VILNIUS GEDIMINAS TECHNICAL UNIVERSITY

Valeriia CHEMERYS

LIGNEOUS BIOCHAR RESEARCH AND DEVELOPMENT OF TECHNOLOGY FOR ENHANCED ADSORPTION OF POTENTIALLY TOXIC ELEMENTS

DOCTORAL DISSERTATION

TECHNOLOGICAL SCIENCES,
ENVIRONMENTAL ENGINEERING (T 004)

VGTU
LEIDYKLA
TECHNIKA
Vilnius 2020

Doctoral dissertation was prepared at Vilnius Gediminas Technical University in 2015–2020.

Supervisor

Prof. Dr Edita BALTRĖNAITĖ-GEDIENĖ (Vilnius Gediminas Technical University, Environmental Engineering – T 004).

The Dissertation Defense Council of Scientific Field of Environmental Engineering of Vilnius Gediminas Technical University:

Chairman

Dr Jurgita MALAIŠKIENĖ (Vilnius Gediminas Technical University, Environmental Engineering – T 004).

Members:

Dr Abhishek DUTTA (KU Leuven, Belgium, Environmental Engineering – T 004),

Assoc. Prof. Dr Eglė JOTAUTIENĖ (Vytautas Magnus University, Environmental Engineering – T 004),

Prof. Dr Habil. Stanislaw Waldemar GAWRONSKI (Warsaw University of Life Sciences, Poland, Environmental Engineering – T 004),

Assoc. Prof. Dr Aušra MAŽEIKIENĖ (Vilnius Gediminas Technical University, Environmental Engineering – T 004).

The dissertation will be defended at the public meeting of the Dissertation Defense Council of Environmental Engineering in the Senate Hall of Vilnius Gediminas Technical University at **10 a. m. on 29 June 2020**.

Address: Saulėtekio al. 11, LT-10223 Vilnius, Lithuania.
Tel.: +370 5 274 4956; fax +370 5 270 0112; e-mail: doktor@vgtu.lt

A notification on the intend defending of the dissertation was send on **28 May 2020**.
A copy of the doctoral dissertation is available for review at VGTU repository http://dspace.vgtu.lt and at the Library of Vilnius Gediminas Technical University (Saulėtekio al. 14, LT-10223 Vilnius, Lithuania).

VGTU leidyklos TECHNIKA 2020-017-M mokslo literatūros knyga

valeriia.chemerys@vgtu.lt

VILNIAUS GEDIMINO TECHNIKOS UNIVERSITETAS

Valeriia CHEMERYS

BIOANGLIES IŠ SUMEDĖJUSIOS BIOMASĖS TYRIMAI BEI TECHNOLOGIJOS KŪRIMAS POTENCIALIAI TOKSIŠKŲ ELEMENTŲ ADSORBCIJAI GERINTI

DAKTARO DISERTACIJA

TECHNOLOGIJOS MOKSLAI,
APLINKOS INŽINERIJA (T 004)

VGTU
LEIDYKLA
TECHNIKA
Vilnius 2020

Disertacija rengta 2015–2020 metais Vilniaus Gedimino technikos universitete.

Vadovė

prof. dr. Edita BALTRĖNAITĖ-GEDIENĖ (Vilniaus Gedimino technikos universitetas, aplinkos inžinerija – T 004).

Vilniaus Gedimino technikos universiteto Aplinkos inžinerijos mokslo krypties disertacijos gynimo taryba:

Pirmininkas

dr. Jurgita MALAIŠKIENĖ (Vilniaus Gedimino technikos universitetas, aplinkos inžinerija – T 004).

Nariai:

dr. Abhishek DUTTA (Leveno katalikiškasis universitetas, Belgija, aplinkos inžinerija – T 004),

doc. dr. Eglė JOTAUTIENĖ (Vytauto Didžiojo universitetas, aplinkos inžinerija – T 004),

prof. habil. dr. Stanislaw Waldemar GAWRONSKI (Varšuvos gyvybės mokslų universitetas, Lenkija, aplinkos inžinerija – T 004),

doc. dr. Aušra MAŽEIKIENĖ (Vilniaus Gedimino technikos universitetas, aplinkos inžinerija – T 004).

Disertacija bus ginama viešame Aplinkos inžinerijos mokslo krypties disertacijos gynimo tarybos posėdyje **2020 m. birželio 29 d. 10 val.** Vilniaus Gedimino technikos universiteto senato posėdžių salėje.

Adresas: Saulėtekio al. 11, LT-10223 Vilnius, Lietuva.
Tel.: (8 5) 274 4956; faksas (8 5) 270 0112; el. paštas doktor@vgtu.lt

Pranešimai apie numatomą ginti disertaciją išsiusti **2020 m. gegužės 28 d.**

Disertaciją galima peržiūrėti VGTU talpykloje http://dspace.vgtu.lt ir Vilniaus Gedimino technikos universiteto bibliotekoje (Saulėtekio al. 14, LT-10223 Vilnius, Lietuva).

Abstract

The dissertation is focused on production and modification ligneous biochar for enhanced adsorption of potentially toxic elements (PTEs) from synthetic solutions and landfill leachate. The main object of the research is adsorption of Cr^{3+}, Cd^{2+}, Pb^{2+}, Zn^{2+}, Ni^{2+}, Cu^{2+} by ligneous biochar. The goal is to assess adsorption of PTEs by biochar and develop technology for modification of ligneous biochar, possessing enhanced adsorption capacity for Cr^{3+}, Cd^{2+}, Pb^{2+}, Zn^{2+}, Ni^{2+}, Cu^{2+}. The thesis approaches several tasks. Tasks 1, 2, 3 are conducted by experimental studies of the key adsorption mechanisms**,** biochar characteristics, modification methods, biochar-hydrogel composite swelling and adsorption studies. Task 4 is conducted by theoretical research and numerical modeling studies of fitting to dynamic intraparticle model for adsorption of PTEs by ligneous biochar.

The dissertation consists of introduction, 3 chapters, general conclusions, recommendations and references. The introduction discusses the research problem, the relevance of the thesis, describes the object of the research, formulates the aim and objectives of the thesis, describes the research methodology, scientific novelty of the thesis, the practical value of the research findings, defended statements. At the end of the introduction, the publications and reports published by the author on the topic of the dissertation and the structure of the dissertation are presented.

Production technologies of biochar from ligneous feedstock, biochar characteristics and modification techniques, as well as mechanisms of adsorption of potentially toxic elements on biochar, equilibrium isotherms and kinetic models of adsorption are presented in Chapter 1. Chapter 2 presents theoretical and experimental methods of selection of feedstock with variable intrinsic properties for biochar production, physical and chemical characteristics of biochar, equilibrium and kinetic modeling of adsorption, modification with H_2O_2, $FeCl_3$, $MgCl_2$ and preparation of biochar-hydrogel composite.

Chapter 3 investigates the effect of modification methods on the adsorption capacity for potentially toxic elements of ligneous biochar and identifies the key mechanisms of adsorption, evaluates the biochar-hydrogel composite potential for application in adsorption of potentially toxic elements from synthetic solutions and landfill leachate, develops the dynamic intraparticle model for adsorption of potentially toxic elements by biochar.

7 publications focusing on the subject of the discussed dissertation were published: 4 articles – in scientific journals included in the Clarivative Analytics Web of Science database (3 of them with citation index), and 3 – in conference proceedings. The 1 patent of the Republic of Lithuania was granted.

Reziumė

Disertacijoje nagrinėjamas bioanglies pagaminimas ir modifikavimas, siekiant pagerinti potencialiai toksiškų elementų (PTE) adsorbciją iš sintetinių tirpalų ir sąvartynų filtrato. Pagrindinis tyrimo objektas yra Cr^{3+}, Cd^{2+}, Pb^{2+}, Zn^{2+}, Ni^{2+}, Cu^{2+} adsorbcija bioanglimi. Tikslas – įvertinti PTE adsorbciją bioanglyje ir sukurti lignino bioanglies modifikavimo technologiją, pasižyminčią padidinta Cr^{3+}, Cd^{2+}, Pb^{2+}, Zn^{2+}, Ni^{2+}, Cu^{2+} adsorbcijos geba. Darbe sprendžiami keli uždaviniai. Pirmieji trys uždaviniai atlikti eksperimentiniais pagrindinių adsorbcijos mechanizmų, bioanglies charakteristikų, modifikavimo metodų, bioanglies-hidrogelio kompozito patinimo ir adsorbcijos tyrimais. Ketvirtasis uždavinys atliktas remiantis teoriniais tyrimais ir skaitmeninio modeliavimo tyrimais, siekiant pritaikyti dinaminį vidinės difuzijos modelį PTE adsorbcijai bioanglyje.

Disertaciją sudaro įvadas, trys skyriai, bendrosios išvados, rekomendacijos ir literatūros sąrašas. Įvadiniame skyriuje aptariama tyrimo problema, darbo aktualumas, aprašomas tyrimo objektas, suformuluojamas darbo tikslas ir uždaviniai, aprašoma tyrimo metodika, darbo mokslinis naujumas, tyrimo išvadų praktinė vertė, ginami teiginiai. Įvado pabaigoje pristatomos disertacijos tema paskelbtos autoriaus publikacijos ir pranešimai konferencijose bei disertacijos struktūra.

Bioanglies iš sumedėjusios biomasės gamybos technologijos, bioanglies charakteristikos ir modifikavimo būdai, taip pat potencialiai toksiškų elementų adsorbcijos bioanglyje mechanizmai, pusiausvyros izotermės ir adsorbcijos kinetiniai modeliai yra aprašyti 1 skyriuje. Antrajame skyriuje pateikti teoriniai ir eksperimentiniai bioanglies atrankos metodai, aprašytos tyrimams naudotos žaliavos su kintančiomis būdingomis savybėmis bioanglies gamyboje, fizikinės ir cheminės bioanglies savybės, pusiausvyros ir kinetinis adsorbcijos modeliavimas, modifikavimas naudojant H_2O_2, $FeCl_3$, $MgCl_2$ tirpalus ir bioanglies-hidrogelio kompozito paruošimo metodika.

Trečiajame skyriuje pateikti tyrimų rezultatai: modifikavimo metodų poveikis potencialiai toksiškų elementų bioanglies adsorbcijos gebai ir nustatomi pagrindiniai adsorbcijos mechanizmai, įvertinamas bioanglies-hidrogelio kompozito potencialas, pritaikant adsorbcijai potencialiai toksiškus elementus iš sintetinių tirpalų ir sąvartyno filtrato, plėtojamas dinaminis vidinės difuzijos modelis potencialiai toksiškų elementų adsorbcijai bioanglyje.

Disertacijos tema paskelbta 7 straipsniai: 4 straipsniai – mokslo žurnaluose, įtrauktuose į Clarivative Analytics Web of Science sąrašą (3 iš jų turi citavimo rodiklį), ir 3 – konferencijų pranešimų leidiniuose. Suteiktas 1 Lietuvos Respublikos patentas.

Notations

Symbols

a_{sp} – geometrical specific surface area, m^2/m^3;
$a_{sp,I}$ – sorbent specific surface area, m^2/m^3;
b – Langmuir equilibrium constant;
C_e – the equilibrium concentration of contaminant molecules in a fluid, mol or mg/l;
$C_{S,*}$ – saturation solute solid concentration, mol/m^3;
D_{Cd} – Cd^{2+} ion diffusivity, m^2/s;
D_{Cr} – Cr^{3+} ion diffusivity, m^2/s;
D_{Cu} – Cu^{2+} ion diffusivity, m^2/s;
D_{Ni} – Ni^{2+} ion diffusivity, m^2/s;
D_p – pore diffusivity based on the cross sectional area, m^2/s;
D_{Pb} – Pb^{2+} ion diffusivity, m^2/s;
D_S – superficial diffusivity, m^2/s;
D_{Zn} – Zn^{2+} ion diffusivity, m^2/s;
d_P – pore diameter, nm;
K_{ads} – linear equilibrium constant;
k_m – mass transfer coefficient;
q_e – the equilibrium mass of sorbed molecules per mass of sorbent, mol or mg/g;

q_{max} – maximum adsorbed amount (total monolayer coverage theoretically), mg/g;

K_f – adsorption coefficient;

n – index of nonlinearity of isotherms;

R_p – particle radius, m;

Shape – Shape factor;

ε – Particle porosity;

ε' – volumetric ratio between the bulk volume and the overall particle volume;

τ – tortuosity factor.

Definitions

Activated carbon – pyrogenic carbonaceous material that undergone activation, e.g. using steam or addition of chemicals (Lehmann & Joseph 2015).

Ash – defined fraction of biomass or pyrogenic carbonaceous material and typically includes inorganic oxides or carbonates (Lehmann & Joseph 2015).

Biochar – heterogeneous substance rich in aromatic carbon and minerals. It is produced by pyrolysis of the sustainably obtained biomass under controlled conditions with clean technology and is used for any purpose that does not involve its rapid mineralization to CO_2 and may eventually become a soil amendment (EBC 2015).

Black carbon – material originated when pyrogenic carbonaceous material dispersed in the environment from wildfires and fossil fuel combustion (Lehmann & Joseph 2015).

Carbonization – thermo-chemical process of formation of carbon from organic matter.

Carbon-negative technology - technology that results in carbon dioxide sequestration (Glaser *et al.* 2009).

Char – material, generated by incomplete combustion processes that occur in natural and man-made fires (Lehmann & Joseph 2015).

Charcoal – material, that produced by thermochemical conversion from biomass for energy generation (Lehmann & Joseph 2015).

Designed biochar – biochar is produced by selecting different feedstocks and using different pyrolysis conditions to form specific physical and chemical characteristics for improving of degraded soils (Ok *et al.* 2015).

Engineered biochar – a biochar-based nanocomposite with improved physicochemical and sorptive properties for various environmental applications including contaminant removal and reclamation of sites containing excessive nutrients (Ok *et al.* 2015).

FTIR − is a technique which is used to obtain an infrared spectrum of absorption or emission of a solid, liquid or gas. It is an easy way to identify the presence of certain functional groups in a molecule (Dwivedi *et al.* 2017).

Hydrochar – a solid product obtained from hydrothermal carbonization or liquefaction, that is different from biochar due to its production process and properties. It has higher hydrogen to carbon ratio and lower aromaticity than biochar (Lehmann & Joseph 2015).

Intrinsic property – a property that is internal in the sense that whether an object has it depends entirely upon what the object is like in itself (Francescotti 1999).

Ligneous biochar – biochar produced from ligneous feedstock (Baltrėnaitė *et al.* 2016).

Macropore – pore, greater than 50 nm length and 50 nm in diameter (IUPAC).

Mesopore – pore, greater than 2 nm, but less than 50 nm in diameter (IUPAC).
Micropore – pore, less than 2 nm in diameter as this value is most commonly used by material scientists in surface area measurements (IUPAC).
Point of zero charge – a pH value at the point, where all the curves intersect. Also is called the zero point of charge (zpc) or pH_0. The knowledge of point of zero charge of the studied materials provides information about the possible attraction and repulsion between sorbent and sorbate but in any case enables to ensure that electrostatic force is one of the mechanisms that takes place in metal sorption (Fiol & Villaescusa 2009).
Potentially Toxic Elements – if present in excessive concentrations maybe hazardous to health and/or inhibit plant growth.
Pyrogenic Carbonaceous Product – general term for a product, that was produced by thermochemical conversion and contain some organic carbon, such as charcoal, biochar, char, black carbon, soot, activated carbon (Lehmann & Joseph 2015).
Pyrolysis – a process where organic substances in biomass are broken down at temperatures ranging from 350 °C to 1000 °C in a low-oxygen thermal process (EBC 2012).
Soot – secondary pyrogenic carbonaceous material and condensation product. Chars, charcoal, biochar, black carbons may contain soot, but it also can be indentified as a separate component from gas condensation processes (Lehmann & Joseph 2015).
Syngenetic elements – elements in the feedstock, that appeared originally (Baltrėnaitė *et al.* 2019).

Abbreviations

BC – biochar;
BET – Brunauer-Emmett-Teller;
BOD – Biological Oxygen Demand;
CEC – cation exchange capacity;
COST – European Cooperation of Science and Technology;
FTIR – Fourier transform infrared spectroscopy;
EBC – European Biochar Certificate;
EBF – European Biochar Foundation;
EBRN – European Biochar Research Network;
EC – electrical conductivity;
GHG – greenhouse gases;
HTT – highest heating temperature;
IBI – International Biochar Initiative;
IDM – intraparticle dynamic model;
PAH – polycyclic aromatic hydrocarbon;
PCM – pyrogenic carbonaceous material;
PTE – potentially toxic element;
SEM – scanning electron microscopy;
SSA – specific surface area.

Contents

INTRODUCTION 1
Problem Formulation 1
Relevance of the Thesis 2
The Object of the Research 3
The Aim of the Thesis 3
The Tasks of the Thesis 3
Research Methodology 3
Scientific Novelty of the Thesis 4
Practical Value of the Research Findings 4
The Defended Statements 5
Approval of the Research Findings 5
Dissertation Structure 6

1. ANALYSIS OF BIOCHAR CHARACTERISTICS, PRODUCTION AND MODIFICATION FOR ENHANCED ADSORPTION OF POTENTIALLY TOXIC ELEMENTS 7
1.1. Production and Properties of Ligneous Biochar 8
1.2. Adsorption Mechanisms, Physical and Chemical Properties of Adsorbent, Solution, Adsorbate 16
1.3. Physical and Chemical Biochar Modification Methods 23
1.4. Intrinsic Properties and Syngenetic Elements Affecting the Adsorption 26

1.5. Theoretical Models for Enhanced Biochar Adsorption, Adsorption Isotherms for Mono- and Multi-Component Adsorptives.....29
1.6. Concept of Biochar-Hydrogel Composite Development 37
1.7. Conclusions of Chapter 1 and Formulation of the Tasks of the Thesis 41

2. METHODOLOGY OF INVESTIGATING THE INFLUENCE OF MODIFICATIONS ON PHYSICAL AND CHEMICAL CHARACTERISTICS OF BIOCHAR FOR INCREASED ADSORPTION CAPACITY 43
2.1. Selection of Feedstock For Biochar Production And Sampling Procedure 44
2.2. Biochar Production 45
2.3. Applied Biochar Modification Techniques 46
2.4. Analysis of Physical and Chemical Characteristics of Feedstock and Biochar ..47
2.5. Methodology of Investigating of Adsorption of Potentially Toxic Elements 51
2.5.1. Selection of the Biochar for Adsorption Experiments…….…….....51
2.5.2. Adsorption Experiments with Synthetic Solutions.....54
2.5.3. Adsorption Experiments with Landfill Leachate ……..……..……..60
2.6. Biochar-Hydrogel Composite Production and Properties…..……..……...62
2.7. Conclusions of Chapter 2 66

3. RESEARCH RESULTS OF BIOCHAR ADSORPTION 69
3.1. Effect of Modification Methods on the Adsorption Capacity for Potentially Toxic Elements of Ligneous Biochar 70
3.1.1. The Influence of Intrinsic Properties and Syngenetic Elements of Ligneous Feedstock on Adsorptive Characteristics of the Biochar.....70
3.1.2. The Influence of Artificial Modifications of Biochar on Adsorptive Characteristics of the Biochar.....77
3.1.3. Adsorption of Potentially Toxic Elements from Synthetic Solutions and Landfill Leachate by Biochar…….……91
3.2. Identification of the Key Mechanisms of the Potentially Toxic Elements Adsorption on Ligneous Biochar …….....……..99
3.3. Evaluation of the biochar-hydrogel composite potential for application in adsorption of potentially toxic elements from synthetic solutions and landfill leachate……...……...……...……100
3.3.1. Characteristics of the Biochar, Hydrogel and Biochar-Hydrogel Composite……..……...…….…….....100
3.3.2. Research of Hydrogel and Biochar-Hydrogel Composite Swelling Under Changing of pH and Temperature……..……..….....103
3.3.3. Adsorption of Potentially Toxic Elements from Landfill Leachate by Biochar-Hydrogel Composites ……...……..…..……...108
3.4. Development of Dynamic Intraparticle Model for Adsorption of Potentially Toxic Elements by Biochar 110
3.4.1. Formation of the Input Data to Dynamic Intraparticle Model Fitting ...110
3.4.2. Results of the Application of the Model for Adsorption of Potentially Toxic Elements by Biochar 113
3.4.3. The Sensitivity Analysis of the Simplified Adsorption Kinetics Model121

3.5. Engineering Technology for Modification of Ligneous Biochar 130
3.6. Conclusions of Chapter 3.....132

GENERAL CONCLUSIONS 135

RECOMMENDATIONS 137

REFERENCES 139

THE LIST OF SCIENTIFIC PUBLICATIONS BY THE AUTHOR ON THE TOPIC OF THE DISSERTATION 151

SANTRAUKA LIETUVIŲ KALBA.....153

ANNEXES[1] 169
Annex A. Physico-Chemical Characteristics of Biochar.....170
Annex B. Equilibrium Data 174
Annex C. Kinetics Data.....177
Annex D. Competing Ions Experimental Data 180
Annex E. Declaration of Academic Integrity 183
Annex F. The Coauthors' Agreements to Present Publications for the Dissertation Defence 184
Annex G. Copies of Scientific Publications by the Author on the Topic of the Dissertation 190

[1] The annexes are supplied in the enclosed compact disc.

Introduction

Problem Formulation

Due to population growth and rapid development of industrialization, the spread of a wide range of potentially toxic elements (PTEs) in surface water and groundwater has become a critical issue worldwide. The most common PTEs in wastewaters are Pb^{2+}, Zn^{2+}, Cu^{2+}, Ni^{2+}, Cr^{3+} and Cd^{2+}, they are long-term pollutants and can not degrade in natural way. If present in excessive concentrations, they may be hazardous to human health and inhibit plant growth. Organisation HELCOM refered these PTEs to the priority lists of contaminants. These PTEs are commonly found in landfill leachate, that distinguished as the most harmful to human beings and ecological environment among all types of wastewater due to high concentration of suspended solids, ammonia nitrogen, chlorinated organic, inorganic salts and other PTEs. It is necessary to control the harmful effects of PTEs and improve the human living environment. Consequently, the need for PTEs removal has become a must.

A variety of treatment technologies are available with different degree of success to control and minimize wastewater pollution with Pb^{2+}, Zn^{2+}, Cu^{2+}, Ni^{2+}, Cr^{3+} and Cd^{2+}. The usual concentration these metal ions in wastewater solution is low (Cr^{3+} 0.2–18 mg/l, Cd^{2+} 0.3–17 mg/l, Pb^{2+} 0.001–2.0 mg/l, Ni^{2+} 0.2–79 mg/l, Zn^{2+} 0.6–370 mg/l, Cu^{2+} 0.005–9.9 mg/l), therefore, conventional methods (e.g.

reverse osmosis, membrane, micro-, ultra- and nanofiltration, coagulation-flocculation, flotation, chemical precipitation, ion exchange, electrochemical methods) may be not efficient for removing of low concentration of PTEs from wastewater (less than 100 mg/l), expensive or generate toxic sludge. Comparatively, adsorption is considered a better and economical alternative in wastewater treatment because of removal of PTEs at low concentrations, flexibility in design and operation. Moreover, adsorbents can be regenerated by suitable desorption process. Today, the most commonly used adsorbent is the activated carbon. However, its widespread use in wastewater treatment is sometimes restricted due to its cost and disposal of the end-of-life adsorbent. Activated carbon could be replaced by biochar (BC), sustainable adsorbent, that is typically processed at lower temperatures in a shorter time period. Commercial price for unmodified BC in 2018 was 3 times lower than for activated carbon, as biochar could be produced from wastes.

Relevance of the Thesis

According to the European Biochar Certificate, ligneous feedstock is the most valuable raw material in terms of its accessibility and ecological acceptance. In 2010 European Union generated 56.8 mln t of ligneous waste. As biochar can be produced from woody residues, large-scale production of a biochar can solve the problem of utilization of woody wastes. In this study woody feedstock was pyrolyzed at 450±10 °C for 2 h, in order to have the following properties for enhanced adsorption of Pb^{2+}, Zn^{2+}, Cu^{2+}, Ni^{2+}, Cr^{3+} and Cd^{2+}: well developed microporous structure and oxygen-containing functional groups on the surface.

Increasing worldwide concern about the development of alternative landfill leachate treatment technologies is growing. BC possesses lower adsorptive characteristics than activated carbon, so it needs to be modified to improve adsorption of PTEs by increasing of specific surface area, porosity and content of oxygenated groups on the surface. To improve biochar's adsorptive properties, it could be prepared from feedstock with certain intrinsic properties and syngenetic elements or modified in artificial way. Selection of feedstock with intrinsic properties and syngenetic elements is cheaper and more accessible, than artificial, but their difference in effect on adsorptive properties of biochar has not been investigated yet. Also influence of intrinsic properties of wood (e.g. lignin, ash, moisture, C, O, H, N, Cr, Cr^{3+}, Cd^{2+}, Pb^{2+}, Zn^{2+}, Ni^{2+}, Cu^{2+} content) on adsorbent characteristics has not been investigated yet.

In order to enhance the efficiency of adsorption of Pb^{2+}, Zn^{2+}, Cu^{2+}, Ni^{2+}, Cr^{3+} and Cd^{2+} during the treatment of landfill leachate, biochar-hydrogel composite

was developed by preparation of biochar-hydrogel composite from the modified biochar with improved adsorption properties.

The Object of the Research

The object of the research is adsorption of Cr^{3+}, Cd^{2+}, Pb^{2+}, Zn^{2+}, Ni^{2+}, Cu^{2+} by ligneous biochar.

The Aim of the Thesis

The aim of the thesis is to assess biochar adsorption of PTEs by developing technology for modification of ligneous biochar, possessing enhanced adsorption capacity for Cr^{3+}, Cd^{2+}, Pb^{2+}, Zn^{2+}, Ni^{2+}, Cu^{2+}.

The Tasks of the Thesis

1. Identify the key mechanisms controlling the maximum adsorption of Cr^{3+}, Cd^{2+}, Pb^{2+}, Zn^{2+}, Ni^{2+}, Cu^{2+} on ligneous biochar from synthetic solutions and landfill leachate.
2. Design and develop device for biochar modification and compare the effect of intrinsic properties, syngenetic elements and artificial modification methods on the adsorption capacity for Cr^{3+}, Cd^{2+}, Pb^{2+}, Zn^{2+}, Ni^{2+}, Cu^{2+} of ligneous biochar from synthetic solutions and landfill leachate.
3. Evaluate biochar-hydrogel composite characteristics and its potential for application in adsorption of Cr^{3+}, Cd^{2+}, Pb^{2+}, Zn^{2+}, Ni^{2+}, Cu^{2+} from landfill leachate.
4. Investigate adsorption parameters (e. g. type of biochar, dosage, time) from fitting to dynamic intraparticle model and conduct sensitivity analysis of simplified adsorption model.

Research Methodology

The research techniques in this dissertation are theoretical, experimental studies and mathematical modelling: equilibrium and kinetic modeling of adsorption (Langmuir, Freundlich isotherms, dynamic intraparticle model), selection of feedstock with variable intrinsic properties for biochar production (e.g. lignin,

moisture, C, O, H, N, PTEs content in feedstock), analysis methods for physical (scanning electronic microscope for morphological structure, Brunauer-Emmett-Teller analyzer for specific surface area) and chemical characteristics (ammonium acetate for cation exchange capacity and oxygen-containing functional groups, pH meter for pH, EC meter for electrical conductivity, CHNO elemental analizer for C, H, N, O content, FTIR for surface functional groups) of biochar using European Biochar Certificate standards, methodology of investigation adsorption of PTEs (Langmuir, Freundlich, Redlich-Peterson, Sips adsorption isotherms, pseudo-first order, pseudo-second order, linear film diffusion, intrapartice pore diffusion, dynamic intraparticle models), atomic absorption spectrophotometer for analysis on PTEs, methodology of modification with H_2O_2, $FeCl_3$, $MgCl_2$, preparation of biochar-hydrogel composite.

Scientific Novelty of the Thesis

1. Influence of intrinsic properties (lignin, ash, moisture, C, O, H, N) and syngenetic elements (Cr^{3+}, Cd^{2+}, Pb^{2+}, Zn^{2+}, Ni^{2+}, Cu^{2+} content) of birch feedstock on adsorptive properties of birch biochar, prepared at 450 °C was investigated.
2. Birch biochar, modified with solution of H_2O_2 of 15% concentration, has 4 higher cation exchange capacity and 15 times higher BET specific surface area than unmodified birch biochar. Moreover, engineering technology for modification of ligneous biochar allows to create H_2O_2-modified biochar with 25% higher cation exchange capacity and up to 2 times higher BET specific surface area, than H_2O_2-modified biochar without the technology.
3. Cationic biochar-hydrogel composite has 7 times higher CEC and 20 times higher BET than unmodified birch biochar. Respectively, composite has higher adsorption efficiency of Cr^{3+}, Cd^{2+}, Pb^{2+}, Zn^{2+}, Ni^{2+}, Cu^{2+} from landfill leachate, than both unmodified birch biochar and H_2O_2-modified birch biochar.
4. The sensitivity analysis of the simplified adsorption model showed that dynamics of the adsorption process could be predicted accurately.

Practical Value of the Research Findings

Engineering technology may be used for preparation of H_2O_2-modified biochar adsorbent for the industrial purposes. H_2O_2-modified biochar and its hydrogel composite may be applied in the industry for adsorption of Cr^{3+}, Cd^{2+}, Pb^{2+}, Zn^{2+},

Ni^{2+}, Cu^{2+} from landfill leachate. Dynamic intraparticle model can give the optimal adsorption parameters (e.g. type of biochar, dosage, time) without kinetic studies. The sensitivity analysis of the simplified adsorption model allows to predict the dynamics of the adsorption process, being a basis for solving important applied optimization problems to maximize the amount of adsorbate by selecting the optimal shape parameter of the adsorbent. Utilization of ligneous wastes is reached due to using them for biochar production.

The Defended Statements

1. Oxidation of biochar with H_2O_2 promotes up to 57% greater adsorption of Cr^{3+}, Cd^{2+}, Pb^{2+}, Zn^{2+}, Ni^{2+}, Cu^{2+} than unmodified biochar.
2. 30−35% lignin content in ligneous feedstock can enhance adsorption of Cr^{3+}, Cd^{2+}, Pb^{2+}, Zn^{2+}, Ni^{2+}, Cu^{2+} in comparison to ligneous feedstock with 18−24% lignin content.
3. Modified biochar-hydrogel composite has up to 2 times higher adsorption capacity of Cr^{3+}, Cd^{2+}, Pb^{2+}, Zn^{2+}, Ni^{2+}, Cu^{2+} from landfill leachate, than unmodified biochar.

Approval of the Research Findings

7 publications focusing on the subject of the discussed dissertation were published: 4 articles – in scientific journals included in the Clarivative Analytics Web of Science database (3 of them with citation index), and 3 – in conference proceedings. The 1 patent of the Republic of Lithuania was granted. 8 presentations on the subject have been presented in conferences at national and international level.

- 2019. 22nd conference for young researchers *Science – Future of Lithuania,* Vilnius, Lithuania.
- 2018. 21st conference for young researchers *Science – Future of Lithuania,* Vilnius, Lithuania.
- 2017. 10th international conference *Challenges in environmental science and engineering* (CESE), Kunming, China.
- 2017. 10th international conference *Environmental Engineering*, Vilnius, Lithuania.
- 2017. 20th conference for young researchers *Science – Future of Lithuania,* Vilnius, Lithuania.

- 2016. 78th conference and exhibition *European Association of Geoscientist and Engineerss* (EAGE), Vienna, Austria.
- 2016. 19th conference for young researchers *Science – Future of Lithuania,* Vilnius, Lithuania.
- 2016. 4th *European Biochar Winter School,* Palermo, Italy.

Dissertation Structure

The scientific work consists of introduction, 3 chapters, general conclusions and recommendations, list of literature, author's publications on the topic of dissertation. The total scope of the dissertation – 185 pages excluding annexes, 58 pictures and 38 tables. 158 literature sources were cited.

1

Analysis of Biochar Characteristics, Production and Modification for Enhanced Adsorption of Potentially Toxic Elements

This Chapter reviews production technologies of biochar, its characteristics and modification techniques. Mechanisms of adsorption of PTEs on biochar, equilibrium isotherms and kinetic models of adsorption are discussed. Value of ligneous feedstock for biochar production, optimal adsorbent characteristics were analyzed. On the basis of literature review, such articles as Chemerys and Baltrėnaitė (2016; 2018a), were published.

1.1. Production and Properties of Ligneous Biochar

Rich in aromatic carbon and minerals, biochar is produced from biomass pyrolysis at temperatures ranging from 350 °C to 1000 °C in low-oxygen environment (EBC 2012). BC is a carbon-rich (10−60%) solid obtained by heating biomass, such as wood, manure with little or no oxygen (pyrolysis or "charring") (Sohi 2012). Using of BC solves different problems: significantly improves the quality and productivity of soil; decreases CO_2 in the atmosphere; biochar production can involve recycling of organic waste; slowing down the process of global climate change by achieving the limit of global average temperature increase 2°C (International Biochar Initiative 2012).

Scientists all over the world investigate biochar properties and methods to increase adsorpion of PTEs from aqueous solutions by biochar. Thus, scientists from Lithuania (Pranas Baltrėnas, Edita Baltrėnaitė-Gedienė, VGTU) created vertical biofilter-adsorber and used diagnostic and simulation models for adsorption on biochar; Pellegrino Conte (University of Palermo, Italy) is focused on water-biochar interactions; Anushka Upamali Rajapaksha (University of Sri Jayewardenepura, Sri Lanka) studies various modifications of biochar as adsorbent of PTEs, Yingwen Xue (Wuhan University, China) investigates chemical modifications of biochar.

Various types of feedstock (e.g. wood, crop residues, animal manure, solid wastes etc) can be used to prepare a biomass (Tan *et al.* 2015) (Fig. 1.1). BC exhibits differing physical and chemical properties depending on the feedstock and the pyrolysis technology.

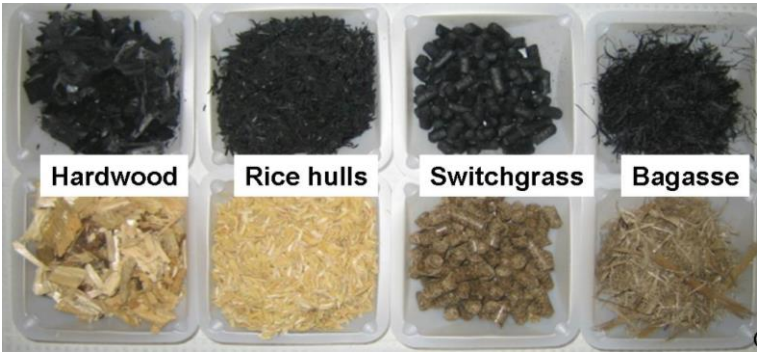

Fig. 1.1. Various feedstock of biochar and produced biochar
(source: International Biochar Initiative 2012)

European Biochar Certificate (EBC) stated that the most valuable material for biochar production is ligneous biomass. Ligneous biomass is a promising alternative and renewable energy source that can be converted via the biomass pyrolysis process into a liquid (bio-oil) and solid products (BC), which are considered to have a variety of applications. In Table 1.1 various types of ligneous biomass are presented.

In terms of waste management, wasted plant biomass is of great importance. Ligneous waste materials include agricultural residues, energy crops, wood residues and municipal paper waste (Nanda *et al.* 2013).

Cellulose, hemicellulose and lignin are three main components in structural composition of ligneous biomass (Fig 1.2). Depending on the type of biomass, cellulose constitutes 40−50%, hemicellulose 20−40% and lignin 10−40% of plant material (Table 1.2).

Table 1.1. General classification of ligneous biomass (Vassilev *et al.* 2010)

Biomass groups	Biomass sub-groups, varieties and species
1. Ligneous biomass	Type of tree specie: coniferous or deciduous; Structure of wood: soft or hard; Form of biomass: stems, branches, foliage, bark, chips, lumps, pellets, briquettes, sawdust, sawmill
2. Herbaceous and agri-cultural biomass	Grasses and flowers (alfalfa, bamboo, brassica, cane, cynara, miscanthus, switchgrass, timothy) Straws (barley, bean, flax, corn, mint, oat, rape, rice, rye, sesame, sunflower, wheat) Other residues (fruits, shells, husks, hulls, pits, pips, grains, seeds, coir, stalks, cobs, kernels, bagasse, fodder, pulps)
3. Contaminated and industrial biomass	Demolition wood, paper-pulp sludge, waste papers, paperboard, chipboard, fibreboard, wood pallets, boxes

Softwoods such as pine contain 42% of cellulose, 27% of hemicelluloses and 28% of lignin, while hardwoods have 45% of cellulose and 20% of lignin (Rutherford *et al.* 2012). A small amount of ash and extractives (15%) is present as well. Woody plant species are richer in lignin due to tightly bound fibers, while herbaceous plants have more loosely bound fibers, consequently, a lower lignin content (Stefanidis *et al.* 2014).

Water, CO_2, nitrogen (N) are involved in production of plant biomass. Environmental stresses (e.g. drought or cold soil) leads to inhibition of root growth in trees, that further reduces adsorption of water and mineral nutrients (N, phosphorus (P), potassium (K), sulfur (S), calcium (Ca), magnesium (Mg), iron (Fe), manganes (Mn), zinc (Zn), copper (Cu), boron (B), molybdenum (Mo),

chlorin (Cl)). Mineral composition of ligneous feedstock influences properties of produced BC.

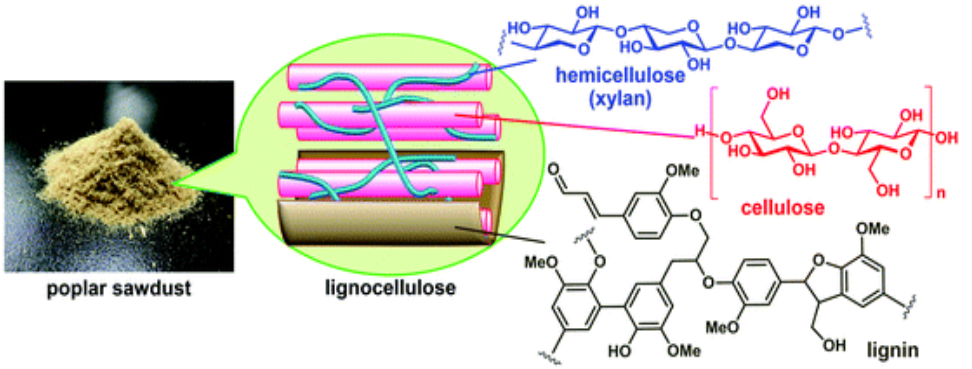

Fig. 1.2. Structure of lignocellulose (source: Kobayashi & Fukuoka 2013)

Table 1.2. Types of ligneous biomass and their average chemical composition (adopted from Isikgor & Becer 2015)

Ligneous biomass		Cellulose, %	Hemicellulose, %	Lignin, %
Hardwood	Poplar	52.1	27.5	15.9
	Oak	40.4	35.9	24.1
Softwood	Pine	46.0	25.5	20.0
	Fir	45.5	22.9	27.9
Agricultural waste	Wheat straw	37.0	26.5	14.0
	Barley hull	34.0	36.0	16.4
	Barley straw	39.5	28.5	8.0
	Rice husk	31.0	20.5	17.7
	Oat straw	33.0	23.0	12.5
	Corn cob	37.5	34.0	11.0
	Corn stalk	37.3	24.3	12.5
	Sugarcane bagasse	35.0	30.0	20.0
Grasses	Switchgrass	37.5	27.5	17.5

Main thermochemical processes to produce BC are slow and fast pyrolysis (Tan *et al.* 2015). Other methods (e.g. hydrothermal carbonization (HTC), flash carbonization, torrefaction, gasification) result not in solid biochar, thus, could be negleted.

Pyrolysis technology can be classified by the residence time, pyrolytic temperature of the pyrolysis material (e.g., slow and fast pyrolysis process), pressure, particle size, and the heating rate and method (e.g., pyrolysis started by the burning of fuels, by electrical heating, or by microwaves) (Nartey & Zhao 2014). The highest heating temperature (HTT) has a great influence on the elemental compositions and the surface functional groups of BC. Various studies demonstrate that with increasing pyrolytic temperature carbon content is enhanced, but N, H, O, S content and most bands are decreased. Pyrolytic temperature significantly changes BC characteristics. BC, produced at higher temperature, shows high pH, cation exchange capacity (CEC) and surface area. Nevertheless, biochar produced at low temperature, contains more active sites and stable carbon–oxygen complexes (Meyer *et al.* 2011).

During pyrolysis biomass is heated in the absence of oxygen. Heating causes disintegration of complex biomolecules, as a result, different gases and solid fuels are generated. If the temperature exceeds 400 °C, the solid fraction is a charcoal, that almost 100% is composed of carbon. If the temperature is in the range 200−300 °C, then the solid fraction is a torrefied mass, and the process is called torrefaction (Tan et al. 2015).

Slow pyrolysis is the most commonly used technology nowadays. BC can be used as an effective adsorbent for adsorption of PTE from aqueous solution (Table 1.3). With the increase of temperature ligneous feedstock is gradually pyrolyzed. Under slow pyrolysis, hemicellulose and cellulose begin to decompose at 250 °C with the majority of mass loss by 400 °C. Lignin loses mass gradually from 200 °C to 720 °C. The major decomposition processes occur between 200 and 500 °C including 4 steps (Meyer *et al.* 2011):

- The partial hemicellulose decomposition;
- The complete hemicellulose decomposition to partial cellulose decomposition;
- The full cellulose and partial lignin decomposition;
- The next decomposition and increasing degree of carbonization .

The yields of BC reduce with the increase of temperature in the range 15−90% (Rutherford *et al.* 2012).

Nearly 46% of BC application in water treatment includes the removal ability of biochar for inorganic PTEs, 39% for organic PTEs, 13% for N and P, and 2% for other PTEs (Tan *et al.* 2015). Table 1.4 illustrates application of different types of BC for specific contaminant removal from water.

The efficiency of BC in adsorption of PTE from water depends on its characteristics. Properties of BC could be divided into physical and chemical (Fig. 1.3). The key parameters influencing properties of BC during pyrolysis include temperature, residence time, heat transfer rate and feedstock type.

Relatively high pyrolysis temperatures generally produce BC that are effective in the sorption of organic contaminants because of increased specific surface area, microporosity, and hydrophobicity; whereas the biochars obtained at low temperatures are more suitable for removing inorganic/polar organic contaminants by oxygen-containing functional groups, which favour electrostatic attraction, and precipitation (Ahmad *et al.* 2014).

Table 1.3. Water treatment from potentially toxic elements using biochar (Mohan et al. 2014b)

Potentially toxic element	Biochar type and the highest heating temperature, °C	References
As^{5+}	Pine wood	Mohan *et al.* 2007
	Oak wood	
Cu^{2+}	Hard wood (450 °C)	Chen *et al.* 2011a
	Peanut straw (400 °C)	Tong *et al.* 2011
	Soybean straw (400 °C)	
	Corn straw	Chen *et al.* 2011a
	Rice hust	Pellera *et al.* 2012
	Compost	
	Orange waste	
	Pig manure	Kołodynska *et al.* 2012
	Cow manure	
Pb^{2+}	Sewage sludge (550 °C)	Lu *et al.* 2012
	Pinewood (300 °C)	Liu & Zhang 2009
	Rice husk (300 °C)	
Cd^{2+}	Pinewood	Mohan *et al.* 2007
	Oak wood	
	Cow manure	Kołodynska *et al.* 2012
	Pig manure	
Zn^{2+}	Corn straw (600 °C)	Chen *et al.* 2011a
	Hard wood (450 °C)	
	Cow manure	Kołodynska *et al.* 2012
	Pig manure	

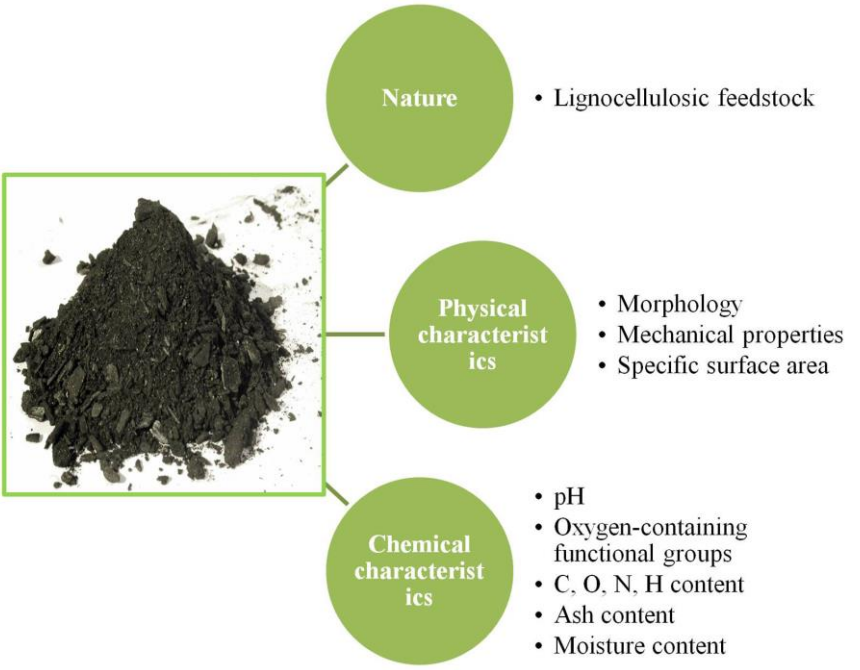

Fig. 1.3. The criteria for selecting the biochar for adsorption of potentially toxic elements (author's figure)

Each type of BC made from the particular feedstock and under the specific production conditions presents a variety of chemical and physical properties. Thus, variety of functional groups on the surface of BC influence sorption by the nature of their surface charge and by the availability of π-electrons. The charge of the functional groups may depend on the pH of the solution, affecting sorption behaviour (Lehmann & Joseph 2009).

The specific surface area of BC is related to pore size distribution. As the highest heating temperature increases, the surface area of BC also increases as more pores are generated. Pores of different length scales can form in BC.

Baltrėnas *et al.* (2015) analysed the morphology of BC produced from birch and pine at different temperatures (Fig 1.4). As determined by N_2-adsorption according to the BET methodology, the BC samples treated at a temperature of 750°C had the largest specific surface area (birch 425.11 and pine 380.36 m^2/g). Less micropores were found in the birch and pine BC samples treated at 300 and 450 °C.

BC physical, chemical and mechanical properties can vary with production conditions, making it challenging to engineer BC that are simultaneously optimized for C sequestration, nutrient storage, water-holding capacity and adsorption (Mohan *et al.* 2014b).

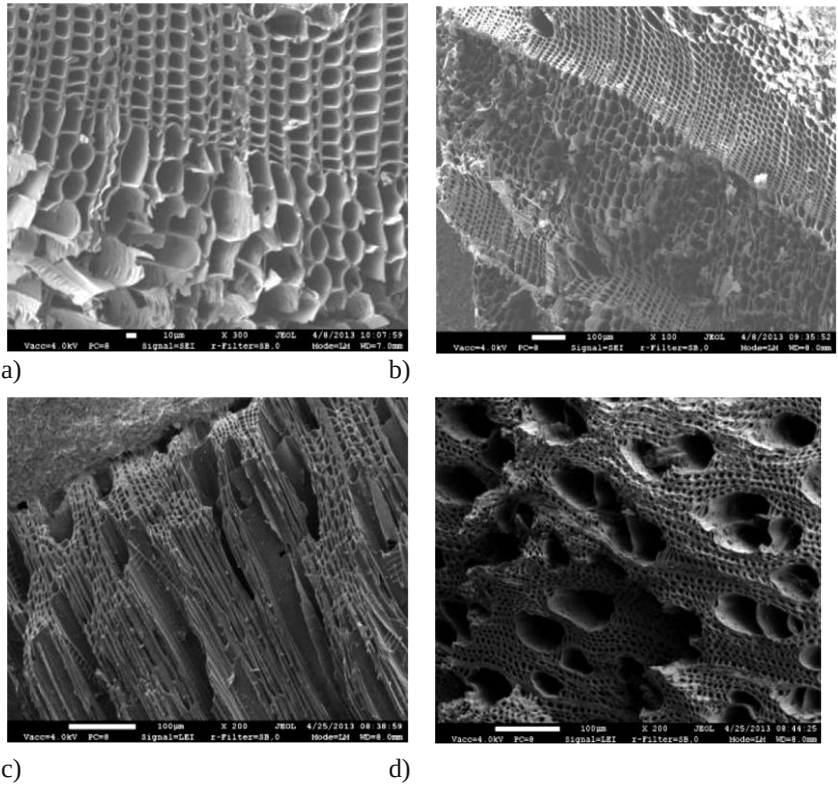

a) b)

c) d)

Fig. 1.4. Scanning electron microscopy (SEM) images of biochar porous structure (Baltrėnas *et al.* 2015): a) Sample P750, ×300; b) Sample P450, ×100; c) Sample B750, ×200; d) Sample B450, ×200; where P − pine, B − birch, 750 and 450 − pyrolysis temperatures

Sun *et al.* 2014 prepared nine types of BC (by slow pyrolysis at 300, 450, 600 °C in N_2-environment) and three hydrochars (by hydrothermal carbonization at 200 °C for 5 h) from hickory wood, bagasse, bamboo. The results showed, that BC produced at 600 °C were more useful for water treatment or environmental remediation due to the largest specific surface area (bamboo 375.5, bagasse 388.3, hickory wood 401 m^2/g).

Table 1.4. Mechanisms of a specific potentially toxic elements adsorption by biochar produced from various types of feedstock

No	Biochar	Adsorbate	Mechanism of adsorption	References
1	Sugar beat tailing (300 °C)	Cr^{6+}	Electrostatic attraction; complexation	Dong *et al.* (2011)
2	Broiler litter (700 °C)	Cu^{2+}	Cation exchange; electrostatic interaction; sorption on mineral ash contents; complexation by surface functional groups	Uchimiya *et al.* (2011)
3	Crop straw (400 °C)	Cu^{2+}	Surface complexation	Tong *et al.* (2011)
4	Dairy manure (200 °C)	Pb^{2+}	Precipitation with phosphate	Cao *et al.* (2011)
5	Sewage sludge (550 °C)	Pb^{2+}	Cation release, functional groups complexation, surface precipitation	Lu *et al.* (2012)
6	Soybean stalk (300–700 °C)	Hg^{2+}	Precipitation, complexation and reduction	Kong *et al.* (2011)

De-ashing and de-mineralization treatments can enhance the adsorption properties of biochar, e.g. rice hull derived biochar exhibited greater removal ability toward methyl violet than water-washed biochar (Ahmad *et al.* 2014).

It was found that increased microporosity, specific surface area, high content of oxygen-containing functional groups on biochar surface enhanced the adsorption of PTE on biochar (Baltrėnas *et al.* 2015). Samsuri *et al.* (2013) showed that the oil palm biochar with lower specific surface area exhibited a higher adsorption capacity for the PTE than the rice husk biochar, suggesting that surface area was less important than oxygen-containing functional groups.

Ratios H/C and O/C are used to characterize the biochar. While H/C indicates the aromatization of biochar (extra molecular stability), O/C indicates the degree of surface hydrophilicity and polarity (reactivity or electrical charge). It was proposed that biochar should have $H/C \leq 0.7$ and $O/C \leq 0.4$. While aromaticity increases with the temperature, polarity decreases with the temperature. The decreasing in the O/C and/or N/C ratios can indicate the increasing in the hydrophobicity and the reduction of functional groups (Suguhuiro *et al.* 2013).

Mineral components in biochar also play an important role. Xu *et al.* (2013) found that PO_4^{3-} and CO_3^{2-} served as additional adsorption sites, contributing to the dairy manure biochar's high adsorption capacity for Cu, Zn, and Cd.

Atomic/ionic size of the PTE is another parameter of concern while considering adsorption onto biochar. Generally, the smaller ionic radius of PTE, the greater adsorption capacity due to enhanced penetration into biochar pores (Ahmad *et al.* 2014).

Surface sorption of PTE corresponds directly with the release of H^+ ions from the biochar, but also with the release of Na, Ca, K, Mg (Uchimiya *et al.* 2011) into solution that indicates retention of metals on protonated (acidic) functional groups but also exchange of ions. In aqueous solutions biochar showed higher adsorption capacity for a single PTE than multiple PTEs are present, because there is a competition for binding sites between PTEs (Lima & Marshall 2005).

The activated carbon (AC) is the most commonly used carbonaceous sorbent for wastewater treatment (Azargohar & Dalai 2006). In comparison to AC, biochar is carbon negative (Glaser *et al.* 2009), produced from wide range of wastes (Ioannidou & Zabaniotou 2007) via slow or fast pyrolysis without obligatory gasification and activation (Nartey & Zhao 2014). Biochar could be a precursor of AC. Biochar was evaluated as a feed to produce activated carbons at 535 °C (Azargohar & Dalai 2006). Activated carbons that resulted had internal surface areas more than 500 m^2/g versus 10 m^2/g for the precursor biochar. This AC was highly microporous, confirmed by SEM analysis. FTIR proved aromatization had occurred (Park *et al.* 2013).

1.2. Adsorption Mechanisms, Physical and Chemical Properties of Adsorbent, Solution, Adsorbate

Being a surface process, adsorption takes place in 4 steps. Bulk solution transport involves the movement of the PTE to be adsorbed through the bulk liquid to the boundary layer of fixed film of liquid surrounding the biochar. Film diffusion transport involves the transport of PTE by diffusion through the stagnant liquid film to the entrance of the pores of the biochar. Pore transport involves the transport of the PTE to be adsorbed through the pores by a combination of molecular diffusion through the pore liquid and/or by diffusion along the surface of the biochar (Nazaroff & Alvarez-Cohen 2001). The main components of adsorption (adsorbent, solution and adsorbate) are shown in Fig. 1.5.

Mechanisms of adsorption of PTEs on biochar are electrostatic attraction, ion exchange, precipitation, surface and innersphere complexation, co-precipitation (Figure 1.6). Adsorption of cations by biochar is mainly controlled by electrostatic attartion and ion exchange. Surface charge play a cruicial role in adsorption. When the surface becomes protonated, adsorbent gains a positive surface charge, that electrostatically attracts and adsorb negative species (anions). When the surface

becomes deprotonated, adsorbent gains a negative surface charge, attracts positive species (cations).

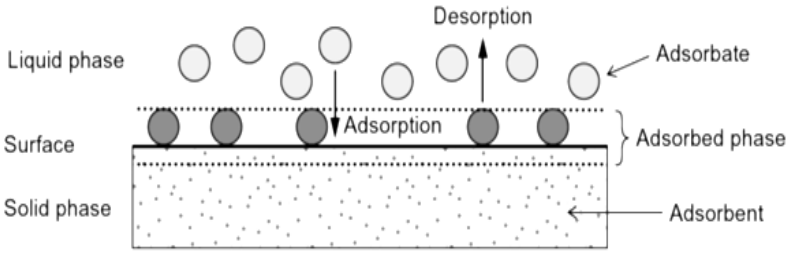

Fig. 1.5. Components in adsorption and desorption processes (source: Christmann 2010)

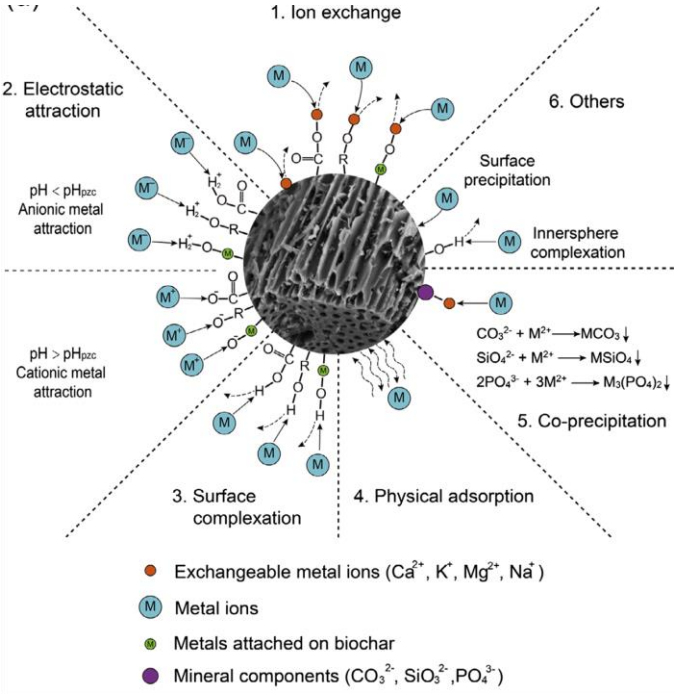

Fig. 1.6. Mechanisms of biochar interactions with inorganic contaminants (source: Tan *et al.* 2015)

With the increase of pH of solution, the competition of metal ions and protons for binding sites decreased and more binding sites are released due to the deprotonation of functional groups (Lu *et al.* 2012). The surface of biochar is negatively charged when $pH_{solution} > pH_{pzc}$ (point of zero charge).

Depending on the type of forces between adsorbate and adsorbent, adsorption could be classified into physical and chemical adsorption (Nazaroff & Alvarez-Cohen 2001). In physical adsorption (physisorption) molecules are held by Van der Waal's forces of attraction, and form multilayer of adsorbate on biochar. It has low enthalpy of the order 20 kJ/mol (Zhou & Toth 2001). In case of chemical adsorption (chemisorption), the force of attraction between adsorbate and adsorbent is chemical bond. During chemisorption, unilayer of adsorbate on biochar is formed. Chemical adsorption has high enthalpy of 80–200 kJ/mol (Zhou & Toth 2001).

Adsorption is affected by characteristics of solution, adsorbent and adsorbate.

Characteristics of solution:

- Higher temperature favors a slight increase in adsorption of PTE onto biochar. For example, the Zn^{2+} adsorption capacity of CS600 increased from 8.65 mg/g at 22°C to 9.84 mg/g at 37°C. These results were consistent with a previous report that Pb^{2+} uptake increased with an increase in temperature for oak wood char and oak bark char in the range of 5–40°C (Mohan *et al.* 2007) and with the work of Liu and Zhang (2009), who suggested that increased temperatures provided heavy metals ions sufficient energy to overcome the diffuse double layer and adsorb onto biochar's interior structure.
- pH has a great importance in cation sorption because it influences chemical speciation of the metal in solution and also on the ionization of chemically active sites on the sorbent, affecting ion exchange and metal deposition reactions to influence metal ion concentrations in aqueous solution (Zhou *et al.* 2018). In Stanila *et al.* (2016), due to ionization of functional groups, adsorption of Pb^{2+} and Ni^{2+} was increased when pH increased from 5 to 7. Decrease in adsorption capacity at pH>7 is due to the formation of soluble PTE complexes and their competition with the active sites. Kilic *et al.* 2013 obtained the highest adsorption of Ni^{2+} and Co^{2+} at pH = 7 for both Ni^{2+} and Co^{2+} ions.
- The adsorbed amount was increased as the contact time increased. Large amounts of metal ions were removed within 150 min for both Ni^{2+} and Co^{2+}. After that the capacity of adsorption remained constant (Kilic *et al.* 2013).
- Catalysts are used for enhancing the adsorption process. The presence of acidic or basic types of catalyst promotes the formation of biochar with

an extended value of surface area, along with significant porosity. Some of hydrated metal oxides, such as manganese (IV) oxide and Fe^{3+} oxide, are especially effective in sorbing PTE ions from aquatic solutions (Duffy 2011).

Characteristics of adsorbent:

- Highly alkaline biochar could increase *pH* of solution above the limits. Raising the pH made toxic metals less soluble, and adsorbing the positively charged metal ions removed them from the solution (Komkienė & Baltrėnaitė 2015).
- Point of zero charge is the pH at which the adsorbent surface charge takes a zero value (pH_{pzc}) (Fiol and Villaescusa 2009). pH_{pzc} provides ensures that electrostatic force is one of the adsorption mechanisms (Fiol and Villaescusa 2009). At pH_{pzc}, the charge of the positive surface sites is equal to that of the negative ones. At solution pH higher than pH_{pzc}, sorbent surface is negatively charged and could interact with metal positive species while at pH lower than pH_{pzc}, solid surface is positively charged and could interact with negative species
- Adsorption is a surface phenomena, therefore, it increases with increase of specific surface area of adsorbent, respectively, porosity of the adsorbent. It is known that adsorption of PTE is affected by micropores with the pore size less than 2 nm.
- Activation of adsorbent surface is done so as to provide more number of vacant sites on surface of adsorbent, i.e. increase content of oxygen-containing functional groups. This can be done by physical (e.g. breaking solid crystal in small pieces, heating charcoal at high temperature, breaking lump of solid into powder etc) or chemical (e.g. activation with salts and acids) methods.

Characteristics of adsorbate:

- Molecules are attached into pores of the BC, therefore, molecule size of adsorbate influence adsorption. More soluble PTEs were removed them from the solution, indicating that solubility of adsorbent affects adsorption (Komkienė & Baltrėnaitė 2015).

Gibb's energy (free enthalpy) indicates the type of adsorption (physical or chemical). Gibb's energy is thermodynamic parameter for adsorption systems (liquid–solid). It is estimated by Equation (1.1):

$$\Delta G^0 = -R \times T \ln (K_c), \quad (1.1)$$

where R = 8.314 J/ K·mol is the gas constant, and T is temperature in K. K_c is the equilibrium constant, and can be calculated from Equation (1.2):

$$K_C = \frac{q_e}{C_e}, \tag{1.2}$$

where q_e is the adsorption capacity (mg/g), C_e is equilibrium concentration of adsorbate (mg/l). The positive values of Gibb's energy indicates that the adsorption is endothermic (Trazzi *et al.* 2016).

For cations (e.g. Cr, Cu, Pb) electrostatic attraction ($pH>pH_{pzc}$) and ion exchange are prevailable mechanisms, because positively charged PTE are adsorbed onto negatively charged surface of biochar. Electrostatic attraction ($pH<pH_{pzc}$) and surface complexation favor adsorption of anionic PTE (e.g. As).

Dong *et al.* (2011) summarized the adsorption of Cr^{6+} by sugar beet tailing biochar, prepared by slow pyrolysis at 300 °C for 2 h in N_2-environment into three parts: first, the negatively charged Cr^{6+} species migrated to the positively charged surfaces of biochar (at low pH) with the help of electrostatic attraction; second, Cr^{6+} was reduced to Cr^{3+} by the participation of hydrogen ions and the electron donors from biochar; third, part of the Cr^{3+} reduced from Cr^{6+} was released to the aqueous solution, and the other part of Cr^{3+} was complexed with the functional groups on biochar. All Cr^{6+} was removed at pH 2 compared to 16% of adsorption efficiency at pH 3.

Abdel-Fattah *et al.* (2015) investigated the adsorption of Ca, Mg, Cr, Pb from aqueous solution by pinewood biochar, prepared by slow pyrolysis for 2 h. Obtained biochar was rich in O-containing groups, calcium, but low BET-surface area. The best adsorption results, being explained with high cation exchange capacity, were for Mg^{2+}, Ca^{2+}, Cr^{6+}, and Pb^{2+} ions were determined as 440 (pH 7.0), 120 (pH 7.0), 680 (pH 1.0), and 520 (pH 6.0) mmol/g.

Kołodynska *et al.* (2012) found that when pH increases, the competition of metal ions and protons for binding sites decreases and more binding sites are released, which results in the increase of adsorption effectiveness. Therefore the maximum adsorption efficiency was achieved at a pH of about 5.0 for Cu^{2+} (6.34 mg/g) and Zn^{2+} (4.25 mg/g) and at pH equal to 6.0 for Cd^{2+} (16.60 mg/g) and Pb^{2+} (19.85 mg/g).

When biochar is used as adsorbent, adsorption takes place by ion exchange when acid surface functionalities are dissociated at the working solution pH. This mechanism also involves the formation of a surface metal complex, because metal cations in aqueous solution are mainly as hexa-aquo cations or as a hydrolyzed form of these, depending on the solution pH. Hence, the adsorption mechanism in this case can be considered, more appropriately, as "proton exchange with formation of surface metal complexes". For hexa-aquo cations, the adsorption mechanism may be either by inner-sphere (IS) or by outer-sphere (OS) surface metal complex formation (Fig. 1.7).

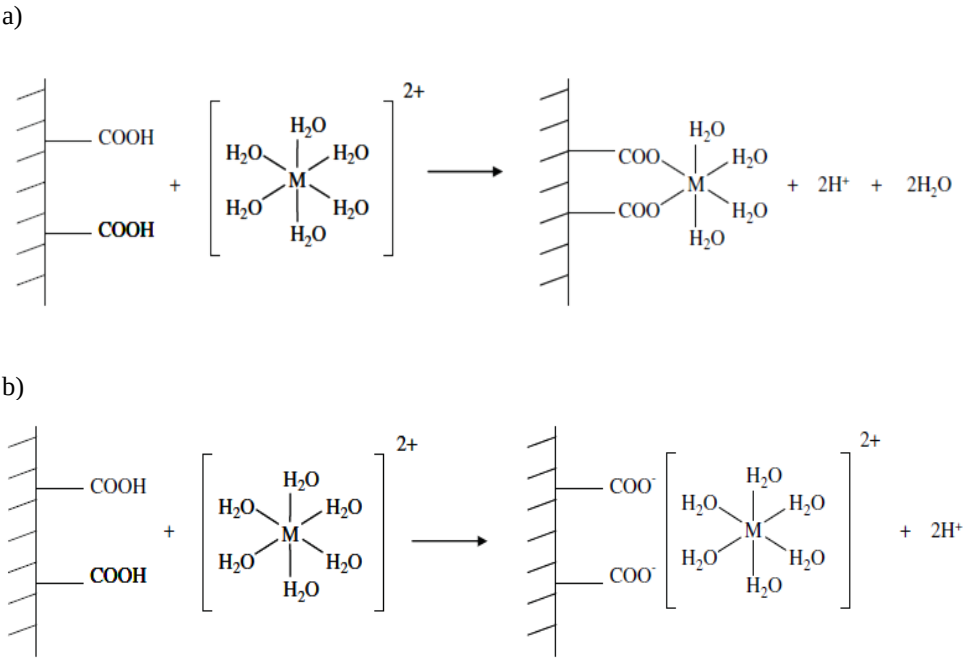

Fig. 1.7. Metal complex formation mechanisms for a divalent hexa-aquo cation: a) inner-sphere surface; b) outer-sphere surface (souce: Moreno-Castilla *et al.* 2010)

Moreno-Castilla *et al.* (2010) revealed that negative surface charge at a given pH increases with higher temperature due to an increase in proton release from surface oxygen complexes of acid character. The adsorption of most metal cations on biochar appears to occur by ion exchange with the surface acid groups of the biochar. This would result in a displacement of protons from the surface acid functional groups. Results obtained indicate that the strength of carboxyl groups involved in metal cation adsorption increased in the order $Cr^{3+} < Cu^{2+} < Zn^{2+} < Mn^{2+}$ due to proton exchange and three and two surface acidic groups were involved in the adsorption of the trivalent and divalent cations, respectively.

Key properties of some commercial adsorbents are indicated in Table 1.5.

According to Seader & Henley (2006), adsorbent should have following properties to be suitable for commercial applications:

- high capacity to minimize the amount of adsorbent needed,
- favorable kinetic and transport properties for rapid sorption,
- chemical and thermal stability to preserve the amount of adsorbent and its properties,

- hardness and mechanical strength to prevent crushing and erosion,
- a free-flowing tendency for ease of filling or emptying vessels,
- no tendency to promote undesirable chemical reactions,
- the capability of being regenerated when used with commercial feedstocks that contain trace quantities of high-molecular-weight species that are strongly sorbed and difficult to desorb,
- relatively low-cost.

Table 1.5. Representative properties of commercial adsorbents (Seader & Henley 2006)

Adsorbent	Nature	Pore diameter D_p, A	Particle porosity ϵ_p	Particle density ρ_p, g/cm^3	Surface area S_g, m^2/g
Activated alumina	Hydrophilic, amorphous	10−75	0.5	1.25	320
Silica gel: Small pore Large pore	Hydrophilic/ Hydrophobic, amorphous	 22−26 100−150	 0.47 0.71	 1.09 0.62	 750−850 300–350
Activated carbon: Small pore Large pore	Hydrophobic, amorphous	 10−25 >30	 0.4−0.6 –	 0.5−0.9 0.6−0.8	 400−1200 200−600
Molecular-sieve carbon	Hydrophobic	2−10	n.a.	0.98	400
Molecular-sieve zeolites	Polar-hydrophilic, crystalline	3−10	0.2−0.5	1.4	600−700
Polymeric adsorbents		40−25	0.4−0.55	n.a.	80−700

To achieve very large surface area for adsorption per unit volume, highly porous solid particles with small diameter interconnected pores are used, with the bulk of the adsorption occurring within the pores. Specific surface areas can be as high as 2000 m^2/g but the range is more usually restricted to 300 to 1200 m^2/g in order to preserve good mechanical strength (Seader & Henley 2006).

1.3. Physical and Chemical Biochar Modification Methods

Adsorption properties of biochar could be further developed through physical and chemical modification techniques. Detailed schematic description of modification of biochar on different stages of production is provided in Fig. 1.8.

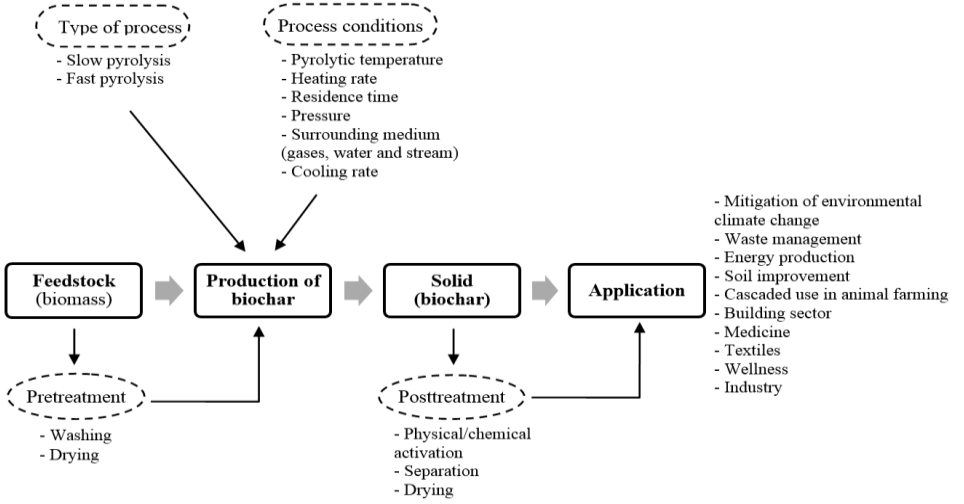

Fig. 1.8. Scheme of biochar production and application (modified from Nartey & Zhao (2014); Schmidt 2012)

Different types of biochar could extend the application of biochar depending on the purpose of use or type of adsorbate (anionic/cationic, polar/non-polar, organic/inorganic, hydrophilic/hydrophobic). Modification of biochar could be made through various methods, e.g acid/base treatment, carboxylation, amination, treatment with organic solvents, surfactant modifications, coating of biochar, impregnation of mineral oxides, steam activation, gas purging, magnetization (Rajapaksha *et al.* 2016). The concept of modified biochar in environmental management to enhance the efficiency of contaminant removal should be developed, e.g to match the properties of biochar to adsorb particular contaminant (Ok *et al.* 2015).

Hence, biochar can be modified at three stages of its production:

- while preparing the feedstock for pyrolysis one can choose different type of feedstock or pre-treat the feedstock with acids, ammonia, salts, steam,

- during pyrolysis process one can set different process conditions,
- after receiving ready biochar product one can apply activation.

Available methods of biochar modification for enhanced adsorption of PTEs are summarized in Table 1.6.

Table 1.6. Chemical modifications of biochar for adsorption of inorganic compounds

Modification method	Biochar feedstock and production temperature, °C	Adsorbate	Mechanism of adsorp-tion	References
KOH	Switchgrass, 300	Cu^{2+}, Cd^{2+}	Surface complexation	Regmi *et al.* (2012)
H_2SO_4+HNO_3, NH_4OH+$Na_2S_2O_4$ +acetic acid (amination)	Saw dust, 500	Cu^{2+}	Surface complexation, ion exchange, co-precipitation	Yang & Jiang (2014)
H_2O_2	Peanut hull, 300	Pb^{2+}, Cu^{2+}, Ni^{2+}, Cd^{2+}	Surface complexation, co-precipitation	Xue *et al.* (2012)
Ca and Fe	Rice husk, 300	Cr^{6+}	Metal precipitation, electrostatic attraction	Agrafioti *et al.* (2014)
Fe	Bamboo, 600	Pb^{2+}, Cr^{6+}	Electrostatic attraction	Zhou *et al.* (2014)
$Fe_2(SO_4)_3$, $FeSO_4$ and NaOH	Oak wood and bar, 450	Cd^{2+}, Pb^{2+}	Metal precipitation	Mohan *et al.* (2014a)

Modified biochar could be distinguished into designed, engineered and smart. Depending on application, designed biochar is produced by selecting various types of feedstock in order to gain specific characteristics, e.g. pellets of biochar, prepared from pyrolized nutshells under 500 °C, can increase carbon sequestration in sandy soil (Novak *et al.* 2009, 2013). Engineered biochar is biochar with enrichment of chemical compounds, e.g. Al (Zhang *et al.* 2013), Mg (Yao *et al.* 2013), Fe and Ca (Agrafioti *et al.* 2014) etc. Smart biochar is the type of engineered biochar, that changes its properties under different stresses (temperature, pH etc), e.g. biochar activated with oxygen plasma (Gupta *et al.* 2015).

Treatment with acids produce positive sites on the surface of biochar and protonation of surface hydroxyl groups causes an increase of electrostatic attraction. Base pretreatment increases the surface area of the biochar (e.g. the

activated ligneous biochar was 367.10 m^2/g, whereas before base activation, it was only 1.22 m^2/g), which can successfully adsorb Cu^{2+} cations from wastewater (Hamid *et al.* 2014). Oxidation of biochar with H_2O_2 increased the content of oxygen-containing functional groups (carboxyl) on the surface of biochar, what encouraged the adsorption (Xue *et al.* 2012). After modification, however, the Langmuir maximum Pb sorption capacity of the biochar from peanut hull increased almost 25 times to about 22.82 mg/g, which is comparable to non-modified biochar (0.88 mg/g), other biochar sorbents (2–150 mg/g) and commercial activated carbons (15–80 mg/g). This indicates that H_2O_2 can be used as an oxidation reagent to modify biochar for effective removal of Pb from water.

Patel & Vashi (2013) showed that H_2SO_4 modification was effective in creating well-developed pores on the surface of neem leaf powder *(Azadirachta indica)* (NLP): surface area increased from 412 to 524 m^2/g, porosity from 24 to 37%.

A new concept of engineering the biochar with impregnation of mineral sorbents showed significant increase in contaminant sorption. Chen *et al.* (2009) found that iron-impregnated activated carbons (bituminous, lignite and wood-based) have been very effective in As^{5+} removal from wastewater due to ion exchange, hydroxyl groups and co-precipitation. The higher removal rate of As^{5+} versus As^{3+} may be due to the easy formation of ferric arsenate, which is undissociated at near neutral pH.

Steam activation is obtained when the initial pyrolysis reactions, occurring in oxygen free atmosphere at moderate temperatures (400−800°C), are complemented by a second stage in which the resulting biochar is subjected to a partial gasification with steam. The steam activation process is known to create new porosities and enlarge diameters of smaller pores developed during pyrolysis. Similarly, steam activation increases the pore volume of the biochar by removing the trapped products (volatile gases) (Rajapaksha *et al.* 2016). Steam activated biochar from chicken litter, alfalfa stems, switchgrass, corn cob showed good removal of Cu^{2+} due to ion exchange (Lima *et al.* 2010). O:C atomic ratio may correlate with its cation-exchange capacity, thus, oxygenation of biochar enhances cation exchange capacity. Physical modification methods are simple and cheaper, but less effective than chemical modification method.

Magnetic adsorbents can easily be recovered after application using low strength external magnetic fields. Magnetic oak wood and oak bark biochars were obtained by fast pyrolysis (400 and 450 °C) during bio-oil production in an auger-fed reactor and used for aqueous Cd^{2+} and Pb^{2+} remediation (Mohan *et al.* 2014a). Adsorption of Pb^{2+} and Cd^{2+} was largest at the highest pH values because carboxylic acids anhydrides, and phenols become carboxylate and phenoxide

anions. Electrostatic attraction bounded free Pb^{2+} and Cd^{2+} and other hydrated Pb and Cd cations.

Magnetic modifications provide better sorption of anionic contaminants due to precipitation with Fe. Zhang *et al.* (2013) pyrolyzed cotton wood treated with $FeCl_3$ at 600°C in N_2-environment. Modified biochar possessed excellent ferromagnetic property (saturation magnetization was 69.2 emu/g, that is close to pure γ-Fe_2O_3-materials of 76 emu/g) and high surface area. Adsorption of As^{5+} from water solution was described by Elovich, pseudo-first- and pseudo-second order kinetic models, and Lagmuir, Freundlich (max 3.147 mg/kg) isotherms. Magnetic orange peel biochars had higher phosphate sorption efficiency than their nonmagnetic analogs, indicating bound iron oxide aggregates assisted in phosphate removal (Chen *et al.* 2011b).

As the adsorption capacity of biochar is influenced by natural composition of feedstock, some natural ways for biochar modification exist, such as syngenetic compounds in feedstock (e.g. metal-contaminated wood or wood treated with fire retardants or antiseptics), that could be used for biochar production (Jones & Quilliam 2014).

1.4. Intrinsic Properties and Syngenetic Elements Affecting the Adsorption

According to the European Biochar Certificate (2012), ligneous feedstock is the most valuable raw material in terms of its availability and waste management reasons. The wood-derived biochar has well-developed microporous structure, that is important characteristic in adsorption of metals. Sawdust of poplar, willow, fir, oak and black locust wood can adsorb the following PTEs in the indicated order Cu>Ni>Zn at particle size of 1 mm (Sciban and Klasnja 2004). *Pinus sylvestris* L. woody biochar was used in biofilter for removal of volatile compounds (Baltrėnas *et al.* 2015). Mohan *et al.* (2007) noted that removal efficiencies of 100% for Pb^{2+} and 50% for Cd^{2+} by oak bark biochar, which are comparable to that of commercial activated carbon, and biochar produced from wood can effectively adsorb Cu^{2+} and Zn^{2+} in aqueous solutions (maximum adsorption capacity of 6.79 and 4.54 mg/g, respectively) (Chen *et al.* 2011a).

Biochar prepared from different types of wood has different properties. The comparative analysis of characteristics of biochar from coniferous and deciduous trees is presented in Table 1.7. Coniferous trees have higher lignin content. The biochar from coniferous tree had higher ash content and pH. Biochar from deciduous tree had higher specific surface area, micropore volume and cation exchange capacity.

Table 1.7. Comparison between biochar from softwood and hardwood (Baltrėnaitė *et al.* 2016)

Parameter	Coniferous tree	Deciduous tree
Lignin content in feedstock, %	25–33	20–25
Specific surface area, m^2/g (750 °C)	380	425
Morphological structure	Better development of meso- and macro-structure; at 750 °C formation of pyrogenous amorphous structure	Better development of microstructure; at 750 °C formation of crystal structure
Ash content, % (300–750 °C)	0.56–1.73	0.55–1.63
Bulk density, g/cm^3 (300–75 °C)	0.53–0.5	0.87–0.68
Yield, % (300..750°C)	28–9	22–15
pH value (300–750 °C)	4.55–9.42	4.58–8.93
Total carbon, % (300–750 °C)	76.4–99.8	65.1–99.8
Cation exchange capacity, cmolc/kg (450–750 °C)	3.41–2.4	5.09–5.71

Moreover, compartments of the trees differ in lignin, ash, moisture content and mineral composition as well. The bark has higher contents of ash (2.5–5%), Al and Si than wood (<2%). Small branches and foliage of trees, short−rotation woods, have the greatest contents of moisture in comparison with stems, barks and large branches of trees (Vassilev *et al.* 2010). Concentration of trace elements in plants varies as follows: leaves > small branches > large branches > stems (Kozlowski, 1997).

Adsorption properties of biochar (e.g. specific surface area, cation exchange capacity, carboxylic surface functional groups) could be further developed through physical, chemical and thermal modification techniques. In recent years, modification of biochar could be made through various “artificial” methods, e.g acid/base treatment, carboxylation, amination, treatment with organic solvents, surfactant modifications, coating of biochar, impregnation of mineral oxides, steam activation, magnetization (Rajapaksha *et al.* 2016),

oxidation of biochar with anaerobic digestion or composting (Inyang *et al.* 2010; Yao *et al.* 2011).

As the adsorption capacity of biochar is influenced by natural composition of feedstock, some natural ways for biochar modification exist and include intrinsic properties of feedstock (moisture, lignin content and morphology) and syngenetic elements in feedstock (elemental composition). Natural modifications are cheaper and more accessable in comparison to artificial modifications.

Experiments show that biochar that holds higher amount of water after drying suppress greenhouse gases production (Spokas and Reicosky 2009). Therefore, higher moisture content in woody feedstock may enhance adsorptive characteristics of the biochar.

It was noted that removal efficiencies of Pb and Cd by oak bark biochar are comparable to that of commercial activated carbon (Mohan *et al.* 2007). Lignin−adsorbent proved 90% of removing Cr^{3+} from real wastewater (Wu *et al.* 2008). As a part of a wood, lignin creates porosity in the biochar structure, promoting adsorption of PTEs by biochar. Therefore, higher lignin content in woody feedstock may enhance adsorptive characteristics of the biochar.

Syngenetic elements in ligneous feedstock are generated during plant growth. In decreasing order of abundance, the elements in wood are commonly C, O, H, N, Ca, K, Si, Mg, Al, S, Fe, P, Cl, Na, Mn, and Ti (Vassilev *et al.* 2010). C, O, H, N content in ligneous feedstock may influence the C, O, H, N content in biochar. While H/C indicates the aromatization of biochar, O/C indicates the degree of surface hydrophilicity and polarity. The decrease in the O/C and/or N/C ratios can indicate the increase in the hydrophobicity and the reduction of polar groups, therefore, decrease of adsorption of PTEs (Suguihiro *et al.* 2013).

As mineral composition of woody feedstock can influence the properties of biochar produced (Tan *et al.* 2015), Xu *et al.* (2013) found that PO_4^{3-} and CO_3^{2-} served as additional adsorption sites, contributing to the dairy manure biochar's high adsorption capacity for Cu, Zn and Cd. Fe particles in modified hickory chips (Hu *et al.* 2015) and Mg particles in modified tomatoes (Yao *et al.* 2013) acted as sorption sites in biochar for electrostatic attraction. Wang *et al.* (2015) found that $KMnO_4$-modified chicory wood BC showed about 3–5 times higher Pb, Cu, Zn, Ni adsorption capacity due to higher SSA, CEC and content of carboxylic groups. Baltrėnaitė *et al.* (2016) established that for effective application in biofiltration systems, selected biochar should contain inorganic nutrients in sufficient quantity (nitrogen 0.4%, phosphorus 0.15%, potassium 0.15%). Therefore, naturally acquired chemical elements in woody feedstock may enhance adsorptive characteristics of the biochar.

Adsorptive characteristics of the biochar, like moisture and ash content, chemical composition (C, O, N, H, Cd, Zn, Pb, Cr, Cu, Ni content), pH, electrical conductivity (EC), cation exchange capacity (CEC), BET specific surface area

(BET SSA) and surface functional groups were selected for investigation. These characteristics of BC are the most important for the adsorption of inorganic PTEs: BET SSA shows the amount of micropores in BC; CEC indicates the amount of carboxylic groups on the BC surface; surface functionality shows which functional groups could serve as adsorption sites. pH and EC influence mechanism of adsorption, H/C indicates the aromatization of biochar, O/C and N/C indicates the degree of surface hydrophilicity and polarity. Other chemical elements not only define if the biochar correspond to the basic/premium EBC requirements, but could serve as adsorption sites as well.

Natural modifications of the biochar imply intrinsic properties of ligneous feedstock, e.g. lignin, moisture and ash content, mineral composition (C, O, H, N, Cu, Zn, Ni, Cr, Cd, Ni), morphology and pore structure (Baltrėnaitė *et al.* 2016). Influence of these intrinsic properties on the properties of biochar to adsorb PTEs has not been investigated yet.

On the topic of intrinsic properties such papers as "A review of lignocellulosic biochar modification towards enhanced biochar selectivity and adsorption capacity of potentially toxic elements" (2018) and "Influence of intrinsic properties of lignocellulosic feedstock on adsorptive properties of biochar" (2018) were published.

1.5. Theoretical Models for Enhanced Biochar Adsorption, Adsorption Isotherms for Mono- and Multi-Component Adsorptives

A liquid-solid adsorption process involves liquid mass transfer, film diffusion (transport of the adsorbate from the bulk phase to the exterior surface of the adsorbent), intraparticle diffusion (transport of adsorbate into the adsorbent by either pore diffusion and/or surface diffusion) and reaction (adsorption on the surface of the adsorbent). Intraparticle diffusion studies at different temperatures show that mechanism of adsorption is mainly dependent on diffusion. Method and level of activation of adsorbent, particle size of adsorbent, concentration and physico-chemical properties of adsorbate are key factors affecting intraparticle diffusion (Wu *et al.* 2008).

Diffusion of ions control intraparticle diffusion within the biochar, e.g. the enhancement in adsorption capacity of PTE ions may be due to the increased rate of intraparticle diffusion rate of PTE ions into the pores (Karthikeyan *et al.* 2005).

The driving force of film diffusion is the concentration gradient located at the interface region between the exterior surface of biochar and the bulk solution

(Xu *et al.* 2013). The flux film diffusion can be expressed in linear form (Fournel *et al*. 2010):

$$\frac{\partial q}{\partial t} = J_f = k_f a(C - C_S), \tag{1.3}$$

where $\frac{dq}{dt}$ – concentration gradient, m^2/s; J_f – the mass transfer flux, $kg/s \cdot m^2$; a – the volumetric surface area, m^2/g; C – PTE concentration in the solution, mg/g; C_s – the adsorbate concentration surface of adsorbent, mg/g; k_f – the film diffusion coefficient. Increasing the flow rate will decrease the film thickness and resistance, whereas larger film resistance can be caused by packing with smaller biochar particles due to the extension of the exterior surface area (Xu *et al.* 2013).

Surface diffusion and pore diffusion proceed in parallel accompanying with Knudsen diffusion and the adsorption reactions (Xu *et al.* 2013). When the pore size is only slightly larger than the diameter of adsorbate ions or molecules, the Knudsen diffusion begins to play a significant role in adsorption of PTEs as shown in Fig. 1.9(b).

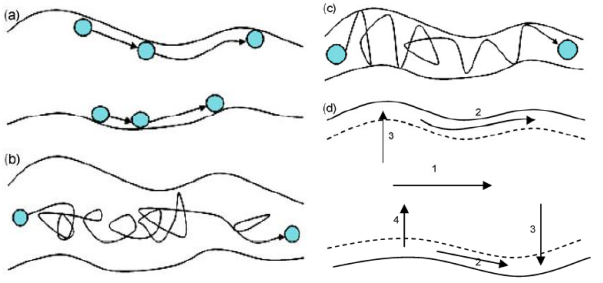

Fig. 1.9. Macroscopic schematic illustration of basic diffusion and adsorption steps inside the pore (Xu *et al.* 2013): a) surface diffusion; b) pore diffusion; c) pore diffusion with significant Knudsen diffusion; d) combination of intraparticle diffusion and adsorption: 1 – pore diffusion, 2 – surface diffusion, 3 – adsorption, 4 – desorption

Isotherms describe the equilibrium relationship between the mass of sorbed PTE per mass of a biochar and the equilibrium concentration of PTE in the fluid. Isotherms are semiempirical relationships. From adsorption theory, there are basically two nonlinear isotherms: the Freundlich model and the Langmuir model (Nazaroff & Alvarez-Cohen 2001).

Langmuir isotherm is valid over a wide range of concentration, though is based on monolayer adsorption.

$$q_e = q_{max} \frac{bC_e}{1 + bC_e}, \tag{1.4}$$

where C_e – the equilibrium concentration of PTE molecules in a fluid, mol or mg/l; q_e – the equilibrium mass of sorbed molecules per mass of sorbent, mol or mg/g; q_{max} – maximum adsorbed amount (total monolayer coverage theoretically), b – Langmuir equilibrium constant.

Freundlich isotherm is based on heterogeneous adsorption, but is not applicable over wide range of concentration.

$$q_e = K_f C_e^{1/n}, \tag{1.5}$$

where C_e – the equilibrium concentration of PTE molecules in a fluid, mol or mg/l; q_e – the equilibrium mass of sorbed molecules per mass of sorbent, mol or mg/g; K_f – adsorption coefficient, n – index of nonlinearity of isotherm.

The maximum adsorption capacity of Cu^{2+} on Silver birch biochar (128.7 mg/g) and Zn^{2+} on Scots pine biochar (107.0 mg/g) and were assessed by extended Freundlich isotherm (Komkienė & Baltrėnaitė 2015).

Flory-Huggins isotherm, which occasionally deriving the degree of surface coverage characteristics of adsorbate onto adsorbent, can express the feasibility and spontaneous nature of an adsorption process.

$$\frac{\theta}{C_o} = K_{FH}(1-\theta)^{n_{FH}}, \tag{1.6}$$

where θ is the degree of surface coverage, K_{FH} is equilibrium constant, n_{FH} is model exponent, C_o – the equilibrium concentration of PTE molecules in a fluid, mg/l.

Redlich-Peterson isotherm is a hybrid isotherm featuring both Langmuir and Freundlich isotherms, which incorporate three parameters into an empirical equation. The model has a linear dependence on concentration in the numerator and an exponential function in the denominator to represent adsorption equilibria over a wide concentration range.

$$q_e = \frac{K_{RP} q_{max} C_e}{1+\alpha_{RP} C_e^n}, \tag{1.7}$$

where C_e – the equilibrium concentration of PTE molecules in a fluid, mol or mg/l; q_e – the equilibrium mass of sorbed molecules per mass of sorbent, mol or mg/g; q_{max} – maximum adsorbed amount, mg/g; K_{RP} is Redlich-Peterson adsorption constant, l/mg; α_{RP} – affinity coefficient, l/mg.

Sips isotherm is a combined form of Langmuir and Freundlich expressions deduced for predicting the heterogeneous adsorption systems and circumventing the limitation of the rising adsorbate concentration associated with Freundlich isotherm model. Depending on adsorbate concentrations, it reduces to Freundlich or Langmuir isotherms.

$$q_e = \frac{K_{LF} C_e^n q_{max}}{1 + K_{LF} C_e^n}, \quad (1.8)$$

where C_e – the equilibrium concentration of PTE molecules in a fluid, mol or mg/l; q_e – the equilibrium mass of sorbed molecules per mass of sorbent, mol or mg/g; q_{max} – maximum adsorbed amount, mg/g; K_{LF} is Sips adsorption constant, l/mg.

Toth isotherm describes heterogeneous adsorption systems within broad concentration range.

$$q_e = \frac{K_T C_e}{(a_T + C_e)^{1/t}}, \quad (1.9)$$

where C_e – the equilibrium concentration of PTE molecules in a fluid, mol or mg/l, q_e – the equilibrium mass of sorbed molecules per mass of sorbent, mol or mg/g, K_T and t are the equation constants. Parameter t characterizes the system heterogeneity.

Similar to the Sips isotherm model, Koble‑Corrigan isotherm incorporated both Langmuir and Freundlich isotherm models for representing the equilibrium adsorption data. The isotherm constants, A, B and n are evaluated from the linear plot using a trial and error optimization.

$$q_e = \frac{A C_e^n}{1 + B C_e^n}, \quad (1.10)$$

where C_e – the equilibrium concentration of PTE molecules in a fluid, mol or mg/l, q_e – the equilibrium mass of sorbed molecules per mass of sorbent, mol or mg/g, A and B are the equation constants.

There are also other isotherms used in adsorption studies, but not mentioned in this Chapter, like Hill, Khan, Radke–Prausnitz etc.

The kinetics of adsorption is described by models. Sorption kinetics shows a strong dependence on the physical and/or chemical characteristics of the biochar which also influences the sorption mechanism. Sorption percentage increases with the increasing initial concentration of metal ions. The particle size and amount of adsorbent, pH and concentration of solutions, residence time and temperature affect the adsorption process. The kinetic data indicated that the mechanism of metal ions sorption by the biochar samples is complex and probably a combination of external mass transfer, intraparticle diffusion through the macro- and micropores of BC and sorption processes.

Kinetic investigations are usually performed in batch reactors, where a known amount of both sorbent and adsorbate are charged, by fixing temperature, stirring rate and all the physical–chemical variables that constitute the system (Russo *et al.* 2015). It allows to measure the evolution with time of the adsorbate concentration in the bulk phase along the experiment time. Kinetic models can be divided into three categories:

(i) adsorption reaction models (ARM), where the adsorption phenomenon is expressed such as a reaction rate expression, e.g. pseudo-first, pseudo-second order models, first-order reversible model;

(ii) adsorption diffusion models (ADM), where the diffusion paths of the sorbate are taken into account, e.g. Weber and Morris intraparticle diffusion model, linear film diffusion model, Elovich equation;

(iii) double exponential model (DEM), a "two-box model", in which the sorbent is subdivided into two types of reaction sites, the first rapidly equilibrated and the second reacting more slowly – there both external and internal diffusion terms are taken into account, e.g. Wilczak and Keinath, dynamic intraparticle model.

Pseudo-first order model is calculated by:

$$\frac{dq}{dt} = k_1(q_e - q)\ , \tag{1.11}$$

where q_e – amount of adsorbate ions on the adsorbent at the equilibrium, mg/g, q – adsorption capacity, mg/g, k_1 – the rate constant of adsorption, l/min. Zhang *et al.* (2013) concluded that the correlation coefficient (R^2 = 0.972) follows the order of first−order> second−order>Elovich, indicating that the first−order model was the most suitable in describing the adsorption kinetics of As^{5+} on biochar/γ-Fe_2O_3.

Pseudo-second order model is calculated by:

$$\frac{dq}{dt} = k_2(q_e - q)^2\ , \tag{1.12}$$

where k_2 − the rate constant of pseudo-second order adsorption, g/ mg·min. Thus, Kilic *et al.* (2013) found that the correlation coefficient for the pseudo-second order kinetic model was higher than the other models (R^2 = 0.999) for both Ni^{2+} and Co^{2+} ions indicating that the adsorption on almond biochar perfectly complies with pseudo-second order reaction and the adsorption process appeared to be controlled by the chemisorption process.

First-order reversible model is calculated by:

$$\ln\left(1 - \frac{C_{AO} - C_A}{C_{AO} - C_E}\right) = -(k_a - k_d)t\ , \tag{1.13}$$

where C_{AO} is initial bulk concentration of adsorptive, mg/l, C_A is concentration of adsorptive in bulk solution at time t, mg/l, C_E is equilibrium concentration of adsorptive, mg/l, k_a is adsorption rate constant, k_d is desorption rate constant, t is the time, min.

Intraparticle diffusion is described by Weber-Morris intraparticle pore diffusion model:

$$q = k_{id}\sqrt{t} + B\ , \tag{1.14}$$

where q – adsorption capacity, mg/g, k_{id} − intraparticle diffusion rate constant, mg·min$^{1/2}$/g, B is initial adsorption, mg/g, t is the time, min.

The Elovich equation was firstly used in the kinetics of chemisorption of gases on solids, it has been successfully applied for the adsorption of PTEs from a liquid solution. The Elovich equation is calculated by:

$$\frac{dq}{dt} = a\ exp(-\beta q)\ , \tag{1.15}$$

where α − the initial adsorption rate, mg/g·min, β − the desorption constant, g/mg, during any one experiment, q – adsorption capacity, mg/g.

Linear film diffusion model is described by:

$$\frac{dC}{dt} = -k_f(C - C_S)\ , \tag{1.16}$$

where C_S is adsorbate concentration at the liquid-solid interface, mg/l, k_f is film diffusion coefficient, l/min, t is the time, min.

There are also other models used in adsorption studies, but not mentioned in this Chapter, like Avrami equation, Crank model, Vermeulen model, Bangham model, multi-exponential, parabolic diffusion, hyperbolic model, two-site nonequilibrium model, branched pore diffusion model, nonlinear film transfer model, second-order reversible reaction model, and mixed-order rate equation etc.

Pseudo-first and pseudo-second order, intraparticle diffusion and Elovich models are usually applied to the adsorption kinetic data by fitting the related adjustable parameters. Even if the fitting can be considered more than satisfactory, it is hard to find a physical meaning of the fitted parameters in all the mentioned cases. New modeling approach wass proposed by Russo *et al.* (2015) for adsorption kinetics investigation performed in batch reactors with a fluid–solid system. Dynamic intraparticle model could be the starting point for designing continuous adsorption columns for water purification. It is based both on film and intraparticle mass transfer. In particular, the mass balances have been developed by taking into account for both the external and internal mass transfer diffusion limitations, solving the dynamic partial differential equations (PDEs) system along the radius of the sorbent particles, considering both the fluid and solid phases that constitute the sorbent particle. Physical parameters have to be evaluated either from existing correlations or by direct measurements, what makes the model predictable (Russo *et al.* 2015).

To describe possible diffusion and equilibria phenomena, four different steps have been taken into account in this model: (i) diffusion from the bulk to the particle surface; (ii) diffusion from the pore mouth into pore (pore liquid diffusion); (iii) equilibrium between the liquid and the solid phase; and (iv)

diffusion of the adsorbate molecule on the sorbent surface. Adsorption mechanism is reported in Fig. 1.10.

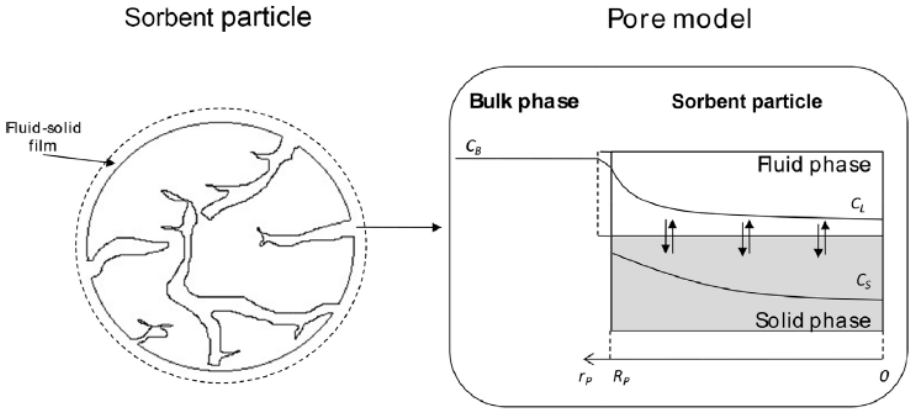

Fig. 1.10. Adsorption model for a fluid-solid system (souce: Russo *et al.* 2015) : C_B − PTE bulk concentration, mol/m^3, C_L – PTE concentration in the liquid of the pores, mol/m^3, C_S – PTE concentration in the solid, mol/m^3, Rp − particle radius, m, r_p − particle radial direction, m

The proposed model takes into account the existence of three different domains: i) the liquid bulk phase that contains the PTE dissolved in the solvent (here pollutant concentration changes with time); ii) a liquid side (liquid intraparticle phase), where the PTE diffuses from the outer particle surface to the center of the particle (here concentration depends on time and radius of the particle); and (iii) a solid side (solid intraparticle phase), where the PTE concentration reaches the equilibrium inside the particle through the Langmuir mechanism (here concentration depends on time and radius of the particle). The PTE can diffuse also on the sorbent surface, with a diffusivity parameter that strongly depends on the interactions between the solute and the sorbent. Conceptually, the pollutant is transferred from the bulk phase to the particle through the liquid film and then it diffuses along the particle radius in the pore, in which the mass transfer is divided into the two parallel contributions of liquid porous diffusion and surface diffusion (Russo *et al.* 2015).

A summary of the assumed hypothesis includes: (1) monomodal particles size, (2) average porosity and tortuosity of the particle, (3) adsorption equilibrium in the pore, (4) particle mass balance adaptable on the basis of the shape factor, (5) isothermal system.

The bulk liquid phase mass balance equation:

$$\varepsilon' \cdot \frac{\partial C_B(t)}{\partial t} = -k_m \cdot a_{sp} \cdot (C_B(t) - C_L(t,r_p)) \Big| R_P) \,, \tag{1.17}$$

where ε' − volumetric ratio between the bulk volume and the overall particle volume, m^3_{BULK}/m^3_P, C_B − PTE bulk concentration, mol/m^3_{BULK}, t − time, s, k_m − mass transfer coefficient, m/s, C_L − PTE concentration in the liquid of the pores, $mol/m^3_{liq,P}$, r_P − particle radial direction, m,

$$a_{sp} = \frac{3}{R_P} \,, \tag{1.18}$$

where a_{sp} − geometrical specific surface area (m^2/m^3), R_P − particle radius (m).

The solid phase mass balance equation:

$$\varepsilon \cdot \frac{\partial C_L(t,r_P)}{\partial t} + (1-\varepsilon) \cdot \frac{\partial C_S(t,r_P)}{\partial t} = \varepsilon \cdot \frac{D_P}{r_P^{shape}} \cdot \frac{\partial}{\partial r_P} \times \left(r_P^{shape} \cdot \frac{\partial C_L(t,r_P)}{\partial r_P} \right) + (1-\varepsilon) \cdot \frac{1}{r_P^{shape}} \cdot \frac{\partial}{\partial r_P} \times \left(\frac{D_S}{1 - C_S(t,r_P)/C_{S,*}} \cdot \frac{\partial C_S(t,r_P)}{\partial r_P} \right), \tag{1.19}$$

where ε − particle porosity, $m^3_{liq,P}/m^3_P$, D_P − pore diffusivity based on the cross sectional area, m^2/s, range 10^{-9}–10^{-11} m^2/s, D_S − superficial diffusivity, m^2/s, range 10^{-13}–10^{-18} m^2/s, C_S – PTE concentration in the solid, $mol/m^3_{sol,P}$, $C_{S,*}$ − saturation solute solid concentration, $mol/m^3_{sol,P}$

$$D_P = D_{AB}^0 \cdot \frac{\varepsilon}{\tau} \,, \tag{1.20}$$

where D^0_{AB} − ion diffusivity, m^2/s, τ − tortuosity factor.

In order to properly describe the system, several physicochemical properties are requested, that are the pore diffusivity (D_P), the film mass transfer parameter (k_m) and the surface diffusivity (D_S). They can be found from correlation in literature, except D_S has to be fitted on experimental data (Russo *et al.* 2015).

The geometry of the problem can be set by simply choosing the right value of the shape factor (shape = 0 for slabs, 1 for cylinders and 2 for spheres).

$$C_S(t,r_P) = C_{S,*} \cdot b \cdot \frac{C_L(t,r_P)}{1 + b \cdot C_L(t,r_P)} \,, \tag{1.21}$$

where b – Langmuir adsorption constant , $m^3_{liq,P}/mol$.

The boundary conditions:

$$\frac{\partial C_L(t,r_P)}{\partial r_P} \Big|_{r_P = 0} \,, \tag{1.22}$$

$$\frac{\partial C_S(t,r_P)}{\partial r_P} \Big|_{r_P = 0} \,, \tag{1.23}$$

$$\varepsilon \cdot D_P \cdot \frac{\partial C_L(t,r_P)}{\partial r_P}\Big|_{r_P = R_P} + (1-\varepsilon) \cdot \frac{D_S}{1 - C_S(t,r_P)\Big|_{r_P = R_P}/C_{S,*}} \cdot \frac{\partial C_S(t,r_P)}{\partial r_P}\Big|_{r_P = R_P} = = k_m \cdot (C_B(t) - C_L(t,r_P)\Big|_{R_P}, \quad (1.24)$$

Equations (1.22) and (1.23) represent the symmetry condition at the center of the particle for both liquid and solid concentrations inside the particle, while Equation (1.24) considers that the external surface of the particle fluxes must be equal to the diffusion flux through the fluid–solid film surrounding the particle (continuity condition).

Due to the IDM, it is possible to estimate physical properties that are difficult to find in the literature, that are the superficial diffusivity and the tortuosity factor.

Russo *et al.* (2015) found, that by increasing the contact time, the liquid of the pores is filled with the adsorbate till a saturation condition is reached. By increasing the initial bulk concentration, the system reaches the saturation in longer time. Particle with bigger radius lead to lower saturation times. The same trends in effect of initial bulk concentration and particle radius were confirmed by simulation of Cu^{2+} in water over activated carbons and Cd^{2+} in water over chitosan (Russo *et al.* 2016). For all simulations the average interval between ±15% of the measured values was obtained, that demonstrated a good fitting of the model.

Russo *et al.* (2016a) investigated adsorption of ions in inorganic media on organic adsorbent, i.e. Cu^{2+} in aqueous solutions over active carbons. The used active carbon has an average particle radius of $1.97 \cdot 10^{-4}$ m (Yao and Wang 2010). The obtained results showed high flexibility of the dynamic intraparticle model that demonstrated to be able to interpret kinetic batch adsorption data. Later investigations demonstrated that the ADIM model can be successfully extended to the prediction of multiscale systems, passing from a batch to a continuous one (Russo *et al.* 2016b).

1.6. Concept of Biochar-Hydrogel Composite Development

It is necessary to control the concentration of potentially toxic elements (PTEs) in wastewater, because being spilled into environment, it is hazardous to human health and can inhibit plant growth. As conventional wastewater treatment

technologies have significant disadvantages (e.g. reverse osmosis is expensive and cannot remove pesticides, solvents, dissolved gases like radon and trihalomethanes, expensiveness, while coagulation/flocculation produces of toxic sludge), there is a need of alternative methods of wastewater treatment. Adsorption of PTEs from wastewater with biochar could be the possible option, as it is effective and economic method (Tan *et al.* 2015; Inyang *et al.* 2016), that offers flexibility in design and operation. Biochar (BC) adsorptive characteristics could be improved via chemical modifications (Rajapaksha *et al.* 2016).

SMART BC concept is the novel aspect in biochar research. According to Drossel *et al.* (2015), smart materials are designed materials, properties of which could be significantly changed in controlled fashion and reversed by applying external stresses (i.e. stimulies), such as temperature, electric or magnetic fields, pH, mechanical stress. The responses are changes in shape, surface, chemical and electrical properties (Schmaljohann 2006) (Fig. 1.11). Recent researches confirm the smart application of BC in supercapacitors or sensors due to high surface areas, porous structure, low cost and low environmental impact (Jiang *et al.* 2013; Suguihiro *et al.* 2013).

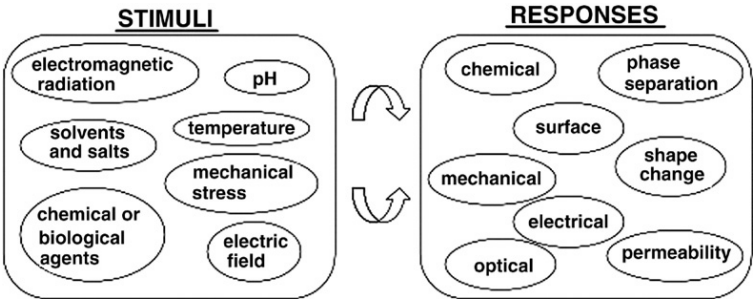

Fig. 1.11. Potential stimuli and responses of synthetic polymers (source: Schmaljohann 2006)

As BC is the precursor of activated carbon (AC), application of AC in healthcare research could be the basis for SMART BC concept in adsorption (Ok *et al.* 2015). Though activated carbon is used in medicine for adsorbability of toxins, pure AC used in health care is not a smart material, because its behavior is not reversible. Reversible behavior could be achieved by combining AC with smart materials and forming composites. A composite is a multicomponent system that enables the straightforward addition of smart elements (Swait *et al.* 2012). Thus, de Guzburg *et al.* (2015) found that activated carbon-based product DAV132 could selectively adsorb drug compounds in the proximal colon due to

pH sensitivity without interfering with drug absorption in the proximal small intestine.

According to Qian *et al*. (2013), key characteristics of BC for its smart application as a sorbent of PTEs are high specific surface area and oxygenated groups on the surface. In order to apply SMART BC in adsorption of PTEs, BC could be combined with hydrogels (a network of polymer chains that are hydrophilic, sometimes found as a colloidal gel in which water is the dispersion medium), that possess flexible swelling and mechanical properties, as well as easy handling and reusability. The swelling property of hydrogel is an important factor in its use for adsorption, e.g. Entheromorpha-based hydrogel could imbibe water up to 60 000% based on its original dry weight (600 g/g), what made it an exceptional material for removal of toxic species and catalysis in aqueous environment (Su *et al.* 2018). Swelling of the hydrogel is the result of ionization/ deionization of the carboxylic acid groups (Yoshida *et al.* 2013), and in combination of hydrogel with biochar, swelling could be used to enhance adsorption selectivity of the biochar-hydrogel composite, as when the hydrogel swells, his pores become larger, so PTEs of larger diameter could be adsorbed due to physical adsorption.

Porous hydrogels have been used extensively in the smart drug delivery systems, e.g. pH−, ion− and temperature−sensitive hydrogels can be used for specific body sites as they swell according to the environmental conditions. Depending on pH sensitivity, hydrogels are divided into cationic (swell at pH lower than 7) and anionic (swell at pH bigger than 7) (Fig. 1.12).

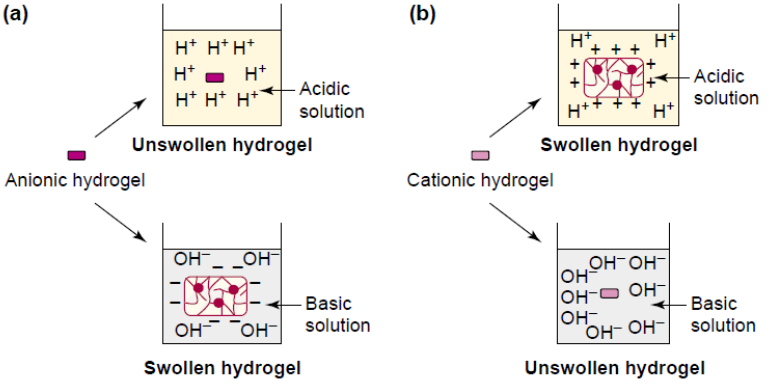

Fig. 1.12. The pH-responsive swelling of hydrogel:
a) anionic; b) cationic (source: Gupta *et al*. 2002)

Depending on the surface charge, cationic hydrogels can mask the taste of drugs and release drugs in the stomach by responding to gastric low pH. Anionic hydrogels respond to intestinal high pH, preventing gastric degradation of drug or assuring colon drug delivery (Yoshida *et al.* 2013). All the pH-sensitive hydrogels contain pendant acidic or basic groups that either accept or release protons in response to changes in environmental pH (Balamuralidhara *et al.* 2011).

As the temperature increases, most hydrogels increase their water-solubility. Temperature-responsive hydrogels swell at high temperature and shrink at low temperature. Swelling depends on the thickness of the hydrogel layers and the surface tension. Hydrogels that are responsive to both temperature and pH can be made by simply incorporating ionizable and hydrophobic functional groups to the same hydrogels (Qiu and Park 2001). Porosity of the hydrogels plays a great role in responsive behavior. Thus, pH-sensitive porous hydrogels (pore diameter 39.20 ± 2.66 μm) exhibited superior pH-dependent swelling properties during controlled release of amoxicillin compared with non-porous hydrogels (Gupta *et al.* 2002). The degree of releasing coomassie brilliant blue drug was the highest at pH 10 for the pH-sensitive coconut-based AC-hydrogel composite due to the extensively developed pore structure of hydrogel and the hydrophilic surface nature of AC with BET surface area 1230 m^2/g and the fraction of 67% micropore structure (Yun *et al.* 2009).

Smart biochar composites could be characterized as 'stimuli-responsive' or 'environment-sensitive'. They possess properties capable to withstand controlled and reversible changes in response to the external stimulation (e.g. temperature, pH, concentration of PTEs). As hydrogel is porous and has oxygen-containing functional groups on its surface, combined with biochar, its composite becomes a better adsorbent than just separate biochar or hydrogel, as the composite has higher BET specific surface area and carboxylic groups content. Hydrogel-biochar composite showed a peak at wavelength 1428 cm^{-1}, that corresponds to O–H bending, i.e. higher content of carboxylic acid on the surface than raw biochar (Meri *et al.* 2018). Algae-based hydrogel showed higher Cu^{2+} removal capacity (197.2 mg/g) (Su *et al.* 2018), than hardwood biochar with 6.79 mg/g (Chen *et al.* 2011), pinewood biochar with 4.46 mg/g (Liu *et al.* 2010). The degree of releasing coomassie brilliant blue drug was the highest at pH 10 for the pH-sensitive coconut-based AC-hydrogel composite due to the extensively developed pore structure of hydrogel and the hydrophilic surface nature of AC with BET surface area 1230 m^2/g and the fraction of 67% micropore structure (Yun *et al.* 2009). Enteromorpha-based hydrogel (EP-g-PKA) showed a higher water swelling capacity at a condition of small grain size (40–60 mesh), low salt concentration (0%), weak acidity condition (pH = 5–6) and low temperature (20°C) (Zhao *et al.* 2016). Su *et al.* (2018) found that this hydrogel showed good swelling behavior and excellent adsorption capacity for Cu^{2+} (197.2 mg/g), thus

could be used for PTEs removal from wastewater. Yun *et al.* (2009) prepared pH-sensitive AC-hydrogel composite that swelled well in the basic condition to release the drug loaded in AC. Karakoyun *et al.* (2011) found 1045% swelling of woody biochar-hydrogel composite and maximum amount of phenol adsorption at pH 10 (28.06 mg/g).

1.7. Conclusions of Chapter 1 and Formulation of the Tasks of the Thesis

The following conclusions can be stated coonsidering the overview of biochar towards adsorption aspect:

1. Main mechanisms of BC interactions with Cr^{3+}, Cd^{2+}, Pb^{2+}, Zn^{2+}, Ni^{2+}, Cu^{2+} are ion exchange and electrostatic attraction.

2. Physical (specific surface area, pore structure) and chemical (oxygen-containing functional groups, cation exchange capacity) properties of BC have significant effect on adsorption of Cr^{3+}, Cd^{2+}, Pb^{2+}, Zn^{2+}, Ni^{2+}, Cu^{2+}.

3. Being more accessible than chemical modifications, natural modifications of BC may increase adsorption of PTEs. They include intrinsic properties (C, O, N, H, moisture, lignin content, morphology and pore structure) and syngenetic elements (trace elements) in ligneous feedstock.

4. Modification with Fe^{3+} and Mg^{2+} was chosen to create additional adsorption sites, while modification with H_2O_2 – to increase content of oxygen-containing functional groups on the BC surface.

5. Langmuir, Freundlich, Redlich-Peterson, Sips isotherms and pseudo-first-order, pseudo-second order models, linear film diffusion and Weber-Morris intraparticle pore diffusion models were chosen for equilibrium and kinetic studies of adsorption of PTEs by biochar. Dynamic intraparticle model, that combines equilibrium and kinetic parts, has not been tested for biochar yet.

6. The concept of biochar-hydrogel composites for adsorption of PTEs needs to be developed for enhanced adsorption of PTEs by BC.

Considering the above, the following tasks can be stated:

1. To compare the efficiency of adsorption of PTEs by chemically modified ligneous biochar and biochar with certain intrinsic properties and to distinquish the most effective modification method.

2. To evaluate influence of intrinsic properties of ligneous feedstock (C, O, N, H, water, lignin content, morphology and pore structure) and syngenetic elements (trace elements) on the adsorptive properties of biochar.

3. Identify adsorption mechanisms of PTEs on biochar.

4. Novel biochar adsorbents of PTEs should be developed through preparation of biochar-hydrogel composite.

5. Investigate adsorption parameters (e. g. type of biochar, dosage, time) from fitting to dynamic intraparticle model and conduct sensitivity analysis of simplified adsorption model.

2

Methodology of Investigating the Influence of Modifications on Physical and Chemical Characteristics of Biochar for Increased Adsorption Capacity

The research methods include theoretical and experimental studies: selection of feedstock with variable intrinsic properties for biochar production (lignin, moisture, macro- and trace elements content in feedstock), analysis methods for physical (SEM, BET analyzer) and chemical characteristics (ammonium acetate, pH meter, CHNO elemental analizer, FTIR) of biochar using EBC standards, methodology of equilibrium and kinetic modeling of adsorption of PTEs (Langmuir, Freundlich, Redlich-Peterson, Sips adsorption isotherms, pseudo-first order, pseudo-second order, linear film diffusion, intrapartice pore diffusion, dynamic intraparticle models), AAS for analysis on PTEs, designed adsorption device for adsorption experiments, methodology of modification with H_2O_2, $FeCl_3$, $MgCl_2$, methodology of preparing biochar-hydrogel composite. The materials from this Chapter were published in Chemerys *et al.* (2020), Chemerys and Baltrėnaitė (2017a; 2017b; 2018b). Lithuanian patent was obtained.

2.1. Selection of Feedstock for Biochar Production and Sampling Procedure

For the experiments lignoeous feedstock was selected. According to the European Biochar Certificate, ligneous feedstock is the most valuable raw material in terms of its accessibility and waste management reasons. The wood-derived biochar has well-developed microporous structure, that is important characteristic in adsorption of metals. According to Confederation of European Paper Industry (CEPI), birch wood was the most consumpted wood among hardwoods (13.4%) in 2016.

To evaluate differences between woody feestock, 4 types of wood species were selected: pine *(Pinus sylvestris* L.*)*, aspen *(Populus tremula* L.*)*, fir *(Picea abies* L.*)*, birch *(Betula pendula* L.*)*. Due to local availability, cost-effectiveness and the prevalence of coniferous trees in Lithuania, pine and fir [pine and fir occupy 33.1% and 19.7% of forest area in Lithuania (Ministry of Environment of Lithuania 2015)] were chosen. Aspen [occupies 3% of forest area in Lithuania (Ministry of Environment of Lithuania 2015)] and birch [occupies 17.5% of forest area in Lithuania (Ministry of Environment of Lithuania 2015)] were chosen among deciduous trees. Woody feedstock was chosen due to higher lignin content, that will result in higher yield of biochar, i.e. pine and fir contain 25−33% of lignin, aspen and birch − 20−23% of lignin.

Aspen, fir and pine, grown in Lithuania, were taken as waste materials in October 2016 from JSC "Vedrana" (Vilnius, Lithuania, 54°63′46″N 25°30′35″E). They were in the form of decks 1–1.5 m long with the cross section area from 10×10 cm to 15×15 cm. The weight of each deck was from 7 to 12 kg. Samples were put into polypropylene bags. Birch was taken in February 2017 from private household in Ignalina region, Lithuania (55°20′52″N 26°14′27″E). Birch wood was cut into pieces of 0.5 m long with the cross section area diameter 20 cm. The weight of each piece was 10 kg. Samples were put into plastic bags to keep conditions.

To evaluate differences between tree compartments, different parts of the pine and birch were taken (e.g. wood, bark). They also contain different content of lignin: pine wood 25–33%, pine bark 50–70%, birch wood 20–25%, birch bark 40%.

To evaluate influence of syngenetic elements, pine and birch (both bark and wood) were taken from potentially contaminated site. Contaminated territory was situated near the highway in Vilnius, Lithuania (54°43'11.99" N 25°20'5.40"E). The source of contamination was automobile traffic. Expected chemical elements in pine and birch growing on the territory were Cd, Zn, Pb, Cr, Cu and Ni.

Respectively, all types of feedstock had different intrinsic properties (moisture, lignin and ash content) and syngenetic elements (C, O, N, H, Cd, Zn,

Pb, Cr, Cu, Ni content), that could influence adsorptive characteristics of the biochar.

Aspen, fir, pine and birch mentioned above were used for $MgCl_2$ and $FeCl_3$ modification. For H_2O_2 modification only birch was used. For the experiment with natural modifications, aspen, fir, pine and birch mentioned above were used, and pine and birch from contaminated territory were taken as well.

For equilibrium and kinetic studies, as well as preparation of smart biochar-hydrogel composite, birch stems with bark were taken from sawmill in Vilnius (Lithuania). Unlike pine wood with mono-size porosity, porosity of birch is various (Fig. 2.1): it consists of 40% large (d>10 μm) and 60% little pores (1 μm<d<10 μm) (Chemerys and Baltrėnaitė (2016)), that could attract PTEs of various size.

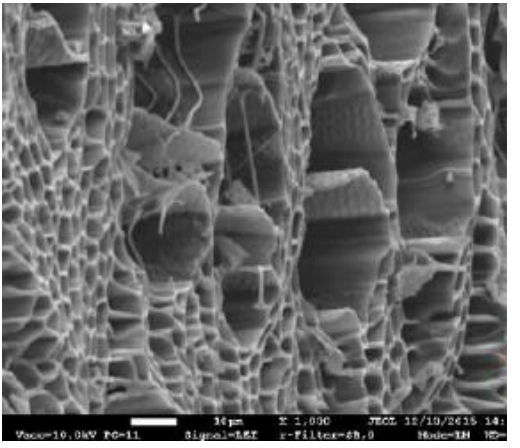

Fig. 2.1. The microstructure of biochar prepared from birch. Magnification is ×1000

Birch wood was selected as its unmodified biochar had the highest CEC (5.15 cmolc/kg) among other tree species. In addition, birch wood had lower pH (8.4) and ash content (3.3%) in comparison to birch bark (9.5 and 11.8%, respectively).

2.2. Biochar Production

Method described in the work by Mancinelli *et al.* (2016) was followed. Air dried feedstock was placed in open crucibles, weighed, and wrapped in aluminium foil in order to create an oxygen-limited environment. An E5CK-T muffle furnace was used with a heating rate of approximately 10 °C/min until the desired pyrolysis

temperature of 450 ± 10 °C was reached. The slow pyrolysis process was performed for 120 min under atmospheric pressure. At the end of the production process, the samples were left to cool in the muffle furnace overnight.

The obtained biochar was grounded after being cooled down to ambient temperature (20 ± 3°C), and a 1–10-mm-diameter fraction was separated by sieves (Retsch, Germany). Biochar yield (%) was calculated according to as follows:

$$Y_{bc} = \frac{W_2}{W_1} \times 100\% , \quad (2.1)$$

where W_1 − the dry mass of the feedstock, g; W_2 − the dry mass of biochar, g.

2.3. Applied Biochar Modification Techniques

To reach the objectives of the thesis, the following modifications techniques were chosen: natural modifications, artificial modification with metal salts ($MgCl_2$, $FeCl_3$) and H_2O_2.

Aim of natural modification was to determine effect of syngenetic elements in wood (C, O, N, H, Cd, Zn, Pb, Cr, Cu, Ni) and intrinsic properties in wood (lignin, moisture and ash content) on the adsorptive properties of biochar.

In order to increase biochar adsorption capacity for cationic PTEs, chemical modifications with H_2O_2, $MgCl_2$, $FeCl_3$ were selected. H_2O_2 is a strong oxidant, which is relatively inexpensive and can decompose to the clean products of H_2O and O_2 (Huff and Lee 2015). Treatment with H_2O_2 leads to an increase in the number of carboxylic groups and the cation exchange capacity of the biochar (Cibati *et al*. 2017), while artificially added Mg and Fe particles may act like additional adsorption sites on the surface of biochar (Yao *et al.* 2013).

Biochar was prepared from pine, aspen, fir and birch. The biochar was crushed by pressing and 0.4-mm-diameter fraction was separated by 400-μm sieve (Retsch, Germany). For modification process, two types of solutions were prepared: 0.37 M $FeCl_3$ and 1 M $MgCl_2$. The biochar was added to modifying solutions with ratio 25% w/w and rotated at 12 rpm for 2 h (RS12 Rotoshake, Gerhardt). After modification the biochar was filtered through cellulose acetate membrane filter (ALBET LabScience, Germany) with particle retention 0.45 μm.

For H_2O_2 modification, the birch biochar was crushed by pressing and 2 fractions (according to commercial size of the activated carbon adsorbent) were separated by sieving: <1.0-mm-diameter (powder form of adsorbent) and 1–3- mm-diameter (granular form of adsorbent). For modification process, three types of solutions were prepared: 3, 15, 30% of H_2O_2. The biochar was added to modifying solutions with ratio 25% w/w. In one case, there was no rotation, in another cases biochar with solution was rotated at 3 rpm for 2 h in self-made

device according to the patent #6434 by Pranas Baltrėnas, Edita Baltrėnaitė and Valeriia Chemerys (2017) (Fig. 2.2).

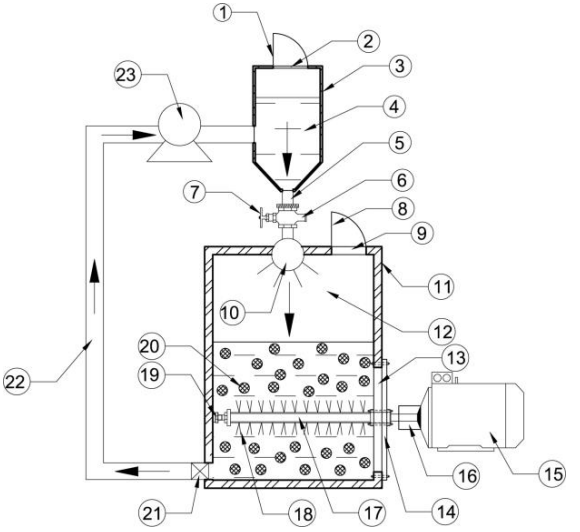

Fig. 2.2. Device for modification the biochar with H_2O_2: 1 – lid, 2 – opening, 3 – body of the tank for H_2O_2, 4 – tank for H_2O_2, 5 – channel, 6 – channel for outflow of H_2O_2, 7 – tap, 8 – lid, 9 – opening, 10 – spray, 11 – body of the modifying tank, 12 – modifying tank, 13 – cavity, 14 – lid, 15 – motor reducer, 16 – clutch, 17 – rotary driven flexible roller, 18 – brush, 19 – slug, 20 – biochar, 21 – filter, 22 – tube, 23 – vacuum pump

This device for modification of biochar with H_2O_2 solution is economically efficient and environmetally friendly. It contains an additional stirring mechanism for increase the contact surface of the biochar with the solution. The purpose of the invention was to activate the biochar surface, and thus improve the adsorption properties of the biochar for the adsorption of cationic metals. Then the biochar was filtered through cellulose acetate membrane filter with particle retention 1.06 μm.

2.4. Analysis of Physical and Chemical Characteristics of Feedstock and Biochar

In experimental part the following characteristics of feedstock were determined:

- Lignin content was determined according to TAPPI T 222 Standard Test Method “Acid-insoluble lignin in wood and pulp” at the Latvian State

Institute of Wood Chemistry. Some of the lignin dissolves in acid solution during the test. In softwoods the amount of soluble lignin is small, about 0.2–0.5%. In hardwoods the content of soluble lignin is about 3–5%. Lignin was calculated by a weight difference as Klason lignin.

- C, O, N, H content was determined using elemental analyzer. Wood was grounded into fine particles. Each sample was packed into aluminium foil container and weighted (mass of the sample tended to be less than 1 g). Eurovector EuroEA3000 of CHNS-O Elemental Analyzers, with its dedicated SW Callidus, allows for the most exact determination of Carbon, Nitrogen, Hydrogen and Sulphur in virtually all existing substances. This is achieved through only three basic steps: sample combustion at high temperature, fast separation of the resultant gaseous species and TCD detection. Determination of Oxygen content is performed on the same instrument in pyrolisys mode by a quick change of configuration.
- Moisture content according to DIN 51718: the sample of the air-dried and crushed (grain size < 1 mm) sample was weighed and dried in oxygen atmosphere at (106 ± 2) ° C for 24h:

$$FH = \frac{m_E - m_R}{m_E} \times 100 \,, \tag{2.2}$$

where FH – moisture content, %, m_E – mass of the sample before drying, g, m_R – mass of the sample after drying, g.

- To determine ash content (550 °C) (analogue DIN 51719) two heating programs were used:
  - heating with a rate of 5°C/min to 106 °C under oxygen atmosphere to constant mass (dry mass Dm < 0.05%).
  - temperature increase with 5 °C/min to 550 °C under oxygen atmosphere, and hold this temperature for 60 min to constant mass (dry mass Dm < 0.05%).
- For the determination of concentrations of PTEs in feedstock, 1 dried woody sample after treatment was taken. To dissolve ashes by acids, each 0.65 g of ash sample was mixed with 3 ml of HNO_3 (65%) and 9 ml of HCl (37%) and poured into special vessels, which were then placed into Milestone ETHOS digester and heated for 45 min. The solution was filtered through qualitative filter paper (grade 201) FRISENETTE® with particle retention 8−12 μm and poured into 50-ml flask and diluted with deionised water to reach the mark of 50 ml. Then filtered through cellulose acetate membrane filter with particle retention 0.45 μm. The concentrations of Cu, Zn, Ni, Cr, Pb, Cd in the samples were determined by the atomic absorption spectrophotometer Buck Scientific's 210VGP.

The following physical properties of biochar were determined:

- Bulk density of the biochar was measured in accordance with EBC guidelines (EBC 2012). The samples of biochar were filled into a graduated cylinder and the mass was determined by weighting:

$$BD_{BC} = \frac{m_{\mathrm{BC}}}{V_{\mathrm{BC}}}, \tag{2.3}$$

where BD_{BC} – bulk density, kg/m^3, m_{BC} – mass of the biochar sample, kg, V_{BC} – volume of the biochar sample in cylinder, m^3.

- The morphology was determined using scanning electron microscope JEOL 7600F at Institute of Building Materials of Vilnius Gediminas Technical University.
- The specific surface area of ligneous biochar was determined by Brunauer-Emmett-Teller (BET) method using nitrogen gas sorption measurements at 77 K with Nova 4200 E-Series, Quantachrome Instruments (US) at the Latvian State Institute of Wood Chemistry. 100 mg of each crushed biochar sample was put on vacuum degasation (300 °C, 17–24h) over night and cooled down.

The following chemical properties of biochar were determined:

- pH was determined by an instrumental method using a glass electrode in a 1:5 (volume fraction) suspension of 0.4 mm fraction of the biochar in deionized water (Komkienė and Baltrėnaitė 2016). After shaking the suspension for 1 h and after allowing deionized water to stand for 1 h, the pH was measured using Mettler Toledo Seven Multi pH meter (Germany).
- Cation exchange capacity (CEC) was determined using ammonium acetate (Komkienė and Baltrenaite 2016). 25 g of biochar was allowed to stand for 15 h after being thoroughly shaken with 125 ml of 1 M NH_4OAc. The biochar was transferred in filter paper-fitted Buchner funnel. The biochar was gently washed four times with 25 ml additions of NH_4-OAc. The leachate was discarded and the biochar was washed with eight separate additions of 95% CH_3CH_2OH to remove excess saturating solution. The adsorbed NH_4 was extracted by leaching the biochar with 1 M KCl. The biochar was removed and the leachate was transferred to a volumetric flask to dilute to 250 ml volume with additional 1 M KCl. The concentration of NH_4–N was determined in the KCl extract by colorimetry (from composed ammonium calibration curve by measuring absorption intensity at the wave length k = 400 nm with photocolorimeter in 1 cm length cells, concentration of NH_4 was calculated using Nessler method. Also NH_4 was determined in the original KCl extracting solution (blank) to adjust for possible NH_4

contamination in this reagent. Cation exchange capacity was calculated using Equation (2.4):

$$CEC = \frac{NH_{4\text{-}in\ extract} - NH_{4\text{-}in\ blank}}{14}, \quad (2.4)$$

where CEC − cation exchange capacity, $cmol_c/kg$; $NH_{4\text{-}in\ extract}$ − ammonium ion concentration in the extract, mg/l; $NH_{4\text{-}in\ blank}$ − ammonium ion concentration in the blank, mg/l.

- Total organic carbon (TOC) was determined according to Komkienė and Baltrėnaitė (2016) using Total Organic Carbon Analyzer TOC-V (SHIMADZU, Japan). Samples of biochar were dried at room temperature, sieved through a 2-mm sieve, crushed, and homogenized. 20 mg of each biochar sample weighed in the combustion cell was placed in the combustion chamber.
- Electrical conductivity in analogy to DIN ISO 11265 was measured by adding 20 g of the sample to 200 ml desalinated water and shaking it for 1 hour, followed by filtration of the solution. The conductivity was measured then in the filtrated water (EBC 2012).
- Moisture, ash and C, O, N, H content in biochar as well as concentrations of PTEs were determined in the same way as in feedstock.
- Content of oxygen-containing functional groups on the biochar surface were determined using FTIR spectroscopy at the Latvian State Institute of Wood Chemistry. 2 mg of each sample were crushed and pressed. Spectrum One (Perkin Elmer, UK) instrument and KBr pellet technique were used (1% solid in KBr) in the range of 4000–450 cm^{-1}, resolution: 4 cm^{-1}, number of scans: 64.
- Water holding capacity (WHC) according to EBC (2012) was measured by soaking the 2 mm fraction of the material in water for a period of 24 hours. After this, the material was placed on a dry sand bed for 2 hours for removing free water. The saturated material was weighed and then dried at 40 °C in a compartment dryer. After drying the material was weighed again for estimate the water holding capacity.
- For the determination of PTEs concentration in liquid solution, it was filtered through qualitative filter paper (grade 201) FRISENETTE® with particle retention 8−12 μm and poured into 100-ml flask. Then filtered through glass microfibers filter 693 VWR® with particle retention 1.2 μm, and cellulose acetate membrane filter with particle retention 0.45 μm.

2.5. Methodology of Investigating of Adsorption of Potentially Toxic Elements

Adsorption efficiency and capacity were compared between mono- and multi-component adsorption tests, unmodified and modified birch biochar, laboratory-prepared and natural (e.i. landfill leachate as a wastewater) solution. Selectivity of adsorption was investigated through multi-component adsorption experiment. During the adsorption experiments, such parameters of solution, as mono- and multicomponent solution, pH, temperature, different PTEs and their initial concentration, were tested. During the adsorption experiments, such parameters of biochar, as type of biochar, dosage, were tested. Equilibrium studies were made by fitting the experimental data to Langmuir, Freundlich, Redlich–Peterson and Sips isotherms. Kinetic studies were made by fitting the data to pseudo-first, pseudo-second, Weber-Morris intraparticle diffusion, linear film diffusion models.

The aim of the study was to compare the effect of modifications on the adsorption capacity and selectivity for Cr^{3+}, Cd^{2+}, Pb^{2+}, Zn^{2+}, Ni^{2+}, Cu^{2+} of modified and non-modified ligneous biochar.

The objectives were set: 1) To investigate efficiency and selectivity of the adsorption by variation of parameters in adsorption testing: parameters of solution and biochar; 2) To investigate equilibrium and kinetics of adsorption; 3) To determine the type of adsorption (physical/chemical) and mechanism of metal adsorption on biochar (ion exchange, electrostatic interaction, precipitation etc.); 4) To investigate adsorption efficiency and selectivity for PTEs by biochar in landfill leachate.

2.5.1. Selection of the Biochar for Adsorption Experiments

In April–September 2018 trial adsorption experiments were made with different biochar, concentration, dosage, type of biochar, mono- and multi-component solution. Results of this experiment helped to correct parameters and select biochar for adsorption experiment in order to have realistic isotherms and modelling data.

These adsorption experiments were performed according to Komkienė and Baltrenaite (2016) in column set-up (Fig. 2.3) at room temperature. Column set-up consists of six experimental columns, made in compliance with ISO 21268–3 of organic glass with internal diameter of 43 mm and height of 50 cm and fitted with metal filters at the bottom in order to prevent the grains passing through (Fig. 2.3). Port between the columns and wooden frame had the options “opened/closed” to regulate velocity of outlet flow.

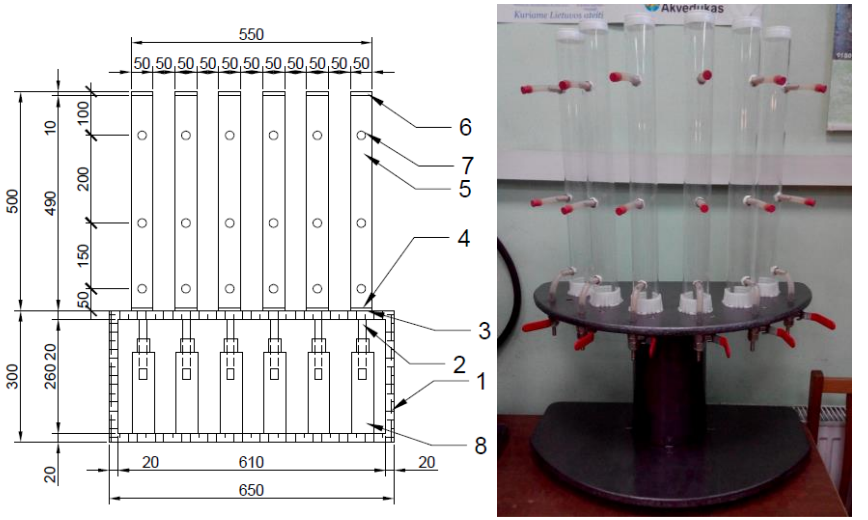

Fig. 2.3. Stand for a column set-up: a) drawing; b) prepared stand. Stand consists of: 1 – wooden frame, 2 – tap, 3 – plastic filter, 4 – metal mesh, 5 – organic glass cylinder, 6 – plastic lid, 7 – channel with rubber tube, 8 – 1000-mL HDPE bottle

At first, mono-component adsorption experiments (using solution of a 1 PTE in a deionized water) were performed. Then – multi-component ads adsorption experiments: 1) using solution of a 6 PTEs of different concentration in a deionized water, 2) using solution of a 6 PTEs of the same concentration in a deionized water.

The effect of adsorbate was investigated by varying 6 PTEs: Cr^{3+}, Cd^{2+}, Pb^{2+}, Zn^{2+}, Ni^{2+}, Cu^{2+}.

For mono-component adsorption, stock solutions of Cr^{3+}, Cd^{2+}, Pb^{2+}, Zn^{2+}, Ni^{2+}, Cu^{2+} were prepared by dissolving analytical grade $Pb(NO_3)_2$, $Cu(NO_3)_2$, $Cd(NO_3)_2$, $Cr(NO_3)_3$, $Ni(NO_3)_2$, $ZnCl_2$ in a deionized water. Adsorption experiments were conducted by mixing 3, 5, 7, 9 g of different biochar with 700 ml of solution of each PTE with specific concentration (Concentration 1 in Table 2.1). After 60 min, the solid and liquid phases were separated. PTEs concentration was analyzed in liquid phase by AAS.

For multi-component adsorption using solution with different concentration of PTEs, multi-component solution was prepared by dissolving analytical grade $Pb(NO_3)_2$, $Cu(NO_3)_2$, $Cd(NO_3)_2$, $Cr(NO_3)_3$, $Ni(NO_3)_2$, $ZnCl_2$ in a deionized water. Adsorption experiments were conducted by mixing 3, 5, 7, 9 g of different biochar with 700 ml of solution with specific concentration (Concentration 2 in Table 2.1). After 60 min, the solid and liquid phases were separated. PTEs concentration was analyzed in liquid phase by AAS.

For multi-component adsorption using solution with the same concentration of PTEs, multi-component solution was prepared by dissolving analytical grade $Pb(NO_3)_2$, $Cu(NO_3)_2$, $Cd(NO_3)_2$, $Cr(NO_3)_3$, $Ni(NO_3)_2$, $ZnCl_2$ in a deionized water. Adsorption experiments were conducted by mixing 3, 5, 7, 9 g of different biochar with 700 ml of solution with specific concentration (Concentration 3 in Table 2.1). After 60 min, the solid and liquid phases were separated. PTEs concentration was analyzed in liquid phase by AAS.

The effect of the initial concentration was investigated by varying the initial concentration of Cr^{3+}, Cd^{2+}, Pb^{2+}, Zn^{2+}, Ni^{2+}, Cu^{2+}.

Concentrations of solutions used are shown in Table 2.1. They were prepared taking into account Lithuanian law about wastewater Nr. D1–236 from 17 May 2006, where maximum permissible concentration (MPC) into wastewater collection system for Cd is 0.1 mg/l, Pb – 0.5 mg/l, Ni – 0.5 mg/l, Cr – 2 mg/l, Cu – 2 mg/l, Zn – 3 mg/l. In addition, uniform concentration of 1 mg/l for all PTEs was tested in multi-component adsorption to find out adsorption selectivity.

Mono-componental solutions of $Pb(NO_3)_2$, $Cu(NO_3)_2$, $Cd(NO_3)_2$, $Cr(NO_3)_3$, $Ni(NO_3)_2$, $ZnCl_2$ were prepared using Concentration 1 (1 PTE in one solution; this is a two-fold MPC concentration), multi-componental solutions were prepared with Concentration 2 (6 PTEs in one solution) and Concentration 3 (6 PTEs in one solution).

Table 2.1. Concentrations of solutions for experiments

PTE	Concentration 1, mg/l	Concentration 2, mg/l	Concentration 3, mg/l
Cd	0.2	0.2	1
Pb	1	1	1
Ni	1	1	1
Cr	4	4	1
Cu	4	4	1
Zn	6	6	1

Sorption isotherms were obtained by equilibrating 3, 5, 7, 9 g of biochar with metal solutions of different initial concentrations from Table 2.1 for 1 h. After separation, the final concentrations of PTEs in the solutions were measured by AAS.

The effect of adsorbent type was investigated by varying 4 types of biochar: unmodified birch biochar and H_2O_2-modified biochar, $MgCl_2$- and $FeCl_3$-modified biochar. Sorption isotherms were obtained by equilibrating 3, 5, 7, 9 g of biochar with metal solutions of different initial concentrations from Table 2.1

for 1 h. After separation, the final concentrations of metal in the solutions were measured by AAS.

The effect of adsorbent dosage was investigated by varying the dosage of biochar in the range 3, 5, 7, 9 g/100 ml (Azmi *et al.* 2016). Sorption isotherms were obtained by equilibrating 3, 5, 7, 9 g of biochar with metal solutions of different initial concentrations from Table 2.1 for 1 h. After separation, the final concentrations of metal in the solutions were measured by AAS.

Adsorption efficiency was calculated using Equation (2.5) (Bousba and Meniai 2013):

$$R = \left(1 - \frac{C_e}{C_o}\right) \times 100\% , \quad (2.5)$$

where R – adsorption efficiency, %; C_0 – the concentration of adsorbate in solution before treatment, mg L^{-1} ; C_e – the concentration of adsorbate in solution after treatment, mg L^{-1}.

2.5.2. Adsorption Experiments with Synthetic Solutions

All adsorption experiments were performed according to Wang *et al.* (2018) in 200-mL shaker tubes at room temperature. At first, mono-component adsorption (solution of a 1 PTE in a deionized water) adsorption experiments were performed. Stock solutions of Cr^{3+}, Cd^{2+}, Pb^{2+}, Zn^{2+}, Ni^{2+}, Cu^{2+} were prepared by dissolving analytical grade $Pb(NO_3)_2$, $Cu(NO_3)_2$, $Cd(NO_3)_2$, $Cr(NO_3)_3$, $Ni(NO_3)_2$, $ZnCl_2$ in a deionized water. Adsorption experiments were conducted by mixing biochar with 50 ml of solution of each PTE with equilibrium concentration (to be found from 2.4.3). The tubes were then agitated at 120 rpm for equilibrium time (to be found from 2.4.2). After equilibrium time, the solid and liquid phases were separated. Effect of adsorbent dosage and particle size, solution pH, temperature and competing ions was investigated.

After mono-component adsorption experiments, the optimal parameters (dosage, pH, initial concentration, temperature, particle size), the best-performed biochar was selected for testing of adsorption of PTEs in landfill leachate. Before adsorption experiments, Cr^{3+}, Cd^{2+}, Pb^{2+}, Zn^{2+}, Ni^{2+}, Cu^{2+} concentrations were analyzed in landfill leachate. After adsorption in landfill leachate, adsorption efficiency, selectivity, mechanisms were investigated.

The effect of adsorbate type was investigated by varying 6 PTEs: Cr^{3+}, Cd^{2+}, Pb^{2+}, Zn^{2+}, Ni^{2+}, Cu^{2+}.

The effect of adsorbent type was investigated by varying 2 types of biochar: unmodified birch biochar and H_2O_2-modified biochar, because these types of biochar favor adsorption of cationic PTEs more than other types of modified biochar from the thesis – $MgCl_2$ and $FeCl_3$-modified biochar. Because of its

pHpzc, $MgCl_2$ and $FeCl_3$-modified biochar suits adsorption of anionic metals. Moreover, our previous adsorption experiments reported lower adsorption efficiency of $MgCl_2$ and $FeCl_3$-modified biochar for Cr^{3+}, Cd^{2+}, Pb^{2+}, Zn^{2+}, Ni^{2+}, Cu^{2+} in comparison to unmodified or H_2O_2-modified biochar.

The effect of contact time on each metal sorption was studied in different time intervals ranging 5, 10, 30, 60, 120, 180, 300 min with the initial metal concentration of 100 mg/l for each PTE. After the completion of the reaction, conical flasks were taken out and the biochar adsorbents were separated followed by the determination of the residual metal concentrations. From this experiment optimal contact time for future experiments was chosen.

The effect of the initial concentration was investigated by varying the initial concentration in the range 10, 30, 50, 100, 150 mg/l. Sorption isotherms were obtained by equilibrating 0.25 g of biochar with metal solutions of different initial concentrations 10, 30, 50, 100, 150 mg/l for 1 h. After separation, the final concentrations of metal in the solutions were measured. From this experiment optimal initial concentration for future experiments was chosen.

The effect of adsorbent dosage was investigated by varying the dosage of biochar in the range 0.3, 1, 5 g/l. Range of values was based on multiple adsorption studies, e.g. Tsai and Chen (2013) showed that with the increase of adsorbent dosage 0.10‑0.30 g/l the number of adsorption sites increased, Chen *et al.* (2011) observed the highest metal sorption efficiencies for hardwood at dosage 1 g/l, Sun *et al.* (2013) removal efficiency of methylene blue dye increased with increasing biochar dose from 2 to 8 g/l.

The suspensions containing different amount of biochar (0.0015, 0.05, 0.25 g) and 50 ml of 100 mg/l metal solution were placed to shaker for 1 h. After separation, the residual metal concentrations in the solutions were measured.

The effect of pH of the solution on adsorption was investigated by varying the pH in the range 2, 4, 5, 6, 7, 10 using 0.1 M KOH and HCl solutions, as in this pH range there is the possibility to obtain better adsorption of the mentioned above PTEs (Kilic *et al.* 2013) than in another pH range. Sorption behaviors of PTEs, for concentration of 100 mg/l of each PTE and 0.25 g of biochar, were studied as a function of pH. After contacting for 1 h, the suspensions were separated and the residual metal concentrations were analyzed.

Effect of temperature was studied with 20, 30, 40 °C. Sorption behaviors of PTEs, for concentration of 100 mg/l of each PTE and 0.25 g of biochar, were studied. After contacting for 1 h, the suspensions were separated and the residual metal concentrations were analyzed.

The effect of the particle size was investigated by varying the dosage between two fractions: (a) fraction 1 (0.4–1 mm), that corresponds to the particle size of powder commercial activated carbon, and (b) fraction 2 (1–3 mm), that

corresponds to the particle size of granular commercial activated carbon. Sorption behaviors of PTEs, for concentration of 100 mg/l of each PTE and 0.25 g of biochar, were studied for the influence of particle size. After contacting for 1 h, the suspensions were separated and the residual metal concentrations were analyzed.

The effect of competing ions was investigated by varying the concentrations of $NaNO_3$/KNO_3/$Ca(NO_3)_2$ in the range 0.01, 0.05, 0.1 M (Zhou *et al.* 2018). $NaNO_3$/ KNO_3/$Ca(NO_3)_2$ were separately added to PTE solutions with concentration of 100 mg/l of each PTE and 0.25 g of biochar; after contacting for 1 h, the suspensions were separated and the residual metal concentrations were analyzed. The aim was to find whether Na^+, K^+, Ca^{2+} ions, that are present in wastewaters, compete with PTEs for the negatively charged adsorption sites. Effect of competing ions on PTEs retention was observed from the figure, where the vertical axis was PTE uptake (mg/g), the horizontal axis was the ratio of initial competing ions to PTE (mol/mol) (Yang and Jiang 2014).

Methodology of equilibrium studies was formed according to Wang *et al.* (2018). Unmodified and modified with H_2O_2 biochar were used for the experiments. Solutions of $Pb(NO_3)_2$, $Cu(NO_3)_2$, $Cd(NO_3)_2$, $Cr(NO_3)_3$, $Ni(NO_3)_2$, $ZnCl_2$ were prepared. For mono-component adsorption equilibrium studies, 0.25 g of biochar were added to Cr^{3+}, Cd^{2+}, Pb^{2+}, Zn^{2+}, Ni^{2+}, Cu^{2+} solutions (50 ml; 10, 30, 50, 100, 150 mg/L), and shaken for 24 h. At the end of each experiment, solutions were sampled, filtered through 0.45 m filter, and analyzed by AAS.

Such two parameter isotherms in linear form, like Langmuir (Equation 2.6) and Freundlich (Equation 2.7) were used (Foo and Hameed 2010):

$$\frac{C_e}{q_e} = \frac{1}{bQ_0} + \frac{C_e}{Q_o}, \tag{2.6}$$

$$\log q_e = \log K_F + \frac{1}{n}\log C_e. \tag{2.7}$$

Such three parameter isotherms in linear form, like Redlich–Peterson (Equation 2.8) and Sips (Equation 2.9) were used (Foo and Hameed 2010):

$$\ln\left(K_{RP}\frac{C_e}{q_e} - 1\right) = g\ln(C_e) + \ln(a_{RP}), \tag{2.8}$$

$$\beta_S \ln(C_e) = -\ln\left(\frac{K_{LF}}{q_e}\right) + \ln(a_{LF}). \tag{2.9}$$

Equilibrium parameters are shown in Table 2.2. Further they were used for dynamic intraparticle model calculations. The most suitable isotherm was determined by R-squared value.

Concentration of PTEs in solution after treatment was measured. For the purpose of the determination of concentrations of PTEs in solution, it was poured

into 50-ml flask. The concentrations of PTEs in the samples were determined by the atomic absorption spectrophotometer Buck Scientific's 210VGP.

Methodology of kinetic studies was formed according to Zhou *et al.* (2018). Unmodified and modified with H_2O_2 biochar were used for the experiments. Solutions of $Pb(NO_3)_2$, $Cu(NO_3)_2$, $Cd(NO_3)_2$, $Cr(NO_3)_3$, $Ni(NO_3)_2$, $ZnCl_2$ were prepared. For mono-component adsorption kinetic studies, 0.25 g of biochar were added to Cr^{3+}, Cd^{2+}, Pb^{2+}, Zn^{2+}, Ni^{2+}, Cu^{2+} solutions (500 ml, 50 mg/l) stirred at 1000 rpm. Aliquots (50 ml) were sampled at different time intervals 5, 10, 30, 60, 120, 180, 300 min, filtered through 0.45 μm filter, and analyzed by AAS.

Table 2.2. List of parameters for equilibrium

Symbol	Description	Unit
b	Langmuir equilibrium constant	–
Ce	equilibrium concentration of adsorbate molecules in a fluid	mg/l
Q_0	maximum adsorbed amount	mg/g
q_e	equilibrium mass of sorbed molecules per mass of sorbent	mg/g
K_f	adsorption coefficient	–
n	index of nonlinearity of isotherms	–
K_{RP}	Redlich-Peterson adsorption constant	l/mg
a_{RP}, a_{LF}	affinity coefficient	l/mg
K_{LF}	Sips adsorption constant	l/mg

For multi-component adsorption kinetic studies, methodology was the same, but was used only one solution with Cr^{3+}, Cd^{2+}, Pb^{2+}, Zn^{2+}, Ni^{2+}, Cu^{2+} (500 ml, 50 mg/l each).

Kinetic and thermodynamic parameters of adsorption of PTEs were tested with adsorption device (Fig. 2.4). In columns (7, 8) such parameters, as adsorbent and adsorbate type, contact time, initial concentration, dosage, pH, temperature, particle size and effect of competing ions were tested.

Among adsorption-reaction models, pseudo-first, pseudo-second order models and first-order reversible model, were applied to the adsorption kinetic data by fitting the related adjustable parameters (Tan and Hameed 2017). Pseudo-first order model linearized form is:

$$\ln(q_e/(q_e - q)) = k_1 t. \tag{2.10}$$

Pseudo-second order model linearized form is:

$$\frac{t}{q} = \frac{1}{k_2 q_e^2} + \frac{t}{q_e}. \tag{2.11}$$

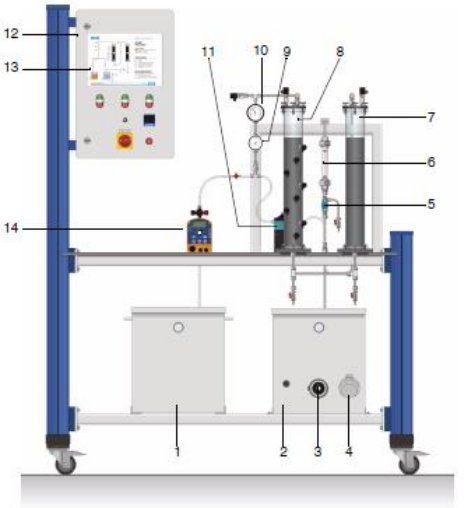

Fig 2.4. Adsorption device (source: Kellow 2011): 1 – Concentrate tank (B2), 2 – Treated water tank (B1), 3 – Heater (H), 4 – Temperature sensor TI (01), 5 – Regulating valve (V15), 6 – Flow rate sensor (FI), 7 – Adsorber (A2), 8 – Adsorber (A1), 9 – Thermometer (TI), 10 – Manometer (PI), 11 – Circulation pump (P1), 12 – Switch cabinet, 13 – Process schematic, 14 – Concentrate pump (P2)

Among adsorption-diffusion models, Weber-Morris intraparticle pore diffusion model and linear film diffusion model were applied (Tan and Hameed 2017). Intraparticle diffusion is described by:

$$q = \mathrm{k_{id}}\sqrt{t} + B. \tag{2.12}$$

Linear film diffusion model is described by:

$$\frac{C}{C_0} = exp(-k_f t). \tag{2.13}$$

Kinetic parameters are shown in Table 2.3.

Adsorption mechanisms were studied by heating of the biochar, determination of pH_{PZC}, adding $NaNO_3$, KNO_3, $Ca(NO_3)_2$. To define if the process was reversible (physical adsorption), the used biochar was heated at 600 °C for 2 h (Greiner *et al.* 2017). The pH of zero point charges (pH_{PZC}) of the unmodified

and modified BCs were determined with the immersion technique according to Jang *et al.* 2018:
(1) 50 mL NaCl solution (0.01 M) was placed in a 100 mL plastic bottle to maintain the ion strength of the solution,
(2) the pH of solution was adjusted to 2, 4, 6, 8, 10 using 0.1M of KOH or 0.1 N HCl solution,
(3) 0.15 g BC was added to the solution,
(4) the final pH of solution was measured after 30 min of shaking at 20 °C and 5000 rpm.

The pH_{PZC} from each set were calculated based on the ΔpH (final−initial pH) = 0. Experiments were performed in triplicate.

Adsorption experiments with $NaNO_3$, KNO_3, $Ca(NO_3)_2$ help to determine ion exchange, surface complexation, co-precipitation.

Table 2.3. List of parameters for kinetics

Symbol	Description	Unit
q	adsorption capacity	mg/g
q_e	adsorption capacity at equilibrium time	mg/g
q_t	adsorption capacity at time t	mg/g
K_1	rate constant of pseudo-first order adsorption	l/min
K_2	rate constant of pseudo-second order adsorption	g/mg·min
K_{id}	intraparticle diffusion rate constant	$mg \cdot min^{1/2}/g$
t	time	min
B	initial adsorption	mg/g
k_f	film diffusion coefficient	1/min
C	adsorbate concentration at the liquid-solid interface	mg/l

Adsorption efficiency was calculated using Equation (2.5). Adsorption capacity was calculated using Equation (2.14) (Bousba and Meniai 2013):

$$q_e = \frac{(C_0 - C_e) \times V}{m}, \tag{2.14}$$

where q_e – adsorption capacity, mg/g; t – time; C_0 – the concentration of the PTEs of initial time, mg/L; C_e – the concentration of the PTEs at equilibrium, mg/L ; V – volume of PTEs solution, L; m – biochar dosage, g.

Adsorption thermodynamics was examined at temperatures of 20, 30, 40 °C, as temperature range 10–45 ºC is favourable for solubility of chemicals in wastewater treatment systems and enhances the reaction rates (Horsfall and Spiff 2005; Mohan *et al.* 2007).

Thermodynamic parameters include Gibbs free energy ($\Delta G°$, Kj/mol), entalphy ($\Delta H°$, Kj/mol) and entropy ($\Delta S°$, j/mol/K).

$$\Delta G° = -RT \cdot \ln K_d , \tag{2.15}$$

$$\ln K_d = -\frac{\Delta H°}{RT} + \frac{\Delta S°}{R}, \tag{2.16}$$

where R = 8.314 J/ K·mol is the gas constant, and T is temperature, K_d is the distribution coefficient for the adsorption (Langmuir constant):

$$K_d = \frac{q_e}{C_e}, \tag{2.17}$$

where q_e is the adsorption capacity (mg/g), C_e is equilibrium concentration of adsorbate (mg/l).

$$\Delta G° = \Delta H° - T\Delta S°. \tag{2.18}$$

The positive values of $\Delta H°$ and $\Delta S°$ suggests the endothermic nature of adsorption (Trazzi *et al.* 2016; Aslan *et al.* 2015).

2.5.3. Adsorption Experiments with Landfill Leachate

The Kazokiškės landfill has been the main site for disposal of Vilnius region municipal wastes for 10 years. It is situated in the Kazokiškes village in north-eastern part of Elektrėnų municipality. Total landfill site area – 30.16 ha, area of waste deposit of 27.1 ha is divided into 6 sections. The waste is deposited in section No 2 of an area of 6.0 ha. Owner and landfill operator is JSC VAATC (Vilnius County Waste Management Center). Annually 339 900 t of waste is disposed. To reduce the operation load of the reverse osmosis for the landfill leachate treatment, adsorption by biochar was suggested.

The aim of the study was to investigate the effect of H_2O_2-modified and unmodified ligneous biochar on the adsorption capacity and selectivity for Cr^{3+}, Cd^{2+}, Pb^{2+}, Zn^{2+}, Ni^{2+}, Cu^{2+} from landfill leachate.

The objectives were set: 1) To investigate efficiency and capacity of the adsorption by variation of parameters of landfill leachate and biochar; 2) To investigate equilibrium and kinetics of adsorption; 3) To determine the type of

adsorption (physical/chemical) and mechanism of metal adsorption on biochar (ion exchange, electrostatic interaction, precipitation etc.).

In April 2019 30 l of landfill leachate were collected from leachate collection point #2 in 2 plastic tanks, and instantaneously transported to the laboratory. They were stored with limited light exposure and temperature 18°C in order to minimize the chemical and biological changes.

The characteristics of leachate samples were analyzed according to standard methods of water and wastewater (APHA 2005). The characteristics of Kazokiskiu landfill samples are presented in Table 2.4.

Table 2.4. Kazokiskiu landfill leachate characteristics

Parameters	Unit	Value
Temperature	°C	20
pH	-	8.3
Electrical conductivity*	S/m	2310
Color	-	black
COD*	mg/l	5537
NH3-N*	mg/l	1397
BOD7*	mg/l	885
BOD7/COD	-	0.16
Total suspended solids*	mg/l	120
Cu	mg/l	55
Cr	mg/l	1400
Zn	mg/l	120
Pb	mg/l	9.5
Cd	mg/l	0.69
Ni	mg/l	135

* data provided by administration of Kazokiskiu landfill

The effect of adsorbate type was investigated by varying 6 PTEs: Cr^{3+}, Cd^{2+}, Pb^{2+}, Zn^{2+}, Ni^{2+}, Cu^{2+}. The effect of adsorbent type was investigated by varying 2 types of biochar: unmodified birch biochar and H_2O_2-modified biochar.

The effect of contact time on each metal sorption was studied in different time intervals ranging 10, 30, 60, 120, 180, 240, 300 min. After the completion of the reaction, conical flasks were taken out and the biochar adsorbents were separated followed by the determination of the residual metal concentrations. From this experiment optimal contact time for future experiments was chosen.

Azmi *et al* (2016) and Shehzad *et al.* (2016) found the optimal dosage for leandfill leachate treatment 7 g/100 ml. Therefore, in this study the effect of adsorbent dosage was investigated by varying the dosage of biochar in the range 50, 70, 100 g/l.

The effect of the temperature was investigated by varying the temperature in the range 20, 30, 40 °C. Sorption behaviors of PTEs, for concentration of 100 mg/l of each PTE and 0.25 g of biochar, were studied as a function of temperature. After contacting for 1 h, the suspensions were separated and the residual metal concentrations were analyzed.

Concentration of PTEs in landfill leachate after treatment was measured. Landfill leachate was poured into 50-ml flask. The concentrations of PTEs in the samples were determined by the atomic absorption spectrophotometer Buck Scientific's 210VGP.

Equilibrium and kinetics studies were conducted. Unmodified, modified with H_2O_2 biochar were used for the experiments. 100 g/l of biochar were added to landfill leachate (500 ml). Aliquots (50 ml) were sampled at different time intervals 10, 30, 60, 120, 180, 240, 300 min, filtered through 0.45 m filter, and analyzed by AAS. Calculations were made according to Subchapter 2.5.2

The influence of the particle size, adsorption efficiency and capacity, thermodynamic calculatons was investigated according to Subchapter 2.5.2.

For quality assurance, each analysis was prepared and analyzed in duplicates. The measurements were carried out three times and the mean of measurements were calculated. The results of arithmetic mean values with values of standard deviation were presented in graphical expression of the results. The standards of calibration were used to calibrate devices in 2019. The quality of experiments was assured by blank samples such as deionized water (for NH_4–N).

2.6. Biochar-Hydrogel Composite Production and Properties

Smart BC concept in adsorption of PTEs could be developed by combining of BC with smart materials and forming composites. In this study biochar was prepared at pyrolysis temperature of 450 °C, because biochar obtained at 300–450 °C is more suitable for adsorption of inorganic PTEs, as it contains both oxygen-containing functional groups and developed microporous structure (Ahmad *et al.* 2014).

Two types of hydrogels were used: cationic, that swells at pH 5–6 (at this pH most of inorganic PTEs are adsorbed from laboratory-based solution), another one – at pH 10 (that corresponds to pH of most of wastewaters). pH and temperature-responsivity characteristics were selected in terms of enhancing of selectivity of adsorption of PTEs. Thus, in this study smart biochar-hydrogel composite is the combination of biochar and hydrogel, that has reversible behavior to changes in temperature and pH.

Biochar-hydrogel composites were prepared with modified and unmodified biochar. Birch biochar modified with H_2O_2, as H_2O_2 modification of the biochar add more oxygenated groups on its surface and increase adsorption of Cu, Zn, Pb, Ni, Cr, Cd by biochar (Xue *et al.* 2012).

Such characteristics of smart biochar-hydrogel composite, like surface functionality, swelling under different pH and temperature, adsorption capacity, were studied. Smart biochar-hydrogel composite is expected to have bigger CEC and adsorption capacity, than a separate biochar, and possess a reversible behavior.

The aim of the study was to evaluate potential of smart biochar-hydrogel composites in adsorption of Cd^{2+}, Pb^{2+}, Zn^{2+}, Ni^{2+}, Cu^{2+}, Cr^{3+} from landfill leachate. The following tasks were set: 1) to prepare smart biochar-hydrogel composites and investigate their characteristics; 3) to test pH- and T-responsivity of smart biochar-hydrogel composites by swelling; 4) to perform tests of smart biochar-hydrogel composites in adsorption of Cd^{2+}, Pb^{2+}, Zn^{2+}, Ni^{2+}, Cu^{2+}, Cr^{3+} from landfill leachate.

2 types of hydrogels (cationic and anionic) were prepared by the classic method of bulk polimerization.

Cationic hydrogel was prepared according to Zhao *et al.* (2016). Materials for the composite preparation were bought from Sigma Aldrich (Germany):

- acyclic acid (AA) (monomer),
- potassium persulfate ($K_2S_2O_8$) (initiator),
- methylene-bis-acrylamide (MBA) (crosslinker),
- ammonium cerium nitrate ($(NH_4)_2 \cdot Ce(NO_3)_6$) (initiator),
- sodium sulfite (Na_2SO_3) (initiator).

10 ml potassium persulfate ($K_2S_2O_8$) solution (20 g/L) and 2 ml Ceric ammonium nitrate ($(NH_4)_2Ce(NO_3)_6$) solution (20 g/L) were added into the three-neck flask and stirred for 15 min. After 15 min 3 ml sodium sulfite (Na_2SO_3) solution (20 g/L) and a premixed AA solution (30 mL) with 54.3% of neutralization degree (ND) were mixed in the three-neck flask and stirred for 45 min. It was followed by adding a 0.05 g of MBA solution (20 g/L) into the flask. The solution was then stirred for 4 h at 50°C. The wet sample was dried at 70 °C for 24 h.

Anionic hydrogel was prepared according to Karakoyun *et al.* (2011). Materials for the composite preparation were purchased from Sigma-Aldrich and Fluka Chemical Companies:

- acrylamide (AAm) (monomer),
- N,N′-methylenebisacrylamide (MBA) (cross linker),
- ammonium persulfate (APS) (initiator).

AAm (1.0 g was dissolved in 1.0 mL water) and 0.00703 mmol N,N′- methylenebisacrylamide (MBA) were mixed. After vortex mixing thoroughly, 0.2 mL 0.0703 mmol aqueous solution of ammonium persulfate (APS) was added to initiate the polymerization and the hydrogel precursor solution was placed in cylindrical plastic pipettes with 3 mm in diameter. After polymerization and crosslinking for 12 h at 25 °C, hydrogels were taken from the plastic pipette, cut to desired sizes and washed several times with deionized water to remove all unreacted monomers and low molecular weight polymeric matter from the hydrogel. Then the hydrogels were dried first in air then in oven at 40 °C for 2 days, and then stored in a desiccator until used.

4 types of smart biochar composites were prepared: 2 with cationic hydrogels and 2 with anionic hydrogels. Further, the composites were named as "cationic" or "anionic" as well. Schematic way of preparation is shown in Fig. 2.5.

2 cationic composites were prepared according to Zhao *et al.* (2016), by combination of the biochar (unmodified, H_2O_2-modified) with cationic hydrogel. Unmodified and H_2O_2-modified biochar was crushed to powder 0.4 mm.

The procedure of the preparation is analogous to 2.6.1. About 1.5 g biochar powder, 10 ml potassium persulfate ($K_2S_2O_8$) solution (20 g/L) and 2 ml Ceric ammonium nitrate ($(NH_4)_2Ce(NO_3)_6$) solution (20 g/L) were added into the three-neck flask and stirred for 15 min. After 15 min 3 ml sodium sulfite (Na_2SO_3) solution (20 g/L) and a premixed AA solution (30 mL) with 54.3% of neutralization degree (ND) were mixed in the three-neck flask and stirred for 45 min. It was followed by adding a 0.05 g of MBA solution (20 g/L) into the flask. The solution was then stirred for 4 h at 50 °C. The wet sample was dried at 70 °C for 24 h.

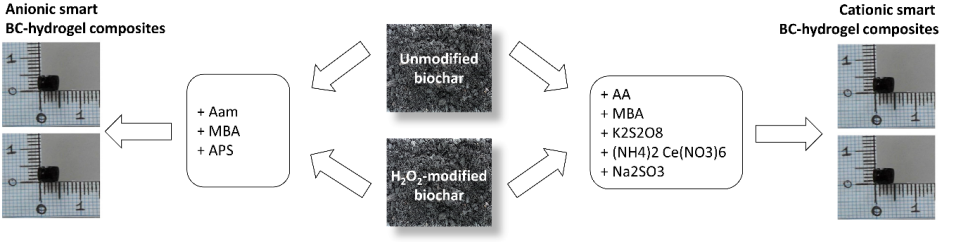

Fig. 2.5. Scheme of preparation of smart biochar-hydrogel composites

2 anionic composites were prepared according to Karakoyun *et al.* (2011), by combination of the biochar (unmodified, H_2O_2-modified) with anionic hydrogel.

Unmodified and H_2O_2-modified biochar was crushed to powder 0.4 mm. Hydrochloric acid (37% Riedel-de Haen, Germany) and sodium hydroxide pellets (Merck, Germany) were used to adjust the pH of sample solutions.

The procedure of the preparation is analogous to 2.6.1. All types of biochar were washed with 0.1 mol/L HCl acid for 6 h, and washed with DI water until a neutral pH was obtained and dried in an oven at 50 °C for three days. The main purpose of washing chars is for de-mineralization and for this goal, generally biochar was exposed to 1 h 0.1 mol/L HCl treatment and washed with deionized water until neutral pH was obtained and then they were dried in an oven. 0.1 g biochar were mixed with AAm (1.0 g was dissolved in 1.0 mL water) and 0.00703 mmol N,N′-methylenebisacrylamide (MBA). After vortex mixing thoroughly, 0.2 mL 0.0703 mmol aqueous solution of ammonium persulfate (APS) was added to initiate the polymerization and the hydrogel precursor solution was placed in cylindrical plastic pipettes with 3 mm in diameter. After polymerization and crosslinking for 12 h at 25 °C, hydrogels were taken from the plastic pipette, cut to desired sizes and washed several times with deionized water to remove all unreacted monomers and low molecular weight polymeric matter from the hydrogel. Then the hydrogels were dried first in air then in a vacuum oven at 40 °C for 2 days, and then stored in a desiccator until used.

Physical and chemical properties, like BET specific surface area, porosity, cation exchange capacity (CEC), surface functionality, EC, pH, pH_{pzc} of the biochar, hydrogels and biochar-hydrogel composites were determined according to p. 2.4, 2.5.

Swelling behavior of hydrogels and biochar-hydrogel composites was studied by varying the effect of pH and temperature. To study the effect of pH on swelling, hydrogels 0.2 g samples (10–20 mesh) were soaked in solutions with pH range (2, 4, 6, 7, 10, 12). pH range was chosen in order to detect hydrogel is cationic or anionic.

A series of biochar-hydrogel composites 0.2 g samples (10–20 mesh) was soaked in solutions with temperature range (20, 30, 40 °C) (Zhao *et al.* 2016). Swelling ratios of the hydrogels were measured gravimetrically after wiping off excess water on the surface with moistened filter paper. The swelling ratio (S) can be calculated by the following formula:

$$S = (W_s\text{-}W_d)/W_d \ , \qquad (2.19)$$

where S is equilibrium swelling ratio (%), W_s is weight of swollen composite (g), W_d is weight of dry composite (g).

The adsorption equilibrium experiments were carried out by mixing different mass of dried anionic and cationic unmod. BC/H_2O_2-mod. BC-hydrogel composites (0.1, 0.25, 0.5, 0.75, 1 g) and 50 ml of landfill leachate at 20 °C

(Karakoyun *et al.* 2011) for 1 h. At the end of each experiment, solutions (50 ml) were sampled, filtered through 0.45 mm filter, and analyzed by AAS. Equilibrium of adsorption was calculated with Langmuir, Freundlich, Redlich-Peterson and Sips isotherms (Equations 2.6–2.9).

Methodology of kinetics studies was formed according to Zhou *et al.* (2018). 10 g dried anionic and cationic unmod. BC/ H_2O_2-mod. BC-hydrogel composites were added to 500 ml of landfill leachate at 20 °C stirred at 1000 rpm. Aliquots (50 ml) were sampled at different time intervals 5, 10, 30, 60, 120, 180, 300 min, filtered through 0.45 mm filter, and analyzed by AAS. Kinetics of adsorption was calculated with pseudo-first order, pseudo-second order, intraparticle diffusion and linear film diffusion kinetic models (Equations 2.10–2.13).

Adsorption efficiency and capacity were calculated according to Subchapter 2.5.2.

Adsorption thermodynamics was examined at temperatures of 20, 30, 40 °C and calculated according to Subchapter 2.5.2. The adsorption equilibrium experiments were carried out by mixing 1 g dried H_2O_2 BC-hydrogel and 50 ml of landfill leachate at 20 °C (Karakoyun *et al.* 2011) at 300 min. After the experiment, samples were filtered through 0.45 m filter, and analyzed by AAS. Calculations were made according to Subchapter 2.5.2.

For quality assurance, each analysis was prepared and analyzed in duplicates. The measurements were carried out three times and the mean of measurements were calculated. The results of arithmetic mean values with values of standard deviation were presented in graphical expression of the results. The standards of calibration were used to calibrate devices in 2019. The quality of experiments was assured by control samples such as KCl (for CEC).

2.7. Conclusions of Chapter 2

1. Such modification ways were chosen for experiments: intrinsic properties and syngenetic elements of ligneous feedstock (lignin, ash and moisture content, C, H, O, N content), chemical modifications with $FeCl_3$, $MgCl_2$, H_2O_2. Treatment with H_2O_2 leads to an increase in the number of carboxylic groups and the cation exchange capacity of the biochar, while artificially added Mg and Fe particles may act like additional adsorption sites on the surface of biochar, increasing the adsorption of PTEs on biochar.

2. To investigate the effect of intrinsic properties, the following ligneous feedstock was selected due to local availability and waste minimization: pine, birch, aspen, fir wood, pine bark, birch bark. Feedstock was taken from control and contaminated site. To investigate effect of chemical modifications with $FeCl_3$ and $MgCl_2$, pine, birch, aspen, fir wood were tested. To investigate effect of

chemical modification with H_2O_2, birch wood was taken, as biochar from birch wood had the higher CEC than other tested types of biochar.

3. Following the EBC requirements, such characteristics of biochar were investigated: density, pH, cation exchange capacity, electrical conductivity, BET, moisture, ash content, C, H, O, N content, as they may have the influence on adsorption of PTEs by biochar.

4. To conduct adsorption experiments, stand for a column set-up and adsorption device were prepared. To improve biochar modification with H_2O_2 process, device for biochar modification with H_2O_2 solution was invented.

5. Langmuir, Freundlich, Redlich–Peterson, Sips isotherms, as the most frequently used in liquid-solid adsorption, were chosen for equilibrium studies. Pseudo-first, pseudo-second order models, linear film diffusion and Weber-Morris intraparticle pore diffusion models, as the most frequently used in liquid-solid adsorption, – for kinetic studies. Dynamic intraparticle model was chosen for fitting and sensitivity analysis, delivering the adsorption parameters without kinetic studies.

6. As H_2O_2 modification of the biochar adds more oxygenated groups on its surface, than other investigated modifications in thesis, H_2O_2-modified biochar was selected for preparation of biochar-hydrogel composites for adsorption of Cr^{3+}, Cd^{2+}, Pb^{2+}, Zn^{2+}, Ni^{2+}, Cu^{2+} . Smart biochar-hydrogel composite is expected to have bigger CEC and adsorption capacity, than a separate biochar, and possess a reversible behavior, that could be found by testing on response to temperature and pH changes of solution.

3

Research results of biochar adsorption

Chapter 3 investigates the effect of modification methods on the adsorption capacity for potentially toxic elements of ligneous biochar and identifies the key mechanisms of adsorption, evaluates the biochar-hydrogel composite potential for application in adsorption of potentially toxic elements from synthetic solutions and landfill leachate, fits the results to dynamic intraparticle model and conduct sensitivity analysis of simplified adsorption model.

The main scientific results were published in jounals with a citation index: Chemerys and Baltrėnaitė (2018b), Chemerys *et al.* (2020) and Leonavičienė *et al.* (2019). Other results were included to conference proceedings: Chemerys and Baltrėnaitė (2016; 2017a; 2017b). Lithuanian patent #6434 was obtained for device and technology for modification of biochar with H_2O_2.

3.1. Effect of Modification Methods on the Adsorption Capacity for Potentially Toxic Elements of Ligneous Biochar

3.1.1. The Influence of Intrinsic Properties and Syngenetic Elements of Ligneous Feedstock on Adsorptive Characteristics of the Biochar

The influence of natural modifications of ligneous biochar on adsorptive characteristics of the biochar is discussed below. Conventions: "P – c" means pine from control site, "B – c" birch from control site, "A – c" aspen clean, "F – c" fir clean, "PB – c" pine bark from control site, "BB – c" birch bark from control site, "P – cm" pine from contaminated site, "B – cm" birch from contaminated site, "PB – cm" pine bark from contaminated site, "BB – cm" birch bark from contaminated site.

Lignin content in ligneus feedstock from control site is summarized in Table 3.1.

Table 3.1. Lignin content in woody feedstock (n = 3, mean value ± SD)

Ligneous feedstock	Lignin content**, %**
P – c	34.93±0.12
B – c	19.06±0.18
PB – c	59.00±0.50
BB – c	54.35±0.11
A – c	18.24 ± 0.01
F – c	28.45 ± 0.11

Rydholm (1965) showed that conifers had more lignin than hardwoods; he reported an average of 27% lignin content for conifers and 21% for hardwoods, while aspen and birch contained only about 18.5% of lignin. Bark of the trees was the highest in lignin. Pine wood has more lignin that birch wood. The results obtained are higher than those indicated in Miranda *et al.* (2012) and Miranda *et al.* (2013), where birch bark had 27.9% and pine bark 33.7% of lignin, respectively.

As a part of a wood, lignin creates porosity in the biochar structure, promoting adsorption of PTEs. It was found that with the increase of lignin content from 19.06 in birch wood to 59% in pine bark, BET specific surface area increases from 20.11 to 362.1 m^2/g. Lignin also had effect on O/C ratio: with the increase

of lignin content, O/C ratio increased from 0.074 to 0.188. Though the high adsorption capacity of lignin could be attributed to polyhydric phenols and other functional groups on the surface (Srivastava *et al.* 2008), in our study lignin in feedstock didn‘t infuence CEC of the biochar.

Bigger amount of lignin (54–59%) in feedstock decrease the moisture, carbon content in BC, but increase the oxygen, nitrogen content, N/C, O/C ratios, pH, EC, BET in BC. Therefore, this property has the highest impact on adsorptive properties, as lignin creates porosity in the biochar and has oxygen-containing functional groups. Thus the BC from birch bark had CEC and BET exceeding BC from birch in 3 and 17 times, respectively. Lignin content in feedstock doesn't influence CEC, ash, hydrogen content, bulk density in BC.

Though excessive moisture in the biochar may block the pores, preventing the adsorption of PTEs by biochar, there was no significant influence of moisture in feedstock on adsorptive properties of BC (Fig. 3.1), except the case when BC from aspen wood (5.8% of moisture in feedstock) had the lowest BET among all types of BC 18.27 (m^2/g).

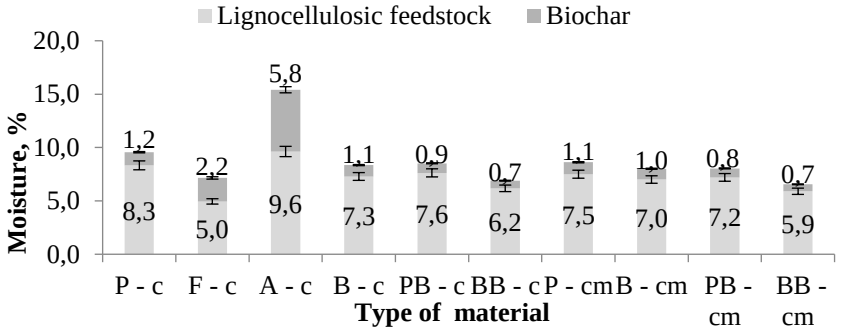

Fig. 3.1. Moisture content in the ligneous feedstock and biochar (n = 3, mean value ± SD)

Bigger amount of ash in feedstock increase ash content of BC. It decrease the moisture, carbon content in BC, but increase the oxygen, nitrogen content, N/C, O/C ratios, pH, EC, CEC, BET in BC. Ash content in feedstock doesn't influence hydrogen content and bulk density in BC. The highest values of ash had the biochar from the contaminated site (Fig. 3.2). The highest ash content was observed for pine bark and birch bark biochar from contaminated site. This could be explained by the metal ions Mg, Fe, Pb, Cu, Ni in these types biochar. Bark of the tree has the highest content of ash than the wood. Miranda *et al.* (2012) reported 2.9% of ash in birch bark tree due to the high content of N, P, Zn. Miranda *et al.* (2013) reported 4.6% of ash in pine bark tree due to the high content of N

(35% of the total ash), Ca (35%), K (17%). Zn, Cu, Ni, Cr and Pb were present at levels under 1% of the total ash.

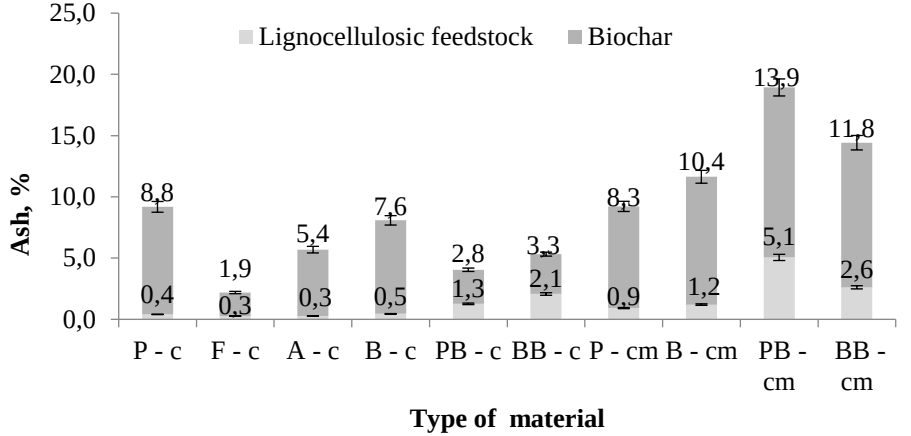

Fig. 3.2. Ash content in the feedstock and biochar (n = 3, mean value ± SD)

On the one hand, minerals in ash can promote the adsorption of PTEs by serving as additional adsorptive sites (Xu *et al.* 2013). On another hand, minerals from ash can block the pores, creating no space for adsorption of PTEs (Zhang *et al.* 2013).

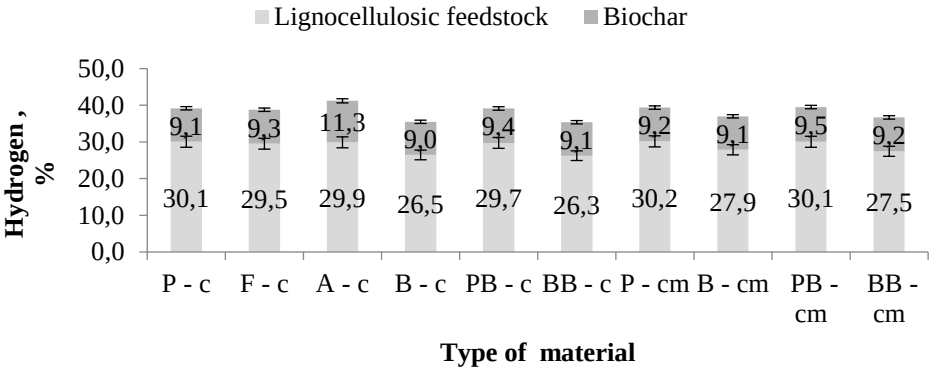

Fig. 3.3. Hydrogen content in the ligneous feedstock and biochar (n = 3, mean value ± SD)

O/C, N/C and H/C ratios of biochar are indicated in Table 3.2. The decreasing in the O/C and/or N/C ratios can indicate the increasing in the hydrophobicity and the reduction of polar groups, therefore, decrease of adsorption of PTEs (Suguihiro *et al.* 2013). The highest potential for adsorption possesses birch bark

biochar due to the highest ratios. Obtained results are higher to those in Sun *et al.* (2014) for hickory wood pyrolyzed at 450 °C, where H/C and O/C ratio was 0.04 and 0.14. H/C and O/C ratios decrease with the increase of temperature (Xiao *et al.* 2014; Rutherford *et al.* 2012).

Table 3.2. H/C, N/C, O/C ratios of biochar

Type of biochar	Ratios		
	H/C ≤ 0.7	N/C	O/C≤ 0.4
P – c	0.110	0.000	0.074
F – c	0.112	0.002	0.098
A – c	0.144	0.000	0.129
B – c	0.109	0.000	0.096
PB – c	0.117	0.003	0.126
BB – c	0.120	0.006	0.188
P – cm	0.115	0.000	0.071
B – cm	0.114	0.000	0.089
PB – cm	0.119	0.004	0.105
BB – cm	0.123	0.006	0.157

Spokas and Reicosky (2009) indicated H/C 0.043, N/C 0.004, O/C 0.119 for pine woodchip biochar at 465 °C, for hardwood char at 538 °C H/C 0.05, N/C 0.007, O/C 0.189, that corresponds to our results on pine and birch bark.

On the contaminated territory enhanced values of Pb, Cd, Zn, Cu, Cr, Ni, Mg, Fe concentration in comparison to control site were found.

After pyrolysis of the ligneous feedstock, content of PTEs in the biochar increased. Bark biochar from contaminated feedstock contained more PTEs than in wood biochar. Obtained biochar corresponded to thresholds for PTEs from EBC (2012): Pb < 120 mg/kg DM(premium), Cd < 1 mg/kg DM (premium), Cu < 100 mg/kg DM (premium), Ni < 30 mg/kg DM (premium), Zn < 400 mg/kg DM (premium), Cr < 80 mg/kg DM (premium). Unlike in the results of Helsen and van den Bulck (2005), when during the pyrolysis of wood Cu and Cr were released. Metal ions Pb, Cu, Ni, Cr, Cd may block the pores of the biochar, thus, decrease adsorption capacity of PTEs by biochar.

Physico-chemical characteristics of the biochar with indication of standard deviation (SD) values are summarized in Table 3.3.

Table 3.3. Physico-chemical properties of the biochar (n = 3, mean value ± SD)

Properties / Type of biochar	Bulk density, g/cm^3	pH	Electrical conductivity, µS/cm	CEC, cmol$_c$/kg
P – c	160.10±5.06	7.55±0.06	113.30±27.48	2.09±0.13
F – c	88.00±6.17	6.54±0.04	51.30±5.13	2.36±0.12
A – c	163.80±12.61	7.82±0.04	92.10±13.24	3.13±0.15
B – c	87.30±2.65	8.36±0.04	125.60±17.50	4.76±0.24
PB – c	106.00±3.74	8.98±0.06	143.90±4.34	11.91±0.89
BB – c	211.20±6.72	9.49±0.07	298.00±33.41	14.88±0.48
P – cm	165.23±4.15	7.68±0.05	119.40±22.33	2.13±0.08
B – cm	89.20±3.85	8.56±0.04	131.28±15.50	4.97±0.21
PB – cm	113.00±4.21	9.11±0.06	152.70±5.87	12.05±0.83
BB – cm	209.05±6.35	9.67±0.06	303.00±13.65	15.11±0.72

CEC – cation exchange capacity

As a physical property, bulk density depends on various factors, namely on material composition, particle shape and size, and specific density of individual particles, which result from the inherent physical structure of the raw material (Miranda *et al.* 2013). Bulk density was the highest in the case of birch bark and the lowest in the case of birch wood, what could be attributed to the pore structure of the biochar from this specie (Table 3.3). The dependency between variation of pH and electrical conductivity exists; the lowest values were observed for fir, the highest values − for birch bark. For coniferous trees pH of biochar was lower than for deciduous trees. Apparently, high hydrogen content in biochar (Fig. 3.3) influenced on decreasing of both pH and electrical conductivity of the biochar. Highest electrical conductivity was observed for birch bark. Bark of the trees had the highest values of cation exchange capacity, what could be attributed to the higher content of carboxylic groups on the surface of the biochar. The results of CEC on pine and birch biochar are similar with those of Komkienė and Baltrėnaitė (2016), 3.41±0.24 cmol$_c$/kg and 5.09±0.42 cmol$_c$/kg, respectively. Kaudal *et al.* (2016) indicated higher value for CEC for pine bark (20 cmol$_c$/kg), lower pH (4.9), electrical conductivity (260 µS/cm), but in that case the biochar was prepared at 650°C for 40 min. Other Figs on biochar characteristics are supplied in Annex A.

Macroporosity analysis results are presented in Fig. 3.4. Pores of different size are generated during thermal treatment of wood and lignin.

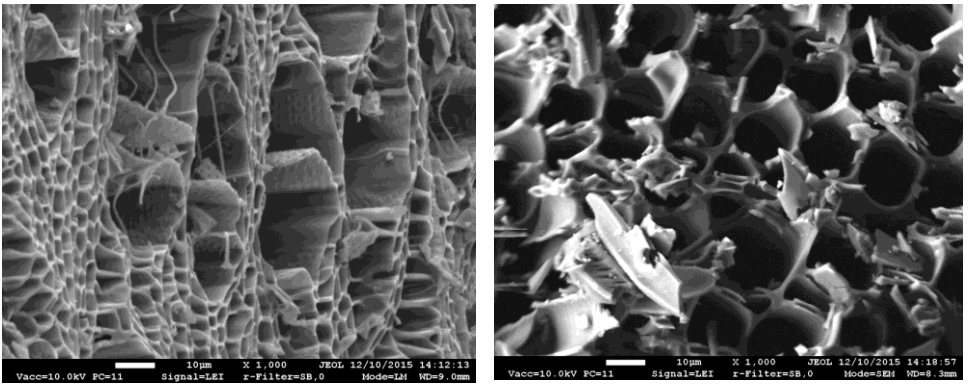

a) b)

Fig. 3.4. SEM images of biochar macroporous structure: a) birch, 450 °C, ×1000; b) pine, 450 °C, ×1000

Pore distribution in pine and birch is organized, even pine has more homogeneous morphology. In contrast to lignin, pores in birch, pine and woodchips are well-defined. Differences in morphology could be explained by the different structure of wood and lignin as non-uniform heteropolymer.

Structural properties of the biochar are shown in Table 3.4. Adsorption of PTEs is affected by micropores with the pore size less than 2 nm (Tan *et al.* 2015).

Table 3.4. Structural properties of the biochar produced from ligneous feedstock (n = 1)

Properties / Type of biochar	BET, m^2/g	Average pore diameter, nm	Total pore volume, cm^3/g	Total micropore volume, cm^3/g
P – c	25.08	2.416	0.152	0.028
F – c	26.61	2.489	0.166	0.025
A – c	18.27	4.146	0.019	0.011
B – c	20.11	4.497	0.023	0.010
PB – c	354.7	2.178	0.193	0.104
BB – c	362.1	2.121	0.192	0.125
P – cm	34.68	2.252	0.195	0.105
B – cm	23.16	2.412	0.140	0.031
PB – cm	283.9	2.250	0.160	0.072
BB – cm	326.1	3.139	0.155	0.106

a)

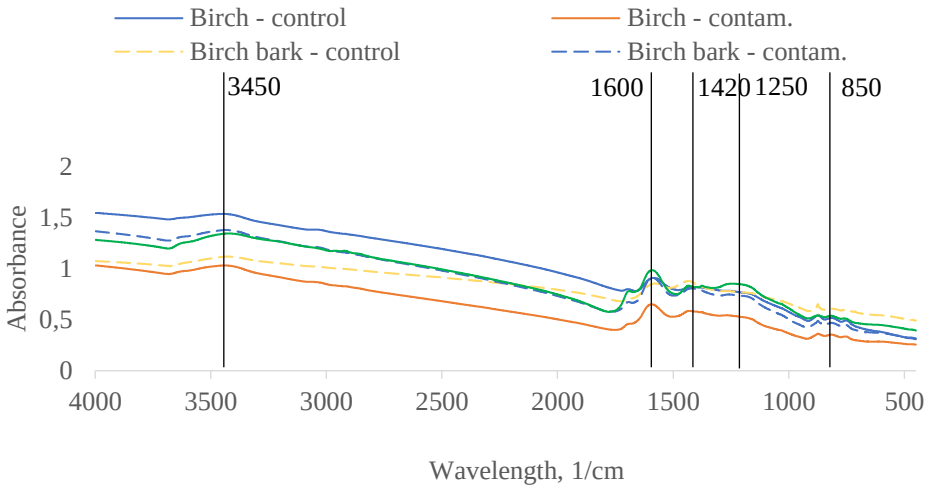

b)

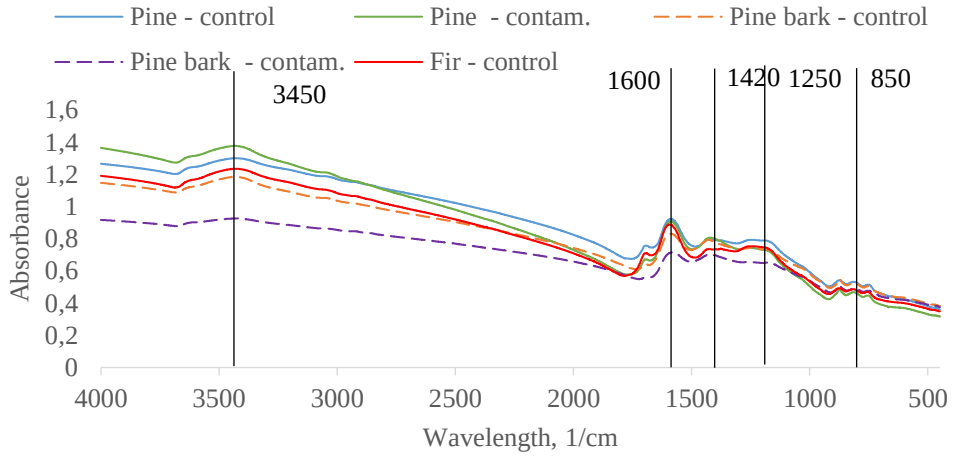

Fig. 3.5. FTIR spectra of the biochar (n = 1): a) birch; b) pine

Pine and birch bark possess higher BET surface area almost in 10 times in comparison with the wood. Respectively, total pore and micropore volumes of pine bark and birch bark were higher as well. Pine and birch from contaminated site have slightly higher BET surface area than pine and birch from reference site. Kaudal *et al.* (2016) reported specific surface area 190 m^2/g for pine bark biochar, but that biochar was prepared at 650 °C for 40 min.

Thus, BET surface area results in decreasing order: Birch (bark) - control > Pine (bark) - control > Birch (bark) > Pine (bark) > Pine > Fir - control > Pine -

control > Birch > Birch - control > Aspen - control. Results on BET surface area for barks are similar to those of birch activated carbon – 400 m^2/g (Cruz, 2012).

The FTIR spectra of the different types of biochar are presented in Fig. 3.5. Number of vacant sites on surface of adsorbent corresponds to the content of oxygen-containing functional groups, e.g. carboxylic and carbonyl groups. The main tendency of the results is similar: peak at 3400 cm^{-1} corresponds to phenolic groups, 1560–1630 cm^{-1} − to aromatic groups, 1418–1422 cm^{-1} − to alkanes. Carboxylic groups usually occur at 2500–3300 cm^{-1} and 1680–1740 cm^{-1}.

The peaks 1315 cm^{-1} and 1700 cm^{-1} corresponded to carboxylic acid functionality, that increased after modification of biochar with H_2O_2 (Huff and Lee 2016). According to the FTIR spectra, biochar from birch – control and birch bark – control had the highest content of carboxylic groups because of the highest peaks.

3.1.2. The Influence of Artificial Modifications of Biochar on Adsorptive Characteristics of the Biochar

Before modification of the biochar with metal salts $FeCl_3$ and $MgCl_2$, physico-chemical characteristics of the pine, fir and aspen biochar were investigated (Table 3.5). Water-holding capacity (WHC) is an ability of biochar to retain water. According to diameter (d), pores are classified as micropores (d<2 nm), mesopores (2 nm<d<50 nm) and macropores (d>50 nm) (Lehmann and Joseph, 2015).

Table 3.5. Physico-chemical characteristics of the biochar

Characteristics / Type of biochar	Yield, %	Bulk density, g/cm^3	TOC, %	WHC, %	Total porosity, %	Pore surface area, m^2/g	Pore volume, cm^3/g
P450	25.0	1.4	88.8	11.8	81.3	8.6	1.5
F450	23.9	1.3	88.4	13.2	80.5	8.2	1.4
A450	19.6	1.7	85.4	16.5	79.2	5.6	1.1
B450	20.1	1.8	87.9	13.5	79.7	5.8	1.2

TOC – total organic carbon, WHC – water holding capacity.

Mercury intrusion porosimetry (MIP) is a suitable technique to describe meso- and macroporous structure, in our case pores with diameter higher than 6.449 nm. Smaller-diameter pores should be investigated by N_2 adsorption at low temperatures.

Prepared in the same conditions, biochar of the different type differ in yield: aspen biochar has the lowest yield because of lower amount of lignin in the aspen feedstock. Moreover, aspen biochar has the lowest total organic carbon content because of lower amount of carbon in the aspen trees than conifer species. Though, aspen has the highest WHC, that could be attributed to the finer structure of aspen biochar. The total porosity of pine was slightly bigger than of aspen, promoting the better adsorption of contaminants. The same tendency for physico-chemical characteristics of woody biochar was observed in Komkienė and Baltrėnaitė (2016).

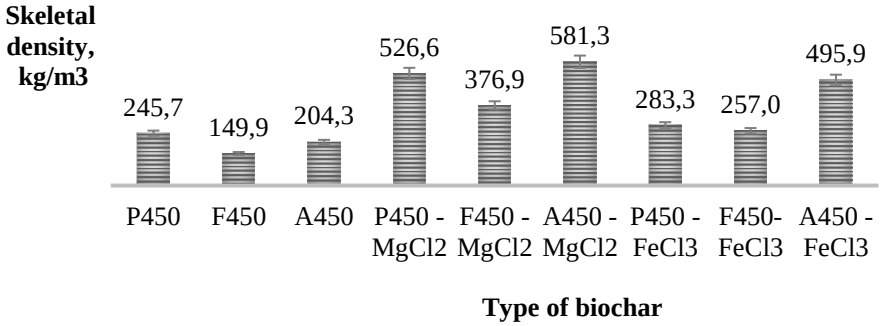

Fig. 3.6. Skeletal density of the biochar before and after modifications ± SD

The density of the modified biochars increased because of adding Mg and Fe particles (Fig. 3.6). Modification of biochar with $MgCl_2$ increased density in almost 2 times in comparison with unmodified biochar. Modification of biochar with $FeCl_3$ influenced density slightly in comparison with $MgCl_2$ modification, because of lower concentration of solution, though the density of $MgCl_2$ is lower than $FeCl_3$ (2.32 g/cm^3 and 2.9 g/cm^3, respectively).

Both type of modification decreased pH of the biochars because of adding of Mg or Fe (Table 3.6). Principally, $MgCl_2$ originated from a weak base $Mg(OH)_2$ and a strong acid HCl. $FeCl_3$ can be considered as a salt from a weak base $Fe(OH)_3$ and HCl acid. Hence, aqueous solutions of $FeCl_3$ and $MgCl_2$ were acidic. pH electrode is sensitive to hydrogen ion activity, that means that modification decreased the hydrogen content.

Both modifications reduced electrical conductivity of the biochars because of adding of Mg or Fe. High electrical conductivity is connected with the high mobility of hydrogen (Karato 2006), which was decreased after modification. Though the electrical conductivity of the biochar from different tree species had been different, after modification the values of electrical conductivity became almost equal.

Table 3.6. pH, EC, moisture and ash content of the biochar before and after modifications ± SD

BC	Modification conditions	Particle size, mm	pH	EC, µS/cm	Ash, %	Moisture, %
P450	–	0.4–1	7.55±0.06	113.30±27.48	1.1±0.02	2.23±0.01
F450	–	0.4–1	6.54±0.04	81.70±5.13	0.9±0.01	2.20±0.02
A450	–	0.4–1	7.82±0.04	92.1±5.38	1.1±0.01	5.78±0.03
B450	–	0.4–1	8.36±0.04	125.60±17.50	1.3±0.01	2.07±0.03
P450	$MgCl_2$	0.4–1	5.78±0.01	15.47±0.05	8.7±0.00	21.5±0.07
F450	$MgCl_2$	0.4–1	5.22±0.02	14.54±0.09	8.2±0.00	23.6±0.08
A450	$MgCl_2$	0.4–1	4.79±0.00	13.91±0.02	9.8±0.01	20.7±0.06
B450	$MgCl_2$	0.4–1	4.89±0.06	12.15±0.03	9.6±0.04	21.4±0.09
P450	$FeCl_3$	0.4–1	2.12±0.00	15.19±0.09	5.3±0.00	23.4±0.06
F450-	$FeCl_3$	0.4–1	2.23±0.01	11.8±0.06	7.1±0.00	25.0±0.04
A450	$FeCl_3$	0.4–1	2.18±0.01	12.19±0.09	9.1±0.00	22.3±0.03
B450	$FeCl_3$	0.4–1	2.19±0.01	11.92±0.04	9.3±0.01	21.6±0.04

Moisture content of the modified biochars increased in comparison to unmodified biochars. Excessive moisture in the biochar may block the pores, preventing the adsorption of PTEs by biochar.

Ash content refers to the mineral content of the biochar. Ash content of the modified biochars increased, that suggested that activation with $FeCl_3$ and $MgCl_2$ was made.

Depending on modification type, in case of $MgCl_2$ ash content decreased in order A450 < P450 < F450, for $FeCl_3$ − A450 < F450 < P450.

The decrease in the O/C and/or N/C ratios can indicate the increasing in the hydrophobicity and the reduction of polar groups, therefore, decrease potential of adsorption of PTEs (Suguihiro *et al.* 2013). Results from Table 3.7 on ratios are higher than those determined by Sun *et al.* (2014) for hickory wood pyrolyzed at 450 °C, where H/C and O/C ratio was 0.04 and 0.14. H/C and O/C ratios decrease with the increase of temperature (Xiao *et al.* 2014; Rutherford *et al.* 2012). Spokas and Reicosky (2009) indicated H/C 0.043, N/C 0.004, O/C 0.119 for pine woodchip biochar at 465 °C, for hardwood char at 538 °C H/C 0.05, N/C 0.007, O/C 0.189, that corresponds to our results on pine and birch bark.

Table 3.7. H/C, N/C, O/C ratios of modified and unmodified biochar

BC	Modification conditions	H/C<0.7	N/C	O/C<0.4
P450	–	0.110	0.0001	0.074
F450	–	0.112	0.002	0.098
A450	–	0.144	0.0001	0.129
B450	–	0.109	0.0003	0.096
P450	$MgCl_2$	0.258	0.001	0.090
F450	$MgCl_2$	0.182	0.001	0.113
A450	$MgCl_2$	0.174	0.002	0.141
B450	$MgCl_2$	0.315	0.000	0.109
P450	$FeCl_3$	0.202	0.000	0.105
F450-	$FeCl_3$	0.153	0.000	0.117
A450	$FeCl_3$	0.162	0.002	0.144
B450	$FeCl_3$	0.271	0.003	0.099

Modification increased cation exchange capacity (CEC) of the biochars (Table 3.8).

Table 3.8. Cation exchange capacity of the biochar before and after modification ± SD

BC	Modification conditions	CEC, $cmol_c/kg$
P450	–	2.09±0.13
F450	–	2.36±0.12
A450	–	3.13±0.15
B450	–	4.76±0.24
P450	$MgCl_2$	2.98±0.16
F450	$MgCl_2$	2.62±0.13
A450	$MgCl_2$	3.62±0.15
B450	$MgCl_2$	4.99±0.17
P450	$FeCl_3$	5.00±0.21
F450	$FeCl_3$	5.95±0.29
A450	$FeCl_3$	5.48±0.25
B450	$FeCl_3$	5.52±0.22

The highest CEC was observed in $FeCl_3$ modification, because the modication with $FeCl_3$ form more oxygen-rich functional groups were formed on

the biochar, especially the C═O group, than $MgCl_2$ activation. Modification with $MgCl_2$ increased BET in 4 times, but with $FeCl_3$ – decreased in 6 times (Table 3.9).

The FTIR spectra of the types of the different types of biochar are presented in Fig. 3.7. Increased cation exchange capacity of the engineered biochar suggested the increased amount of oxygen-containig functional groups, promoting enhanced adsorption of cationic metals through ion exchange.

Table 3.9. Structural properties of the modified and unmodified biochar

BC	Modification conditions	BET, m^2/g	Average pore diameter, nm	Total pore volume, cm^3/g	Total micropore volume, cm^3/g
P450	–	25.08	2.416	0.152	0.028
F450	–	26.61	2.489	0.166	0.025
A450	–	18.27	4.146	0.019	0.011
B450	–	20.11	4.497	0.023	0.010
P450	$MgCl_2$	33.62	13.80	0.116	0.013
F450	$MgCl_2$	82.59	5.42	0.112	0.037
A450	$MgCl_2$	20.23	3.43	0.068	0.009
B450	$MgCl_2$	96.45	4.16	0.100	0.042
P450	$FeCl_3$	18.38	4.33	0.021	0.009
F450	$FeCl_3$	17.22	7.81	0.034	0.004
A450	$FeCl_3$	6.19	3.45	0.019	0.003
B450	$FeCl_3$	3.30	6.25	0.005	0.001

$FeCl_3$ modification adds more phenolic groups on the surface, than $MgCl_2$ modification.

Ahmed *et al.* (2016) stated that modification method with metal salts influences physical and chemical properties of biochar, i.e. H/C, O/C and N/C molar ratios, CEC, ash content, facilitating enhanced removal of organic and inorganic contaminants, although with reduced pore volumes.

Unmodified aspen biochar showed lower values of yield (19.5%), porosity (79%) and TOC (85%) in comparison with conifer trees (23–25%, 81%, 88–89% respectively), but higher WHC (16.5% to 11–13%).

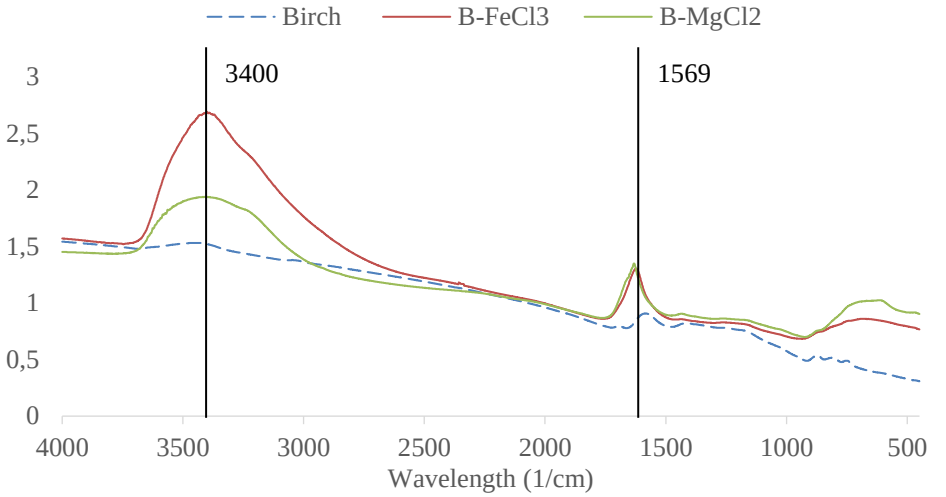

Fig. 3.7. Effect of modifications on biochar surface

The most important characteristics for adsorption of cationic metals are pH, CEC, ash content. Results showed that modifications significantly decreased pH of the biochars, i.e. modification with $FeCl_3$ decreased pH of the biochar in 3 times, while $MgCl_2$ modification decreased pH on 20%. Increased ash content (in 9 times) showed the adding of Mg into the biochar. $FeCl_3$ results in higher CEC because of adding of oxygen functional groups on the surface of biochar.

For modification of the biochar with H_2O_2, biochar was marked as follows: first letter *B* means biochar, last letter *P* or *G* means powder or granular fraction, respectively. Numbers 3, 15, 30% indicate concentration of H_2O_2 solution and *r* indicates that modification was made using rotation.

Higher bulk density is associated with higher mechanical strength. The bulk density is related to the mechanical strength, which is the characteristic used to define the biochar ability to withstand wear and tear during its use. In adsorption systems, the media should remain stable with time. Modification with H_2O_2 increased bulk density of the biochar, confirming that there was almost no weight loss from the H_2O_2 treatment (Fig. 3.8).

Biochar, modified with rotation, had the higher bulk density than biochar, modified without rotation. Biochar with powder particle size (0.4–1 mm-diameter) had higher bulk density than biochar with granular particle size (1- 3 mm-diameter). Xue *et al.* (2012) reported increase in bulk density from 240 to 250 kg/m^3, when hydrochar was modified with 10% of H_2O_2 solution. Results on bulk density of birch biochar are lower in comparison to those of Baltrėnaitė *et al.* (2017) for woodchips pyrolized at 450 °C – 440 kg/m^3.

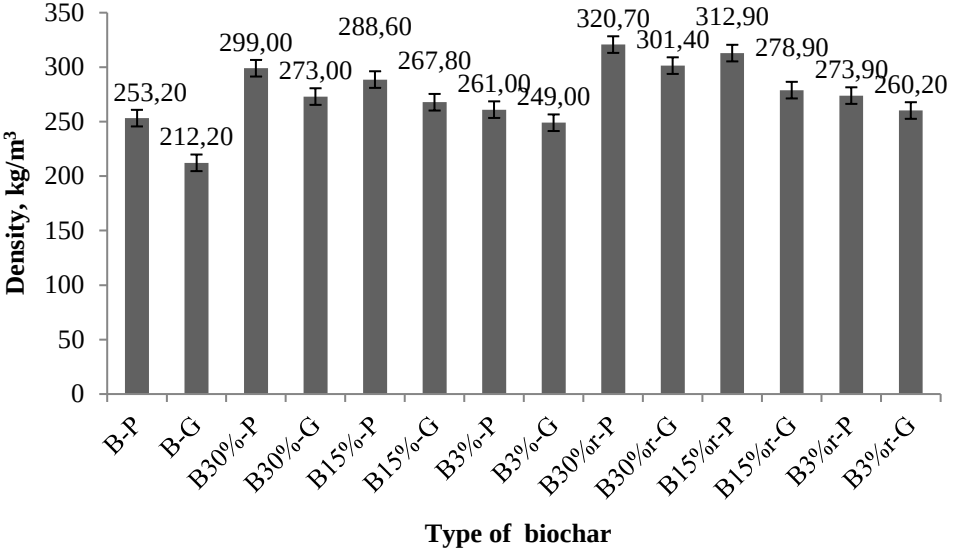

Fig. 3.8. Density of the unmodified and modified biochar (n = 3, mean value ± SD)

It is known that adsorption of PTEs through complexation, electrostatic attraction and ion exchange is affected by micropores with the pore size less than 2 nm (Tan *et al.* 2015). Modification with H_2O_2 increased BET specific surface area (Table 3.10). Biochar, modified with rotation, had the higher BET SSA than biochar, modified without rotation. Biochar with powder particle size (<1 mm) had higher BET SSA than biochar with granular particle size (1–3 mm). Respectively, B30%r-P biochar had the highest BET SSA (321.7 m^2/g), that exceeds BET SSA of unmodified biochar almost in 15 times (20.11 m^2/g). Results on BET SSA are lower to those of birch activated carbon – 400 m^2/g (Cruz 2012). B3%-G biochar had the lowest BET SSA (50.7 m^2/g), that exceeds BET SSA of unmodified biochar only in 2.5 times (20.11 m^2/g). Baltrėnas *et al.* (2015) showed higher result for unmodified birch than indicated in the current study – 73.19 m^2/g.

The pH of the modified biochar was lower in comparison to unmodified biochar (8.64 for powder fraction and 8.36 for granular fraction), which could be attributed to the weak acidic nature of the created carboxyl surface functional groups (Fig. 3.9).

Xue *et al.* (2012) reported decrease in pH from 6.2 to 4.4, when hydrochar was modified with 10% of H_2O_2 solution. Biochar, modified with rotation, had even lower pH than biochar, modified without rotation. Biochar with powder particle size (<1 mm) had higher pH than biochar with granular particle size (1– 3 mm), because lower particle size favors modification with solution. Higher concentration of H_2O_2 solution corresponds to higher decrease in pH. Therefore,

the highest pH had B3%-P biochar among all modified types of biochar, the lowest – B30%r-G biochar.

Table 3.10. Specific surface area and pore characteristics of the biochar produced from ligneous feedstock

Type of biochar	BET, m^2/g	Average pore diameter, nm	Total pore volume, cm^3/g	Total micropore volume, cm^3/g
B	20.11	4.497	0.023	0.010
B30%-P	264.9	2.329	0.154	0.116
B30%-G	236.4	2.477	0.146	0.081
B15%-P	152.3	2.893	0.11	0.091
B15%-G	121.9	3.239	0.099	0.142
B3%-P	82.8	3.39	0.079	0.048
B3%-G	50.7	3.51	0.059	0.032
B30%r-P	321.7	2.269	0.183	0.111
B30%r-G	310.4	2.333	0.181	0.171
B15%r-P	301.5	2.31	0.174	0.172
B15%r-G	289.9	2.29	0.166	0.165
B3%r-P	277.0	2.33	0.161	0.158
B3%r-G	205.8	2.44	0.126	0.119

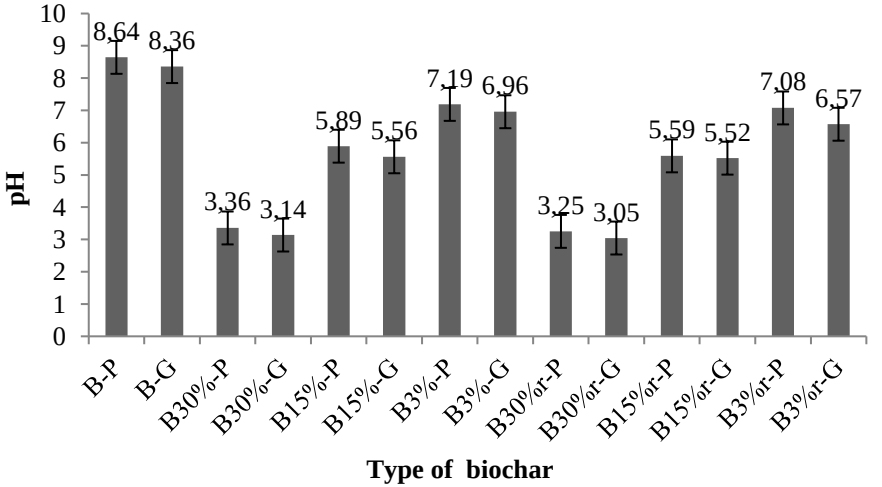

Fig. 3.9. pH of the unmodified and modified biochar (n = 3, mean value ± SD)

Electrical conductivity depends on the inorganic content of the biochar and thus could be used to calculate the salinity of the material (Allaire *et al.* 2015). Lower conductivity is associated with the higher degree of aromatic condensation in char (Brewer 2012). Electrical conductivity (EC) of the modified biochar was higher in comparison to unmodified biochar, which could be attributed to the increase in oxygen content (Fig. 3.10). Biochar, modified with rotation, had even higher EC than biochar, modified without rotation. Higher concentration of H_2O_2 solution corresponds to higher increase in EC. Therefore, the highest EC had B30%r-P biochar among all modified types of biochar, the lowest – B3%-G biochar. Biochar with powder particle size (<1 mm) had higher EC than biochar with granular particle size (1–3 mm), because lower particle size favors modification with solution.

Modification with H_2O_2 increased moisture content (Fig. 3.11). Biochar, modified with rotation, had the higher moisture content than biochar, modified without rotation. Biochar with powder particle size (<1 mm) had lower moisture content than biochar with granular particle size (1–3 mm). The highest value for moisture was determined for the B30%r-G biochar. The lowest moisture content among the modified types of biochar was determined for B3%-P biochar.

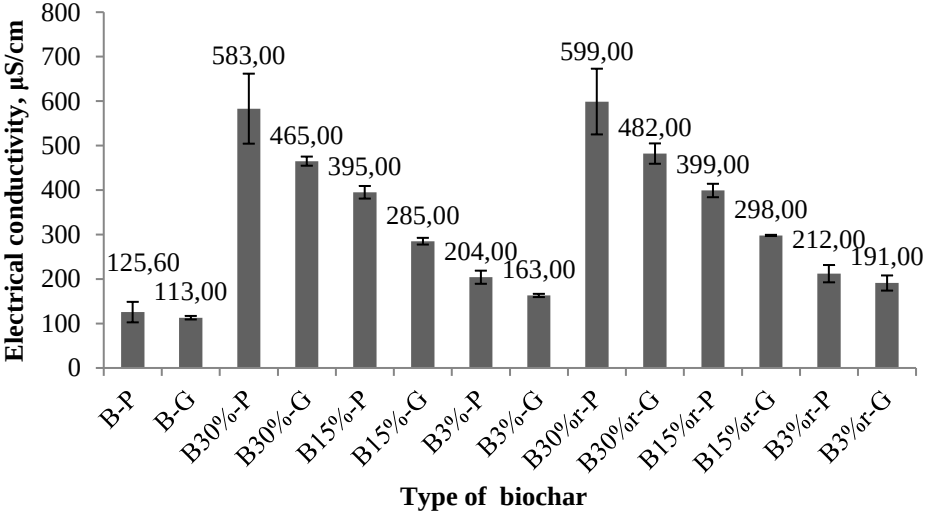

Fig. 3.10. Electrical conductivity of the unmodified and modified biochar (n = 3, mean value ± SD)

Ash is the residue, remaining after combustion under specified conditions, which is composed primarily of oxides and sulfates. The ash fraction of biochar is enriched with inorganic non-crystalline (amorphous) and poorly to well-crystallized (mineral) constituents. The inorganic constituents of the ash fraction

of biochar are usually metal carbonates, silicates, phosphates, sulfates, chlorides and oxy-hydroxides.

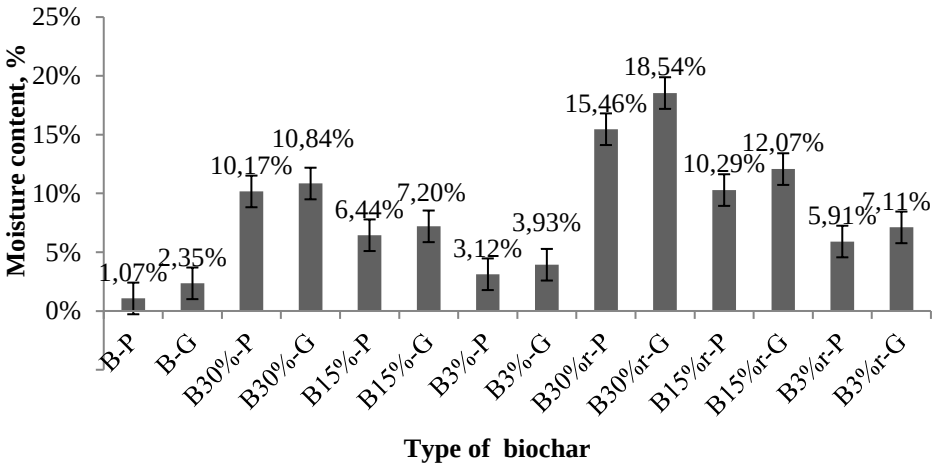

Fig. 3.11. Moisture content in the unmodified and modified biochar (n = 3, mean value ± SD)

Modification with H_2O_2 decreased ash content of the modified biochar. Biochar, modified with rotation, had the higher ash content than biochar, modified without rotation. Biochar with powder particle size (<1 mm) had higher ash content than biochar with granular particle size (1–3 mm). The highest values of ash had B3%-P biochar, the lowest – B30%r-G biochar. On the one hand, minerals in ash can promote the adsorption of PTEs by serving as additional adsorptive sites (Xu *et al.* 2013). On another hand, metal ions from ash can block the pores, creating no space for adsorption of PTEs (Zhang *et al.* 2013).

Three types of ratios, in particular, O/C, H/C and N/C, were calculated to attribute biochar hydrophilicity, aromaticity and polarity level (Table 3.11). Correlation between higher O:C ratio and higher CEC was found. The decrease in the O/C and/or N/C ratios can indicate the increasing in the hydrophobicity and the reduction of polar groups, therefore, decrease potential of adsorption of PTEs (Suguihiro *et al.* 2013). Modification with H_2O_2 increased H/C, N/C and O/C ratios.

Biochar, modified with rotation, had the highest ratios than biochar, modified without rotation. Respectively, B30%r-P biochar had the highest ratios (H/C = 0.212, N/C = 0.0032, O/C = 0.293).

Table 3.11. Hydrogen, nitrogen and oxygen to carbon ratios of biochar

Type of biochar	Ratios		
	H/C ≤ 0.7	N/C	O/C≤ 0.4
B-P	0.109	0.0003	0.096
B-G	0.101	0.0003	0.092
B30%-P	0.182	0.0027	0.248
B30%-G	0.162	0.0022	0.228
B15%-P	0.137	0.0014	0.204
B15%-G	0.126	0.0011	0.170
B3%-P	0.119	0.0004	0.115
B3%-G	0.104	0.0003	0.103
B30%r-P	0.212	0.0032	0.293
B30%r-G	0.181	0.0027	0.275
B15%r-P	0.174	0.0016	0.222
B15%r-G	0.141	0.0012	0.180
B3%r-P	0.128	0.0007	0.122
B3%r-G	0.116	0.0005	0.109

Modification with H_2O_2 increased CEC of the biochar (Fig. 3.12). Biochar, modified with rotation, had the higher CEC than biochar, modified without rotation. This increase in CEC can be attributed to an increase in the presence of acidic oxygen functional groups on the surface of the biochar materials.

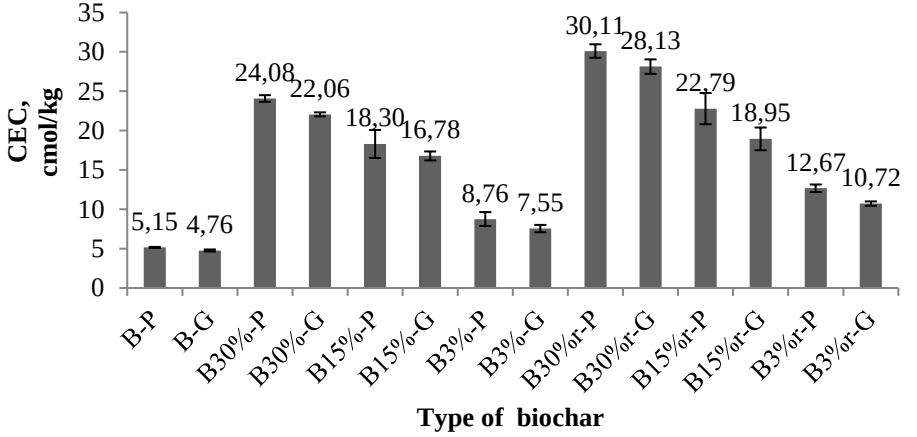

Fig. 3.12. Cation exchange capacity of modified and unmodified biochar

Respectively, B30%r-P biochar had the highest CEC (30.11 $cmol_c/kg$). For comparison, unmodified hydrochar (Huff and Lee 2016) had 17.95 $cmol_c/kg$, modified with 3% H_2O_2 solution – 23.3 $cmol_c/kg$, 20% H_2O_2 solution – 25.43 $cmol_c/kg$, 30% H_2O_2 solution – 31.37 $cmol_c/kg$.

FTIR was used in this study to describe the development and alterations in functional group chemistry of the studied types of biochar modified in different ways. The FTIR spectra of the types of the different types of biochar are presented in Fig. 3.13-3.15.

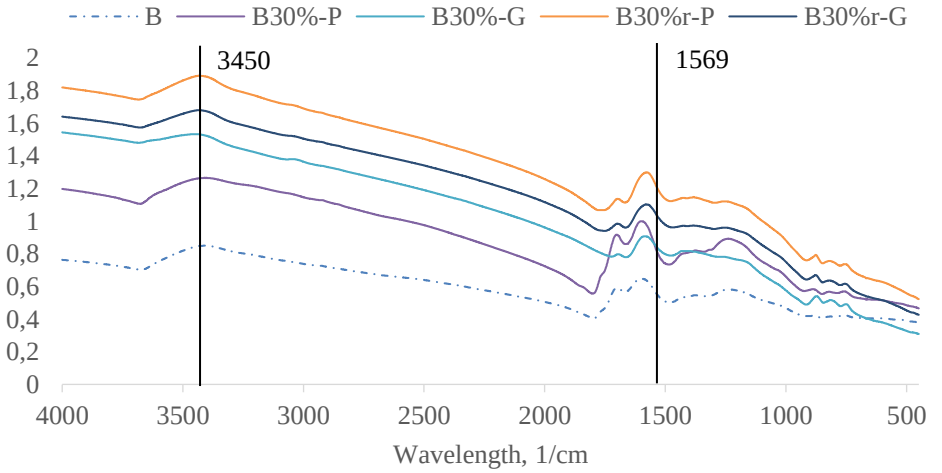

Fig. 3.13. FTIR spectra of unmodified biochar and modified with 30% H_2O_2 solution

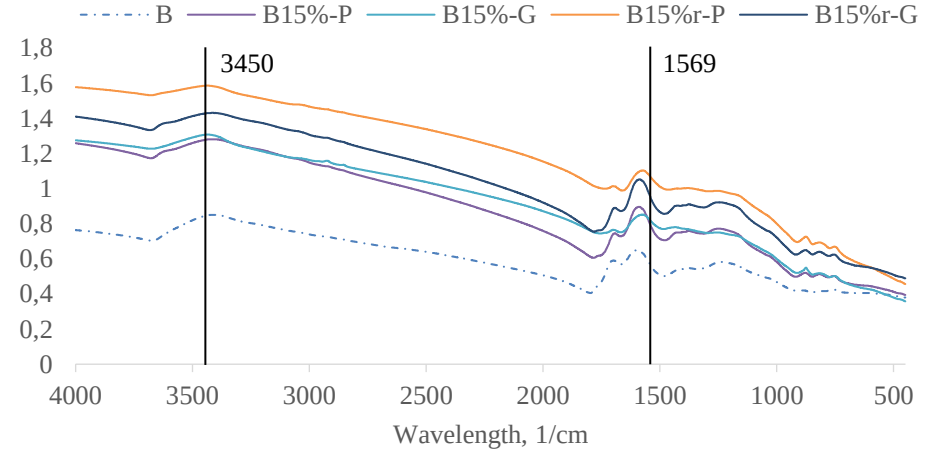

Fig. 3.14. FTIR spectra of unmodified biochar and modified with 15% H_2O_2 solution

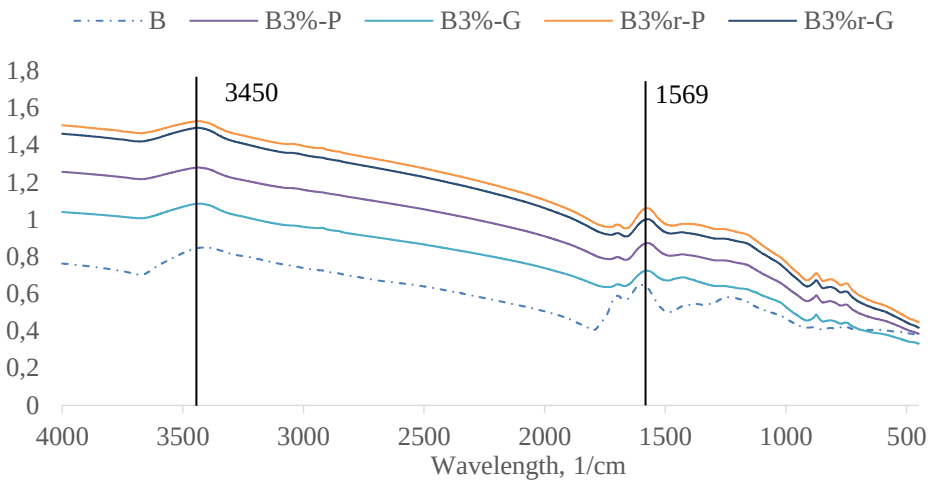

Fig. 3.15. FTIR spectra of unmodified biochar and modified with 3% H_2O_2 solution

Number of vacant sites on surface of adsorbent corresponds to the content of oxygen-containing functional groups, e.g. carboxylic and carbonyl groups. Huff and Lee (2016) stated that the peaks 1315 cm^{-1} and 1700 cm^{-1} corresponded to carboxylic acid functionality, that increased after modification of biochar with H_2O_2.

From Fig. 3.16 peaks at 1500–1750 cm^{-1} corresponded to carboxylic groups, while peaks at 3250–3500 cm^{-1} corresponded to phenolic groups on the biochar surface. Modification with H_2O_2 increased content of carboxylic groups, especially in case of rotation during modification.

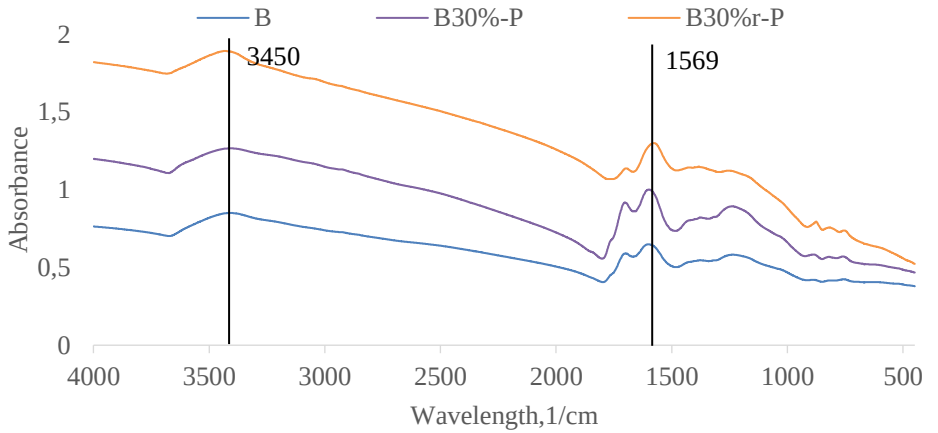

Fig. 3.16. Effect of H_2O_2 modification and rotation of BC surface

With the increasing of the percentage of H_2O_2-solution content of carboxylic and phenolic groups increases; the highest peak for carboxylic groups was observed for 30%-modified biochar with rotation. Rotation process favors modification of biochar and increases content of phenolic and oxygen-containing functional groups.

It was found that H_2O_2 modification can activate birch-derived biochar and increase cation exchange capacity 6-fold (from 5.15 $cmol_c/kg$ to 30.11 $cmol_c/kg$) and BET specific surface area 15-fold (from 20.11 m^2/g to 321.7 m^2/g). Increase in cation exchange capacity can be attributed to the increase of acidic carboxylic functional groups on the surface of the biochar, as evidenced by FTIR and the pH.

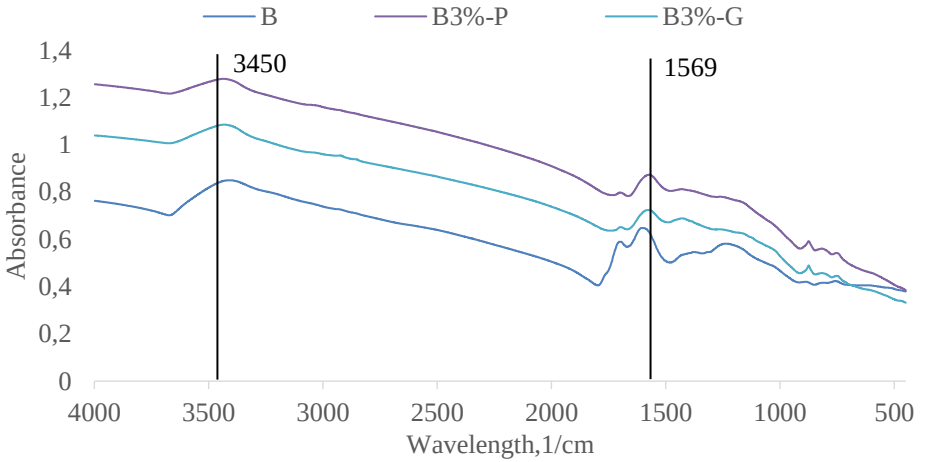

Fig. 3.17. Effect of H_2O_2 modification and particle size of BC surface

Smaller particle size favors modification of biochar and increases content of phenolic and oxygen-containing functional groups (Fig. 3.17).

Concentration of modification solution favors modification of biochar and increases content of phenolic and oxygen-containing functional groups (Fig. 3.18).

Increase in specific surface area may be explained by the increase in micropore volume as a result of oxygenation of the biochar. H_2O_2 modification influences other physico-chemical characteristics of the biochars. It increases density in 1.26 times, electric conductivity in 4.77 times, H/C in 2 times and O/C ratios in 3 times, reduces pH in 2.66 times and ash content in 2 times.

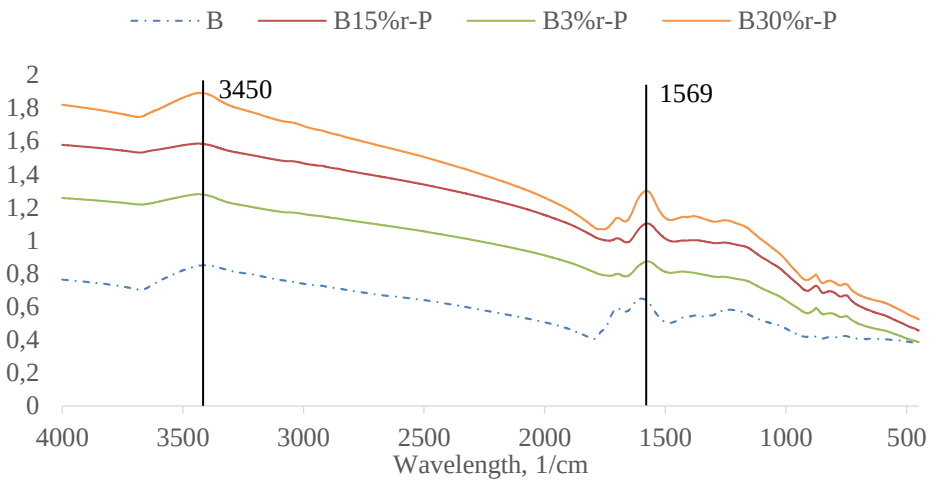

Fig. 3.18. Effect of H_2O_2 modification and solution concentration of BC surface

Smaller biochar particle size and rotation favor modification process. Thus, biochar with smaller particle size (0.4–1 mm) has CEC and BET specific surface area than biochar with particle size 1–3 mm modified in the same way. Biochar modified with rotation, has higher cation exchange capacity on 25%, specific surface area on 21%, N/C and O/C ratios.

3.1.3. Adsorption of Potentially Toxic Elements from Synthetic Solutions and Landfill Leachate by Biochar

From preliminary adsorption experiments, H_2O_2-modified biochar at dosage 9 g/l showed the highest adsorption efficiency in all types of solutions than other tested types of biochar:

1) mono-component solutions (Cd 0.2 mg/l, Pb 1 mg/l, Cu 4 mg/l, Ni 1 mg/l, Cr 4 mg/l, Zn 6 mg/l): Zn 93%, Cd 96%, Cr 96%, Cu 98%, Pb 96%, Ni 92%;

2) multi-component solution with different initial concentration of PTEs (Cd 0.2 mg/l, Pb 1 mg/l, Cu 4 mg/l, Ni 1 mg/l, Cr 4 mg/l, Zn 6 mg/l): Zn 91%, Cd 95%, Cr 79%, Cu 95%, Pb 95%, Ni 90%;

3) multi-component solutions with equal initial concentration of PTEs (Cd 1 mg/l, Pb 1 mg/l, Cu 1 mg/l, Ni 1 mg/l, Cr 1 mg/l, Zn 1 mg/l): Zn 79%, Cd 74%, Cr 77%, Cu 85%, Pb 95%, Ni 89%.

Therefore, this type of modified biochar along with unmodified biochar was chosen for further adsorption experiments.

Firstly, adsorption of PTEs from synthetic aqueous solutions was investigated. The percentage of PTE removed from solution decreased as a

function of the initial amount of PTE added to solution. This decrease could be ascribed to the ratio of PTE in solution to the available sorption sites. At lower initial concentration, this ratio is lower which influences PTE uptake but at higher initial PTE concentration, the ratio is higher and the available sorption site quickly becomes saturated which decreases.

Table 3.12. Maximum adsorption efficiency at initial concentration of PTEs 10 mg/l

Biochar	Ni, %	Cr, %	Pb, %	Cd, %	Zn, %	Cu, %
H_2O_2-m. BC	82.3	81.2	95.5	85.3	84.9	85.6
Birch BC	65.5	58.7	86.8	66.1	61	72.7

Cu^{2+} adsorption efficiency onto the manure biochar was 87.2% and for Pb^{2+} – 94.3% (Kołodynska *et al.* 2012). The adsorption capacities of rice husk biochar and MgO–BCR for Cd^{2+} reached 6.36 and 18.1 mg/g, respectively (Xiang *et al.* 2018) at initial concentration 100 mg/l. Zhou *et al.* (2018) found that ferromanganese modified biochar at initial concentration 50 mg/l exhibited maximum Cu^{2+} and Cd^{2+} adsorption capacities of 64.9 and 101.0 mg/g, respectively, exceeding the corresponding values of biochar (21.7 and 28.0 mg/g, respectively).

pH of solution has a great importance in cation sorption because it influences chemical speciation of the metal in solution and also on the ionization of chemically active sites on the sorbent, affecting ion exchange and metal deposition reactions to influence metal ion concentrations in aqueous solution (Zhou *et al.* 2018).

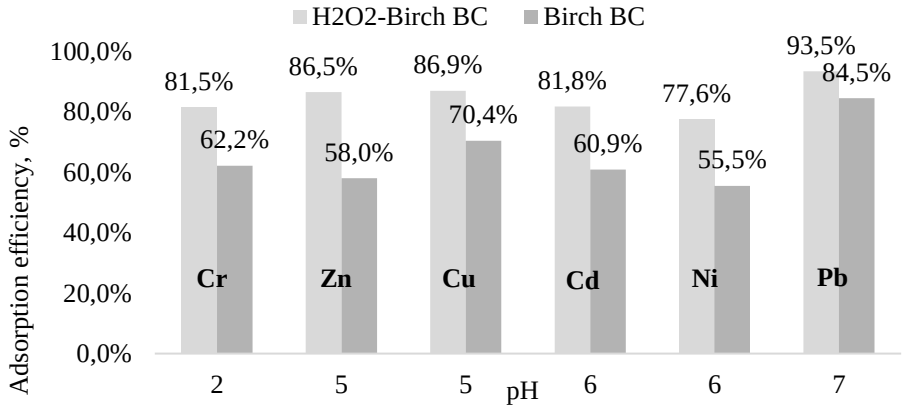

Fig. 3.19. Maximum adsorption efficiency of biochar depending on PTEs and pH

As pH influence on Cr^{3+}, Cd^{2+}, Pb^{2+}, Zn^{2+}, Ni^{2+}, Cu^{2+} adsorption was tested with various pH of solution (2, 4, 5, 6, 7, 8, 10), Fig. 3.19 represents summarized data including only that pH values for Cr^{3+}, Cd^{2+}, Pb^{2+}, Zn^{2+}, Ni^{2+}, Cu^{2+}, where adsorption efficiency was the highest.

During experiments was found, that adsorption efficiency increased from pH = 2, and after reaching its maximum, adsorption efficiency was decreased. Cr was exception, as the maximum adsorption efficiency was reached at pH = 2.

The highest adsorption was obtained of Ni^{2+} and Co^{2+} were carried out at pH = 7 for both Ni^{2+} and Co^{2+} ions (Kilic *et al.* 2013). Zama *et al.* (2017) observed high Pb^{2+} adsorption by mulberry wood biochar (97.5–99.8 %) due to organic functional groups, mineral content, ionic content and π-electrons, and peanut shells biochar – Cd^{2+} (50–90%) due to electrostatic attraction at pH 5.5. Due to ion exchange, date seed biochar adsorbed 69% and 72% of the Cu^{2+} and Ni^{2+} at pH = 6 (Mahdi *et al.* 2018).

Table 3.13. Maximum adsorption efficiency at contact time 300 min

Biochar	Ni, %	Cr, %	Pb, %	Cd, %	Zn, %	Cu, %
H_2O_2-m. BC	84.4	82.7	95.7	86.4	87.5	86.9
Birch BC	58.2	60.7	88.6	68.4	59	74.1

Adsorption efficiency and capacity was increased with the increase of the contact time, reaching its maximum at 300 min (Table 3.13). In study of Kilic *et al.* (2013) large amounts of metal ions Ni^{2+} and Co^{2+} were removed within 150 min. After that the capacity of adsorption remained constant.

Table 3.14. Maximum adsorption efficiency at biochar dosage 5 g/l

Biochar	Ni, %	Cr, %	Pb, %	Cd, %	Zn, %	Cu, %
H_2O_2-m. BC	76.1	74.9	93.5	81.4	80	79.5
Birch BC	48.6	50.7	84.5	59.2	55.3	67.3

Applying an optimum dosage of biochar to contaminants removal is crucial for its cost-effective application. Adsorption efficiency and capacity were the highest at higher biochar dosage, reaching its maximum at 5 g/l; that can be attributed to the increase in available adsorption surface and the availability of more adsorption sites (Table 3.14).

Adsorption efficiency and capacity increased with the increase of temperature (Fig. 3.20), because of decreasing viscosity and increasing molecular

motion allowing the uptake of molecules into the pores more easily, reaching its maximum at 40 °C. The range of temperatures which favours the adsorption process was 10–45 ºC with optimal temperature at 40 ºC (Horsfall and Spiff 2005).

a)

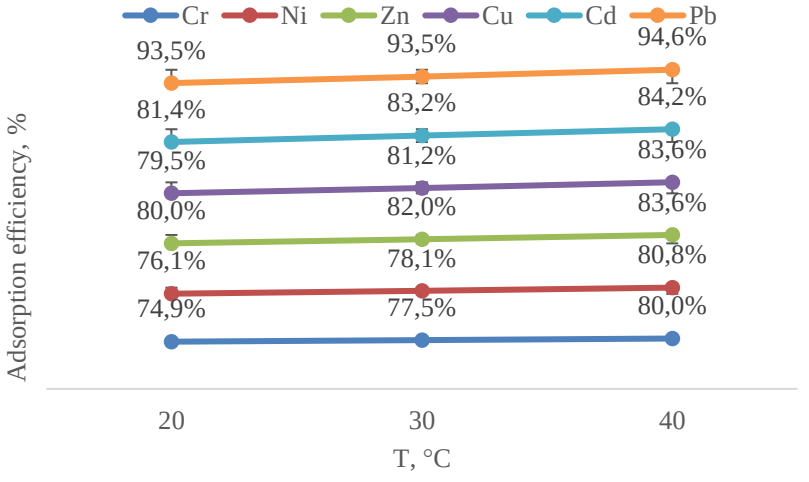

b)

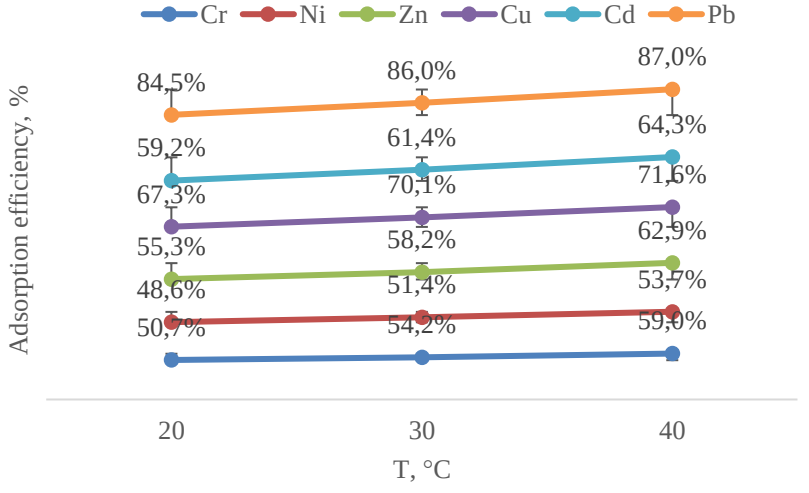

Fig. 3.20. Effect of temperature on adsorption efficiency of PTEs on: a) H_2O_2-modified biochar; b) unmodified biochar

Temperature, higher than 10 °C favors the increase in adsorption of PTEs onto biochar due to providing to PTEs ions sufficient energy to overcome the diffuse double layer and adsorb onto biochar's interior structure (Liu and Zhang 2009). It leads to higher mass transfer rate from bulk to the boundary layer around the surface of the carbon particle. At temperature higher than 40 ºC adsorption decreases, because the thickness of the boundary layer decreases due to the increased tendency of the PTE ion to escape from the biomass surface to the solution phase (Aksu & Kutsal 1991).

Pb(II) uptake increased with an increase in temperature for oak wood char and oak bark char in the range of 5–40 °C (Mohan *et al.* 2007).

Table 3.15. Maximum adsorption efficiency at particle size 0.4–1.0 mm

Biochar	Ni, %	Cr, %	Pb, %	Cd, %	Zn, %	Cu, %
H_2O_2-m. BC	76.1	74.9	93.5	81.4	80	79.5
Birch BC	48.6	50.7	84.5	59.2	55.3	67.3

Adsorption efficiency and capacity were higher at lower particle size (Table 3.15). Particle size has significant effects on biochar chemical composition and pore structure. For instance, small biomass particle sizes gave chars with larger BET surface areas and micropore volume (Sun *et al.* 2012). No significant influence of competing ions on adsorption efficiency could be found in Annex D.

Results on isotherm fitting and kinetic parameters of Cr^{3+}, Cd^{2+}, Pb^{2+}, Zn^{2+}, Ni^{2+}, Cu^{2+} adsorption by unmodified birch BC and H_2O_2-modified birch BC could be found in Annex B,C.

In this study, the R_L values were all within the range of 0–1, indicating the favorable nature for adsorption of PTEs from solution on biochar. The 1/n values in this study for PTEs also fell into the range of 0–1, indicating the favorable adsorption of PTEs on biochar. The well-fitted model indicated that the adsorption would take place on a heterogeneous surface. The values in this study are in the range with other studies' values (Shukla and Pai (2005), Gazi *et al.* (2018), Agrafioti *et al.* (2014), Yang *et al.* (2013), Komkienė and Baltrėnaitė (2016), Wu *et al.* (2017), Xiang *et al.* (2018), Wang *et al.* (2015)).

Adsorption kinetics study is important in order to determine the uptake rate of adsorbate at the solid-phase interface. In this study, pseudo-second order model fitted for H_2O_2-modified biochar, and intraparticle diffusion model – for birch biochar. The values in this study correspond to other studies' values (Ghasemi *et al.* 2012, Nethaji *et al.* 2013, Mahdi *et al.* 2018).

Thermodynamic studies are necessary to conclude whether the adsorption process is spontaneous. Gibb's free energy change, $\Delta G°$, is the fundamental

criterion of spontaneity. Results on thermodynamics are indicated in the Table 3.16.

Reactions occur spontaneously at a given temperature if ΔG° is a negative value. In all cases ΔG° decreases with an increase in temperature -that indicates that the adsorption process becomes more favorable at higher temperatures.

The positive value of ΔH° in all cases indicates that the adsorption reaction is endothermic. The positive value of ΔS° in all cases suggests that some structural changes occur on the adsorbent, and the randomness at the solid/liquid interface in the adsorption system increases during the adsorption process.

Table 3.16. Thermodynamic parameters of PTEs adsorption on biochar in laboratory solutions

Biochar	T, K	Ni			Cr			Pb		
		ΔG°	ΔH°	ΔS°	ΔG°	ΔH°	ΔS°	ΔG°	ΔH°	ΔS°
H_2O_2-Birch BC	293.15	1.10	10.64	0.03	1.25	10.99	0.03	-2.56	7.53	0.03
H_2O_2-Birch BC	303.15	0.85			0.95			-2.66		
H_2O_2-Birch BC	313.15	0.45			0.59			-3.24		
Birch BC	293.15	4.06	7.85	0.01	3.85	12.76	0.03	-0.21	7.98	0.03
Birch BC	303.15	3.91			3.64			-0.53		
Birch BC	313.15	3.80			3.24			-0.77		
Biochar	T, K	Ni			Cr			Pb		
		ΔG°	ΔH°	ΔS°	ΔG°	ΔH°	ΔS°	ΔG°	ΔH°	ΔS°
H_2O_2-Birch BC	293.15	0.33	7.47	0.02	0.55	9.43	0.03	0.62	10.46	0.03
H_2O_2-Birch BC	303.15	0.02			0.24			0.36		
H_2O_2-Birch BC	313.15	-0.16			-0.06			-0.05		
Birch BC	293.15	3.01	8.26	0.02	3.40	11.98	0.03	2.16	7.66	0.02
Birch BC	303.15	2.89			3.23			1.91		
Birch BC	313.15	2.66			2.82			1.78		

ΔG°, Kj/mol; ΔH°, Kj/mol; ΔS°, kj/mol/K

The next step of adsorption experiments was to investigate adsorption of potentially toxic elements from landfill leachate.

Table 3.17. Maximum adsorption efficiency at contact time 300 min

Biochar	Ni, %	Cr, %	Pb, %	Cd, %	Zn, %	Cu, %
H_2O_2-m. BC	53.7	50.5	54.5	21.4	58.4	52.4
Birch BC	38.1	43.8	40.1	18.1	31.6	29.4

Adsorption efficiency and capacity was increased with the increase of the contact time, reaching its maximum at 300 min (Table 3.17). Azmi *et al.* (2016) found the optimum contact time 180 min with removal of color at 80%, COD at 72.98%, NH3-N at 33.06%. In the early stage, there were larger surface sites that lead to higher adsorption capacity at a short period of time. However, as the contact time prolonged and approached to equilibrium, the availability of sorption sites decrease and becomes difficult to occupy due to repulsive forces between the PTE molecules on the solid and bulk phases. As a consequence, the removal rates slow down due to the competition for the adsorption sites. Shehzad *et al.* (2016) found the optimum removals for color, COD, and NH3-N were obtained at 3 h, as 71.93, 75.73, and 78.32%, respectively.

Table 3.18. Maximum adsorption efficiency at biochar dosage 100 g/l

Biochar	Ni, %	Cr, %	Pb, %	Cd, %	Zn, %	Cu, %
H_2O_2-m. BC	64.6	64.2	65.7	25.8	49.9	47.9
Birch BC	42.9	47.2	51.1	20.5	44.2	40.6

Biochar dosage predicts the cost of biochar per unit of PTE to be treated. Adsorption efficiency and capacity were the highest at higher biochar dosage, reaching its maximum at 100 g/l (Table 3.18). Azmi *et al.* (2016) found the optimum AC dosage 70 g/l with removal efficiency of 94.74% color, 83.61% COD, and 46.65% NH3-N. Shehzad *et al.* (2016) found the optimum biochar dosage 70 g/l with color, COD, and NH3-N removal efficiencies of 95.10, 84.94, and 95.77%, respectively.

Table 3.19. Maximum adsorption efficiency at particle size 0.4–1.0 mm

Biochar	Ni, %	Cr, %	Pb, %	Cd, %	Zn, %	Cu, %
H_2O_2-m. BC	64.6	64.2	72.4	49.9	66.6	62.8
Birch BC	23.8	29.6	67.4	35	25.6	40.6

Adsorption efficiency and capacity were higher at lower particle size.

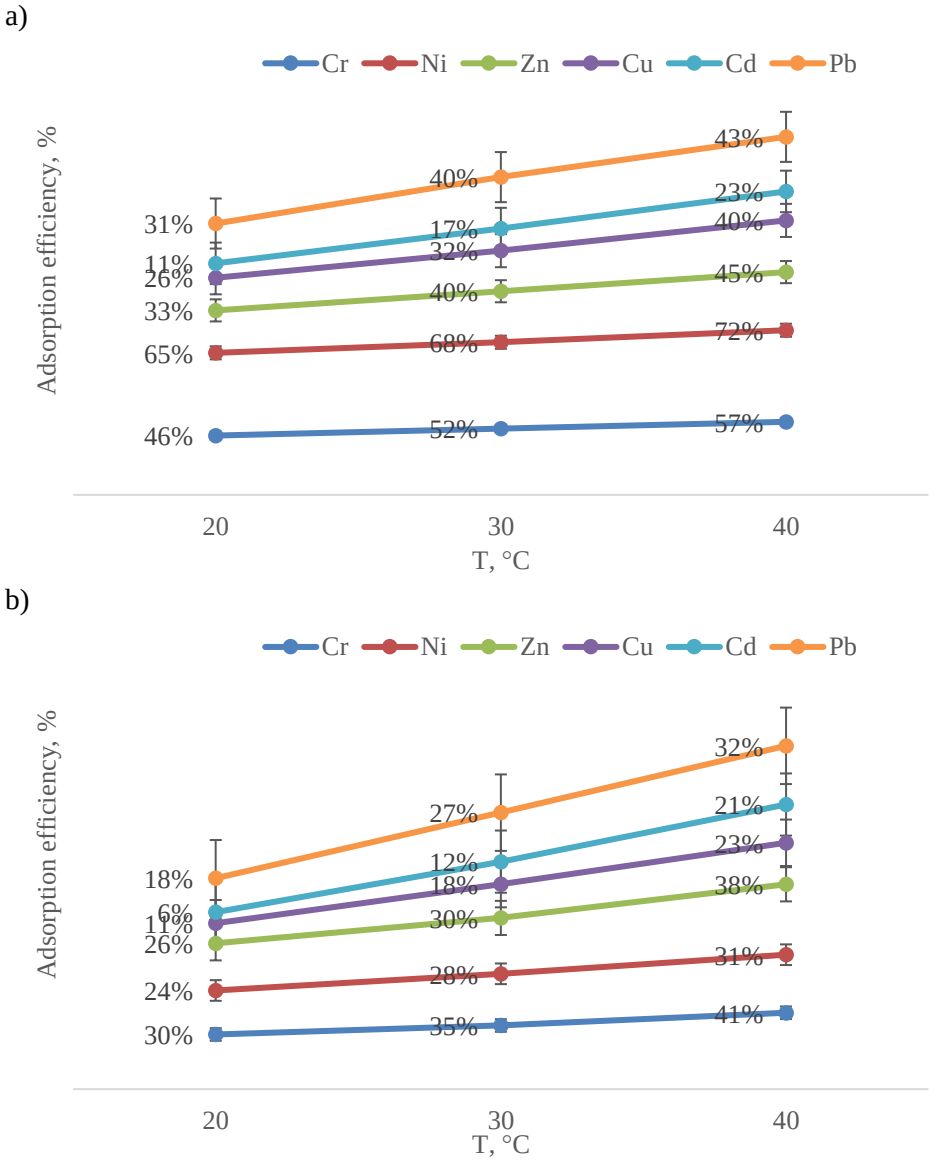

Fig. 3.21. Effect of temperature on adsorption efficiency of PTEs on a) H_2O_2-modified biochar, b) unmodified biochar

Adsorption efficiency and capacity increased with the increase of temperature, reaching its maximum at 40 °C (Fig. 3.21). The data kindly procured by the staff of Kazokiškės landfill, indicated the following values after reverse osmosis treatment of landfill leachate: BOD7 22.4 mg/l, Zn <40 mg/l, Ni 7 mg/l, Cr 14 mg/l, Pb 1 mg/l, Cu 3 mg/l, Cd 0.36 mg/l. According to the Lithuanian law about wastewater Nr. D1–236 from 17 May 2006, requirements to the maximum allowable concentration (MAC) of PTEs in the landfill leachate to the wastewater treatment plant are the following: Zn − 3 mg/l, Ni − 0.5 mg/l, Cr − 2 mg/l, Pb − 0.5 mg/l, Cu − 2 mg/l. H_2O_2-modified biochar showed adsorption efficiency of PTEs than unmodified biochar. However, leachate treated with biochar didn't meet the requirements, that indicates that H_2O_2-modified biochar is not so efficient as reverse osmosis.

3.2. Identification of the Key Mechanisms of the Potentially Toxic Elements Adsorption on Ligneous Biochar

Various mechanisms are responsible for adsorption of PTEs on biochar. Increased values of BET SSA and total micropore volume, decreased average pore diameter indicate that physical adsorption will take place. Increased CEC shows the increased content of oxygen-containing functional groups, and surface complexation mechanism. EDX analysis determined Mg, Al, Si, K, Ca in biochar (Table 3.20), and these elements participate in ion exchange.

Table 3.20. All elements analysed on the birch biochar (normalized values), %

Element	C	O	Mg	Al	Si	K	Ca
Value, %	78.81	18.06	0.19	0.41	1.63	0.51	0.40

With the increase of pH of solution, the competition of metal ions and protons for binding sites decreased and more binding sites are released due to the deprotonation of functional groups (Lu *et al.* 2012). The surface of biochar is negatively charged when $pH_{solution} > pH_{pzc}$ (point of zero charge).

Pinus-taeda biochar had pH_{PZC} 5.08, and the same biochar activated with NaOH – 6.83 (Jang *et al.* 2018). Thus, the surface charge of BC was protonated and has a positive charge. Banik *et al.* (2018) found that pH_{PZC} of the Al-treated biochar exceeded its pH and was ~10, supporting the hypothesis, that alumina biochar produced at high temperatures (700–900 °C) is effective for adsorption of anionic PTEs due to its positive charge.

Table 3.21. Comparison of pH and pHpzc of different types of biochar (mean ± SD)

Type of biochar	pH	pH_{pzc}
Unmodified biochar	8.36±0.04	6.73±0.10
H_2O_2-modified biochar (15%)	5.59±0.14	5.08±0.17
MgCl2-modified biochar	4.89±0.06	6.58±0.11
FeCl3-modified biochar	2.19±0.01	3.63±0.23

On the opposite, pH_{PZC} of raw wood was lower, than pH of the raw wood (4.8 and 6.2), suggesting that the surface of the wood was negatively charged, and, thus, favorable for adsorption of cations. More examples are coming next. pH_{PZC} of the biochar decreased after modification of corn straw biochar with ferromanganese oxides – from 10 to 9.2 (Zhou *et al.* 2018). The pH_{PZC} of Douglas fir biochar dropped from 9.2 to 6.2 after magnetite (Fe_3O_4) modification (Karunanayake *et al.* 2018). Hao *et al.* (2018) found that pH_{PZC} of straw biochar was decreased by the magnetic modification (7.18 to 7.11), indicating the difference between the surface chemistry. The phenomenon can attribute to the partial oxidation of carbonaceous materials surfaces by Fe_3O_4 coating and the increase of surface acidic functional groups. Acidic oxidation of the wheat straw biochar decreased its pH_{PZC} from 8 to 6.2, and alkaline oxidation – from 8 to 7.3 (Fan *et al.* 2018).

From Table 3.21 could be seen, that for unmodified biochar and modified with H_2O_2 (where $pH>pH_{pzc}$) electrostatic attraction may favor adsorption of cationic metals. For Mg- and Fe-modified biochar (where $pH<pH_{pzc}$), electrostatic attraction may favor adsorption of anionic metals.

Thus, mechanisms of adsorption are electrostatic attraction, ion exchange, surface complexation and physical adsorption.

3.3. Evaluation of the Biochar-Hydrogel Composite Potential for Application in Adsorption of Potentially Toxic Elements from Synthetic Solutions and Landfill Leachate

3.3.1. Characteristics of the Biochar, Hydrogel and Biochar-Hydrogel Composite

Structural properties of biochar, hydrogel and composites are shown in Table 3.22.

Table 3.22. Structural of the biochar, hydrogel and composites

Type of biochar	BET, m^2/g	Average pore diameter, nm	Total micropore volume, cm^3/g
Unmodified biochar	20.11	4.50	0.010
H_2O_2-modified biochar (15%)	301.50	2.31	0.172
Anionic hydrogel	68.35	3.76	0.035
Cationic hydrogel	115.67	2.12	0.064
Anionic composite with unmod. BC	79.20	3.95	0.042
Anionic composite with H_2O_2-mod. BC	288.33	3.43	0.151
Cationic composite with unmod. BC	125.79	3.18	0.076
Cationic composite with H_2O_2-mod. BC	401.14	2.01	0.232

It is known that adsorption of PTEs through complexation, electrostatic attraction and ion exchange is affected by micropores with the pore size less than 2 nm (Tan *et al.* 2015). Modification with H_2O_2 increased BET specific surface area (SSA). Results on BET SSA are lower to those of birch activated carbon – 400 m^2/g (Cruz 2012). Baltrėnas *et al.* (2015) showed higher result for unmodified birch than indicated in the current study – 73.19 m^2/g.

Chemical properties of biochar are shown in Table 3.23.

For further experiments on swelling, it was decided not to proceed with composites with unmodified biochar, as their CEC and BET won't make impact on adsorption selectivity and capacity. The pH of the modified biochar was lower in comparison to unmodified biochar, which could be attributed to the weak acidic nature of the created carboxyl surface functional groups. Xue *et al.* (2012) reported decrease in pH from 6.2 to 4.4, when hydrochar was modified with 10% of H_2O_2 solution.

Modification with H_2O_2 increased CEC of the biochar. This increase in CEC can be attributed to an increase in the presence of acidic oxygen functional groups on the surface of the biochar materials. For comparison, unmodified hydrochar (Huff and Lee 2016) had 17.95 $cmol_c/kg$, modified with 3% H_2O_2 solution – 23.3 $cmol_c/kg$, 20% H_2O_2 solution – 25.43 $cmol_c/kg$, 30% H_2O_2 solution – 31.37 $cmol_c/kg$.

FTIR was used in this study to describe the development and alterations in functional group chemistry of the studied types of biochar modified in different ways. Number of vacant sites on surface of adsorbent corresponds to the content of oxygen-containing functional groups, e.g. carboxylic and carbonyl groups. Huff and Lee (2016) stated that the peaks 1315 cm^{-1} and 1700 cm^{-1} corresponded to carboxylic acid functionality, that increased after modification of biochar with H_2O_2.

Table 3.23. pH and CEC of the biochar, hydrogel and composites (mean value ± SD)

Biochar	pH	pHpzc	EC, mS/cm	CEC (cmolc/ kg)
Unmodified biochar	8.36 ± 0.11	6.73 ± 0.10	125.60 ± 17.50	5.15 ± 0.24
H_2O_2-modified biochar (15%)	5.59 ± 0.14	5.08 ± 0.17	399.00 ± 21.32	22.79 ± 0.76
Anionic hydrogel	8.13 ± 0.75	7.78 ± 0.49	518.33 ± 3.51	7.51 ± 0.54
Cationic hydrogel	4.51 ± 0.53	4.22 ± 0.63	614.67 ± 9.07	12.33 ± 0.35
Anionic composite with unmod. BC	9.36 ± 0.82	8.95 ± 0.45	574.33 ± 7.77	9.78 ± 0.63
Anionic composite with H_2O_2-mod. BC	7.28 ± 0.56	7.02 ± 0.39	793.33 ± 8.62	28.65 ± 0.29
Cationic composite with unmod. BC	5.82 ± 0.72	5.13 ± 0.36	707.00 ± 5.00	18.37 ± 0.87
Cationic composite with H_2O_2-mod. BC	5.09 ± 0.38	4.83 ± 0.31	952.00 ± 8.00	37.12 ± 0.95

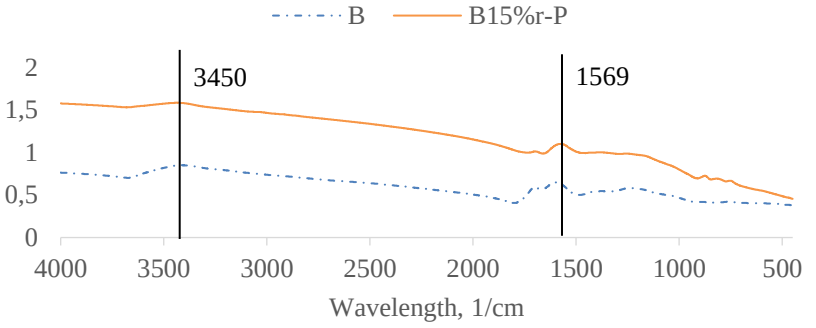

Fig. 3.22. FTIR spectra of modified and unmodified biochar

From Fig. 3.22 peaks at 1500–1750 cm^{-1} corresponded to carboxylic groups, while peaks at 3250–3500 cm^{-1} corresponded to phenolic groups on the biochar surface. Modification with H_2O_2 increased content of carboxylic groups. With the increasing of the percentage of H_2O_2-solution content of carboxylic and phenolic groups increases.

3.3.2. Research of Hydrogel and Biochar-Hydrogel Composite Swelling under Changing of pH and Temperature

Hydrogels responsive to temperature and pH can be made by simply incorporating ionizable and hydrophobic functional groups to the same hydrogels (Qui and Park 2001). Swelling of the hydrogel is the result of ionization/ deionization of the carboxylic acid groups (Yoshida *et al.* 2013), and in combination of hydrogel with biochar, swelling could be used to enhance adsorption selectivity of the biochar-hydrogel composite, as when the hydrogel swells, his pores become larger, so PTEs of larger diameter could be adsorbed due to physical adsorption.

From the Fig. 3.23, it could be seen that anionic hydrogel swells the most at 40°C, because the water gains an enthalpy and the hydrophilic group in hydrogels are turned into an intramolecular hydrogen bond (Zhao *et al.* 2016), and reaches its maximum at t = 240 min (636%). The lowest swelling was observed at 20°C and 240 min (362%).

With the hydrogel soaked in hot water extending, a part of hydrogen bonds that were existed in the network structure were destroyed, consequently the hydrogels would become less hydrophilic, resulting in a lower swelling capacity. Anionic hydrogel in this study swells in 8 times faster than biochar-hydrogel composites from Karakoyun *et al.* (2011).

Cationic hydrogel swells more at 20 °C and reaches its maximum at t = 240 min (268%). The lowest swelling was observed at 40 °C and 240 min (103%). Swelling of cationic hydrogel was lower than for anionic, because of the composition: acyclic acid as monomer leads to the quick polymerization, achieved at high acidity of water phases, which results in the formation of highly cross-linked polymers and thus, lower swelling. The results on cationic hydrogel are twice lower than in Zhao *et al.* (2016), as their enteromorpha-based hydrogel (EP-g-PKA) showed swelling capacity of 700%at 20 °C at 300 min.

Similar swelling tendency could be observed for biochar-hydrogel composites. From the Fig. 3.24, it could be seen that anionic composite swells more at 40 °C, and reaches its maximum at t = 240 min (869%). The lowest swelling was observed at 20 °C and 240 min (548%). Cationic composite swells more at 20 °C and reaches its maximum at t = 240 min (434%). The lowest swelling was observed at 40 °C and 240 min (175%).

From the Fig. 3.25, it could be seen that anionic hydrogel swells more at pH 7, 10, 12, and reaches its maximum when pH is 12 (971%) and t = 180 min. When pH is acidic, the swelling reaches it maximum at 120 min (pH = 2 – 161%, pH = 4 – 281%, pH = 6 – 364%) and then the volume of hydrogel decreases. Cationic hydrogel swells more at pH 2, 4, 6, and reaches its maximum when pH is 2 (354%) and t = 150 min. When pH is neutral or basic, the swelling reaches it maximum at 30–60 min (pH =7 – 105%, pH = 10 – 69%, pH = 12 – 65%) and

then the volume of hydrogel decreases. The lower swelling capacity of cationic hydrogel was due to the higher protonation degree of carboxylic groups of hydrogel.

a)

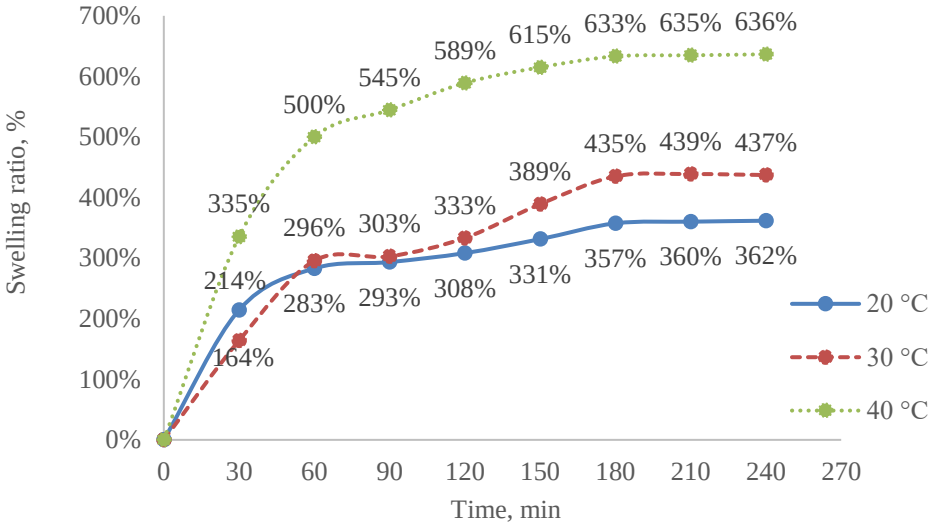

b)

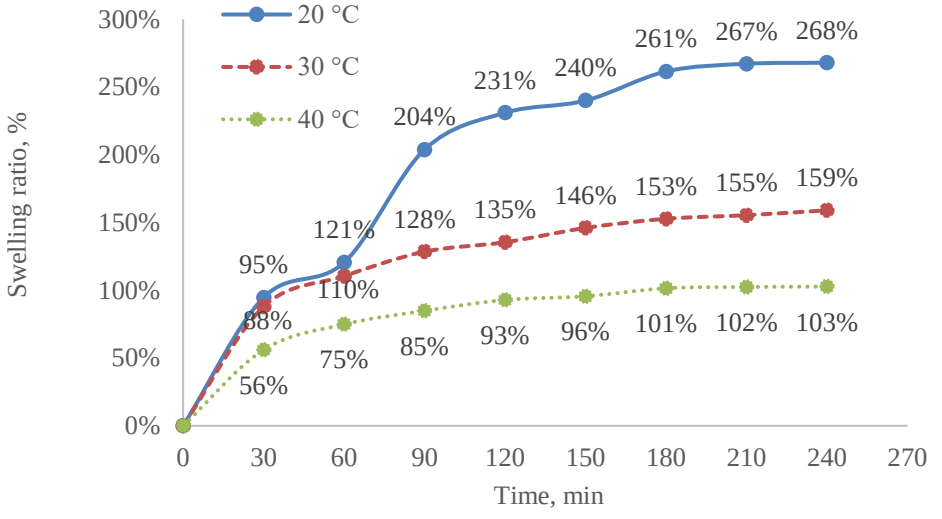

Fig. 3.23. Influence of the temperature on hydrogel swelling:
a) anionic hydrogel; b) cationic hydrogel

a)

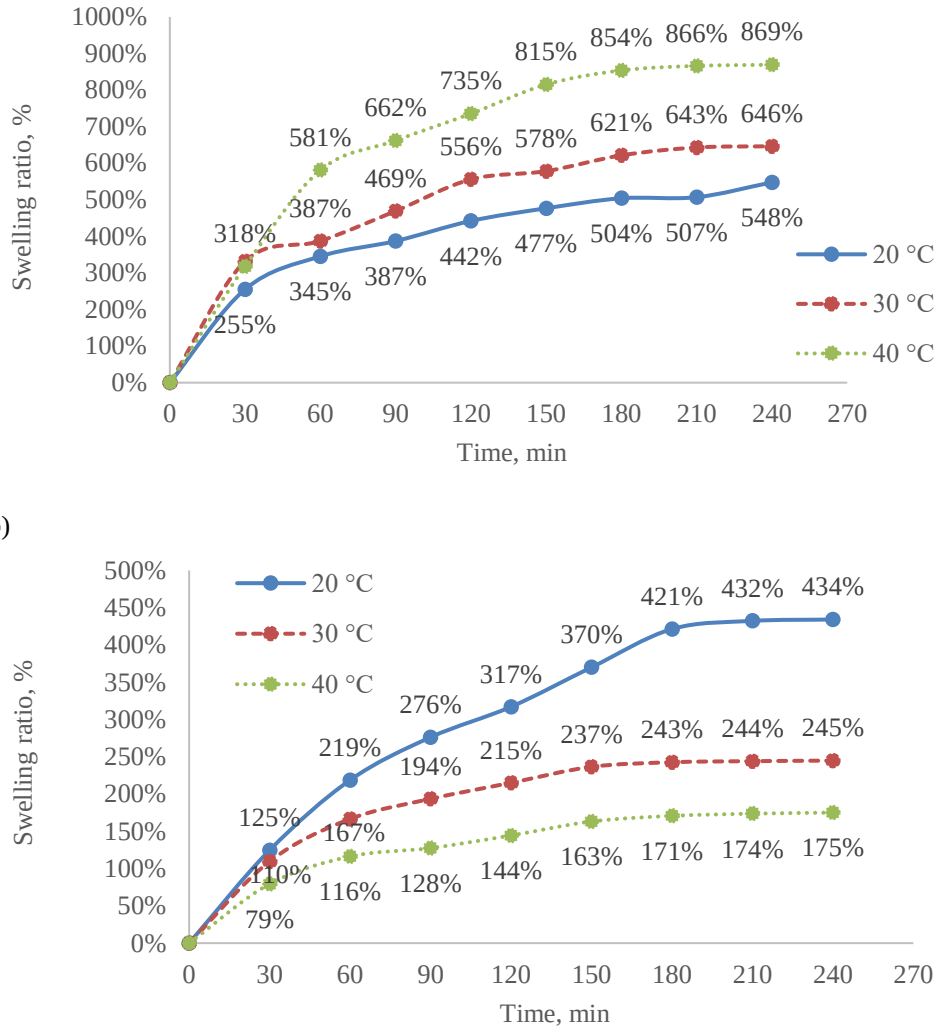

Fig. 3.24. Influence of the temperature on biochar-hydrogel composite swelling: a) anionic composite; b) cationic composite

As the pH value continued to increase, the water swelling capacity of hydrogel began to decrease; this could be explained by 'charge screening effect' of excessive Na^+ in the swelling media (Zhao *et al.* 2016). When pH value was between 2 and 6, the carboxylic groups became ionized and the electrostatic repulsion between the molecular chains was predominated in the system, which led to the network more expanding.

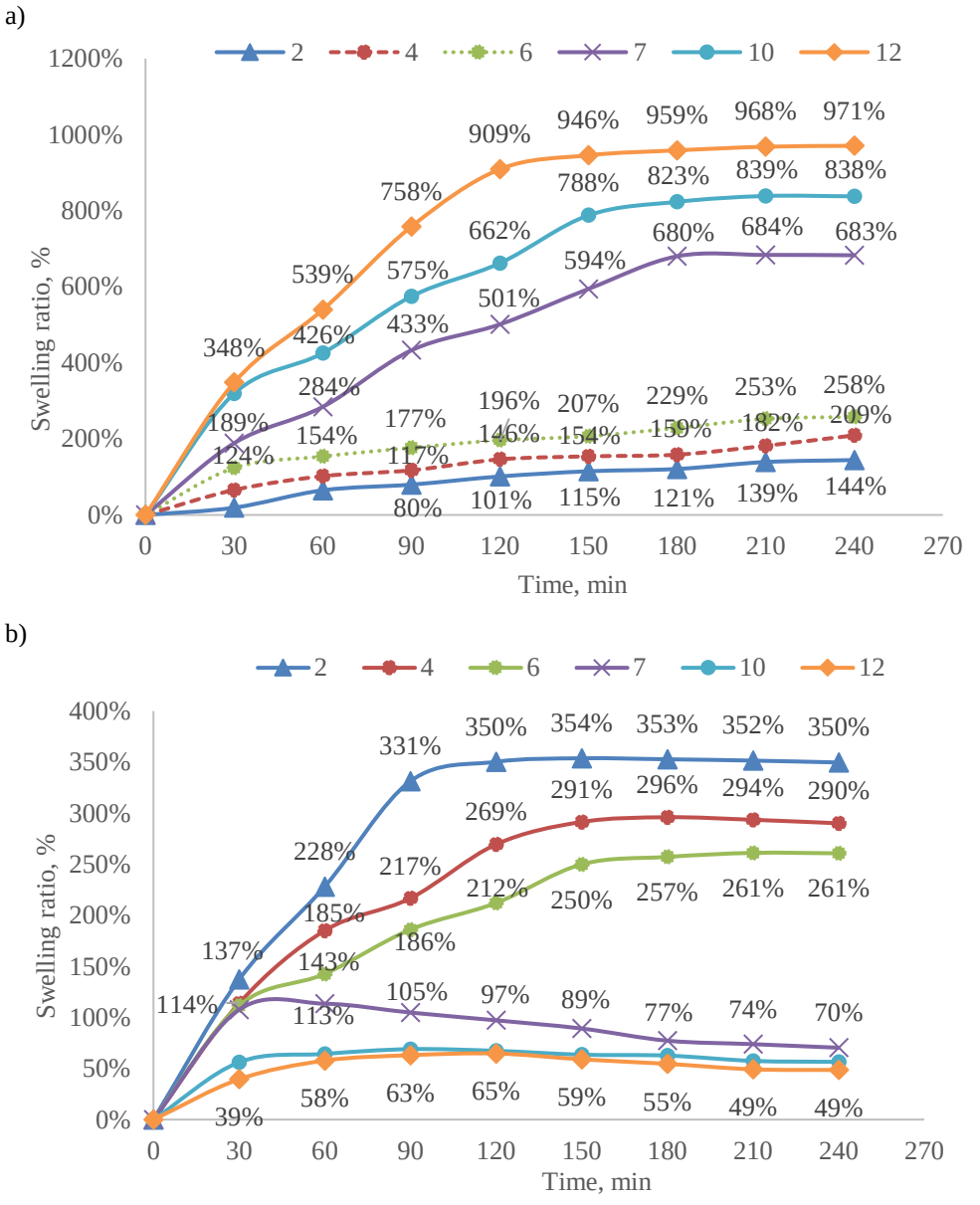

Fig. 3.25. Influence of the pH on hydrogel swelling:
a) anionic hydrogel; b) cationic hydrogel

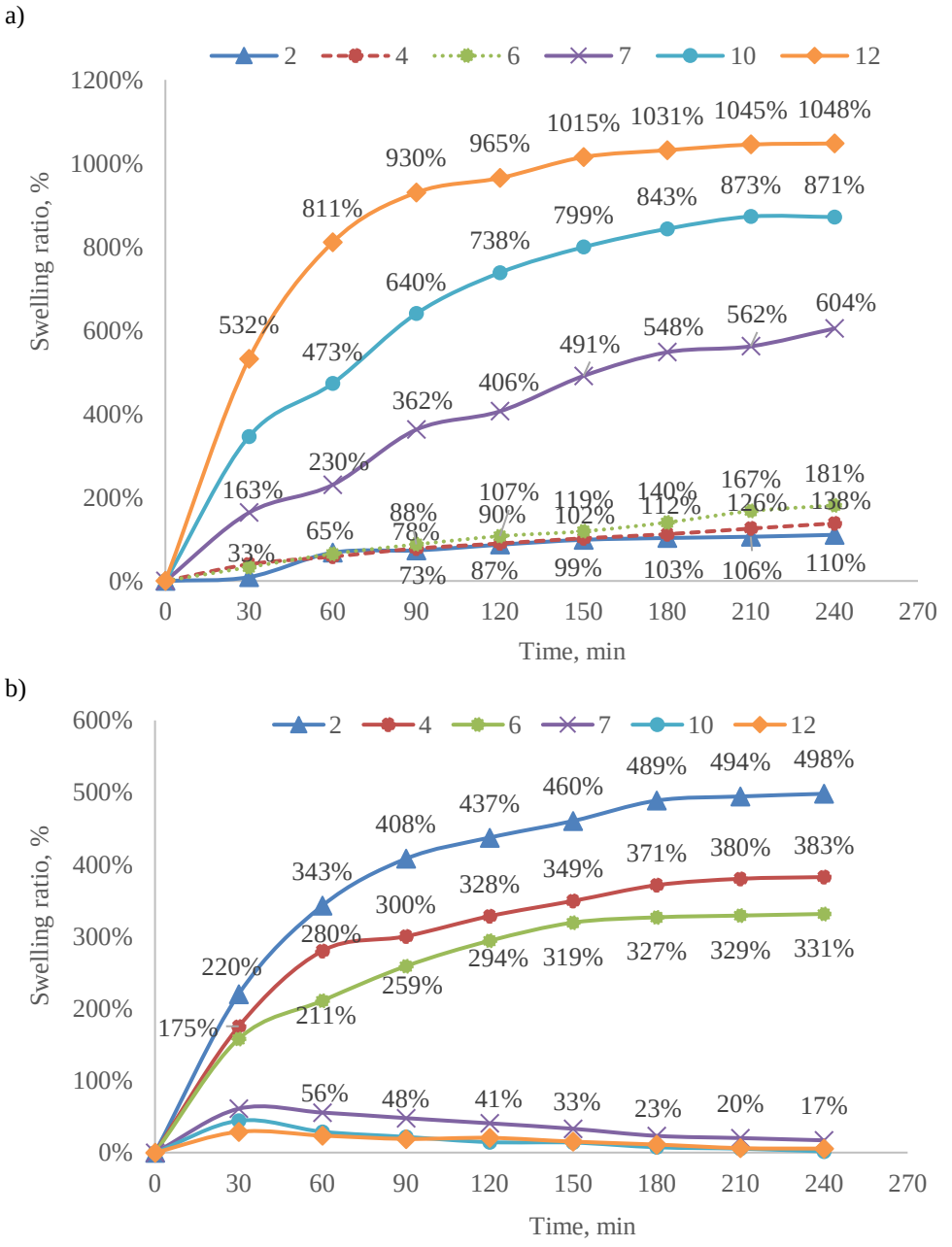

Fig. 3.26. Influence of the pH on biochar-hydrogel composite swelling:
a) anionic composite; b) cationic composite

Karakoyun et al (2011) found 1045% swelling of woody biochar-hydrogel composite and maximum amount of phenol adsorption at pH 10 (28.06 mg/g). Enteromorpha-based hydrogel (EP-g-PKA) showed a higher water swelling capacity at weak acidity condition (pH = 5–6) and low temperature (20°C) at 300 min – 700% (Zhao *et al.* 2016).

The degree of releasing coomassie brilliant blue drug was the highest at pH 10 for the pH-sensitive coconut-based AC-hydrogel composite due to the extensively developed pore structure of hydrogel and the hydrophilic surface nature of AC with BET surface area 1230 m^2/g and the fraction of 67% micropore structure (Yun *et al.*, 2009).

Su *et al.* (2018) found that this hydrogel showed good swelling behavior and excellent adsorption capacity for Cu^{2+} (197.2 mg/g), thus could be used for PTEs removal from wastewater. pH and temperature-responsivity characteristics were selected in terms of enhancing of selectivity of adsorption of PTEs. Yun *et al.* (2009) prepared pH-sensitive AC-hydrogel composite that swelled well in the basic condition to release the drug loaded in AC.

From the Fig. 3.26, it could be seen that anionic composite swells more at pH 7, 10, 12, and reaches its maximum when pH is 12 (1048%) and t = 240 min. When pH is acidic, the swelling reaches it maximum at 240 min (pH = 2 – 110%, pH = 4 – 138%, pH = 6 – 181%) and then the volume of composite decreases.

Cationic composite swells more at pH 2, 4, 6, and reaches its maximum when pH is 2 (498%) and t = 240 min. When pH is neutral or basic, the swelling reaches it maximum at 30–60 min (pH = 7 – 105%, pH = 10 – 69%, pH = 12 – 65%) and then the volume of composite decreases.

Both anionic hydrogel and composite swell with the increase of the temperature, while cationic hydrogel and its composite act the opposite. Also anionic hydrogel and its composite swell at pH>7, while cationic hydrogel and its composite swell at acidic pH.

3.3.3. Adsorption of Potentially Toxic Elements from Landfill Leachate by Biochar-Hydrogel Composites

Adsorption efficiency and capacity was increased with the increase of the dosage and contact time, reaching its maximum at 300 min and dosage 20 g/l. Maximum values are shown in Table 3.24, 3.25.

Isotherm and kinetic studies showed the favorable nature for adsorption of PTEs from solution on biochar-hydrogel composite, because R_L and 1/n values were all within the range of 0–1 (Annex B, C). The well-fitted Langmuir model for composites with unmodified biochar indicated that the adsorption would take place with a homogeneous surface, while Freundlich for composites with

modified biochar indicated the adsorption with a heterogeneous surface. In this study, pseudo-second order model fitted for all composites.

Table 3.24. Maximum adsorption efficiency at dosage 20 g/l

Adsorbent	Ni, %	Cr, %	Pb, %	Cd, %	Zn, %	Cu, %
Anionic hydrogel	6.8	9.8	8.5	10.3	7.6	5.2
Cationic hydrogel	22.8	26.3	14.8	19.0	19.2	17.9
Anionic composite with H_2O_2-mod. BC	11.3	13.2	13.4	14.1	10.3	10.6
Cationic composite with H_2O_2-mod. BC	64.6	61.2	57.3	27.7	72.2	57.2

Thermodynamic studies confirmed the spontaneous nature of adsorption (negative $\Delta G°$). In all cases $\Delta G°$ decreases with an increase in temperature – that indicates that the adsorption process becomes more favorable at higher temperatures.

Table 3.25. Maximum adsorption capacity at dosage 20 g/l

Adsorbent	Ni, mg/g	Cr, mg/g	Pb, mg/g	Cd, mg/g	Zn, mg/g	Cu, mg/g
Anionic hydrogel	0.46	6.83	0.64	0.14	0.46	0.14
Cationic hydrogel	1.54	8.42	0.87	0.27	1.15	0.49
Anionic composite with H_2O_2-mod. BC	0.76	9.25	1.06	0.75	0.62	0.29
Cationic composite with H_2O_2-mod. BC	4.36	12.81	1.27	0.91	4.33	1.57

The positive value of $\Delta H°$ in all cases indicates that the adsorption reaction is endothermic. The positive value of $\Delta S°$ in all cases suggests that some structural changes occur on the adsorbent, and the randomness at the solid/liquid interface in the adsorption system increases during the adsorption process.

3.4 Development of Dynamic Intraparticle Model for Adsorption of Potentially Toxic Elements by Biochar

3.4.1. Formation of the Input Data to Dynamic Intraparticle Model Fitting

Dynamic intraparticle model (DIM) describes sorption from a mathematical point of view without assuming a specific sorption mechanism. Two types of sites of the adsorbent were assumed to describe adequately sorption at high sorbate-sorbent ratios, e.g. in these studies 400, in others – 13 (Chiron *et al.* 2003), 100 and 400 (Wilczak and Keinath 1993).

To calculate DIM, solute concentration in the liquid of the pores and solute concentration on the solid surface should be investigated. Concerning the C_S, it is computed by considering the ratio between the moles adsorbed by the solid volume, that can be directly calculated from the experimental data normally reported as adsorbate mol/g of sorbent. Result of the model is finding optimal parameters of adsorption by conductiong only equilibrium experiments.

In Table 3.26–3.27 parameters for DIM simulation based on the experimental data from selection of the BC are indicated. From isotherm fitting, were taken Langmuir adsorption constant *b* and Saturation solute solid concentration $C_{S,*}$. Physical system was chosen to be a sphere (neither cylinder nor slab), thus, *shape factor* was 2 and mass transfer coefficient k_m was established as 100 (Russo *et al.* 2016). All BC particles were crushed to the size of 1 mm, thus, Particle radius *Rp* was 0.001 m. Pore diameter d_P and particle porosity ε of the BC were analysed with mercury porosimeter at the Institute of Thermal Insulation. Pore diffusivity *Dp* was taken from the typical order of magnitudes of this parameter from range 10^{-9}–10^{-11} m^2/s (Duong 1998). Superficial diffusivity D_S was taken from the typical order of magnitudes of this parameter from range 10^{-13}–10^{-18} m^2/s (Duong 1998). Solute bulk concentration C_B was calculated from the ratio initial concentration of PTE (g/l) in the solution to its molecular weight (g/mol).

Additionally, model was fitted to Freundlich isotherm, and parameters like *K*, 1/*n* and *n* were taken from isotherm fitting.

The complex of pore volume and surface diffusion model is considered. Model is based on assumptions, that the system is isothermal, all particles are spherical and of the same size, equilibrium in the pore exists and average porosity and tortuosity of the particle (tortuosity factor is the geometric factor, found from the ratio between the actual diffusion path length and the net distance in the direction of flux, or the radial distance; it is independent of temperature and the nature of the diffusing species). In the particle two processes are considered: the solute diffusion from the particle surface to the center of the particle and the adsorption equilibrium in the particle represented by Langmuir isotherm.

Table 3.26. Parameters for DIM simulation for H2O2-modified biochar from mono-component laboratory solution

Symbol	Description	Unit	Cr^{3+}	Cd^{2+}	Cu^{2+}	Ni^{2+}	Pb^{2+}	Zn^{2+}
Langmuir fitting								
C_B	solute bulk concentration	mol/m^3_{BULK}	0.658	0.89	1.574	1.704	0.483	1.53
b	Langmuir adsorption constant	m^3_{liq}/mol	0.0204	0.013	0.0228	0.0233	0.1081	0.0179
$C_{S,*}$	saturation solute solid concentration (q_{max} Langmuir)	mol/m^3_{sol}	833.33	1666.67	1000	769.23	833.33	1250
Rp	particle radius	m	0.001	0.001	0.001	0.001	0.001	0.001
k_m	mass transfer coefficient	-	100	100	100	100	100	100
D_p	pore diffusivity based on the cross sectional area	m^2/s	10^{-10}	10^{-10}	10^{-10}	10^{-10}	10^{-10}	10^{-10}
D_S	superficial diffusivity	m^2/s	10^{-15}	10^{-15}	10^{-15}	10^{-15}	10^{-15}	10^{-15}
Shape	Shape factor (sphere)	-	2	2	2	2	2	2
d_P	pore diameter	nm	2.31	2.31	2.31	2.31	2.31	2.31
ε	Particle porosity	-	0.85	0.85	0.85	0.85	0.85	0.85
Freundlich fitting								
K	Freundlich capacity factor		1.76	2.6	3.27	2.06	39.36	2.83
1/n	Freundlich intensity parameter		0.8046	0.8728	0.8024	0.7799	0.7461	0.8455
n	index of nonlinearity of isotherms		1.243	1.146	1.246	1.282	1.34	1.183

Table 3.27. Parameters for DIM simulation for unmodified biochar from mono-component laboratory solution

Symbol	Description	Unit	Cr^{3+}	Cd^{2+}	Cu^{2+}	Ni^{2+}	Pb^{2+}	Zn^{2+}
Langmuir fitting								
C_B	solute bulk concentration		0.658	0.89	1.574	1.704	0.483	1.53
b	Langmuir adsorption constant	m^3_{liq}/mol	0.0081	0.0122	0.0135	0.0269	0.0228	0.0064
$C_{S,*}$	saturation solute solid concentration (q_{max} Langmuir)	mol/m^3_{sol}	714.29	666.67	833.33	322.58	1250	1000
Rp	particle radius	m	0.001	0.001	0.001	0.001	0.001	0.001
k_m	mass transfer coefficient	-	100	100	100	100	100	100
D_p	pore diffusivity based on the cross sectional area	m^2/s	10^{-10}	10^{-10}	10^{-10}	10^{-10}	10^{-10}	10^{-10}
D_S	superficial diffusivity	m^2/s	10^{-15}	10^{-15}	10^{-15}	10^{-15}	10^{-15}	10^{-15}
Shape	Shape factor (sphere)	-	2	2	2	2	2	2
d_P	pore diameter	nm	4.497	4.497	4.497	4.497	4.497	4.497
ε	Particle porosity	-	0.8	0.8	0.8	0.8	0.8	0.8
Freundlich fitting								
K	Freundlich capacity factor		5.61	2.71	1.47	1.47	4.22	5.27
1/n	Freundlich intensity parameter		0.8378	0.8208	0.8362	0.6605	0.8652	0.8746
n	index of nonlinearity of isotherms		1.194	1.218	1.196	1.514	1.156	1.143

3.4.2. Results of the Application of the Model for Adsorption of Potentially Toxic Elements by Biochar

Adsorbent is a very porous material and based on Russo *et al.* (2015), three concentrations are taken into account: solute bulk concentration (C_B), concentration of the solute in the liquid (inside the particle) C_L and concentration of the solute in the solid (C_S). Experimental data from Cu, Ni, Cd, Zn, Ni, Pb mono-component adsorption on different types of biochar was fitted to dynamic intraparticle model.

Effect of solute bulk concentration on adsorption is discussed below. This is the 1st domain of the dynamic intraparticle model – liquid bulk phase that contains the solute dissolved in the solvent (here pollutant concentration changes with time). Here the pollutant is transferred from the bulk phase to the particle through the liquid film via film diffusion (external diffusion) (Russo *et al.* 2015).

Concentration in the bulk helps to define adsorption mechanism, as it describes film diffusion (external diffusion), which is the transport of adsorbate from the bulk phase to the external surface of adsorbent. Film diffusion is influenced by initial concentration of the PTE and functional groups on the biochar surface. Fig. 3.26–3.27 show the change of the normalized (according to the initial time concentration) bulk concentration.

By increasing of contact time, C_B descreases. It could be seen, how fast the film diffusion happens – process reaches the saturation, i. e. the moment, when PTE is not transferred inside the biochar particle. A rapid adsorption occurred during the first 30 min. Carboxylic groups acted like active adsorption sites for PTEs on the biochar surface.

When Wilczak and Keinath (1993) fitted adsorption of on activated carbon to double exponential model, the sorption occurred rapidly at the outset but was followed by a slow and prolonged secondary sorption step. Chiron *et al.* (2003) found 90% removal for both Cu^{2+} and Pb^{2+} occurred within 1 h, and maximum duration of experiment was 250 min. A rapid adsorption occurred during the first 30 min after which equilibrium was slowly achieved. Each metal was adsorbed via a two-step mechanism, namely, external particle diffusion and intraparticle diffusion.

Adsorption process with an initial fast adsorption event, followed by a slow adsorption event, can be due to the presence of two distinct types of adsorption sites on the surface (Wilczak and Keinath 1993), the first rapidly equilibrated and the second reacting more slowly, or due to a system limited by interparticle diffusion (Chiron *et al.* 2003).

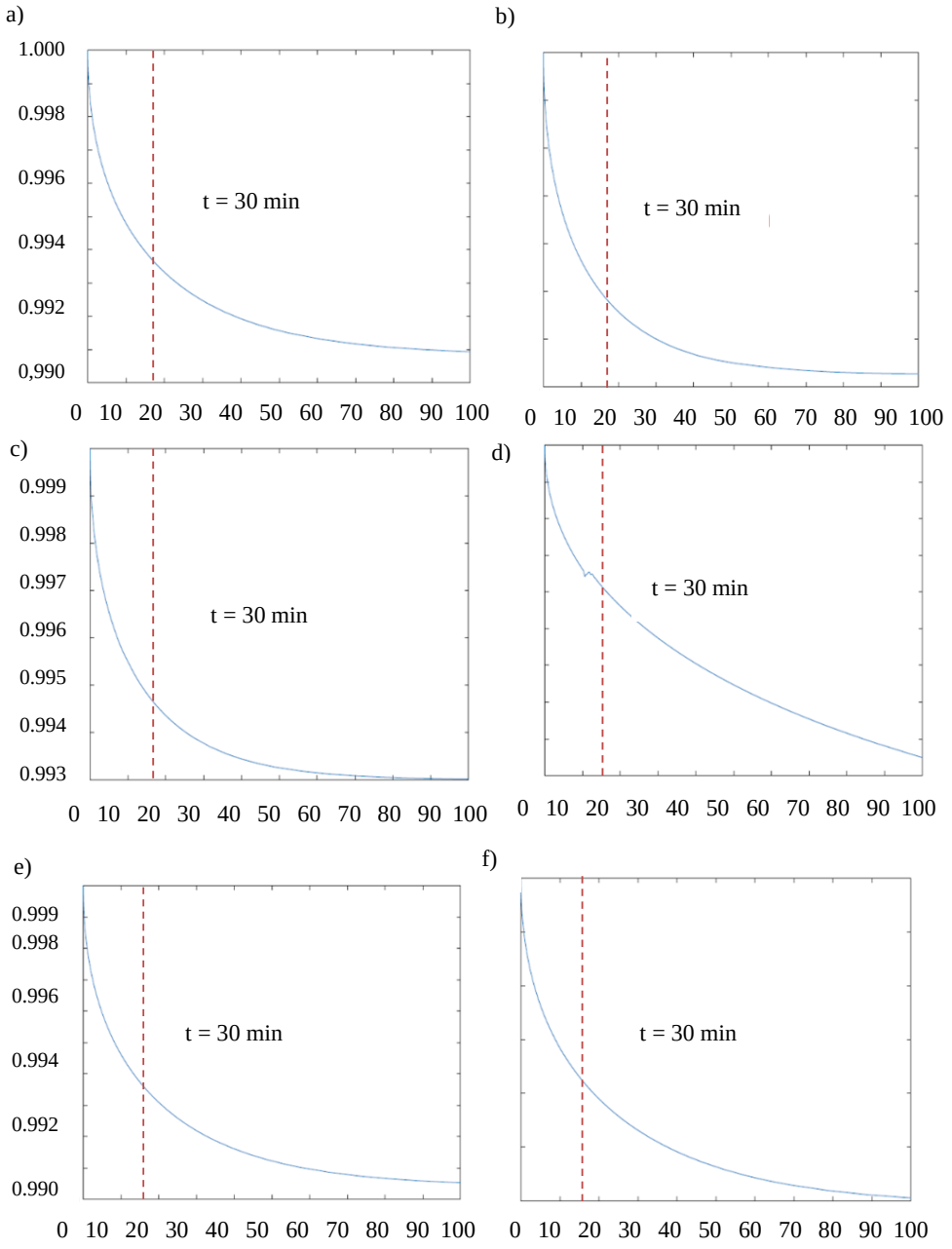

Fig. 3.26. Potentially toxic elements normalized concentration in bulk along time (C_B) (t = 60 min) on H_2O_2-modified biochar: a) Cr, b) Cd, c) Cu, d) Pb, e) Zn, f) Ni. Vertical axis – C_B (mol/m^3), horizontal axis – t, s $\times 10^2$

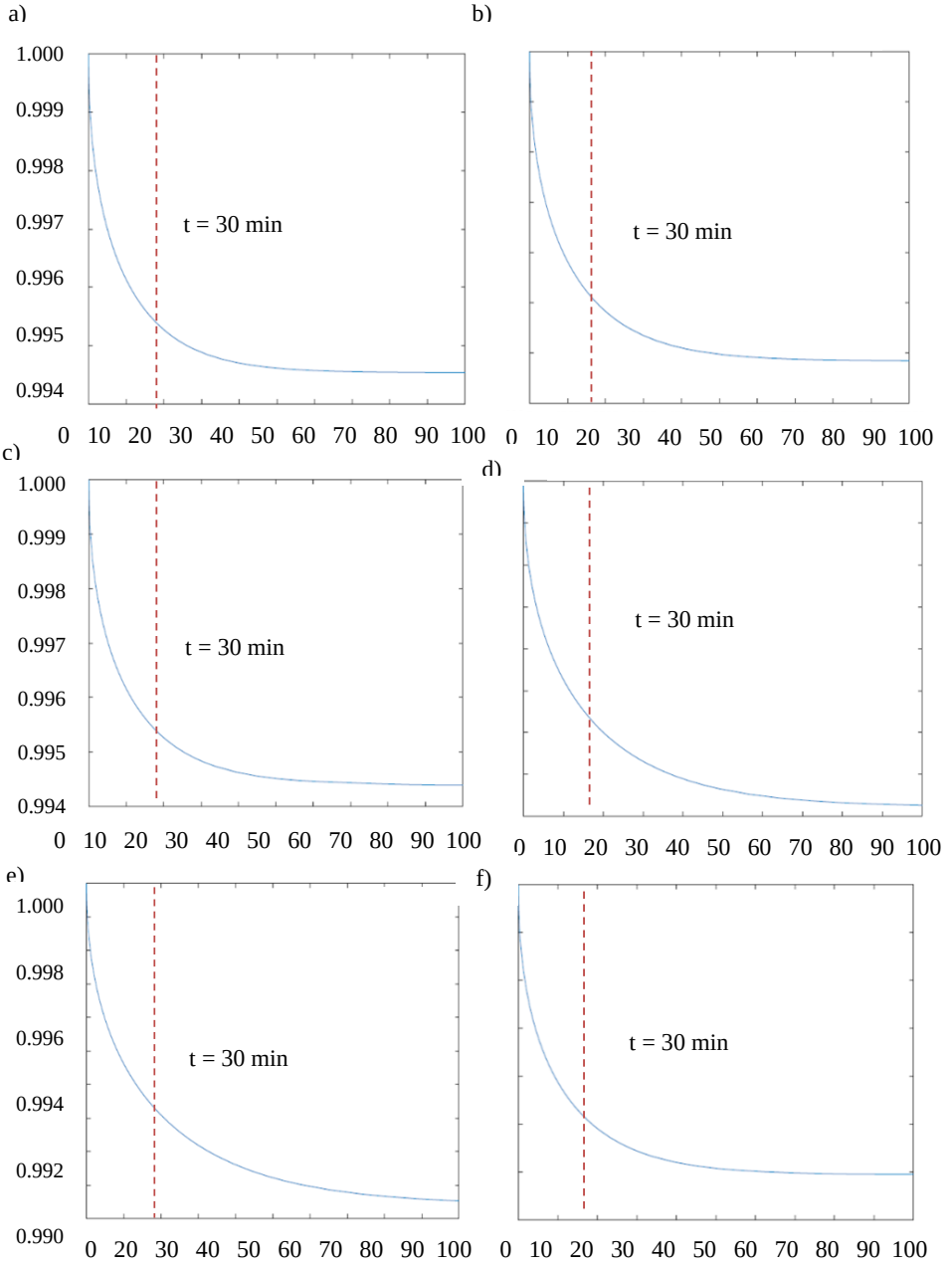

Fig. 3.27. Potentially toxic elements normalized concentration in bulk along time (C_B) (t = 60 min) on unmodified biochar: a) Cr, b) Cd, c) Cu, d) Pb, e) Zn, f) Ni. Vertical axis – C_B (mol/m^3), horizontal axis – t, s $\times 10^2$

Effect of concentration in the liquid of the biochar pores on adsorption is discussed below. This is the 2nd domain of the dynamic intraparticle model – a liquid side (liquid intraparticle phase), where the solute diffuses from the outer particle surface to the center of the particle (here concentration depends on time and radius of the particle). After the pollutant is transferred from the bulk phase to the particle through the liquid film, then it diffuses along the particle radius in the pore, in which the mass transfer here is liquid porous diffusion (pore diffusion) (Russo *et al.* 2015).

Concentration in the liquid of the biochar pores helps to define adsorption mechanism, as it describes the transport of PTEs from the external surface into the pores. Activation of adsorbent, particle size of adsorbent, concentration and physico-chemical properties of adsorbate are key factors affecting intraparticle diffusion. Fig. 3.28–3.29 show the concentration (normalized according to the concentration on the surface of the particle) distribution in the liquid inside the particle at different time.

Intraparticle diffusion happens slower, than film diffusion, because adsorption slows as surface coverage nears saturation. With the increasing of contact time, PTE concentration in the liquid of the pores increases, and reaches the saturation within 60 min. Results are referred to the pore-size distribution of biochar. Micropores (pores of internal width < than 2nm) and mesopores (2– 50 nm) are of importance to many liquid–solid adsorption processes. Macropores (> 50nm) serve the transport of adsorbate molecules to the meso- and micropores.

Effect concentration in the solid on adsorption is discussed below. This is the 3rd domain of dynamic intraparticle model – a solid side (solid intraparticle phase), where the PTE concentration reaches the equilibrium inside the particle through the Langmuir mechanism (here concentration depends on time and radius of the particle). The PTE can diffuse also on the sorbent surface, with a diffusivity parameter that strongly depends on the interactions between the solute and the sorbent. After the pollutant is transferred from the bulk phase to the particle through the liquid film, then it diffuses along the particle radius in the pore, in which the mass transfer here is surface diffusion (Russo *et al.* 2015).

Concentration in the solid helps to define adsorbate distribution in the biochar particle and assume adsorption mechanism, as it describes surface diffusion, which is the transport of adsorbate on the internal surface of adsorbent. By increasing the contact time, Cr in pores is attached to biochar till a saturation condition is reached. Fig. 3.30–3.31 show how fast the pores (without the liquid inside) attach PTEs until the saturation condition is reached.

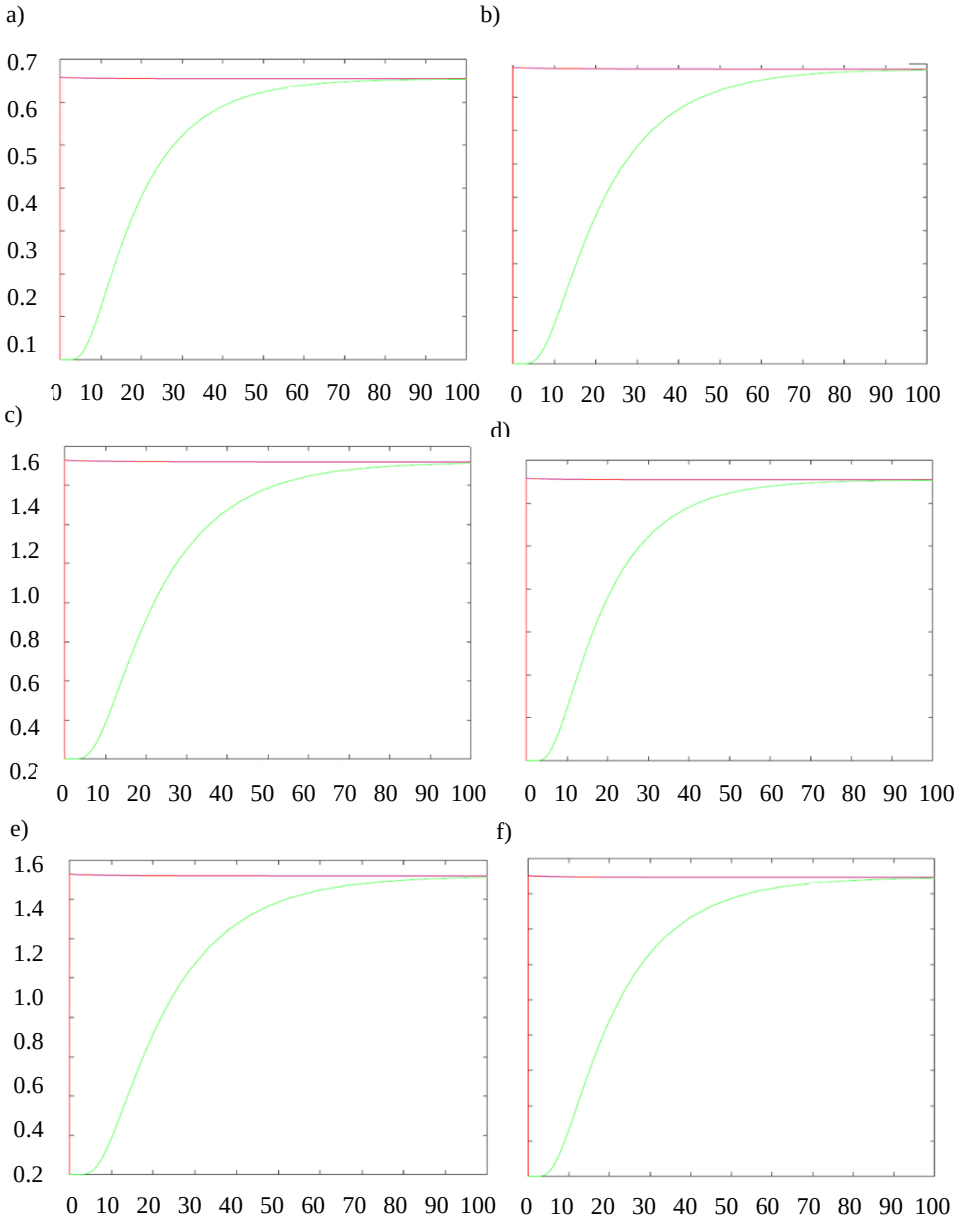

Fig. 3.28. Potentially toxic elements concentration in the liquid of the biochar pores (C_L) (green line) on H_2O_2-modified biochar: a) Cr, b) Cd, c) Cu, d) Pb, e) Zn, f) Ni. Vertical axis – C_L (mol/m3), horizontal axis – t, s $\times 10^2$

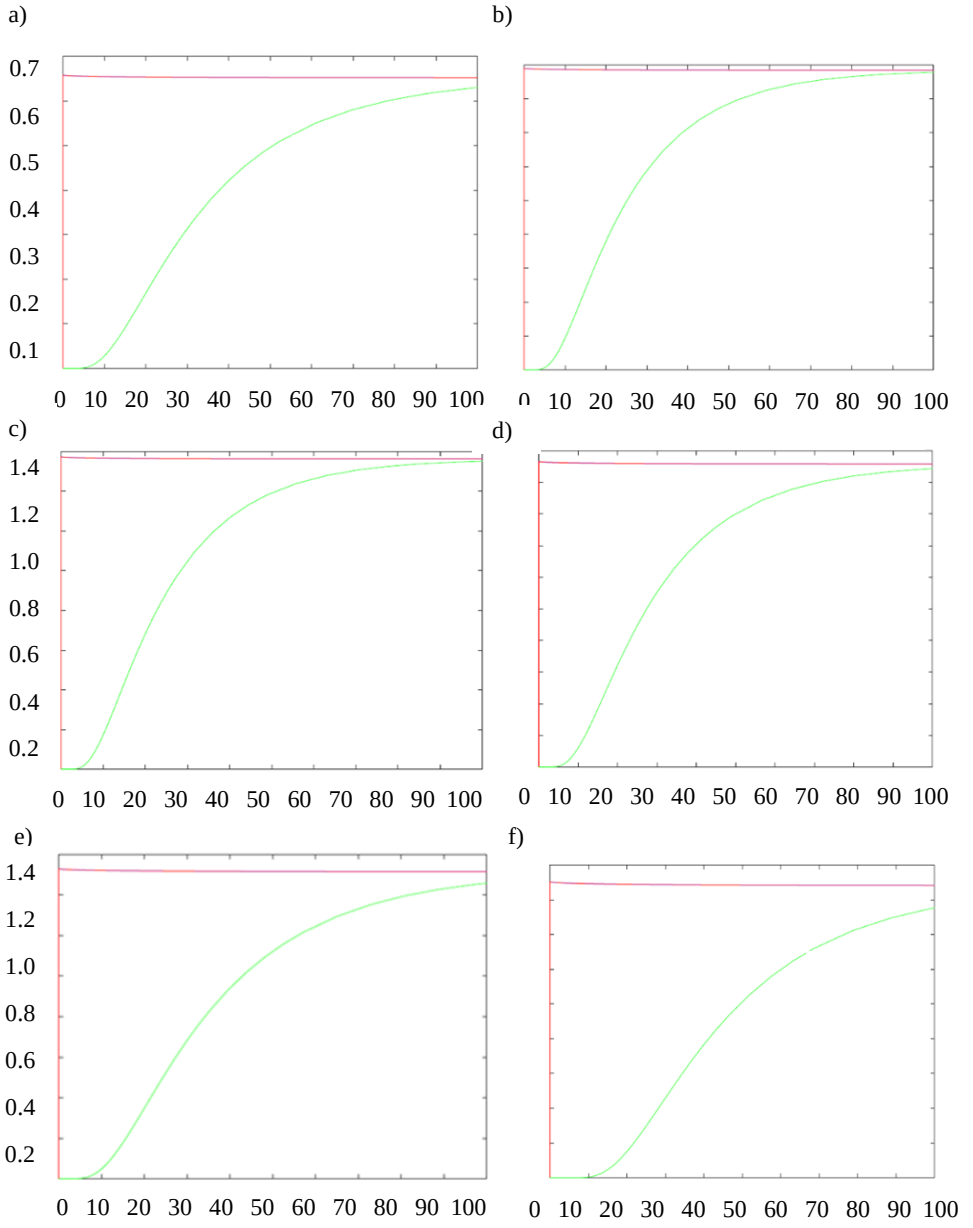

Fig. 3.29. Potentially toxic elements concentration in the liquid of the biochar pores (C_L) (green line) on unmodified biochar: a) Cr, b) Cd, c) Cu, d) Pb, e) Zn, f) Ni. Vertical axis – C_L (mol/m3), horizontal axis – t, s $\times 10^2$

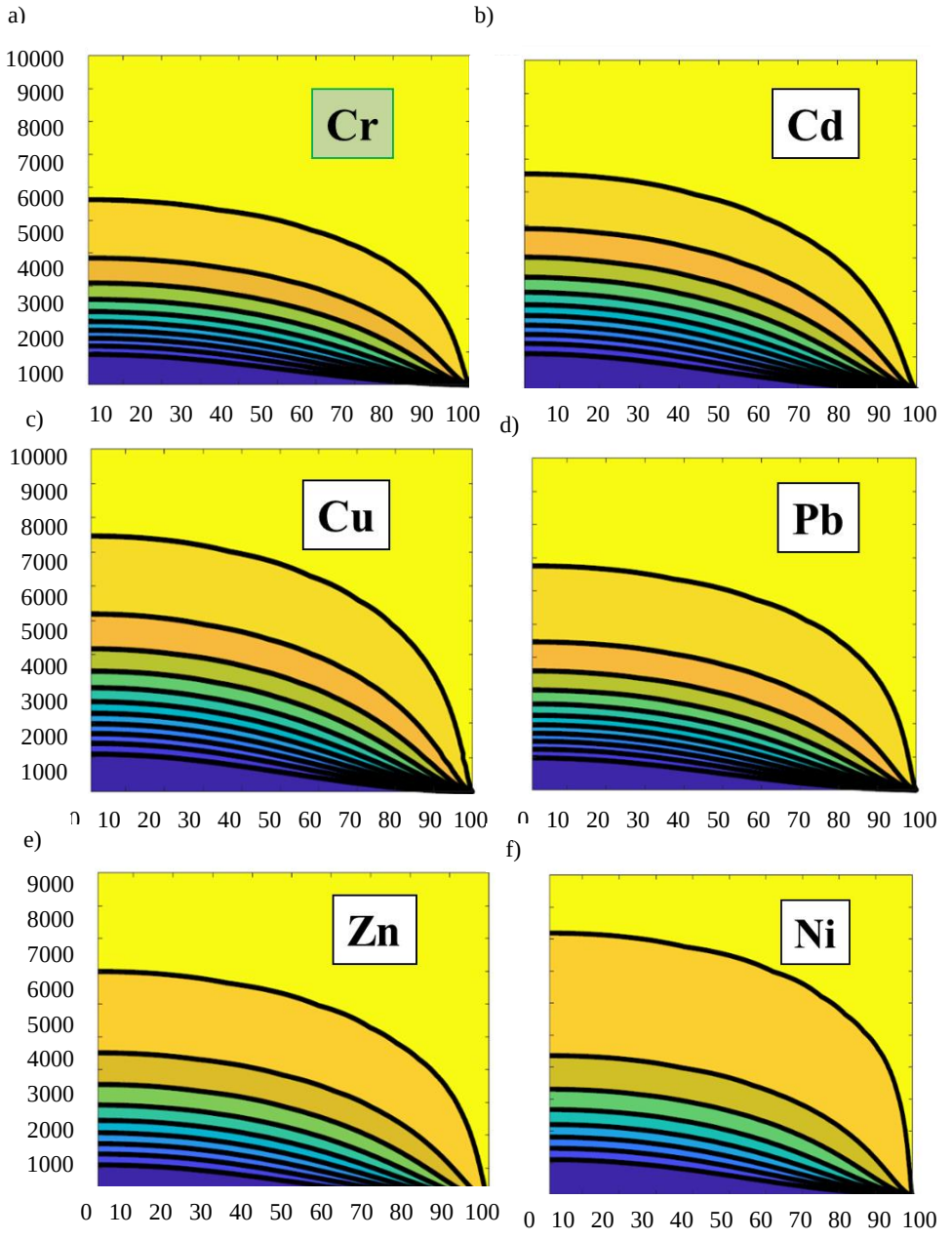

Fig. 3.30. Potentially toxic elements concentration in the solid along time and particle radius (C_S) on H_2O_2-modified biochar: a) Cr, b) Cd, c) Cu, d) Pb, e) Zn, f) Ni. Vertical axis – t, s, horizontal axis – particle radius, m×10^5

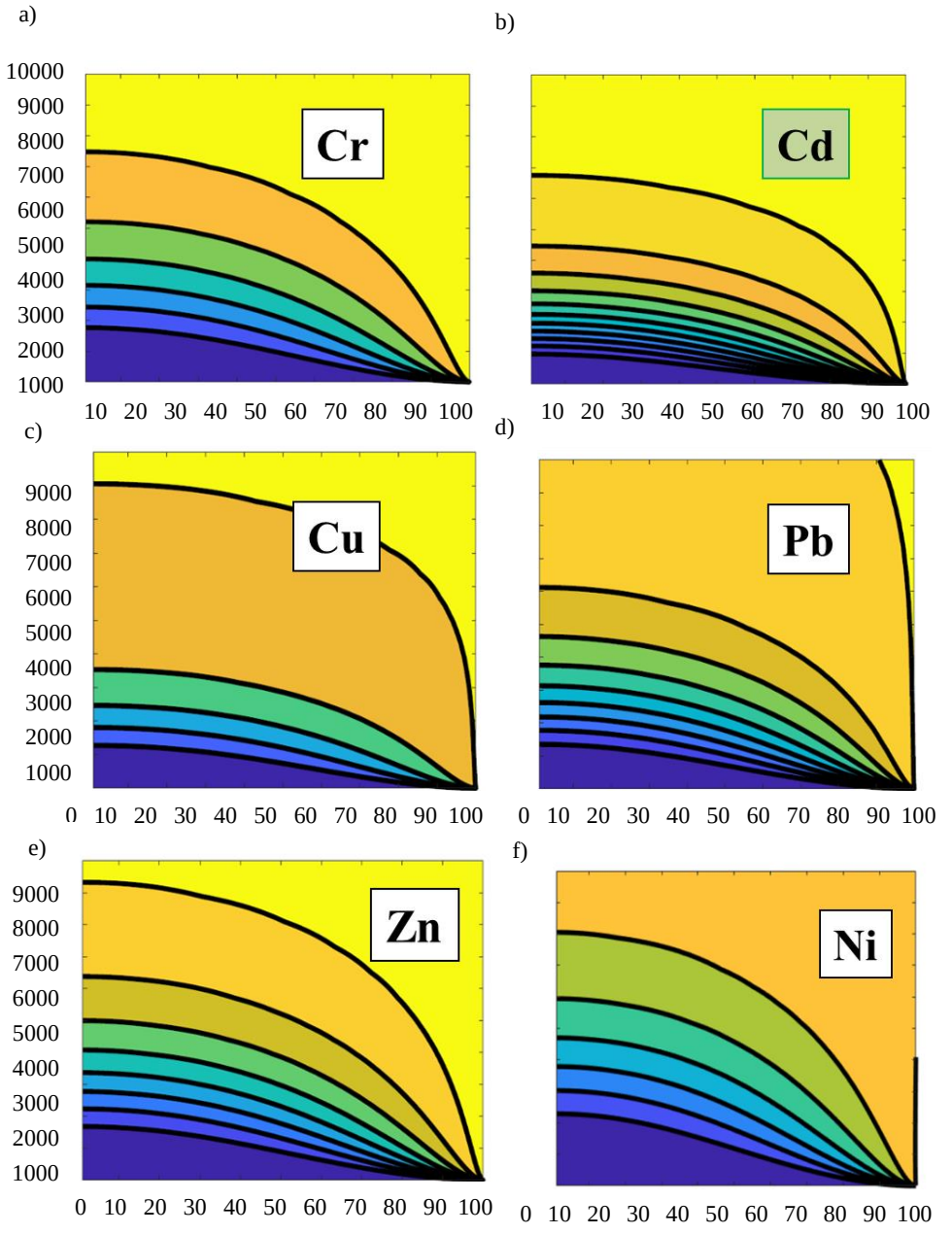

Fig. 3.31. Potentially toxic elements concentration in the solid along time and particle radius (C_S) on unmodified biochar: a) Cr, b) Cd, c) Cu, d) Pb, e) Zn, f) Ni. Vertical axis – t, s, horizontal axis – particle radius, m×10^5

Concentration maximum is present along the time near to the particle surface, because the boundary conditions at the surface has a direct dependence on bulk concentration, that changes along the time. PTEs concentration in unmodified and H_2O_2-modified biochar was in distributed manner, suggesting that surface diffusion was a step of adsorption. Time to reach the center of the particles was achieved in all cases, except Ni on unmodified BC, where saturation wasn't achieved.

3.4.3. The Sensitivity Analysis of the Simplified Adsorption Kinetics Model

Some of the adsorption models are based on adsorption reaction models and the adsorption kinetics is represented as the rate of chemical reactions. Other authors investigate the influence of the model parameters (mass transfer coefficient, surface diffusion or pore diffusivity) (Kavand *et al.* 2017). Less works are dedicated to the direct numerical simulation of reactive flow when the scientists should choose the appropriate solute transport model (Iliev et al. 2017).

The mathematical models with mass transfer diffusion are more complicated, but these models are most realistic. Some authors analyzed and compared the adsorption results obtained using different diffusion models (Souza *et al.* 2017). In this case the system of partial differential equations (PDEs) with appropriate boundary conditions is nonlinear and quite complicated. Thus numerical methods are used for solving such problems. For approximation of the system of PDEs different numerical methods are applied. In Kangro and Kalis (2018) the conservative averaging method was used. In Iliev et al. (2017), the finite volume method is applied to approximate the system of PDE. For solving adsorption problems a various computational software was used. For example, in Iliev et al. (2017) calculations were performed by combining the special commercial software package (GeoDict) and a general non-commercial software (Pore-Chem). The results of (Kangro and Kalis 2018; Russo *et al.* 2015) were obtained by using MATLAB software.

In this study, the special methods for appropriate numerical approximation of the dynamic intraparticle model for adsorption kinetics are considered and the sensitivity of the solution with respect of main transport and kinetic parameters is investigated. On the basis of this analysis it is shown how the adsorption process can be controlled efficiently. The obtained results make a basis for solving some important applied optimization problems to maximize the amount of adsorbate by selecting the optimal shape parameter of the adsorbent.

The main aim of this Chapter is to analyze the sensitivity of the solution with respect to the main parameters of the mathematical model. Such a control analysis is done for a linearized and normalized mathematical model.

The approximation of the mathematical model was done by using the method of lines (Leonavičiene *et al.* 2019). First, the semi-discrete finite volume scheme is constructed to approximate in space the nonlinear PDE. In order to simplify notations, it is restricted to the Langmuir adsorption model.

The uniform spatial mesh $\overline{\omega_h} = \omega \cup \{r_J\}$ is defined as

$$\omega_h = \left\{r_j : r_j = \left(j - \frac{1}{2}\right)h,\ j = 1,\dots,J-1\right\}, r_J = R_p, h = \frac{R_p}{J-0.5}. \quad (3.1)$$

Multiplying equation by r^2, integrating it over finite volume $[r_{j-0.5}; r_{j+0.5}]$ and approximating the obtained fluxes by central difference formula we obtain the semi-discrete scheme for j = 1; …; J – 1:

$$\frac{r_{j+1/2}^3 - r_{j-1/2}^3}{3}\left(\varepsilon + (1-\varepsilon)\frac{bC_{S,*}}{\left(1+bC_{L,j}\right)^2}\right)\frac{\partial C_{L,j}(t)}{\partial t} =$$

$$= r_{j+1/2}^2\left(\varepsilon D_p + (1-\varepsilon)D_s\frac{bC_{S,*}}{1+0.5b\left(C_{L,j+1}+C_{L,j}\right)}\right)\frac{C_{L,j+1}-C_{L,j}}{h} -$$

$$- r_{j-1/2}^2\left(\varepsilon D_p + (1-\varepsilon)D_s\frac{bC_{S,*}}{1+0.5b\left(C_{L,j-1}+C_{L,j}\right)}\right)\frac{C_{L,j}-C_{L,j-1}}{h}. \quad (3.2)$$

Boundary conditions are approximated in a similar way. For example, the condition is approximated by the semi-discrete equation:

$$\frac{h}{2}r_J^2\left(\varepsilon + (1-\varepsilon)\frac{bC_{S,*}}{\left(1+bC_{L,J}\right)^2}\right)\frac{\partial C_{L,J}(t)}{\partial t} =$$

$$-r_{J-1/2}^2\left(\varepsilon D_P + (1-\varepsilon)D_S \times \frac{bC_{S,*}}{1+0.5b(C_{L,J}+C_{L,J-1})}\right)\frac{C_{L,J}-C_{L,J-1}}{h}$$

$$+r_J^2 k_m(C_{B(t)} - C_{L,J}). \quad (3.3)$$

The proposed finite volume scheme approximates the given nonlinear differential problem with the second order accuracy. Due to properties of nonlinear coefficients it is straightforward to show that for implicit approximations of the time derivatives the fully discrete scheme is also unconditionally stable and the discrete solution converges to the exact solution of the differential problem. In this case the known theoretical results can be applied to prove that the solution of the semi-discrete scheme converges in the L_∞ norm with the order equal to the accuracy of approximation.

By adding the mass balance equation for the bulk concentration C_B

$$\frac{\partial C_B(t)}{\partial t} = -k_m A\left(C_B(t) - C_{L,J}(t)\right), \quad (3.4)$$

we obtain a large system of nonlinear ODEs with respect to functions $C_{L,j}(t)$, j = 1; …; J and $C_B(t)$.

In the computational experiments MATLAB ode15s solver was used.
For sensitivity analysis, the simplified adsorption kinetics model with initial and boundary conditions was introduced:

$$\frac{\partial C_B(\bar{t})}{\partial \bar{t}} = -\alpha\left(C_B(\bar{t}) - C_L(\bar{t},1)\right), 0 < \bar{t} < \mathrm{T}, \tag{3.5}$$

$$\frac{\partial C_L(\bar{t},\bar{r})}{\partial \bar{t}} = \frac{1}{\bar{r}^2}\frac{\partial}{\partial \bar{r}}\left(\bar{r}^2\frac{\partial C_L(\bar{t},\bar{r})}{\partial \bar{r}}\right), 0 < \bar{r} < 1, \tag{3.6}$$

$$\bar{r}^2\frac{\partial C_L(\bar{t},\bar{r})}{\partial \bar{r}}\Big|_{\bar{r}=0} = 0,\ \frac{\partial C_L(\bar{t},\bar{r})}{\partial \bar{r}}\Big|_{\bar{r}=1} = \beta\left(C_B(\bar{t}) - C_L(\bar{t},1)\right), \tag{3.7}$$

$$C_B(0) = C_B^o,\ C_L(0,\bar{r}) = C_L^o, 0 \le \bar{r} \le 1\,. \tag{3.8}$$

These equations are obtained from model approximation (Leonavičiene *et al.* 2019) using dimensionless variables

$$r = R_p\bar{r}, t = \frac{cR_p^2}{D}\bar{t}, 0 < \bar{r} < 1, 0 < \bar{t} < T = \frac{TD}{cR_p^2}, \tag{3.9}$$

and linearizing nonlinear equation on the equilibrium isotherm:

$$C_S(\bar{t},\bar{r}) = f\left(C_L(\bar{t},\bar{r})\right), \tag{3.10}$$

with $c = \varepsilon + (1-\varepsilon)f'(C_L)$.

The combined diffusion coefficient is selected as:

$$D = \varepsilon D_p + (1-\varepsilon)D_S\frac{f(C_L)}{C_L}\,. \tag{3.11}$$

New mass transport parameters α and β are computed as:

$$\alpha = \frac{Ak_mcR_p^2}{D},\ \beta = \frac{k_mR_p}{D}\ . \tag{3.12}$$

Linearized and normalized mathematical model (3.5) – (3.8) for the sensitivity analysis with respect to the parameters of adsorption system were used. Simplified model on the data reported by Russo *et al.* (2015) and Souza *et al.* (2017) was tested. In Russo *et al.* (2015) the Langmuir isotherm for the equilibrium was used. For the set of parameters reported in Russo *et al.* (2015) the full adsorption kinetics model was solved.

In Figure 3.32 the change of the bulk concentration ($C_B(t)$) and the change of the concentration of the solute in the liquid on the surface of the particle ($C_L(t; R_p)$) and at the center of the particle ($C_L(t; 0)$) along the time are seen. Bulk concentration reaches the saturation very fast.

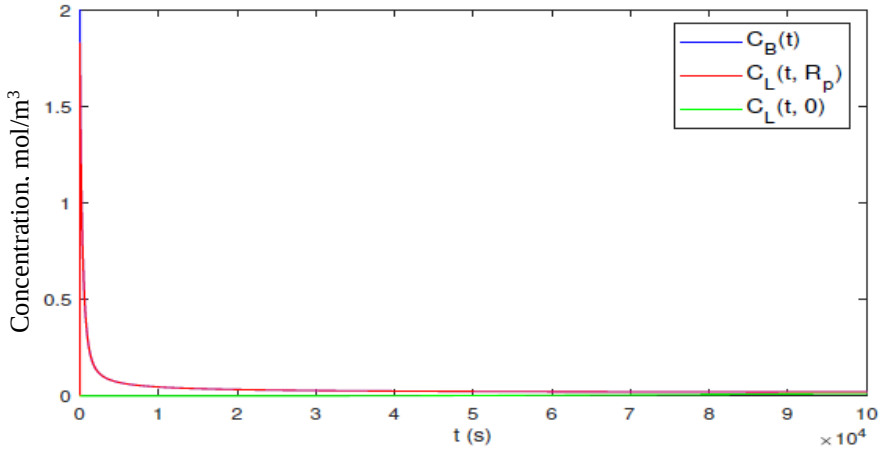

Fig. 3.32. Bulk concentration, concentration of the solute in the liquid on the surface of the particle and concentration of the solute in the liquid at the center of the particle for the data reported in Russo *et al.* (2015)

This is determined by the boundary condition: the change in the bulk concentration causes the change of the concentration of the solute in the liquid phase on the surface of the particle. But still a slow transport (diffusion) process inside of the particle. Therefore, the concentration of the solute in the liquid at the center of the particle changes very slowly along the time.

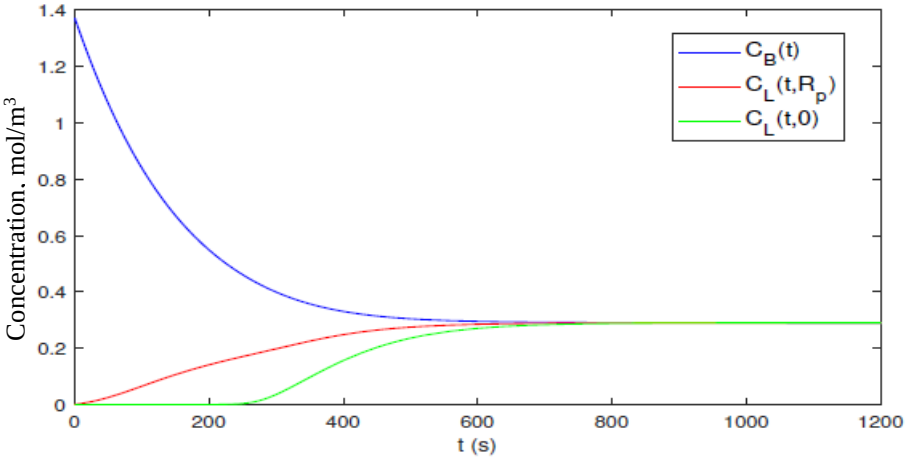

Fig. 3.33. Bulk concentration, concentration of the solute in the liquid on the surface of the particle and concentration of the solute in the liquid at the center of the particle for the data reported in Souza *et al.* (2017)

The second example illustrates an opposite situation when the concentration of the solute in the liquid at the center of the particle changes much faster and it reaches equilibrium state only shortly after surface concentration (Figure 3.33).

In this case the data reported in Souza *et al.* (2017) with the Redlich-Peterson isotherm was used. Some model parameters are estimated or converted using the provided data in order to compare the change of the concentrations for the two analyzed problems.

These two examples illustrate different properties of the adsorption process. In the presented figures qualitatively different results were observed.

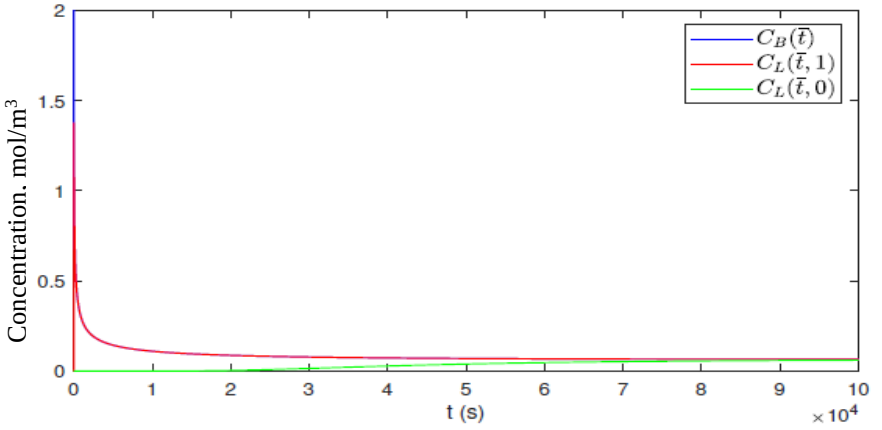

Fig. 3.34. Dynamics of the concentrations obtained from the simplified model for the data reported in Russo *et al.* (2015)

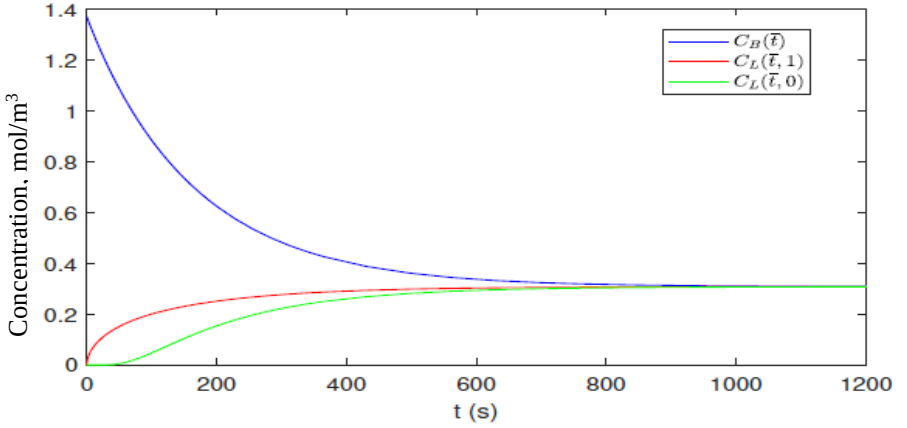

Fig. 3.35. Dynamics of the concentrations obtained from the simplified model for the data reported in Souza *et al.* (2017)

Next the linearized and normalized mathematical model were used to the discussed problems and concentrate on the dynamics of the bulk concentration

($C_B(\bar{t})$), concentration of the solute in the liquid on the surface of the particle ($C_L(\bar{t}; 1)$) and concentration of the solute in the liquid at the center of the particle ($C_L(\bar{t}; 0)$). The Figures 3.34 and 3.35 show that with the simplified model the dynamics of the process could be predicted quite accurately.

For sensitivity analysis, in order to investigate the influence of physical parameters on solutions, a detailed analysis of the second example based on data provided in Souza *et al.* (2017) was performed. With this set of parameters it was found that the simplified model parameters are $\alpha = 4.14$ and $\beta = 0.4$. The parameter α controls the decay of the bulk concentration. The higher is the value of this parameter the faster bulk concentration $C_B(\bar{t})$ decreases and the process reaches the equilibrium with the lower concentration (see Figure 3.36). The concentration on the surface of the particle $C_L(\bar{t}; 1)$ does not increases so fast.

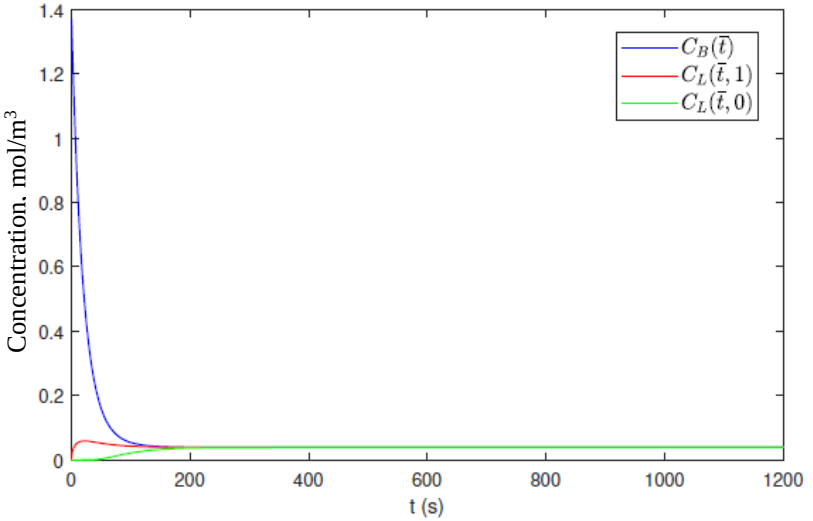

Fig. 3.36. Dynamics of the concentrations obtained from the simplified model ($\alpha = 41.4$, $\beta = 0.4$) for the data reported in Souza *et al.* (2017)

The parameter β affects the change in concentration on the surface of the particle: the higher the value of this parameter the faster concentration $C_L(\bar{t}; 1)$ increases (Figure 3.36).

The adsorption kinetics depends not only on the absolute values of parameters, but also on their ratio. The influence of the ratio α/β in Figure 3.37 ($\alpha/\beta \approx 1$), Figure 3.38 ($\alpha/\beta \approx 10$) and Figure 3.39 ($\alpha/\beta \approx 0.1$) could be seen. The ratio of parameters influences the equilibrium concentration and the time required to reach this concentration. If α/β is large then the system fast reaches equilibrium with lower the bulk concentration. In the case when $\alpha/\beta << 1$ the system reaches equilibrium with high bulk concentration and needs more time.

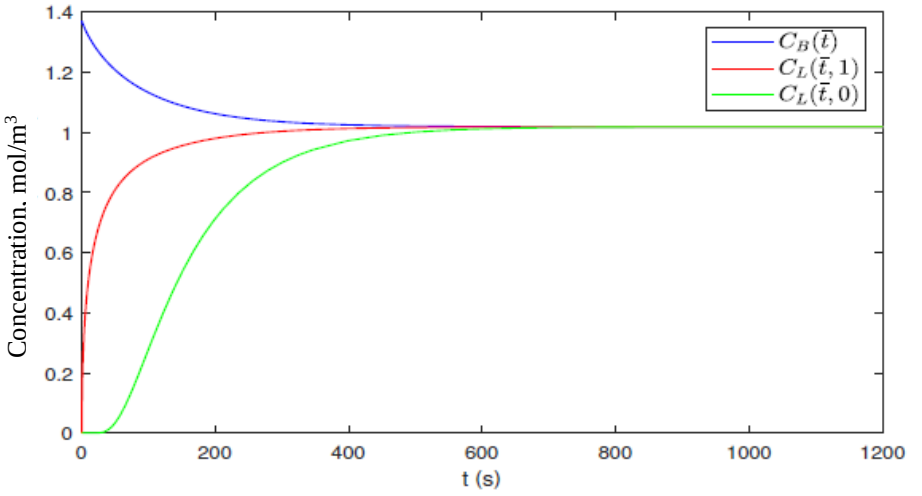

Fig. 3.37. Dynamics of the concentrations obtained from the simplified model ($\alpha = 4.14$, $\beta = 4$) for the data reported in Souza *et al.* (2017)

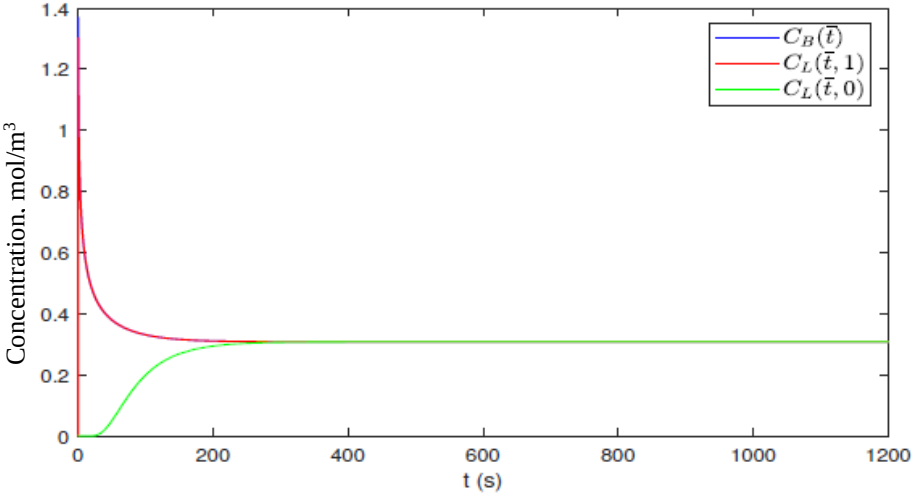

Fig. 3.38. Dynamics of the concentrations obtained from the simplified model ($\alpha/\beta \approx 10$) for the data reported in Souza *et al.* (2017)

Which physical parameters influence such changes? From the (3.12) it was found that $\alpha/\beta = A_c R_p$. This means that the adsorption process depends on the properties of the adsorbent and solution, on the isotherm used for equilibrium and the radius of the particle. In Figure 3.40 the concentrations obtained using Langmuir isotherm estimated from the data reported in Souza *et al.* (2017) were

presented. The results show that in our case when isotherms fit quite well to the given data the same adsorption process development (see Fig. 3.35 for comparison) could be observed.

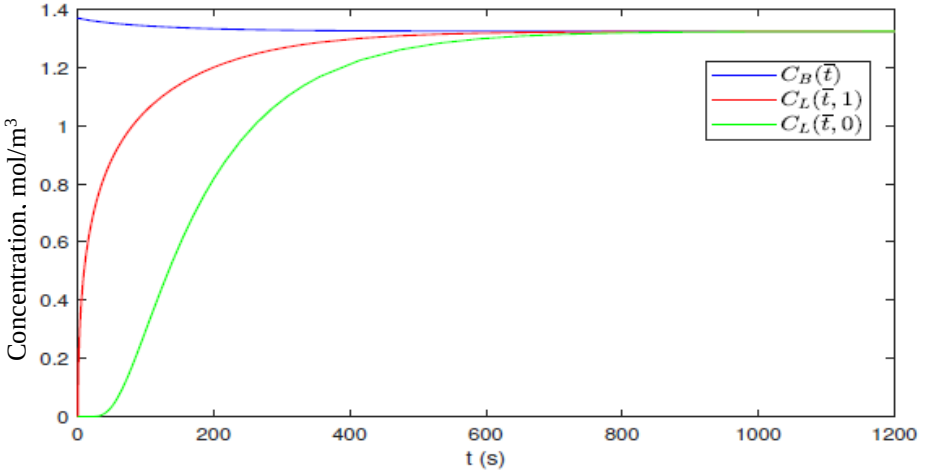

Fig. 3.39. Dynamics of the concentrations obtained from the simplified model ($\alpha/\beta \approx 0.1$) for the data reported in Souza *et al.* (2017)

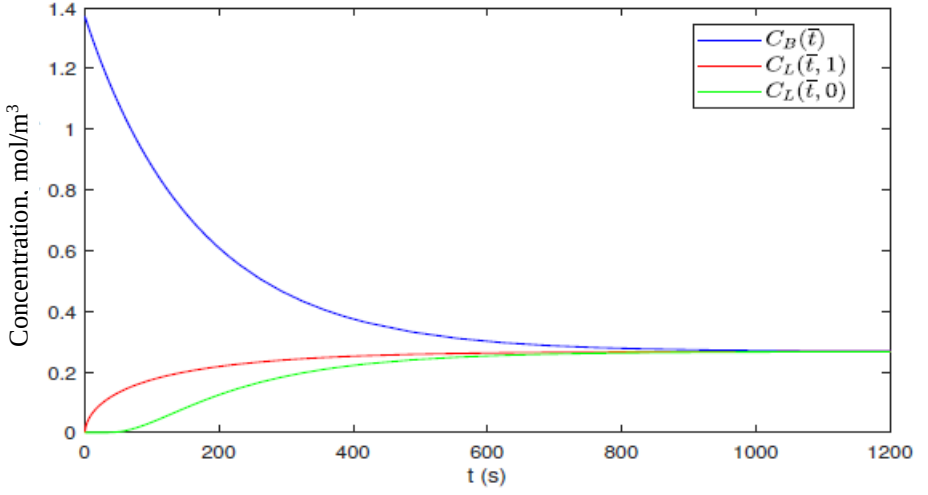

Fig. 3.40. Dynamics of the concentrations obtained from the simplifed model with Langmuir isotherm for the data reported in Souza *et al.* (2017)

After performed simulations it could be observed that the linearized and normalized mathematical model works well and the dynamics of the process with

a different set of physical parameters could be predicted quite accurately. As it could be seen from calculations with a full adsorption model the bulk concentration decreases for both examples (see Figure 3.32 and Figure 3.33), but for the first example the process is faster. Let us compare the results obtained using the full and the simplified models for the data reported in Russo *et al.* (2015). In this case the full model (see Figure 3.32) shows that the bulk concentration decreases very fast and the pore concentration of the solute in the liquid increases till a saturation is reached. During a short time interval (depending on the physical parameters) the concentration of solute in the liquid at the surface of the particle increases very fast and a quasi-stationary solution is fastly reached. Then both solutions decay together. The change of the concentration on the surface of the particle implies the change of the concentration in the pore. This process is very slow for this example. And the pore is fully filled only after a long time interval. It could be seen that the saturation at the center of the particle even after 100 000 s is still not reached.

Analogous information is obtained from the simplified model (see Figure 3.34). Using this model the concentration of solute in the liquid at the surface of the particle increases very fast and reaches the value of bulk concentration. The change in the concentration inside the particle is a slow process and needs time to reach the center of the particle. We should note that the quasistationary concentration and the rate of adsorption process differ from the full model solutions. Such differences can be explained by the influence of the parameters c and D used in simplified model. The values of these parameters do not change according to time in the simplified model and such simplification implies the quantitative changes in solutions. But the main trend of the adsorption process is modelled quite accurately.

The sensitivity of the solution with respect of main physical system parameters is analyzed using the simplified model. This analysis allows to predict the dynamics of the adsorption process. The results obtained with the linearized and normalized mathematical model are compared with the simulations done for a full nonlinear mathematical model. The results of the numerical experiments show that we can predict the main trend of the adsorption process using the proposed simplified linear model. The obtained results can be applied for optimization problems.

3.5. Engineering Technology for Modification of Ligneous Biochar

Biochar needs to be produced at pyrolysis temperature of 450 °C, because biochar obtained at 300–450 °C is more suitable for adsorption of inorganic PTEs, as it

contains both oxygen-containing functional groups and developed microporous structure (Ahmad *et al.* 2014).

Higher adsorption capacity for cationic PTEs could be achieved via modification of the biochar. The adsorption of PTEs on the biochar is mainly controlled by the interaction between the ions of metals in solution and oxygen-containing functional groups (hydroxyl and carboxyl groups) on the surface of the biochar. Thus, modification with the strong oxidant will result in the increase of cation exchange capacity of the biochar via the increase of the content of oxygen-containing functional groups on the surface.

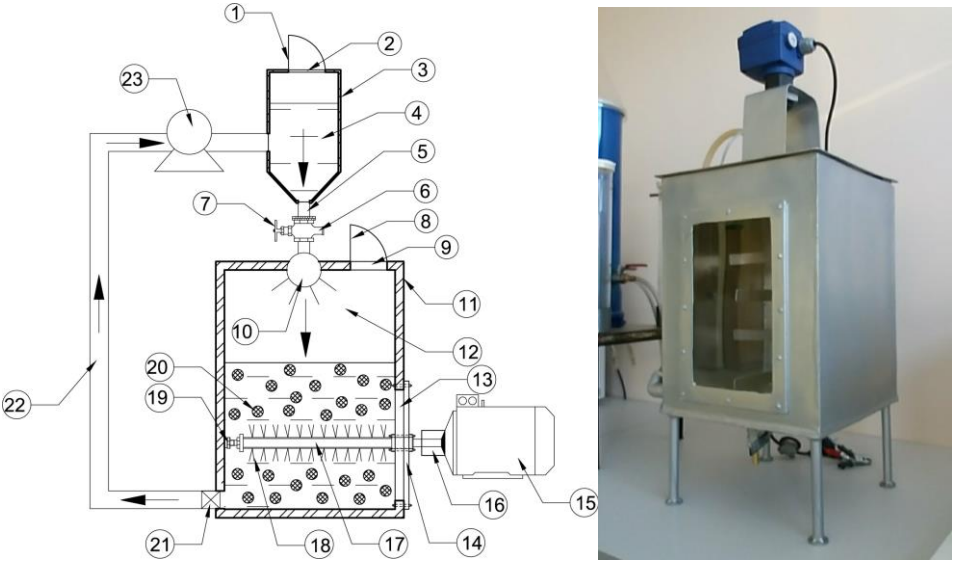

Fig. 3.41. Device for modification the biochar with H_2O_2: a – technical drawing, b – prepared device. Device consists of: 1 – lid, 2 – opening, 3 – body of the tank for H_2O_2, 4 – tank for H2O2, 5 – channel, 6 – channel for outflow of H_2O_2, 7 – tap, 8 – lid, 9 – opening, 10 – spray, 11 – body of the modifying tank, 12 – modifying tank, 13 – cavity, 14 – lid, 15 – motor reducer, 16 – clutch, 17 – rotary driven flexible roller, 18 – brush, 19 – slug, 20 – biochar, 21 – filter, 22 – tube, 23 – vacuum pump

One of such modification agents could be oxidant H_2O_2, being cheaper than acids and decomposed to H_2O и O_2, not forming salts after modification procedure, that could block the pores of the biochar.

For intensification of the modification process, a device for modification the biochar with H_2O_2 solution was invented (patent #6434 by Pranas Baltrėnas, Edita Baltrėnaitė and Valeriia Chemerys (2017)). The invention relates to a technical

field for the treatment of contaminated water. Modification is based on the mixing of biochar particles with H_2O_2 solution.

This device for modification of biochar with H_2O_2 solution (Fig. 3.41) is economically efficient and environmetally friendly. It contains an additional stirring mechanism for increase the contact surface of the biochar with the solution. The purpose of the invention was to activate the biochar surface, and thus improve the adsorption properties of the biochar for the adsorption of cationic metals.

The modification process presumes using of the ligneous biochar of 0.2 to 1 cm fraction to prevent flotation of particles, as well as water contamination by fine particles <0.2 cm. To achieve a sufficient biochar saturation, biochar to solution mixing ratio is 1:3. Modification device's 4/5 volume is filled: the volume of the biochar is 1/5 and the volume of the H_2O_2 solution is 3/5. Biochar with H_2O_2-solution needs to be rotated at 3 rpm for 2 h. Then the biochar needs to be separated from the solution with cellulose acetate membrane filter with particle retention 1.06 μm, and dried.

The improved modification process due to mixing makes it possible to create a biochar with a large number of carboxyl groups. In addition, the method is simple, economical, and does not require manual work. The device consists of the tank, mixer and a permanent H_2O_2 solution supply and disposal system. The mixing is carried out in a vertical plane by a rotary driven flexible roller with brushes supported by motor reducer. Rotary driven flexible roller with brushes increases the efficiency of mixing, simplifies construction, reduces energy consumption. In addition, the vacuum pump optimizes the overall system performance by adjusting the removal of excess H_2O_2 from the modification tank and returning this solution back to the H_2O_2 solution tank. After the modification, the excess solution is returned to the H_2O_2 solution tank, and the biochar is removed through the opening on the side of the device. The solution should be changed after each modification process.

3.6. Conclusions of Chapter 3

1. Surface complexation, electrostatic attraction, ion exchange and physical adsorption control adsorption of Cr^{3+}, Cd^{2+}, Pb^{2+}, Zn^{2+}, Ni^{2+}, Cu^{2+} on the biochar;

2. The most important intrinsic characteristics of ligneous feedstock, that influence adsorptive characteristics of biochar: lignin, as it creates pores; ash – as it may contain trace elements, that act like adsorption sites; nitrogen and carbon content – as they influence N/C and O/C ratios in biochar.

3. From natural modifications it was found, that with the increase of lignin content from 19.06 in birch wood to 59% in pine bark, BET SSA increased from

20.11 to 362.1 m^2/g. Also with the increase of lignin content, O/C ratio increased from 0.074 in pine bark 0.188 in birch bark. The difference between BET SSA of biochar from stem wood and stem bark was about 10 times: 25.08 and 354.7 m^2/g in pine, 20.11 and 362.1 m^2/g in birch. Thus, bigger amount of lignin (54–59%), ash (11.8–13.9%), nitrogen (0.4%) and lower carbon content (75–76%) in ligneous feedstock favor the adsorptive characteristics of BC.

4. Modification with H_2O_2 adds carboxylic groups on the BC surface, while $FeCl_3$ and $MgCl_3$ – adds phenolic groups. Modification with $FeCl_3$ and $MgCl_3$ decreased BET SSA, because Fe and Mg particles blocked biochar pores. Unmodified and H_2O_2-modified BC (where $pH>pH_{pzc}$) are suitable for adsorption of cationic PTEs through electrostatic attraction, while Mg- and Fe-modified BC (where $pH<pH_{pzc}$) are more suitable for adsorption of anionic PTEs.

5. Higher BET SSA and CEC are favorable for adsorption of cationic PTEs. From the adsorption perspective, the most suitable modified biochar was BC - H_2O_2 (15%) with the BET 301.5 m^2/g and CEC 22.79 $cmol_c/kg$. Modification with H_2O_2 increased O/C ratio in 3 times, and N/C ratio – 9 times.

6. The highest adsorption capacity of PTEs from laboratory solutions was reached by H_2O_2-modified BC when when concentration was 10 mg/l: 20.10 mg/g (Ni), 20.56 mg/g (Cr), 26.68 mg/g (Pb), 23.77 mg/g (Cd), 23.35 mg/g (Zn), 22.72 mg/g (Cu). That exceeded results for unmodified biochar up to 2 times.

7. Combination of BC with cationic hydrogel increased CEC of unmodified BC from 5.15 to 37.12 $cmol_c/kg$ and BET from 20.11 to 401.14 m^2/g. Swelling of cationic hydrogel was lower than anionic, because of the acyclic acid in composition, that leads to formation of highly cross-linked polymers and thus, lower swelling. Cationic hydrogel swells at 20 °C and reaches its maximum at 240 min (434%). The lowest swelling was observed at 40 °C (175%). Cationic hydrogel swells at acidic pH (2, 4, 6) and reaches its maximum when pH is 2 (498%) at 240 min.

8. Adsorption efficiency of PTEs by biochar from landfill leachate was lower than from laboratory solutions. H_2O_2-modified BC showed maximum adsorption capacity from landfill leachate at particle size 0.4–1.0 mm: 3.54 mg/g (Ni), 5.14 mg/g (Cr), 1.01 mg/g (Pb), 0.74 mg/g (Cd), 4.12 mg/g (Zn), 1.05 mg/g (Cu). The results were higher than unmodified birch biochar at dosage 100 g/l: 2.10 mg/g (Ni), 2.56 mg/g (Cr), 0.68 mg/g (Pb), 0.37 mg/g (Cd), 3.35 mg/g (Zn), 0.72 mg/g (Cu). Cationic composite with H_2O_2-modified BC had the highest adsorption capacity from landfill leachate at 300 min and dosage 20 g/l: 4.36 mg/g (Ni), 12.81 mg/g (Cr), 1.27 mg/g (Pb), 0.91 mg/g (Cd), 4.33 mg/g (Zn), 1.57 mg/g (Cu).

9. Dynamic intraparticle model was firstly fitted for adsorption of Cr^{3+}, Cd^{2+}, Pb^{2+}, Zn^{2+}, Ni^{2+}, Cu^{2+} by biochar. Concentration in the bulk and concentration in the liquid of the biochar pores helped to define adsorption mechanism.

Concentration in the solid helps to define PTEs distribution in the biochar particle and define adsorption mechanism. Rapid adsorption occurred during the first 30 min due to film diffusion, while the pore and surface diffusion process was slow. Concentration maximum was present along the time near to the particle surface.

10. The sensitivity of the solution with respect of main physical system parameters was analyzed using the simplified model. This analysis allows to predict the dynamics of the adsorption process. The obtained results predict the main trend of the adsorption process using the proposed simplified linear model. Thus, sensitivity analysis is a basis for solving important applied optimization problems to maximize the amount of adsorbate by selecting the optimal shape parameter of the adsorbent.

11. Technology for modification of ligneous biochar allows to create H_2O_2-modified biochar with 25% higher cation exchange capacity and content of carboxyl and carbonyl groups on the surface of the biochar, and up to 2 times higher BET specific surface area, than H_2O_2-modified biochar without the technology. Also it was found, that BC of smaller particle size (0.4–1.0 mm), had higher CEC and BET SSA, than BC of patricle size 1.0–3.0 mm, that was modified in the same way.

General Conclusions

1. Key mechanisms controlling the maximum adsorption of Cr^{3+}, Cd^{2+}, Pb^{2+}, Zn^{2+}, Ni^{2+}, Cu^{2+} on ligneous biochar were surface complexation, electrostatic attraction, ion exchange, physical adsorption.

2. Specific surface area and cation exchange capacity were the main properties affecting adsorption of Cr^{3+}, Cd^{2+}, Pb^{2+}, Zn^{2+}, Ni^{2+}, Cu^{2+} on biochar.

3. Influence of intrinsic properties of ligneous feedstock on adsorption was investigated for the first time. The most important intrinsic characteristics of ligneous feedstock, that influence adsorptive characteristics of biochar: lignin, as it creates pores; ash – as it may contain trace elements, that act like adsorption sites; nitrogen and carbon content – as they influence N/C and O/C ratios in biochar. From natural modifications it was found, that bigger amount of lignin (54–59%), ash (11.8–13.9%), nitrogen (0.4%) and lower carbon content (75– 76%) in ligneous feedstock favor the adsorptive characteristics of BC.

4. Modification with H_2O_2 added carboxylic groups on the BC surface, while $FeCl_3$ and $MgCl_3$ – phenolic groups. Unmodified and H_2O_2-modified BC were found to be suitable for adsorption of cationic PTEs through electrostatic attraction, while Mg- and Fe-modified BC were more suitable for adsorption of anionic PTEs.

5. From the adsorption perspective, the most suitable modified biochar was BC – H_2O_2 (15%) with the BET 301.5 m^2/g and CEC 22.79 $cmol_c/kg$. Modification with H_2O_2 increased O/C ratio in 3 times, and N/C ratio – 9 times.

6. The highest adsorption capacity of PTEs from laboratory solutions was reached by H_2O_2-modified BC when when concentration was 10 mg/l: 20.10 mg/g (Ni), 20.56 mg/g (Cr), 26.68 mg/g (Pb), 23.77 mg/g (Cd), 23.35 mg/g (Zn), 22.72 mg/g (Cu). That exceeded results for unmodified biochar up to 2 times.

7. Combination of BC with cationic hydrogel increased CEC of unmodified BC from 5.15 to 37.12 $cmol_c$/kg and BET from 20.11 to 401.14 m^2/g. Swelling of cationic hydrogel was lower than anionic, because of the acyclic acid in composition, that leads to formation of highly cross-linked polymers and thus, lower swelling. Cationic hydrogel swells at 20 °C and reaches its maximum at 240 min (434%). The lowest swelling was observed at 40 °C (175%). Cationic hydrogel swells at acidic pH (2, 4, 6) and reaches its maximum when pH is 2 (498%) at 240 min.

8. Biochar adsorption efficiency from landfill leachate was lower than from laboratory solutions. The adsorption capacity from landfill leachate decreased in the following order: cationic composite with H_2O_2-modified BC (with contact time 300 min and biochar dosage 20 g/l) > H_2O_2-modified BC (with particle size 0.4–1.0 mm) > unmodified birch biochar (with biochar dosage 100 g/l).

9. Dynamic intraparticle model was firstly fitted for adsorption of Cr^{3+}, Cd^{2+}, Pb^{2+}, Zn^{2+}, Ni^{2+}, Cu^{2+} by ligneous biochar. Concentration in the bulk and in the liquid of the biochar pores helped to define adsorption mechanism. Concentration in the solid helps to define PTEs distribution in the biochar particle and define adsorption mechanism. Rapid adsorption occurred during the first 30 min due to film diffusion, while the pore and surface diffusion process was slow. Concentration maximum was present along the time near to the particle surface.

10. The sensitivity of the solution with respect of main physical system allows to predict the dynamics of the adsorption process – the main trend of the adsorption process – using the proposed simplified linear model. Sensitivity analysis is a basis for solving important applied optimization problems to maximize the amount of adsorbate by selecting the optimal shape parameter of the adsorbent.

11. Technology for modification of ligneous biochar allows to create H_2O_2-modified biochar with 25% higher cation exchange capacity and content of carboxyl and carbonyl groups on the surface of the biochar, and up to 2 times higher BET specific surface area, than H_2O_2-modified biochar without the technology. Also it was found, that BC of smaller particle size (0.4–1.0 mm), had higher CEC and BET SSA, than BC of patricle size 1.0–3.0 mm, that was modified in the same way.

Recommendations

1. In the patented modification device, different chemical solutions could be used in order to modify the biochar towards enhanced adsorption from synthetic solutions and landfill leachate. For enhanced adsorption of Cr^{3+}, Cd^{2+}, Pb^{2+}, Zn^{2+}, Ni^{2+}, Cu^{2+}, it is recommended to use H_2O_2 solution to increase specific surface area and cation exchange capacity.
2. In terms of sustainability, it is recommended to choose birch forestry wastes with bigger amount of lignin (54–59%), ash (11.8–13.9%), nitrogen (0.4%) as the feedstock, prepare biochar adsorbent at 450 °C for 2 h, crush it to particle size 0.4–1 mm and modify with H_2O_2 solution in special device with rotation.
3. It is recommended to use H_2O_2-modified biochar-hydrogel composites for enhanced adsorption of Cr^{3+}, Cd^{2+}, Pb^{2+}, Zn^{2+}, Ni^{2+}, Cu^{2+} from landfill leachate.

References

Abdel-Fattah, T. M., Mahmoud, M. E., Ahmed, S. B., Huff, M. D., Lee, J. W., & Kumar, S. (2015). Biochar from woody biomass for removing metal contaminants and carbon sequestration. *Journal of Industrial and Engineering Chemistry*, *22*, 103–109.

Agrafioti, E., Kalderis, D., & Diamadopoulos, E. (2014). Ca and Fe modified biochars as adsorbents of arsenic and chromium in aqueous solutions. *Journal of environmental management*, *146*, 444–450.

Ahmad, M., Rajapaksha, A. U., Lim, J. E., Zhang, M., Bolan, N., Mohan, D., Ok, Y. S. (2014). Biochar as a sorbent for contaminant management in soil and water: a review. *Chemosphere*, *99*, 19–33.

Ahmed, M. B., J. L. Zhou, H. H. Ngo, W. Guo, and M. Chen. 2016. "Progress in the preparation and application of modified biochar for improved contaminant removal from water and wastewater." *Bioresour. Technol.* 214 (1): 836–851.

Aksu, Z., & Kutsal, T. (1991). A bioseparation process for removing lead (II) ions from wastewater by using C. vulgaris. *Journal of Chemical Technology & Biotechnology*, *52*(1), 109–118.

Allaire, S. E.; Lange, S. F.; Auclair, I. K.; Quinche, M.; Greffard, L.; (The Char Team). Report: Analyses of Biochar Properties; CRMR-2015-SA-5; Centre de Recherche sur les Matériaux Renouvelables, Université Laval: Quebec, QC, Canada, 2015; 59p.

Apha, A. (2005). WEF, 2005. *Standard methods for the examination of water and wastewater*, *21*, 258–259.

Aslan S., Polat A. & Ugur Savas Topcu (2015) Assessment of the adsorption kinetics, equilibrium and thermodynamics for the potential removal of Ni2+ from aqueous solution using waste eggshell, *Journal of Environmental Engineering and Landscape Management*, 23:3, 221–229.

Azargohar, R., Dalai, A.K., 2006. Biochar as a precursor of activated carbon. *Appl. Biochem. Biotechnol.* 131 (1–3), 762–773.

Azmi, N. B., Bashir, M. J., Sethupathi, S., & Ng, C. A. (2016). Anaerobic stabilized landfill leachate treatment using chemically activated sugarcane bagasse activated carbon: kinetic and equilibrium study. *Desalination and Water Treatment*, *57*(9), 3916–3927.

Balamuralidhara, V., Pramodkumar, T. M., Srujana, N., Venkatesh, M. P., Gupta, N. V., Krishna, K. L., & Gangadharappa, H. V. (2011). pH sensitive drug delivery systems: A review. *Am J Drug Discov Dev*, *1*(1), 25.

Baltrėnaitė, E., Baltrėnas, P., & Huisingh, D. (2019). Technogenic metallic elements in biomass and their effects on biomass product properties. *Journal of Water Supply: Research and Technology—AQUA*, *68*(8), 623–644.

Baltrėnaitė, E., Baltrėnas, P., Lietuvninkas, A. (2016). *The sustainable role of the tree in environmental protection technologies*. Monograph. Dordrecht: Springer International Publishing.

Baltrėnas, P., Baltrėnaitė, E., & Spudulis, E. (2015). Biochar from Pine and Birch Morphology and Pore Structure Change by Treatment in Biofilter. *Water, Air, & Soil Pollution*, *226*(3), 1–14.

Banik, C., Lawrinenko, M., Bakshi, S., & Laird, D. A. (2018). Impact of Pyrolysis Temperature and Feedstock on Surface Charge and Functional Group Chemistry of Biochars. *Journal of environmental quality*.

Bousba, S., & Meniai, A. H. (2013). Adsorption of 2-chlorophenol onto sewage sludge based adsorbent: Equilibrium and kinetic study. *Chemical Engineering Transactions*, *35*, 859–864.

Brewer, C. E. (2012). Biochar characterization and engineering.

Cao, X., Ma, L., Liang, Y., Gao, B., & Harris, W. (2011). Simultaneous immobilization of lead and atrazine in contaminated soils using dairy-manure biochar. *Environmental science & technology*, *45*(11), 4884–4889.

Chen, X., Chen, G., Chen, L., Chen, Y., Lehmann, J., McBride, M. B., & Hay, A. G. (2011a). Adsorption of copper and zinc by biochars produced from pyrolysis of hardwood and corn straw in aqueous solution. *Bioresource technology*, *102*(19), 8877–8884.

Chen, B., Chen, Z., Lv, S., 2011b. A novel magnetic biochar efficiently sorbs organic pollutants and phosphate. *Bioresour. Technol.* 102 (2), 716–723.

Chen, B., Chen, Z., 2009. Sorption of naphthalene and 1-naphthol by biochars of orange peels with different pyrolytic temperatures. *Chemosphere* 76, 127–133.

Chiron, N., Guilet, R., & Deydier, E. (2003). Adsorption of Cu (II) and Pb (II) onto a grafted silica: isotherms and kinetic models. *Water Research*, *37*(13), 3079–3086.

Christmann, K. (2010). Adsorption. Lecture Series 2010/2011: "Modern Methods in Heterogeneous Catalysis Research", Institut für Chemie und Biochemie, Freie Universität, Berlin,Availablefrom http://www.fhierlin.mpg.de/acnew/department/pages/teaching/pages/teaching__wintersemester__2010_2011/klaus_christmann__adsorption__101105.pdf

Cibati, A., Foereid, B., Bissessur, A., & Hapca, S. (2017). Assessment of Miscanthus× giganteus derived biochar as copper and zinc adsorbent: study of the effect of pyrolysis temperature, pH and hydrogen peroxide modification. *Journal of Cleaner Production*, *162*, 1285–1296.

COST. 2011. *FA COST Action TD1107: Biochar as option for sustainable resource management* [online]. Available from internet: <http://www.cost.eu/domains_actions/fa/Actions/TD1107>.

de Gunzburg, J., Ducher, A., Modess, C., Wegner, D., Oswald, S., Dressman, J., ... & Siegmund, W. (2015). Targeted adsorption of molecules in the colon with the novel adsorbent-based Medicinal Product, DAV132: A proof of concept study in healthy subjects. *The Journal of Clinical Pharmacology*, *55*(1), 10–16.

Deutsche Norm, Testing of solid fuels. Determination of the water content and the moisture of analysis sample, DIN 51718, 1995.

Deutsche Norm, Testing of solid fuels. Determination of ash content, DIN 51719, 1978.

DIN ISO 11265, Ausgabe:1997-06 Bodenbeschaffenheit e Bestimmung der spezifischen elektrischen Leitfähigkeit (ISO 11265:1994 þ ISO 11265:1994/ Corr.1:1996). DIN Deutsches Institut für Normung e. V., Berlin.

Dong, X., Ma, L. Q., & Li, Y. (2011). Characteristics and mechanisms of hexavalent chromium removal by biochar from sugar beet tailing. *Journal of hazardous materials*, *190*(1), 909–915.

Drossel, W. G., Kunze, H., Bucht, A., Weisheit, L., & Pagel, K. (2015). Smart 3–Smart Materials for Smart Applications. *Procedia CIRP*, *36*, 211–216.

Duffy, S. J. (2011). *Environmental chemistry: a global perspective*. Oxford university press.

Dwivedi, D., Lepková, K., & Becker, T. (2017). Carbon steel corrosion: a review of key surface properties and characterization methods. *RSC advances*, *7*(8), 4580–4610.

EBC. 2012. European Biochar Certificate - Guidelines for a Sustainable Production of Biochar [online]. Version 6.1 of 19th June 2015. European Biochar Foundation [cited 10 January 2017]. Available from Internet: http://www.european-biochar.org/en/analytical%20methods.

EUROSTAT 2015. *Municipal wastes statistics*. Available from Internet: http://ec.europa.eu/eurostat/statistics-explained/index.php/Municipal_waste_statistics

Fan, Q., Sun, J., Chu, L., Cui, L., Quan, G., Yan, J., ... & Iqbal, M. (2018). Effects of chemical oxidation on surface oxygen-containing functional groups and adsorption behavior of biochar. *Chemosphere*, *207*, 33–40.

Fiol, N., & Villaescusa, I. (2009). Determination of sorbent point zero charge: usefulness in sorption studies. *Environmental Chemistry Letters*, *7*(1), 79–84.

Foo, K. Y., & Hameed, B. H. 2010. Insights into the modeling of adsorption isotherm systems. *Chemical engineering journal*, *156*(1), 2–10.

Fournel, L., Mocho, P., Brown, R., & Le Cloirec, P. (2010). Modeling breakthrough curves of volatile organic compounds on activated carbon fibers. *Adsorption*, *16*(3), 147–153.

Francescotti, R. (1999). How to define intrinsic properties. *Noûs*, *33*(4), 590–609.

Ghasemi, Z., Seif, A., Ahmadi, T. S., Zargar, B., Rashidi, F., & Rouzbahani, G. M. (2012). Thermodynamic and kinetic studies for the adsorption of Hg (II) by nano-TiO2 from aqueous solution. *Advanced Powder Technology*, *23*(2), 148–156.

Glaser, B., Parr, M., Braun, C., & Kopolo, G. (2009). Biochar is carbon negative. *Nature Geoscience*, *2*(1), 2–2.

Greiner, B. G. (2017). Thermal Regeneration of Biochar for Adsorption of Synthetic Organic Contaminants in the Presence of Dissolved Organic Matter.

Gupta, P., Vermani, K., & Garg, S. (2002). Hydrogels: from controlled release to pH-responsive drug delivery. *Drug discovery today*, *7*(10), 569–579.

Gupta, R. K., Dubey, M., Kharel, P., Gu, Z., Fan, Q. H. (2015). Biochar activated by oxygen plasma for supercapacitors. *J. Power Sources* 274, 1300.

Hamid, S. B. A., Chowdhury, Z. Z., & Zain, S. M. (2014). Base Catalytic Approach: A Promising Technique for the Activation of Biochar for Equilibrium Sorption Studies of Copper, Cu (II) Ions in Single Solute System. *Materials*, *7*(4), 2815–2832.

Horsfall Jnr, M., & Spiff, A. I. (2005). Effects of temperature on the sorption of Pb2+ and Cd2+ from aqueous solution by Caladium bicolor (Wild Cocoyam) biomass. *Electronic Journal of Biotechnology*, *8*(2), 43–50.

Hu, X., Ding, Z., Zimmerman, A. R., Wang, S., Gao, B. (2015). Batch and column sorption of arsenic onto iron-impregnated biochar synthesized through hydrolysis. *Water Res.* 68, 206.

Huff, M. D., & Lee, J. W. (2016). Biochar-surface oxygenation with hydrogen peroxide. *Journal of Environmental Management*, *165*, 17–21.

Iliev, O., Lakdawala, Z., Neßler, K. H., Prill, T., Vutov, Y., Yang, Y., & Yao, J. (2017). On the pore-scale modeling and simulation of reactive transport in 3D geometries. *Mathematical Modelling and Analysis*, *22*(5), 671–694.

International Biochar Initiative. 2012. *Biochar Production Units* [online]. Available from internet: <http://www.biochar-international.org/technology>.

International Union of Pure and Applied Chemistry Physical Chemistry Division Commission on Colloid and Surface Chemistry, Subcommittee on Characterization of Porous Solids: "Recommendations for the characterization of porous solids (Technical Report)", Pure Appl. Chem., Vol. 66(8), (1994), pp. 1739–1758.

Inyang, M. I., Gao, B., Yao, Y., Xue, Y., Zimmerman, A., Mosa, A., ... & Cao, X. (2016). „A review of biochar as a low-cost adsorbent for aqueous heavy metal removal." *Critical Reviews in Environmental Science and Technology*, 46(4), 406–433.

Ioannidou, O., & Zabaniotou, A. (2007). Agricultural residues as precursors for activated carbon production—a review. *Renewable and Sustainable Energy Reviews*, *11*(9), 1966–2005.

Isikgor, F. H., and Becer, C. R. (2015). Lignocellulosic biomass: a sustainable platform for the production of bio-based chemicals and polymers. *Polym. Chem.* 6 (25), 4497.

ISO/TS 21268-3:2007-07, Soil quality - Leaching procedures for subsequent chemical and ecotoxicological testing of soil and soil materials - Part 3: Up-flow percolation test.

Jang, H. M., Yoo, S., Choi, Y. K., Park, S., & Kan, E. (2018). Adsorption isotherm, kinetic modeling and mechanism of tetracycline on Pinus taeda-derived activated biochar. *Bioresource technology*, *259*, 24–31.

Jiang, J., Zhang, L., Wang, X., Holm, N., Rajagopalan, K., Chen, F., & Ma, S. (2013). Highly ordered macroporous woody biochar with ultra-high carbon content as supercapacitor electrodes. *Electrochimica Acta*, *113*, 481–489.

Jiang, S., Huang, L., Nguyen, T. A., Ok, Y. S., Rudolph, V., Yang, H., & Zhang, D. (2016). Copper and zinc adsorption by softwood and hardwood biochars under elevated sulphate-induced salinity and acidic pH conditions. *Chemosphere*, *142*, 64–71.

Jones, D. L., & Quilliam, R. S. (2014). Metal contaminated biochar and wood ash negatively affect plant growth and soil quality after land application. *Journal of hazardous materials*, *276*, 362–370.

Kangro, I., & Kalis, H. (2018). On mathematical modelling of the solid-liquid mixtures transport in porous axial-symmetrical container with Henry and Langmuir sorption kinetics. *Mathematical Modelling and Analysis*, *23*(4), 554–567.

Karakoyun, N., Kubilay, S., Aktas, N., Turhan, O., Kasimoglu, M., Yilmaz, S., & Sahiner, N. (2011). Hydrogel–Biochar composites for effective organic contaminant removal from aqueous media. *Desalination*, *280*(1-3), 319–325.

Karato, S. I. (2006). Influence of hydrogen-related defects on the electrical conductivity and plastic deformation of mantle minerals: a critical review. *GEOPHYSICAL MONOGRAPH-AMERICAN GEOPHYSICAL UNION*, *168*, 113.

Karthikeyan, T., Rajgopal, S., & Miranda, L. R. (2005). Chromium (VI) adsorption from aqueous solution by Hevea Brasilinesis sawdust activated carbon. *Journal of hazardous materials*, *124*(1-3), 192–199.

Karunanayake, A. G., Todd, O. A., Crowley, M., Ricchetti, L., Pittman Jr, C. U., Anderson, R., ... & Mlsna, T. (2018). Lead and cadmium remediation using magnetized and nonmagnetized biochar from Douglas fir. *Chemical Engineering Journal*, *331*, 480–491.

Kavand, M., Asasian, N., Soleimani, M., Kaghazchi, T., & Bardestani, R. (2017). Film-pore-[concentration-dependent] surface diffusion model for heavy metal ions adsorption: single and multi-component systems. *Process Safety and Environmental Protection*, *107*, 486–497.

Kaudal, B. B., D. Chen, D. B. Madhavan, A. Downie, and A. Weatherley. 2016. "An examination of physical and chemical properties of urban biochar for use as growing media substrate." *Biomass Bioenergy* 84: 49–58.

Kılıc, M., Kırbıyık, C., Çepelioğullar, Ö., & Pütün, A. E. (2013). Adsorption of heavy metal ions from aqueous solutions by bio-char, a by-product of pyrolysis. *Applied Surface Science*, *283*, 856–862.

Kellow, M. (2011). Energy and Environment, Experiment instructions, CE 583. *Adsorption. GUNT, Geratebau, Barsbuttel, Germany*.

Kobayashi, H., & Fukuoka, A. (2013). Synthesis and utilisation of sugar compounds derived from lignocellulosic biomass. *Green Chemistry*, *15*(7), 1740–1763.

Kołodyńska, D., Wnętrzak, R., Leahy, J. J., Hayes, M. H. B., Kwapiński, W., & Hubicki, Z. (2012). Kinetic and adsorptive characterization of biochar in metal ions removal. *Chemical Engineering Journal*, *197*, 295–305.

Komkienė, J., and Baltrenaitė, E. (2016). Biochar as adsorbent for removal of heavy metal ions [Cadmium (II), Copper (II), Lead (II), Zinc (II)] from aqueous phase. *International Journal of Environmental Science and Technology* 13 (2), 471–482.

Kong, H., He, J., Gao, Y., Wu, H., & Zhu, X. (2011). Cosorption of phenanthrene and mercury (II) from aqueous solution by soybean stalk-based biochar. *Journal of agricultural and food chemistry*, *59*(22), 12116–12123.

Kozlowski, T. T., Pallardy, S. G., Pospisilova, J. (1997). *Physiology of Woody Plants*. 2nd edition. San Diego: Academic Press.

Lehmann, J.; Joseph, S. 2009. *Biochar for Environmental Management: Science and Technology*. London: Earthscan. 405 p.

Lehmann, J.; Joseph, S. 2015. *Biochar for Environmental Management: Science, Technology and Implementation*. Abingdon: Routledge. 928 p.

Lima, I. M., Boateng, A. A., Klasson, K. T., 2010. Physicochemical and adsorptive properties of fast-pyrolysis bio-chars and their steam activated counterparts. *Journal of Chemical Technology & Biotechnology* 85, 1515–1521

Lima, I. M., & Marshall, W. E. (2005). Granular activated carbons from broiler manure: physical, chemical and adsorptive properties. *Bioresource Technology*, *96*(6), 699–706.

Liu, Z., & Zhang, F. S. (2009). Removal of lead from water using biochars prepared from hydrothermal liquefaction of biomass. *Journal of Hazardous Materials*, *167*(1-3), 933–939.

Lu, H., Zhang, W., Yang, Y., Huang, X., Wang, S., & Qiu, R. (2012). Relative distribution of Pb 2+ sorption mechanisms by sludge-derived biochar. *Water research*, *46*(3), 854–862.

Mahdi, Z., Yu, Q. J., & El Hanandeh, A. (2018). Investigation of the kinetics and mechanisms of nickel and copper ions adsorption from aqueous solutions by date seed derived biochar. *Journal of environmental chemical engineering*, *6*(1), 1171–1181.

Mancinelli, E., Baltrėnaitė, E., Baltrėnas, P., Paliulis, D. and Passerini, G., 2016. Trace metals in biochars from biodegradable by-products of industrial processes. *Water, Air, & Soil Pollution*, *227*(6), p.198.

Meri, N. H., Alias, A. B., Talib, N., Rashid, Z. A., Wan, W. A., & Ghani, A. K. (2018, May). Effect of Chemical Washing Pre-treatment of Empty Fruit Bunch (EFB) biochar on Characterization of Hydrogel Biochar composite as Bioadsorbent. In *IOP Conference Series: Materials Science and Engineering* (Vol. 358, No. 1, p. 012018). IOP Publishing.

Meyer, S., Glaser, B., & Quicker, P. (2011). Technical, economical, and climate-related aspects of biochar production technologies: a literature review. *Environmental science & technology*, *45*(22), 9473–9483.

Miranda, I., J. Gominho, I. Mirra, and H. Pereira. 2012. "Chemical characterization of barks from Picea abies and Pinus sylvestris after fractioning into different particle sizes." *Ind. Crop. Prod.* 36 (1): 395–400.

Miranda, I., J. Gominho, I. Mirra, and H. Pereira. 2013. "Fractioning and chemical characterization of barks of Betula pendula and Eucalyptus globulus." *Ind. Crop. Prod.* 41: 299–305.

Mohan, D., & Pittman, C. U. (2007). Arsenic removal from water/wastewater using adsorbents—a critical review. *Journal of Hazardous materials*, *142*(1), 1–53.

Mohan, D., Pittman Jr, C. U., Bricka, M., Smith, F., Yancey, B., Mohammad, J., ... & Gong, H. (2007). Sorption of arsenic, cadmium, and lead by chars produced from fast pyrolysis of wood and bark during bio-oil production. *Journal of colloid and interface science*, *310*(1), 57–73.

Mohan, D., Kumar, H., Sarswat, A., Alexandre-Franco, M., Pittman Jr., C.U., 2014a. Cadmium and lead remediation using magnetic oak wood and oak bark fast pyrolysis bio-chars. *Chem. Eng. J.* 236, 513–528.

Mohan, D., Rajput, S., Singh, V. K., Steele, P. H., & Pittman, C. U. (2011). Modeling and evaluation of chromium remediation from water using low cost bio-char, a green adsorbent. *Journal of Hazardous Materials*, *188*(1), 319–333

Mohan, D., Sarswat, A., Ok, Y. S., & Pittman, C. U. (2014b). Organic and inorganic contaminants removal from water with biochar, a renewable, low cost and sustainable adsorbent–a critical review. *Bioresource technology*, *160*, 191–202.

Moreno-Castilla, C., Álvarez-Merino, M. A., Pastrana-Martínez, L. M., & López-Ramón, M. V. (2010). Adsorption mechanisms of metal cations from water on an oxidized carbon surface. *Journal of colloid and interface science*, *345*(2), 461–466.

Nanda, S., Mohanty, P., Pant, K. K., Naik, S., Kozinski, J. A., Dalai, A. K. (2013). Characterization of North American lignocellulosic biomass and biochars in terms of their candidacy for alternate renewable fuels. *Bioenergy Res.* 6 (2), 663.

Nartey, O.D., and Zhao, B. (2014). Biochar preparation, characterization, and adsorptive capacity and its effect on bioavailability of contaminants: an overview. *Adv. Mater. Sci. Eng.* 2014.

Nazaroff, W. W. and Alvarez-Cohen. (2001). *L.: Environmental engineering science. John Wiley and Sons*. Collegiate Division.

Nethaji, S., Sivasamy, A., & Mandal, A. B. (2013). Preparation and characterization of corn cob activated carbon coated with nano-sized magnetite particles for the removal of Cr (VI). *Bioresource technology*, *134*, 94–100.

Novak, J. M., Lima, I., Xing, B., Gaskin, J. W., Steiner, C., Das, K. C., ... & Schomberg, H. (2009). Characterization of designer biochar produced at different temperatures and their effects on a loamy sand. *Ann. Environ. Sci*, *3*(2).

Novak, J. M., & Busscher, W. J. (2013). Selection and use of designer biochars to improve characteristics of southeastern USA Coastal Plain degraded soils. In *Advanced biofuels and bioproducts* (pp. 69–96). Springer New York.

Ok, Y. S., Chang, S. X., Gao, B., & Chung, H. J. (2015). SMART biochar technology – a shifting paradigm towards advanced materials and healthcare research. *Environmental Technology & Innovation*, *4*, 206–09.

Park, J., Hung, I., Gan, Z., Rojas, O.J., Lim, K.H., Park, S., 2013. Activated carbon from biochar: influence of its physicochemical properties on the sorption characteristics of phenanthrene. *Bioresour. Technol.* 149, 383–389.

Park, J. H., Ok, Y. S., Kim, S. H., Cho, J. S., Heo, J. S., Delaune, R. D., & Seo, D. C. (2016). Competitive adsorption of heavy metals onto sesame straw biochar in aqueous solutions. *Chemosphere*, *142*, 77–83.

Patel, H. & Vashi, R. T. (2013) A comparison study of removal of methylene blue dye by adsorption on Neem leaf powder (NLP) and activated NLP, *Journal of Environmental Engineering and Landscape Management*, 21:1, 36–41.

Pellera, F. M., Giannis, A., Kalderis, D., Anastasiadou, K., Stegmann, R., Wang, J. Y., & Gidarakos, E. (2012). Adsorption of Cu (II) ions from aqueous solutions on biochars prepared from agricultural by-products. *Journal of Environmental Management*, *96*(1), 35–42.

Qian, L., & Chen, B. (2013). Dual role of biochars as adsorbents for aluminum: the effects of oxygen-containing organic components and the scattering of silicate particles. *Environmental science & technology*, *47*(15), 8759–8768.

Qiu, Y., & Park, K. (2001). Environment-sensitive hydrogels for drug delivery. *Advanced drug delivery reviews*, *53*(3), 321–339.

Rajapaksha, A. U., Chen, S. S., Tsang, D. C., Zhang, M., Vithanage, M., Mandal, S., Gao, B., Bolan, N. S., Ok, Y. S. (2016). Engineered/designer biochar for contaminant removal/immobilization from soil and water: Potential and implication of biochar modification. *Chemosphere* 148, 276–291.

Regmi, P., Moscoso, J. L. G., Kumar, S., Cao, X., Mao, J., & Schafran, G. (2012). Removal of copper and cadmium from aqueous solution using switchgrass biochar produced via hydrothermal carbonization process. *Journal of environmental management*, *109*, 61–69.

Russo, V., Tesser, R., Trifuoggi, M., Giugni, M., & Di Serio, M. (2015). A dynamic intraparticle model for fluid–solid adsorption kinetics. *Computers & Chemical Engineering*, *74*, 66–74.

Russo, V., Tesser, R., Masiello, D., Trifuoggi, M., & Di Serio, M. (2016a). Further verification of adsorption dynamic intraparticle model (ADIM) for fluid–solid adsorption kinetics in batch reactors. *Chemical Engineering Journal*, *283*, 1197–1202.

Russo, V., Masiello, D., Trifuoggi, M., Di Serio, M., & Tesser, R. (2016b). Design of an adsorption column for methylene blue abatement over silica: from batch to continuous modeling. *Chemical Engineering Journal*, *302*, 287–295.

Rutherford, D. W., Wershaw, R. L., Rostad, C. E., Kelly, C. N. (2012). Effect of formation conditions on biochars: Compositional and structural properties of cellulose, lignin, and pine biochars. *Biomass Bioenergy* 46, 693.

Rydholm, S. A. 1965. Pulping processes. New York: Interscience Publishers.

Samsuri, A.W., Sadegh-Zadeh, F., Seh-Bardan, B.J. (2013). Adsorption of As (III) and As (V) by Fe coated biochars and biochars produced from empty fruit bunch and rice husk. *J. Environ. Eng.* 1 (4), 981.

Schmaljohann, D. (2006). Thermo-and pH-responsive polymers in drug delivery. *Advanced drug delivery reviews*, *58*(15), 1655–1670.

Schmidt, H. P. 2012. 55 Uses of Biochar. *Ithaka Journal* 2012: 286–289.

Šćiban, M., & Klašnja, M. (2004). Wood sawdust and wood originate materials as adsorbents for heavy metal ions. *Holz als Roh-und Werkstoff*, *62*(1), 69–73.

Seader J.; Henley, E. 2006. Separation Process Principles. Second edition. John Wiley & Sons.

Shehzad, A., Bashir, M. J., Sethupathi, S., & Lim, J. W. (2016). An insight into the remediation of highly contaminated landfill leachate using sea mango based activated bio-

char: optimization, isothermal and kinetic studies. *Desalination and Water Treatment*, *57*(47), 22244–22257.

Shukla, S. R., & Pai, R. S. (2005). Adsorption of Cu (II), Ni (II) and Zn (II) on dye loaded groundnut shells and sawdust. *Separation and purification Technology*, *43*(1), 1–8.

Sohi, S. P. (2012). Carbon storage with benefits. *Science*, *338*(6110), 1034–1035.

Souza, P. R., Dotto, G. L., & Salau, N. P. G. (2017). Detailed numerical solution of pore volume and surface diffusion model in adsorption systems. *Chemical Engineering Research and Design*, *122*, 298–307.

Spokas, K. A., & Reicosky, D. C. (2009). Impacts of sixteen different biochars on soil greenhouse gas production.

Srivastava, N. K., and Majumder, C. B. (2008). Novel biofiltration methods for the treatment of heavy metals from industrial wastewater. *Journal of Hazardous Materials* 151, 1–8.

Stanila, A., Mihaiescu, T., Socaciu, C., & Diaconeasa, Z. (2016). Removal of Copper and Lead Ions from Aqueous Solution Using Brewer Yeast as Biosorbent. *Revista de Chimie (Bucharest)*, *67*(7), 1276–1280.

Stefanidis, S. D., Kalogiannis, K. G., Iliopoulou, E. F., Michailof, C. M., Pilavachi, P. A., Lappas, A. A. (2014). A study of lignocellulosic biomass pyrolysis via the pyrolysis of cellulose, hemicellulose and lignin. *J. Anal. Appl. Pyrolysis* 105, 143.

Su, R., Li, Q., Huang, R., Zhao, L., Yue, Q., Gao, B., & Chen, Y. (2018). Biomass-based soft hydrogel for triple use: Adsorbent for metal removal, template for metal nanoparticle synthesis, and a reactor for nitrophenol and methylene blue reduction. *Journal of the Taiwan Institute of Chemical Engineers*.

Suguihiro, T. M., de Oliveira, P. R., de Rezende, E. I. P., Mangrich, A. S., Junior, L. H. M., & Bergamini, M. F. (2013). An electroanalytical approach for evaluation of biochar adsorption characteristics and its application for lead and cadmium determination. *Bioresour. Technol. 143*, 40–45.

Sun, Y., Gao, B., Yao, Y., Fang, J., Zhang, M., Zhou, Y., ... & Yang, L. (2014). Effects of feedstock type, production method, and pyrolysis temperature on biochar and hydrochar properties. *Chemical Engineering Journal*, *240*, 574–578.

Swait, T. J., Rauf, A., Grainger, R., Bailey, P. B., Lafferty, A. D., Fleet, E. J., ... & Hayes, S. A. (2012). Smart composite materials for self-sensing and self-healing. *Plastics, Rubber and Composites*, *41*(4-5), 215–224.

Tan, X.; Liu, Y.; Zeng, G.; Wang, X.; Hu, X.; Gu, Y.; Yang, Z. 2015. Application of biochar for the removal of pollutants from aqueous solutions. *Chemosphere* 125: 75–85.

Tan, K. L., and B. H. Hameed. 2017. Insight into the adsorption kinetics models for the removal of contaminants from aqueous solutions. *Journal of the Taiwan Institute of Chemical Engineers*, 74, 25–48.

TAPPI Test Method T222. Acid-Insoluble Lignin in Wood and Pulp.

Tong, X. J., Li, J. Y., Yuan, J. H., & Xu, R. K. (2011). Adsorption of Cu (II) by biochars generated from three crop straws. *Chemical Engineering Journal*, *172*(2), 828–834.

Trazzi, P. A., Leahy, J. J., Hayes, M. H., & Kwapinski, W. (2016). Adsorption and desorption of phosphate on biochars. *Journal of Environmental Chemical Engineering*, *4*(1), 37–46.

Tsai, W. T., & Chen, H. R. (2013). Adsorption kinetics of herbicide paraquat in aqueous solution onto a low-cost adsorbent, swine-manure-derived biochar. *International Journal of Environmental Science and Technology*, *10*(6), 1349–1356.

Uchimiya, M., Wartelle, L. H., Klasson, K. T., Fortier, C. A., Lima, I. M. 2011. Influence of pyrolysis temperature on biochar property and function as heavy metal sorbent in soil. *Journal of Agricultural and Food Chemistry*. 59:2501–2510.

Vassilev, S. V., Baxter, D., Andersen, L. K., Vassileva, C. G. (2010). An overview of the chemical composition of biomass. *Fuel* 89 (5), 913.

Wang, H., Gao, B., Wang, S., Fang, J., Xue, Y., & Yang, K. (2015). Removal of Pb (II), Cu (II), and Cd (II) from aqueous solutions by biochar derived from KMnO4 treated hickory wood. *Bioresource technology*, *197*, 356–362.

Wang, Q., Wang, B., Lee, X., Lehmann, J., & Gao, B. (2018). Sorption and desorption of Pb (II) to biochar as affected by oxidation and pH. *Science of The Total Environment*, *634*, 188–194.

Wilczak, A., & Keinath, T. M. (1993). Kinetics of sorption and desorption of copper (II) and lead (II) on activated carbon. *Water Environment Research*, *65*(3), 238–244.

Wu, W., Li, J., Lan, T., Müller, K., Niazi, N. K., Chen, X., ... & Yuan, G. (2017). Unraveling sorption of lead in aqueous solutions by chemically modified biochar derived from coconut fiber: a microscopic and spectroscopic investigation. *Science of the Total Environment*, *576*, 766–774.

Wu, Y., Zhang, S., Guo, X., & Huang, H. (2008). Adsorption of chromium (III) on lignin. *Bioresource technology*, *99*(16), 7709–7715.

Xiao, X., B. Chen, and L. Zhu. 2014. "Transformation, morphology, and dissolution of silicon and carbon in rice straw-derived biochars under different pyrolytic temperatures." *Environ. Sci. Technol.* 48 (6): 3411–3419.

Xu, X., Cao, X., Zhao, L., Wang, H., Yu, H., Gao, B. (2013). Removal of Cu, Zn, and Cd from aqueous solutions by the dairy manure-derived biochar. *Environ. Sci. Pollut. Res.* 20 (1), 358.

Xue, Y., Gao, B., Yao, Y., Inyang, M., Zhang, M., Zimmerman, A. R., & Ro, K. S. (2012). Hydrogen peroxide modification enhances the ability of biochar (hydrochar) produced from hydrothermal carbonization of peanut hull to remove aqueous heavy metals: batch and column tests. *Chemical engineering journal*, *200*, 673–680.

Yang, G. X., & Jiang, H. 2014. Amino modification of biochar for enhanced adsorption of copper ions from synthetic wastewater. *Water research*, *48*, 396–405.

Yao, Y., Gao, B., Inyang, M., Zimmerman, A. R., Cao, X., Pullammanappallil, P., & Yang, L. (2011). Biochar derived from anaerobically digested sugar beet tailings: characterization and phosphate removal potential. *Bioresource technology*, *102*(10), 6273–6278.

Yao, Y., Gao, B., Chen, J., Zhang, M., Inyang, M., Li, Y., ... & Yang, L. (2013). Engineered carbon (biochar) prepared by direct pyrolysis of Mg-accumulated tomato tissues: characterization and phosphate removal potential. *Bioresource technology*, *138*, 8–13.

Yao, Z. Y., Qi, J. H., & Wang, L. H. (2010). Equilibrium, kinetic and thermodynamic studies on the biosorption of Cu (II) onto chestnut shell. *Journal of Hazardous Materials*, *174*(1-3), 137–143.

Yoshida, H., Matsusaki, M., & Akashi, M. (2013). Multilayered blood capillary analogs in biodegradable hydrogels for in vitro drug permeability assays. *Advanced Functional Materials*, *23*(14), 1736–1742.

Yun, J. M., Im, J. S., Oh, A. R., Lee, Y. S., & Kim, H. I. (2009). Controlled release behavior of ph-responsive composite hydrogel containing activated carbon. *Carbon letters*, *10*(1), 33–37.

Zama, E. F., Zhu, Y. G., Reid, B. J., & Sun, G. X. (2017). The role of biochar properties in influencing the sorption and desorption of Pb (II), Cd (II) and As (III) in aqueous solution. *Journal of cleaner production*, *148*, 127–136.

Zhang, M., Gao, B., 2013. Removal of arsenic, methylene blue, and phosphate by biochar/AlOOH nanocomposite. *Chem. Eng. J.* 226, 286–292.

Zhang, M., Gao, B., Varnoosfaderani, S., Hebard, A., Yao, Y., Inyang, M., 2013. Preparation and characterization of a novel magnetic biochar for arsenic removal. *Bioresour. Technol.* 130, 457–462.

Zhao, L., Li, Q., Xu, X., Kong, W., Li, X., Su, Y., ... & Gao, B. (2016). A novel Enteromorpha based hydrogel optimized with Box–Behnken response surface method: synthesis, characterization and swelling behaviors. *Chemical Engineering Journal*, *287*, 537–544.

Zhou, L., & Toth, J. (2001). Adsorption: Theory, Modeling and Analyzing.

Zhou, Q., Liao, B., Lin, L., Qiu, W., & Song, Z. (2018). Adsorption of Cu (II) and Cd (II) from aqueous solutions by ferromanganese binary oxide–biochar composites. *Science of the Total Environment*, *615*, 115–122.

Zhou, Y., Gao, B., Zimmerman, A. R., Chen, H., Zhang, M., & Cao, X. (2014). Biochar-supported zerovalent iron for removal of various contaminants from aqueous solutions. *Bioresource technology*, *152*, 538–542.

List of Scientific Publications by the Author on the Topic of the dissertation

Articles in Reviewed Scientific Journals

Chemerys, V., Baltrėnaitė, E., Baltrėnas, P., Dobele, G. (2020). Influence of H_2O_2-modification on adsorptive properties of birch-derived biochar. *Polish Journal of Environmental Studies*, 29(1), 579–588. (Clarivate Analytics Web of Science) [IF = 1.186].

Leonavičienė, T., Čiegis, R., Baltrėnaitė, E. and Chemerys, V. (2019). Numerical analysis of liquid-solid adsorption model. *Mathematical Modelling and Analysis*, *24*(4), 598–616. (Clarivate Analytics Web of Science) [IF = 1.038].

Chemerys, V., & Baltrėnaitė, E. (2018b). Influence of Intrinsic Properties of Lignocellulosic Feedstock on Adsorptive Properties of Biochar. *Journal of Environmental Engineering*, *144*(9), 04018075-1–04018075-11. (Clarivate Analytics Web of Science) [IF = 1.657].

Chemerys, V., & Baltrėnaitė, E. (2018a). A review of lignocellulosic biochar modification towards enhanced biochar selectivity and adsorption capacity of potentially toxic elements. *Ukrainian Journal of Ecology*, *8*(1), 21–32. (Clarivate Analytics Web of Science).

Articles in Other Editions

Chemerys, V., & Baltrėnaitė, E. (2017b). Effect of modification with $FeCl_3$ and $MgCl_2$ on adsorption characteristics of woody biochar. Conference proceedings of the *10th International Conference „Environmental Engineering"*, that took place on the 27–28 April, Vilnius, 1–8.

Chemerys, V., & Baltrėnaitė, E. (2017a). Pine-derived biochar as option for removal of metals and decreasing of bod_5 in landfill leachate. Presentation at the *20th conference of young scientists „Science – Future of Lithuania"*, that took place on the 20 March, Vilnius, 406–412.

Chemerys, V., & Baltrėnaitė, E. (2016). Modified biochar: a review on modifications of biochar towards its enhanced adsorptive properties. Presentation at the *19th conference of young scientists „Science – Future of Lithuania"*, that took place on the 7 April, Vilnius, 19–25.

Patent

Baltrėnas, P., Baltrėnaitė, E., Chemerys, V. Bioanglies modifikavimo H_2O_2 vandeniniu tirpalu įrenginys ir būdas. Vilnius: Lietuvos respublikos valstybinis patentų biuras, 8 p. (in Lithuanian).

Summary in Lithuanian

Įvadas

Problemos formulavimas

Dėl gyventojų skaičiaus augimo ir sparčios pramonės plėtros plataus spektro potencialiai toksiškų elementų (PTE) plitimas paviršiniame ir požeminiame vandenyje tapo kritine problema visame pasaulyje. Šie PTE dažniausiai būna sąvartynų filtrate, kuris yra kenksmingiausias žmonėms ir ekologinei aplinkai tarp visų tipų nuotekų dėl didelės suspenduotų kietų medžiagų, amonio azoto, chlorintų organinių, neorganinių druskų ir kitų PTE koncentracijos. Būtina kontroliuoti kenksmingą PTE poveikį ir pagerinti žmogaus gyvenamąją aplinką. Todėl PTE pašalinimo poreikis tapo būtinybe.

Dažniausi PTE nuotekose yra Pb^{2+}, Zn^{2+}, Cu^{2+}, Ni^{2+}, Cr^{3+} ir Cd^{2+} junginiai; jie yra ilgalaikiai teršalai ir negali natūraliai susiskaidyti. Jei jų koncentracija yra per didelė, jie gali būti pavojingi žmonių sveikatai ir slopinti augalų augimą. Organizacija HELCOM įtraukė šiuos PTE į prioritetinius teršalų sąrašus. Siekiant suvaldyti ir sumažinti nuotekų užterštumą Pb^{2+}, Zn^{2+}, Cu^{2+}, Ni^{2+}, Cr^{3+}, Cd^{2+}, naudojamos įvairios valymo technologijos. Įprasta šių metalų jonų koncentracija nuotekų tirpale yra maža (Cr^{3+} 0,2–18 mg/l, Cd^{2+} 0,3–17 mg/l, Pb^{2+} 0,001–2,0 mg/l, Ni^{2+} 0,2–79 mg/l, Zn 0,6–370 mg/l, Cu^{2+} 0,005–9,9 mg/l), todėl įprasti valymo metodai (pvz., atvirkštinė osmozė, membraninis, mikro-, ultra- ir nanofiltravimas, krešėjimo-flokuliacija, flotacija, cheminis nusodinimas, jonų mainai, elektrocheminiai metodai) gali būti neveiksmingi dėl mažos PTE koncentracijos nuotekose (mažiau kaip 100 mg/l), jie yra brangūs arba sukuria toksišką dumblą. Lyginant su kitais valymo metodais, adsorbcija laikoma geresne ir ekonomiškesne nuotekų valymo

alternatyva dėl mažų PTE koncentracijų pašalinimo ir lankstaus dizaino. Be to, adsorbentai gali būti regeneruojami tinkamu desorbcijos procesu, kadangi adsorbcija kartais yra grįžtamoji. Šiandien dažniausiai naudojamas adsorbentas yra aktyvuota anglis. Tačiau platus jos naudojimas nuotekoms valyti kartais yra ribojamas dėl jos didelių sąnaudų bei sorbento sunaikinimo pasibaigus eksploatavimo laikui. Aktyvuota anglis gali būti pakeista bioanglimi (BA), tvaru adsorbentu, kuri paprastai yra apdorojama žemesnėje temperatūroje per trumpesnį laiką. Nemodifikuotos BA komercinė kaina 2018 m. buvo 3 kartus mažesnė nei aktyvuotos anglies, nes bioanglis gaminama iš atliekų.

Darbo aktualumas

Remiantis Europos Bioanglies Sertifikatu lignino žaliava dėl savo prieinamumo ir ekologinio tinkamumo yra pati vertingiausia žaliava. 2010 m. Europos Sąjungoje susidarė 56,8 mln. t komunalinių atliekų. Kadangi BA gali būti gaminama iš sumedėjusių liekanų, didelė BA gamybos apimtis gali išspręsti sumedėjusių atliekų tvarkymo problemą. Šiame tyrime lignino žaliava 2 valandas buvo pirolizuojama esant 450 ± 10 °C temperatūrai, kad būtų padidintos Pb^{2+}, Zn^{2+}, Cu^{2+}, Ni^{2+}, Cr^{3+}, Cd^{2+} adsorbavimo savybės: gerai išvystyta mikroporinė struktūra ir deguonies turinčios funkcinės grupės paviršiuje.

Šiais laikais visame pasaulyje nuolat didėja susirūpinimas nuotekų valymo technologijų plėtra. BA turi silpnesnes adsorbcines savybes, negu aktyvuota anglis, todėl ją reikia modifikuoti, kad būtų pagerinta PTE adsorbcija didinant savitąjį paviršiaus plotą, poringumą ir deguonimi prisotintų grupių kiekį paviršiuje. Siekiant pagerinti BA adsorbcines savybes, ji gali būti pagaminta iš žaliavų, turinčių tam tikrų būdingų savybių ir singenetinių elementų, arba modifikuota dirbtiniu būdu. Žaliavų, turinčių būdingų savybių ir singenetinių elementų, pasirinkimas yra pigesnis ir prieinamesnis nei dirbtinis, tačiau jų skirtumų poveikis BA adsorbcinėms savybėms nėra ištirtas. Taip pat dar nera ištirtas būdingų medienos savybių (pvz., lignino, pelenų, drėgmės, C, O, H, N, Cr^{3+}, Cd^{2+}, Pb^{2+}, Zn^{2+}, Ni^{2+}, Cu^{2+} kiekio) poveikis adsorbento savybėms.

Siekiant pagerinti Pb^{2+}, Zn^{2+}, Cu^{2+}, Ni^{2+}, Cr^{3+}, Cd^{2+} adsorbcijos gebą sąvartyno filtrato apdorojimo metu, buvo sukurtas bioanglies-hidrogelio kompozitas, paruoštas iš modifikuotos bioanglies, pasižyminčios patobulintomis adsorbcijos savybėmis.

Tyrimų objektas

Tyrimų objektas yra Cr^{3+}, Cd^{2+}, Pb^{2+}, Zn^{2+}, Ni^{2+}, Cu^{2+} adsorbcija naudojant bioanglį iš sumedėjusios biomasės.

Darbo tikslas

Darbo tikslas – įvertinti PTE adsorbciją bioanglimi, sukurus lignino bioanglies modifikavimo technologiją, didinančią Cr^{3+}, Cd^{2+}, Pb^{2+}, Zn^{2+}, Ni^{2+}, Cu^{2+} adsorbcijos gebą.

Darbo uždaviniai

Norint pasiekti apibrėžtą darbo tikslą, buvo iškelti šie uždaviniai:

1. Nurodyti pagrindinius mechanizmus, kontroliuojančius maksimalią Cr^{3+}, Cd^{2+}, Pb^{2+}, Zn^{2+}, Ni^{2+}, Cu^{2+} adsorbciją iš sintetinių tirpalų ir sąvartyno filtrato lignino bioanglimi.

2. Sukurti bioanglies modifikavimo įrenginį ir palyginti būdingų savybių, singenetinių elementų ir dirbtinio modifikavimo metodų poveikį Cr^{3+}, Cd^{2+}, Pb^{2+}, Zn^{2+}, Ni^{2+}, Cu^{2+} adsorbcijos gebai bioanglimi iš sintetinių tirpalų ir sąvartyno filtrato.

3. Įvertinti bioanglies-hidrogelio kompozito tūrio padidėjimą keičiant tirpalo pH ir įvertinti jo panaudojimo galimybes sąvartyno filtrato adsorbcijai Cr^{3+}, Cd^{2+}, Pb^{2+}, Zn^{2+}, Ni^{2+}, Cu^{2+}.

4. Optimizuoti adsorbcijos parametrus (pvz., bioanglies rūšį, dozavimą, laiką) nuo pritaikymo prie dinaminio vidinės difuzijos modelio ir atlikti supaprastinto adsorbcijos modelio jautrumo analizę.

Tyrimų metodikos

Šios disertacijos tyrimo metodai yra teoriniai, eksperimentiniai tyrimai ir matematinis modeliavimas: adsorbcijos pusiausvyros ir kinetinis modeliavimas (Langmuir, Freundlich izotermes, dinaminis vidinės difuzijos modelis), žaliavos, turinčios kintamų būdingų savybių bioanglies gamyboje, parinkimas (pvz., ligninas, drėgmė, C, O, H, N, PTE kiekis žaliavoje), analizės metodai fizikinių savybių tyrimams (morfologines struktūras skenuojantis elektroninis mikroskopas, savitasis paviršiaus ploto Brunauer-Emmett-Teller analizatorius) ir cheminių savybių (amonio acetatas katijonų mainų gebai ir deguonies turinčioms funkcinėms grupėms, pH metras, EL matuoklis elektros laidis, CHNO elementų analizatorius C, H, N, O kiekiui, FTIR paviršiaus funkcinėms grupėms) naudojant Europos bioanglies sertifikato standartus, PTE adsorbcijos tyrimo metodika (Langmuir ir Freundlich izotermės, dinaminis vidinės difuzijos modelis), atominės absorbcijos spektrofotometras PTE kiekio nustatymui, modifikavimo H_2O_2 ir metalų druskomis ($FeCl_3$, $MgCl_2$) metodika, bioanglies-hidrogelio kompozito paruošimo metodika.

Darbo mokslinis naujumas

1. Ištirta beržo žaliavos būdingų savybių (lignino, pelenų, drėgmės, C, O, H, N kiekio) ir singenetinių elementų (Cr^{3+}, Cd^{2+}, Pb^{2+}, Zn^{2+}, Ni^{2+}, Cu^{2+} kiekio) įtaka bioanglies adsorbcinems savybėms.

2. Beržo bioanglis, modifikuota naudojant 15% koncentracijos H_2O_2 tirpalą, turi 4 didesnę katijonų mainų gebą ir 15 kartų didesnį BET paviršiaus plotą nei nemodifikuota beržo bioanglis. Be to, lignino bioanglies modifikavimo technologija leidžia sukurti H_2O_2 modifikuotą bioanglį, turinčią 25% didesnę katijonų mainų gebą ir karboksilinių bei karbonilinių grupių kiekį bioanglies paviršiuje, ir iki 2 kartų didesnį BET savitąjį paviršiaus plotą nei bioanglis, modifikuota nenaudojant H_2O_2 minėtą technologiją.

3. Katijoninis bioanglies-hidrogelio kompozitas turi 7 kartus didesnę KMG ir 20 kartus didesnį BET, nei nemodifikuotas beržo bioanglis. Atitinkamai, kompozitas turi didesnį Cr^{3+}, Cd^{2+}, Pb^{2+}, Zn^{2+}, Ni^{2+}, Cu^{2+} adsorbcijos efektyvumą iš sąvartyno filtrato, nei nemodifikuota ir H_2O_2 modifikuota beržo bioanglys.

4. Jautrumo analizė naudojant supaprastintą adsorbcijos modelį parodė, kad adsorbcijos proceso dinamiką galima tiksliai numatyti.

Darbo rezultatų praktinė reikšmė

Lignino bioanglies modifikavimo technologija gali būti panaudojama H_2O_2-modifikuoto bioanglies adsorbento gamybai pramoniniams tikslams. H_2O_2 modifikuota bioanglis ir jos hidrogelio kompozitas gali būti panaudojami pramonėje Cr^{3+}, Cd^{2+}, Pb^{2+}, Zn^{2+}, Ni^{2+}, Cu^{2+} adsorbcijai iš sąvartyno filtrato. Dinaminis vidinės difuzijos modelis geba nustatyti optimalius adsorbcijos parametrus (pvz., bioanglies rūšį, dozavimą, laiką) be kinetinių tyrimų. Jautrumo analizė leidžia numatyti adsorbcijos proceso dinamiką, ir taip pat yra bazė išspręsti svarbias taikomas optimizavimo problemas, siekiant maksimaliai padidinti adsorbcijos gebą pasirinkus optimalų adsorbento formos parametrą. Medienos atliekos yra panaudojamos bioanglies gamybai.

Ginamieji teiginiai

1. Bioanglies oksidacija naudojant H_2O_2 tirpalą skatina iki 57% didesnę Cr^{3+}, Cd^{2+}, Pb^{2+}, Zn^{2+}, Ni^{2+}, Cu^{2+} adsorbciją nei nemodifikuota bioanglis.

2. 30–35% lignino kiekis medienos žaliavoje gali padidinti Cr^{3+}, Cd^{2+}, Pb^{2+}, Zn^{2+}, Ni^{2+}, Cu^{2+} adsorbciją, lyginant su ligninėmis žaliavomis, turinčiomis 18–24% lignino.

3. Modifikuoto bioanglies-hidrogelio kompozito adsorbcijos geba Cr^{3+}, Cd^{2+}, Pb^{2+}, Zn^{2+}, Ni^{2+}, Cu^{2+} iš sąvartyno filtrato yra net 2 kartus didesnė, nei nemodifikuotos bioanglies.

Darbo rezultatų aprobavimas

Disertacijos tema paskelbta 7 straipsniai: 4 straipsniai – mokslo žurnaluose, įtrauktuose į „Clarivative Analytics Web of Science“ sąrašą (3 iš jų turi citavimo rodiklį), ir 3 – konferencijų pranešimų leidiniuose. Suteiktas 1 Lietuvos Respublikos patentas. 8 pranešimai šia tema buvo pristatyti nacionalinio ir tarptautinio lygio konferencijose:

– 2019. 22-oji jaunųjų mokslininkų konferencija *Moslas – Lietuvos Ateitis,* Vilnius, Lietuva.
– 2018. 21-oji jaunųjų mokslininkų konferencija *Moslas – Lietuvos Ateitis,* Vilnius, Lietuva.
– 2017. 10-oji tarptautinė konferencija *Challenges in environmental science and engineering* (CESE), Kunming, Kinija.
– 2017. 10-oji tarptautinė konferencija *Environmental Engineering*, Vilnius, Lietuva.
– 2017. 20-oji jaunųjų mokslininkų konferencija *Moslas – Lietuvos Ateitis,* Vilnius, Lietuva.
– 2016. 78-oji konferencija ir paroda *European Association of Geoscientist and Engineerss* (EAGE), Viena, Austrija.
– 2016. 19-oji jaunųjų mokslininkų konferencija *Moslas – Lietuvos Ateitis,* Vilnius, Lietuva.
– 2016. 4-oji žiemos mokykla *European Biochar Winter School*, Palermo, Italija.

Disertacijos struktūra

Mokslinį darbą sudaro įvadas, 3 skyriai, bendrosios išvados ir rekomendacijos, literatūros sąrašas, autorių publikacijos ir pranešimai disertacijos tema mokslinėse konferencijose. Bendra disertacijos apimtis – 185 puslapiai, be priedų, 58 paveikslų ir 38 lentelės. Pacituoti 158 literatūriniai šaltiniai.

1. Bioanglies paruošimo metodai, charakteristikos ir modifikavimo būdai potencialiai toksiškų elementų adsorbcijai gerinti

Bioanglis (BA), turinti daug anglies ir mineralų, gaminama iš biomasės pirolizės, esant temperatūrai nuo 350 °C iki 1000 °C žemo deguonies aplinkoje (EBC 2012). BA gali būti naudojamas potencialių toksiškų metalų (PTE) adsorbcijai iš vandeninių tirpalų. Pagrindiniai bioanglies Cr^{3+}, Cd^{2+}, Pb^{2+}, Zn^{2+}, Ni^{2+}, Cu^{2+} adsorbcijos mechanizmai yra jonų mainai ir elektrostatinė trauka.

BA, priklausomai nuo žaliavos ir pirolizės technologijos, pasižymi skirtingomis fizinėmis ir cheminėmis savybėmis. Europos Bioanglies Sertifikatas (EBC) teigė, kad pati vertingiausia medžiaga BA gaminimui yra sumedėjusi biomasė, pvz., žemės ūkio atliekos, energetiniai augalai, medienos ir komunalinio popieriaus atliekos (Nanda ir kt. 2013). Lėtinė pirolizė yra dažniausiai naudojama technologija BA gamybai. BA, gaminama žemoje temperatūroje, turi daugiau aktyvių vietų ir stabilių anglies-deguonies kompleksų (Meyer ir kt. 2011). Nustatyta, kad padidėjęs mikroporingumas, savitasis paviršiaus plotas, deguonies turinčio funkcinių grupių kiekis bioanglies paviršiuje, didina PTE adsorbciją.

Be bioanglies (S1.1 pav.), tirpalas (jo temperatūra, pH) ir adsorbatas (jo koncentracija, molekulės dydis, tirpumas) taip pat turi įtakos adsorbcijos procesui. Bioanglis traukia katijoninius PTE, kai bioanglies paviršius yra neigiamai įkrautas ($pH_{tirpalas} > pH_{pzc}$ (nulio įkrovos taškas)).

Bioanglį galima modifikuoti įvairiais metodais, pvz., apdorojant rūgštimi / šarmu, karboksilinimu, apdorojimu organiniais tirpikliais, mineralinių oksidų impregnavimu, aktyvinimu garais, dujų valymu ir įmagnetinimu (Rajapaksha ir kt. 2016). Siekiant padidinti BA adsorbcijos gebą, buvo pasirinktos cheminės modifikacijos naudojant H_2O_2, $MgCl_2$, $FeCl_3$ tirpalus. Apdorojimas H_2O_2 tirpalu padidina karboksilo grupių kiekį ir katijonų mainų gebą (Cibati ir kt. 2017; Huff ir Lee 2015; Xue ir kt. 2016), o dirbtinai pridėtos Mg ir Fe dalelės veikė kaip papildomos adsorbcijos vietos bioanglies paviršiuje (Yao ir kt. 2013; Zhang ir kt. 2013; Agrafioti ir kt. 2014).

Tarp natūralių modifikavimo būdų, kuriems įtakos turi natūrali žaliavos sudėtis, buvo pasirinktos būdingos žaliavos savybės (drėgmės, lignino kiekis ir porų struktūra) bei singenetiniai elementai žaliavoje (elementinė sudėtis). Baltrėnaitė ir kt. (2016) parodė skirtumus tarp BA savybių pagamintos iš medienos: BA iš spygliuočių medienos turėjo didesnį lignino kiekį, šiek tiek didesnį pelenų kiekį ir pH nei BA iš lapuočių medienos; tuo tarpu BA iš lapuočių medienos turėjo 10% didesnį savitąjį paviršiaus plotą, mikroporų

kiekį ir 2 kartus didesnę katijonų mainų gebą. Taigi tyrimams buvo parinktos 4 medienos rūšys: pušis *(Pinus sylvestris L.)*, drebulė *(Populus tremula L.)*, eglė *(Picea abies L.)* ir beržas *(Betula pendula L.)*.

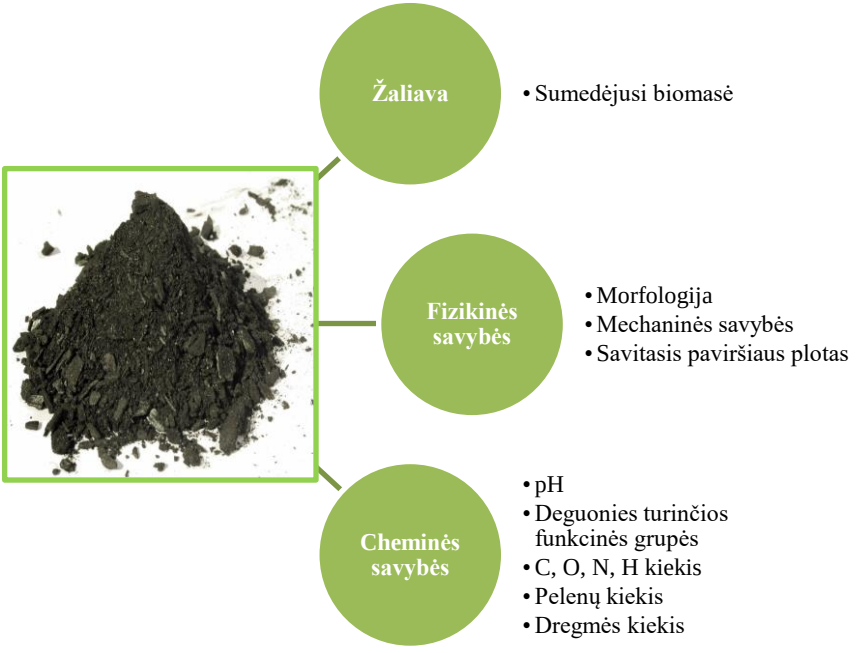

S1.1 pav. Kriterijai bioanglies parinkimo potencialiai toksiškų elementų adsorbcijai

Buvo ištirtos bioanglies adsorbcinės savybės: drėgmės ir pelenų kiekis, cheminė sudėtis (C, O, N, H, Cd, Zn, Pb, Cr, Cu, Ni kiekis), pH, elektrinis laidis (EC), katijonų mainų geba (KMG), BET savitasis paviršiaus plotas (BET SPP) ir paviršiaus funkcinės grupės.

Langmuir, Freundlich, Redlich-Peterson, Sips izotermės, pirmosios eilės ir antrosios eilės pseudo kinetiniai modeliai, linijinės plėvelės difuzijos ir Weber-Morris porų difuzijos modeliai buvo pasirinkti pusiausvyros ir kinetikos adsorbcijos nustatymui. Dinaminis vidinės difuzijos modelis, apimantis pusiausvyrą ir kinetines dalis, naudojant bioanglį dar nebuvo išbandytas.

Siekiant pagerinti PTE adsorbciją bioanglyje, buvo sukurtas bioanglies-hidrogelio kompozitas. Kadangi hidrogelis yra porėtas ir jo paviršiuje yra deguonies turinčios funkcinės grupės, jungdamasis su bioanglimi (Su ir kt. 2018; Karakoyun ir kt. 2011), kompozitas tampa geresniu adsorbentu nei atskira bioanglis, nes kompozitas turi didesnį BET SPP ir karboksilo grupių kiekį – aplinkai nekenksmingas ir efektyvus adsorbentas. Hidrogelio tūrio padidėjimas dėl pH ir tirpalo temperatūros pokyčių taip pat gali padidinti kompozito adsorbcijos selektyvumą, nes kai hidrogelis išsipučia, jo poros tampa didesnės, todėl didesnio diametro PTE gali būti adsorbuoti dėl fizinės adsorbcijos.

Atlikus mokslinės literatūros analizę, buvo iškelti šie uždaviniai:

1. Palyginti PTE adsorbcijos efektyvumą tarp chemiškai modifikuotos lignino bioanglies ir bioanglies su būdingomis savybėmis ir išskirti efektyviausią modifikavimo metodą.

2. Įvertinti lignino žaliavų būdingų savybių (C, O, N, H, vandens, lignino kiekį, morfologiją ir porų struktūrą) bei singenetinių elementų (mikroelementų) įtaką bioanglies adsorbcinėms savybėms.

3. Nustatyti PTE adsorbcijos mechanizmus bioanglyje.

4. Sukurti bioanglies-hidrogelio kompozitą PTE adsorbcijai.

5. Pritaikyti dinaminį vidinės difuzijos modelį PTE adsorbcijai bioanglyje ir atlikti supaprastinto adsorbcijos modelio jautrumo analizę.

2. Natūralių ir cheminių modifikavimo metodų poveikis potencialiai toksiškų elementų adsorbcijai bioanglimi

Iš natūralių modifikacijų nustatyta, kad padidėjus lignino kiekiui nuo 19,06 beržo medienoje iki 59% pušies žievėje, BET savitasis paviršiaus plotas padidėja nuo 20,11 iki 362,1 m^2/g. Padidėjus lignino kiekiui, O/C koeficientas padidėjo nuo 0,074 pušies medienoje iki 0,188 beržo žievėje. Skirtumas tarp BET paviršiaus ploto kamieno medienos ir kamieno žievės bioanglyje siekė beveik 10 kartų: 25,08 ir 354,7 m^2/g pušyje, 20,11 ir 362,1 m^2/g berže.

Modifikavimo proceso efektyvumui padidinti buvo sukurtas bioanglies modifikavimo įrenginys naudojant H_2O_2 tirpalą (Patentas #6434) (S2.1 pav). Išradimas susijęs su užterštos vandens valymo technine sritimi. Modifikacija vykdoma bioanglies dalelių sumaišymu su H_2O_2 tirpalu. Šis prietaisas yra ekonomiškai efektyvus ir aplinkai nekenksmingas. Jame yra papildomas mechaninis elementas, skirtas padidinti bioanglies ir tirpalo sąlyčio paviršių.

Didžiausias BET buvo nustatytas modifikavus bioanglį H_2O_2 tirpalu, kurio koncentracija siekė 30%, nes mikroporų kiekio padidėjimą lėmė bioanglies deguonies oksigenacija (S2.2 pav.). Bioanglis, kuri buvo modifikuota naudojant $FeCl_3$, turi mažiausią BET, nes Fe dalelės gali užblokuoti bioanglies poras.

Didžiausia KMG buvo nustatyta bioanglyje po jos modifikacijos naudojant H_2O_2 tirpalą, kurio koncentracija siekė 30%, nes didesnė modifikavimo tirpalo koncentracija padidino deguonies turinčių funkcinių grupių kiekį (S2.3 pav.). Mažiausia KMG – $MgCl_2$ modifikuotoje bioanglyje.

Bioanglies modifikavimas, naudojant H_2O_2 tirpalą, prideda karboksilines grupes BA paviršiuje, o $FeCl_3$ ir $MgCl_3$ prideda fenolines grupes. Modifikavimas, naudojant H_2O_2, padidino O/C koeficientą 3 kartus (S2.4 pav.), o N/C koeficientą – 9 kartus (S2.5 pav.). Tai rodo sumažėjusį hidrofobiškumą ir padidėjusį funkcinės grupės kiekį, todėl padidėja potencialas PTE adsorbuoti (Suguihiro ir kt. 2013).

Įrenginio tikslas buvo suaktyvinti bioanglies paviršių ir taip pagerinti bioanglies adsorbcijos savybes adsorbuojant katijoninius metalus. Nustatyta, kad bioanglis, modifikuota pagal technologiją, turėjo 25% didesnę KMG, 21% savitojo paviršiaus ploto, N/C ir O/C koeficiantai. Taip pat bioanglis, kurios dalelių dydis mažesnis (0,4–1,0 mm),

turėjo didesnius KMG ir BET, nei bioanglis, kurios dalelių dydis 1,0–3,0 mm, modifikuota tokiu pačiu būdu.

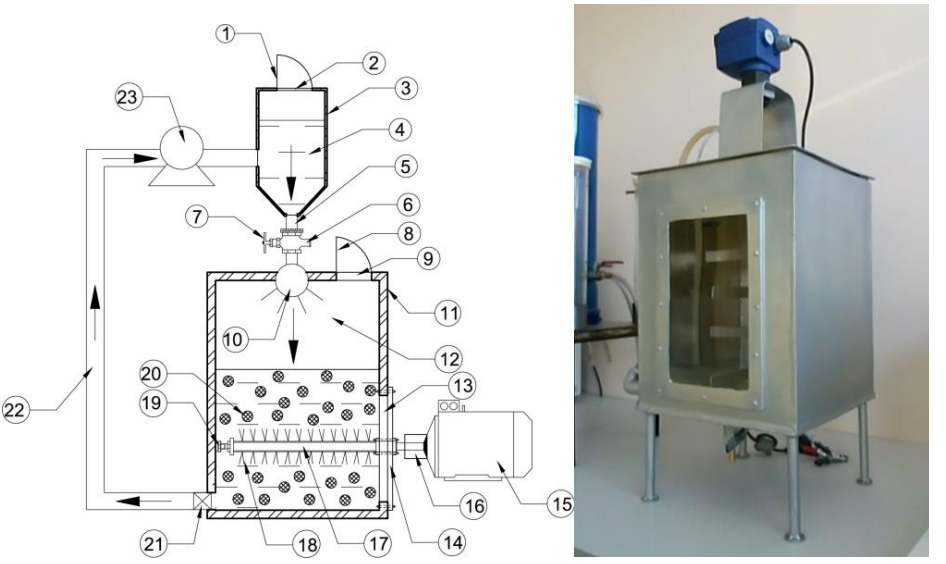

a) b)

S2.1 pav. Bioanglies modifikavimo įrenginys: a) – brėžinys; b) – pagamintas įrenginys. Įrenginį sudaro: 1 – H_2O_2 talpos dangtis, 2 – anga, 3 – H_2O_2 talpos korpusas, 4 – H_2O_2 talpa, 5 – kanalas, 6 – H_2O_2 pašalinimo kanalas, 7 – sklendė, 8 – dangtis, 9 – anga, 10 – purkštuvas, 11 – modifikuojančios talpos korpusas, 12 – modifikavimo talpa, 13 – ertmė, 14 – dangtis, 15 – elektrinis variklis, 16 – mova, 17 – besisukantis lankstus velenas, 18 – šepetėliai, 19 – įvorė, 20 – bioanglis, 21 – filtras, 22 – žarna, 23 – siurblys.

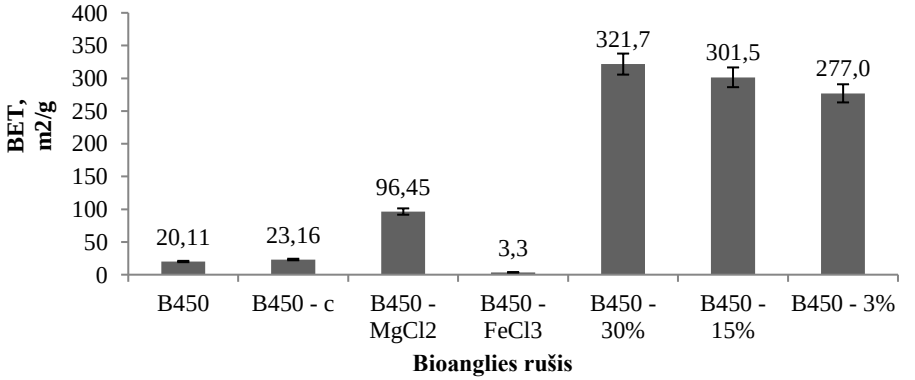

S2.2 pav. Modifikacijos įtaka Brunauer-Emmett-Teller savitąjam paviršiaus plotui

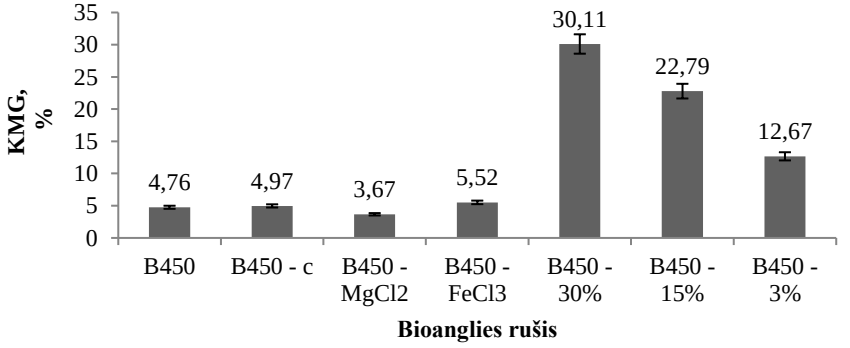

S2.3 pav. Modifikacijos įtaka katijonų mainų gebai

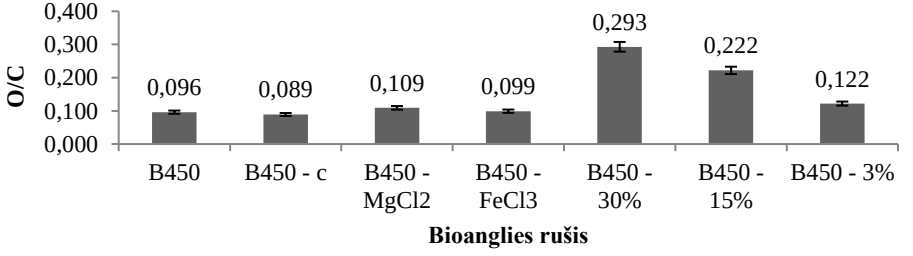

S2.4 pav. Modifikacijos įtaka O/C koeficientui

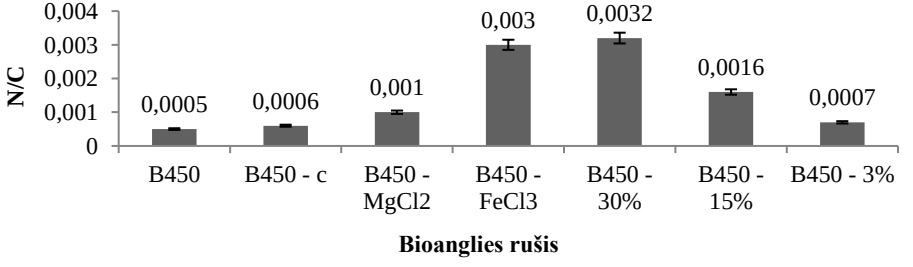

S2.5 pav. Modifikacijos įtaka N/C koeficientui

S2.1 lentelė rodo, kad nemodifikuotos bioanglies ir modifikuotos su H_2O_2 (kur $pH>pH_{pzc}$) elektrostatinė trauka gali skatinti katijoninių metalų adsorbciją. Mg ir Fe modifikuotos bioanglies (kai $pH<pH_{pzc}$) elektrostatinė trauka gali skatinti anijoninių

metalų adsorbciją. Taigi adsorbcijos mechanizmai yra elektrostatinė trauka, jonų mainai, paviršiaus kompleksavimas ir fizikinė adsorbcija.

S2.1 lentelė. Skirtingų bioanglies rūšių pH ir pHpzc palyginimas (vidurkis ± SD)

Bioanglies rūšis	pH	pHpzc
Nemodifikuota bioanglis	8,36±0.04	6,73±0.10
H_2O_2-modifikuota bioanglis (15%)	5,59±0.14	5,08±0.17
$MgCl_2$- modifikuota bioanglis	4,89±0.06	6,58±0.11
$FeCl_3$- modifikuota bioanglis	2,19±0.01	3,63±0.23

H_2O_2 modifikuota bioanglis, kurios koncentracija siekė 9 g/l, parodė aukščiausią adsorbcijos efektyvumą tiek vienkomponenčiuose, tiek daugiakomponenčiuose tirpaluose lyginant su kitomis ištirtomis bioanglies rūšimis, todėl minėta modifikuotos bioanglies rūšis kartu su nemodifikuota bioanglimi buvo pasirinktos adsorbcijos eksperimentiniams tyrimams atlikti.

3. Potencialiai toksiškų elementų adsorbcija iš sintetinių tirpalų ir sąvartyno filtrato naudojant bioanglį ir bioanglies-hidrogelio kompozitą

Didžiausia PTE adsorbcijos geba iš sintetinių tirpalų buvo pasiekta H_2O_2-modifikuota bioanglimi, kai koncentracija siekė 10 mg/l: 20,10 mg/g (Ni), 20,56 mg/g (Cr), 26,68 mg/g (Pb), 23,77 mg/g (Cd), 23,35 mg/g (Zn), 22,72 mg/g (Cu). Tai viršijo nemodifikuotos bioanglies rezultatus beveik 2 kartus.

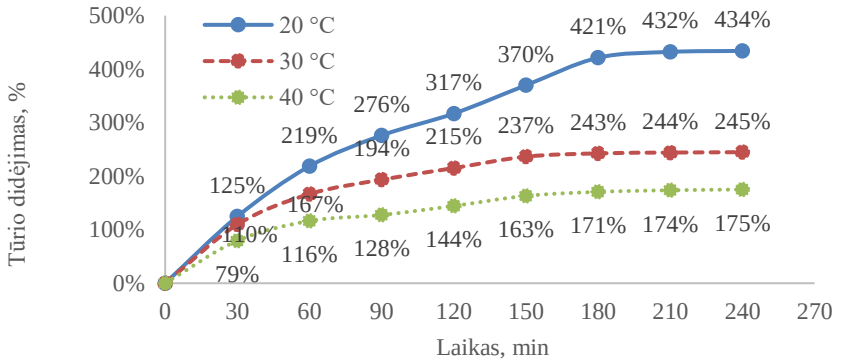

S3.1 pav. Temperatūros įtaka katijoninio bioanglies-hidrogelio kompozito tūrio didėjimui

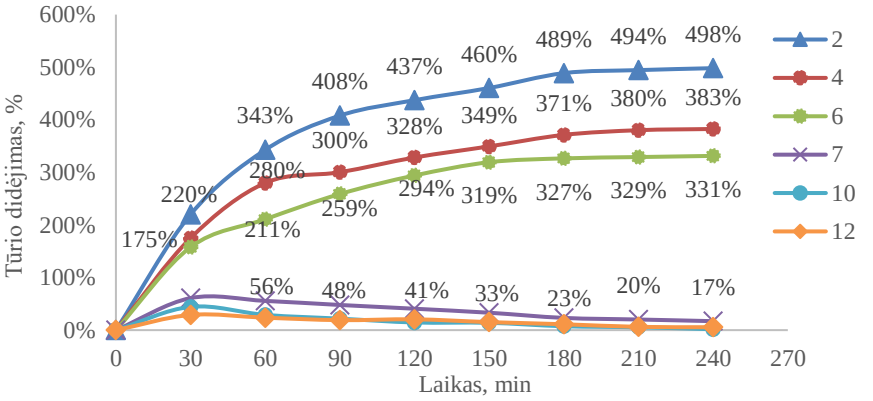

S3.2 pav. pH įtaka katijoninio bioanglies-hidrogelio kompozito tūrio didėjimui

Adsorbcijos rezultatų pritaikymas Langmuir, Freundlich, Redlich-Peterson ir Sips izotermėms parodė, kad adsorbcija vyksta heterogeniniu paviršiumi. Visos R_L ir 1/n vertės buvo 0–1 intervale, patvirtindamos efektyvią PTE adsorbciją iš tirpalo. Termodinaminiai tyrimai parodė teigiamą ΔH° vertę, kadangi adsorbcijos reakcija buvo endoterminė.

BA derinimas su katijoniniu hidrogeliu padidino nemodifikuotos bioanglies KMG nuo 5,15 iki 37,12 cmolc/kg, o BET – nuo 20,11 iki 411,14 m2/g.

Katijoninio kompozito tūrio didėjimas buvo mažesnis nei anijoninio kompozito dėl sudėtyje esančios aciklinės rūgšties, dėl kurios susidaro tinklinės struktūros polimerai. Katijoninis kompozitas išsipučia būdamas 20 °C tirpale (S3.1 pav.) ir pasiekia savo didžiausią tūrį per 240 min (434%). Mažiausias patinimas pastebėtas būdamas 40 °C tirpale (175%). Katijoninis kompozitas išsipučia būdamas rūgščiame tirpale (pH 2, 4, 6) ir pasiekia savo didžiausią tūrį, kai pH yra 2 (498%) per 240 min (S3.2 pav.).

S3.1 lentelė. Didžiausia bioanglies adsorbcijos geba iš sąvartyno filtrato

Adsorbentas	Ni, mg/g	Cr, mg/g	Pb, mg/g	Cd, mg/g	Zn, mg/g	Cu, mg/g
Nemodifikuota BA (bioanglies koncentracija 100 g/l)	2,10	2,56	0,68	0,37	3,35	0,72
H_2O_2-modifikuota BA (dalelių dydis 0,4–1,0 mm)	3,54	5,14	1,01	0,74	4,12	1,05
Katijoninis kompozitas su H_2O_2-modifikuota BA (bioanglies koncentracija 20 g/l)	4,36	12,81	1,27	0,91	4,33	1,57

S3.1 lentelė rodo, kad bioanglies PTE adsorbcijos efektyvumas iš sąvartyno filtrato buvo mažesnis nei iš sintetinių tirpalų. Modifikuotos bioanglies-hidrogelio kompozitas turi 2 kartus didesnį PTE adsorbcijos efektyvumą iš sąvartyno filtrato nei H_2O_2-modifikuota bioanglis.

Dinaminio vidinės difuzijos modelio pritaikymo potencialiai toksiškų elementų adsorbcijos bioanglyje rezultatai pateikti žemyn.

Tūrio koncentracija (C_B) padeda apibrėžti adsorbcijos mechanizmą. Didėjant kontaktiniam laikui, PTE koncentracija mažėja. Buvo pastebėta greita plėvelės difuzija, taip pat nustatytas lėtas adsorbcijos žingsnis. Dėl elektrostatinės traukos ir paviršiaus kompleksavimo per pirmąsias 30 minučių įvyko greita adsorbcija (karboksilinės grupės veikė kaip aktyvios PTE adsorbcijos vietos) (S3.3 pav.). PTE adsorbcija H_2O_2 modifikuotoje bioanglyje įvyko greičiau nei nemodifikuotoje bioanglyje.

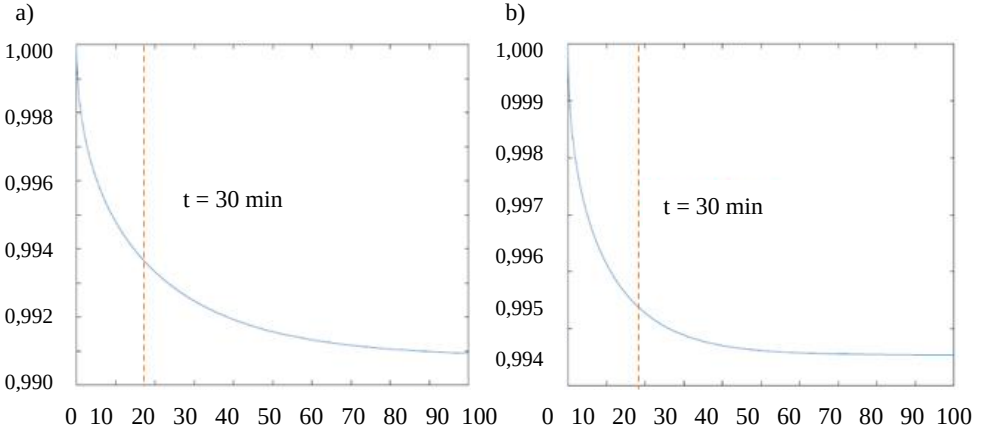

S3.3 pav. Cr normuota tūrio koncentracija pagal laiką (C_B) (t = 60 min):
a) H_2O_2-modifikuota bioanglis; b) nemodifikuota bioanglis.
Vertikalioji ašis – C_B (mol/m^3), horizontalioji ašis – t, s $\times 10^2$

PTE koncentracija bioanglies porų skystyje (C_L) padeda nustatyti adsorbcijos mechanizmą. Padidėjus kontaktiniam laikui, PTE koncentracija porų skystyje pamažu didėjo, tačiau per 60 minučių nepasiekė prisotinimo (S3.4 pav.). PTE buvo adsorbuoti dėl elektrostatinės traukos ir fizikinės adsorbcijos, o dalelių difuzija buvo lėtesnė, dėl didesnio paviršiaus ploto kuris siekė 301,5 m^2/g.

PTE koncentracija kietoje medžiagoje (C_S) padeda apibrėžti PTE pasiskirstymą bioanglies dalelėse ir adsorbcijos mechanizmą. Paaiškėjo, kad paviršiaus difuzija yra vienas iš pagrindinių žingsnių PTE adsorbcijos procese bioanglyje. Koncentracijos maksimumas buvo visą laiką šalia dalelių paviršiaus (S3.5 pav.), nes paviršiaus sąlygos yra tiesiogiai priklausomos nuo tūrio koncentracijos, kuri keičiasi visą laiką. Laikas pasiekti dalelių centrą buvo pasiektas visais atvejais, išskyrus Ni, esant nemodifikuotoje BA.

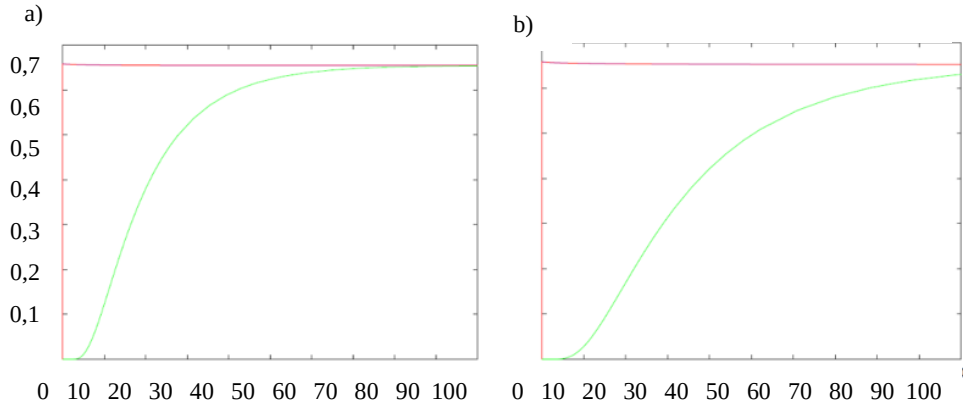

S3.4 pav. Cr koncentracija bioanglies porų skystyje pagal laiką (C_L) (t = 60 min) (žalia linija): a) H_2O_2-modifikuota bioanglis; b) nemodifikuota bioanglis. Vertikalioji ašis – C_L (mol/m3), horizontalioji ašis – t. s $\times 10^2$

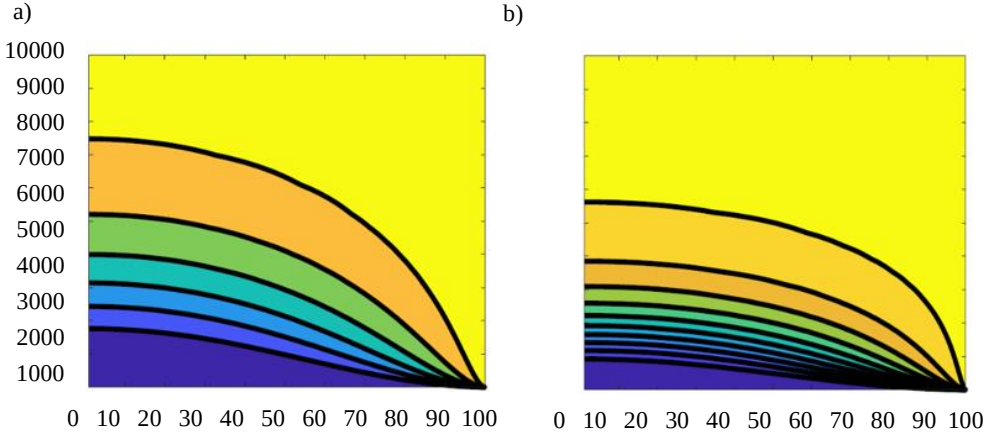

S3.5 pav. Cr koncentracija kietoje medžiagoje pagal laiką ir dalelių spindulį (C_S) (t = 60 min): a) H_2O_2-modifikuota bioanglis; b) nemodifikuota bioanglis. Vertikalioji ašis – t, s, horizontalioji ašis – dalelių spindulys, m$\times 10^5$

Supaprastinto matematinio modelio aproksimacija buvo atlikta linijiniu metodu. Tirpalo jautrumas pagrindinių transportavimo ir kinetinių parametrų atžvilgiu buvo išanalizuotas naudojant supaprastintą modelį.

$$\frac{\partial C_B(\bar{t})}{\partial \bar{t}} = -\alpha\left(C_B(\bar{t}) - C_L(\bar{t},1)\right), 0 < \bar{t} < \mathrm{T}, \qquad \text{(S3.1)}$$

$$\frac{\partial C_L(\bar{t},\bar{r})}{\partial \bar{t}} = \frac{1}{\bar{r}^2}\frac{\partial}{\partial \bar{r}}\left(\bar{r}^2\frac{\partial C_L(\bar{t},\bar{r})}{\partial \bar{r}}\right), 0 < \bar{r} < 1, \qquad \text{(S3.2)}$$

$$\overline{r}^2 \frac{\partial C_L(\overline{t},\overline{r})}{\partial \overline{r}}\Big|_{\overline{r}=0} = 0,\ \frac{\partial C_L(\overline{t},\overline{r})}{\partial \overline{r}}\Big|_{\overline{r}=1} = \beta\left(C_B(\overline{t}) - C_L(\overline{t},1)\right), \quad \text{(S3.3)}$$

$$C_B(0) = C_B^o,\ C_L(0,\overline{r}) = C_L^o, 0 \le \overline{r} \le 1\ . \quad \text{(S3.4)}$$

Linijinis ir normalizuotas matematiniai modeliai (S3.1) – (S3.4) buvo panaudoti jautrumo analizei su adsorbcijos sistemos parametrais. Supaprastintas modelis buvo išbandytas naudojant Russo ir kt. (2015), Souza ir kt. (2017) duomenis.

Atlikus matematinį modeliavimą, buvo pastebėta, kad linijinis ir normalizuotas matematiniai modeliai veikė gerai, o adsorbcijos dinamiką, naudojant skirtingų fizikinių parametrų, galima numatyti gana tiksliai.

Bendrosios išvados

Apibendrinus analizės rezultatus, galima teigti, kad:

1. Pagrindiniai mechanizmai, kontroliuojantys maksimalią Cr^{3+}, Cd^{2+}, Pb^{2+}, Zn^{2+}, Ni^{2+}, Cu^{2+} adsorbciją bioanglyje – paviršiaus kompleksiškumas, elektrostatinė trauka, jonų mainai, fizikinė adsorbcija.

2. Savitasis paviršiaus plotas ir katijonų mainų geba buvo pagrindinės savybės, turinčios įtakos Cr^{3+}, Cd^{2+}, Pb^{2+}, Zn^{2+}, Ni^{2+}, Cu^{2+} adsorbcijai bioanglyje.

3. Pirmą kartą ištirta sumedėjusios žaliavos būdingų savybių įtaka adsorbcijai. Nustatytos svarbiausios žaliavos būdingos savybės, turinčios įtakos bioanglies adsorbcinėms savybėms: ligninas, nes jis sukuria poras; pelenai, kadangi juose gali būti mikroelementų, veikiančių kaip adsorbcijos vietos; azoto ir anglies kiekis, kadangi turi įtaką N/C ir O/C koeficiantų vertėms bioanglyje.Atlikus natūralių modifikavimo metodų tyrimus nustatyta, kad didesnis lignino (54–59%), pelenų (11,8–13,9%), azoto (0,4%) ir mažesnis anglies kiekis (75–76%) sumedėjusioje žaliavoje gerina BA adsorbcines savybes.

4. Bioanglies modifikavimas, naudojant H_2O_2 tirpalą, prideda karboksilines grupes BA paviršiuje, o $FeCl_3$ ir $MgCl_3$ prideda fenolines grupes. Nemodifikuota ir H_2O_2-modifikuota bioanglys labiau tinka katijoninių PTE adsorbcijai dėl elektrostatinės traukos, tuo tarpu Fe- ir Mg-modifikuotos bioanglys tinkamesnės anijoninių PTE adsorbcijai.

5. Adsorbcijos požiūriu tinkamiausia modifikuota bioanglis buvo BA - H_2O_2 (15%) su BET 301,5 m^2/g ir KMG 22,79 cmolc/kg, nes didesnis BET paviršiaus plotas ir KMG sudaro palankias sąlygas katijonų adsorbcijai dėl mikroporų. Modifikavimas naudojant H_2O_2 padidino O/C koeficientą 3 kartus, o N/C koeficientą – 9 kartus.

6. Didžiausia PTE adsorbcijos geba iš sintetinių tirpalų buvo pasiekta H_2O_2-modifikuota bioanglimi, kai koncentracija siekė 10 mg/l: 20,10 mg/g (Ni), 20,56 mg/g (Cr), 26,68 mg/g (Pb), 23,77 mg/g (Cd), 23,35 mg/g (Zn), 22,72 mg/g (Cu). Tai viršijo nemodifikuotos bioanglies rezultatus beveik 2 kartus.

7. BA derinimas su katijoniniu hidrogeliu padidino nemodifikuotos bioanglies KMG nuo 5,15 iki 37,12 cmolc/kg, o BET – nuo 20,11 iki 401,14 m^2/g. Katijoninio kompozito tūrio didėjimas buvo mažesnis nei anijoninio kompozito dėl sudėtyje esančios aciklinės rūgšties, dėl kurios susidaro tinklinės struktūros polimerai. Katijoninis kompozitas išsipučia būdamas 20 °C tirpale ir pasiekia savo didžiausią tūrį per 240 min (434%). Mažiausias patinimas pastebėtas būdamas 40 °C tirpale (175%). Katijoninis kompozitas

išsipučia būdamas rūgščiame tirpale (pH 2, 4, 6) ir pasiekia savo didžiausią tūrį, kai pH yra 2 (498%) per 240 min.

8. Bioanglies PTE adsorbcijos efektyvumas iš sąvartyno filtrato buvo mažesnis nei iš sintetinių tirpalų. Adsorbento adsorbcijos gebą iš sąvartyno filtrato sumažėjo tokia tvarka: Katijoninis kompozitas su H_2O_2-modifikuota BA (su laiku 300 min ir bioanglies koncentracija 20 g/l) > H_2O_2-modifikuota BA (su dalelių dydžiu 0,4–1,0 mm) > nemodifikuota BA (su bioanglies koncentracija 100 g/l).

9. Pirmą kartą buvo išbandytas dinaminis vidinės difuzijos modelis Cr^{3+}, Cd^{2+}, Pb^{2+}, Zn^{2+}, Ni^{2+}, Cu^{2+} adsorbcijai naudojant bioanglį. Tūrio koncentracija ir koncentracija bioanglies porų skystyje padeda spręsti adsorbcijos mechanizmą. Koncentracija kietoje medžiagoje padeda apibrėžti PTE pasiskirstymą bioanglies dalelėse ir adsorbcijos mechanizmą. Dėl plėvelės difuzijos per pirmąsias 30 minučių įvyko greita adsorbcija, o porų ir paviršiaus difuzijos procesai įvyko lėčiau. Koncentracijos maksimumas buvo visą laiką šalia dalelių paviršiaus.

10. Tirpalo jautrumo analizė fizikinės sistemos atžvilgiu leidžia numatyti adsorbcijos proceso dinamiką – pagrindinę adsorbcijos proceso tendenciją – naudojant siūlomą supaprastintą linijinį modelį. Jautrumo analizė yra bazė išspręsti svarbias optimizavimo problemas, siekiant maksimaliai padidinti adsorbcijos gebą pasirinkus optimalų adsorbento formos parametrą.

11. Lignino bioanglies modifikavimo technologija leidžia sukurti H_2O_2 modifikuotą bioanglį, turinčią 25% didesnę katijonų mainų gebą ir karboksilinių bei karbonilinių grupių kiekį bioanglies paviršiuje, ir iki 2 kartų didesnį BET savitąjį paviršiaus plotą nei bioanglis, modifikuota nenaudojant H_2O_2 minėtą technologiją. Taip pat bioanglis, kurios dalelių dydis mažesnis (0,4–1,0 mm), turėjo didesnius KMG ir BET, nei bioanglis, kurios dalelių dydis 1,0–3,0 mm, modifikuota tokiu pačiu būdu.

Rekomendacijos

Siūlomos tokios rekomendacijos:

1. Patentuotame modifikavimo įrenginyje galima naudoti įvairius cheminius tirpalus, siekiant modifikuoti bioanglį taip, kad padidėtų adsorbcija iš vandeninių tirpalų ir sąvartyno filtrato. Norint patobulinti Cr^{3+}, Cd^{2+}, Pb^{2+}, Zn^{2+}, Ni^{2+}, Cu^{2+} adsorbciją, rekomenduojama padidinti sąvitąjį paviršiaus plotą ir katijonų mainų gebą.

2. Tvariam naudojimui, rekomenduojama rinktis beržo miškų atliekas su didesniu lignino (54–59%), pelenų (11,8–13,9%), azoto (0,4%) kiekiu. Žaliava ruošiama pirolizės būdu 450 °C 2 valandas, susmulkinama iki 0,4–1,0 mm dydžio dalelių ir bioanglis modifikuojama naudojant H_2O_2 tirpalą modifikavimo įrenginyje.

3. H_2O_2 tirpalu modifikuoti bioanglies-hidrogelio kompozitai gali būti naudojami Cr^{3+}, Cd^{2+}, Pb^{2+}, Zn^{2+}, Ni^{2+}, Cu^{2+} adsorbcijai iš sąvartynų filtrato.

Annexes[2]

Annex A. Physico-chemical characteristics of biochar

Annex B. Equilibrium data

Annex C. Kinetics data

Annex D. Competing ions experimental data

Annex E. Declaration of academic integrity

Annex F. The coauthors' agreements to present publications for the dissertation defence

Annex G. Copies of scientific publications by the author on the topic of the dissertation

[2]The annexes are supplied in the enclosed compact disc

Valeriia CHEMERYS

LIGNEOUS BIOCHAR RESEARCH AND
DEVELOPMENT OF TECHNOLOGY FOR ENHANCED
ADSORPTION OF POTENTIALLY TOXIC ELEMENTS

Doctoral Dissertation

Technological Sciences,
Environmental Engineering (T 004)

BIOANGLIES IŠ SUMEDĖJUSIOS BIOMASĖS TYRIMAI
BEI TECHNOLOGIJOS KŪRIMAS POTENCIALIAI
TOKSIŠKŲ ELEMENTŲ ADSORBCIJAI GERINTI

Daktaro disertacija

Technologijos mokslai,
aplinkos inžinerija (T 004)

2020 05 28. 15,75 sp. l. Tiražas 20 egz.
Vilniaus Gedimino technikos universiteto
leidykla „Technika“,
Saulėtekio al. 11, 10223 Vilnius,
http://leidykla.vgtu.lt
Spausdino UAB „BMK leidykla“,
A. Mickevičiaus g. 5, LT-08119 Vilnius